

5-Methylated Polyprenylated Acylphloroglucinols Derivatives as Low-Voltage-Gated Ca^{2+} Channels Inhibitors

Ya-Li Hu,^{‡a} Ding Dong,^{‡ab} Jian-Jun Zhao,^a Kun Hu,^a Ling-Mei Kong,^a Yun-Xia Hu,^{ab} Xing-Ren Li,^a Song-Yu Li,^a Yin Nian ^{*a} and Gang Xu ^{*a}

^aKey Laboratory of Phytochemistry and Natural Medicines and Yunnan Key Laboratory of Natural Medicinal Chemistry, Kunming Institute of Botany, Chinese Academy of Sciences, Kunming 650201, People's Republic of China

^bUniversity of Chinese Academy of Sciences, Beijing 100049, People's Republic of China

Supporting Information

Table of contents

- SI-1. Experimental procedures (Page S2–S3).
- SI-2. Physical data of the new compounds (Page S4–S6).
- SI-3. Structure elucidation of new compounds (S7–S12)
- SI-4. Biological assays (S13–S18)
- SI-5. The NMR spectroscopic data of new compounds (S19–S26)
- SI-6. The original NMR and MS spectra of new compounds (Page S27–S94).
- SI-7. Computational methods and results (Page S95–S119).

SI-1. Experimental procedures.

General experimental procedures. X-ray data were collected on Bruker APEX DUO instrument using Cu K α radiation. Melting points were recorded on an RDY-1B micro melting point apparatus. Optical rotations were measured on a Jasco P-1020 polarimeter with MeOH as solvent. UV spectra were recorded on a Shimadzu UV-2401PC spectrometer. IR spectra were determined by using a Bruker FT-IR Tensor-27 infrared spectrophotometer with KBr disks. 1D and 2D NMR spectra were recorded on a Bruker Avance III 600 spectrometer. ESIMS and HRESIMS data were acquired on Agilent G6230 TOF and Agilent 6540 Q-TOF mass spectrometers. Semi-preparative HPLC was performed on an Agilent 1100 HPLC. Silica gel (100-200 and 200-300 mesh, Qingdao Marine Chemical Co., Ltd., Qingdao, People's Republic of China), and MCI gel (75–150 μ m, Mitsubishi Chemical Corporation, Tokyo, Japan) were used for column chromatography. Fractions were monitored by TLC (GF 254, Qingdao Marine Chemical Co., Ltd.), and spots were visualized by heating silica gel plates immersed in 10%H₂SO₄ in ethanol.

Plant material. The aerial parts of *Hypericum ascyron* L. were collected in Haba Snow Mountain of Shangri-La, Yunnan Province, P. R. China, in August 2015. The plant was identified by Dr. Yong-Zeng Zhang, Kunming Institute of Botany, Kunming, P. R. China. A voucher specimen was deposited with Kunming Institute of Botany with identification number 2015H01.

Extraction and isolation. The air-dried and powdered entire plants of *H. ascyron* L. (16.0 kg) were extracted with MeOH at room temperature and then filtered. The solvent was evaporated in vacuo and the obtained crude extract (5.0 kg) was subjected to a silica gel column chromatography eluted with petroleum ether/acetone in gradient (1:0–1:1, v/v) to afford five fractions (Fr. A–E).

Fraction A (109 g) was separated over a MCI-gel column (MeOH-H₂O from 7:3 to 10:0) to obtain five fractions (Fr. A1–A5). Fraction A3 (18.2 g) and A4 (16.7 g) were further chromatographed over silica gel, MCI, RP-18, preparative and semi-preparative HPLC to yield **4** (4.5 mg, t_R = 11.45min, 95% MeOH), **5** (2.0 mg, t_R = 15.53 min, 90%

MeOH), **6** (8.5 mg, t_R = 12.64 min, 90% MeOH), **7** (18.5 mg, t_R = 3.42 min, 90% MeOH), **9** (2.0 mg, t_R = 13.71 min, 90% MeOH), **12** (5.0 mg, t_R = 16.13 min, 95% MeOH), **13** (5.0 mg, t_R = 17.51 min, 95% acetonitrile), **18** (2.5 mg, t_R = 22.73 min, 85% MeOH), **19** (3.5 mg, t_R = 11.91 min, 90% MeOH), **16** (15.5 mg, t_R = 10.30 min, 90% MeOH), **20** (1.5 mg, t_R = 17.58 min, 95% acetonitrile), and **23** (2000.0 mg, t_R = 6.99 min, 95% MeOH).

Fraction B (77 g) was separated over an MCI-gel column (MeOH-H₂O from 7:3 to 10:0, v/v) to obtain seven fractions (Fr. B1–B7). Fraction B4 (16.8 g) was further chromatographed over silica gel, RP-18, Sephadex LH-20, preparative and semi-preparative HPLC to obtain **10** (10.0 mg, t_R = 17.13 min, 90% MeOH), **11** (4.3 mg, t_R = 8.87 min, 85% MeOH), **17** (5.0 mg, t_R = 24.75 min, 85% MeOH), **14** (4.5 mg, t_R = 24.24 min, 85% MeOH), **15** (4.0 mg, t_R = 26.29 min, 85% MeOH), **21** (1.5 mg, t_R = 13.67 min, 80% MeOH), **22** (2.0 mg, t_R = 13.72 min, 80% MeOH), **25** (30.0 mg, t_R = 17.41 min, 80% MeOH), **24** (20.0 mg, t_R = 10.72 min, 85% MeOH), **26** (200.0 mg, t_R = 23.42 min, 75% MeOH), and **27** (160.0 mg, t_R = 11.37 min, 85% MeOH).

Fraction C (63.0 g) was separated over an MCI-gel column (MeOH-H₂O from 6:4 to 10:0, v/v) to obtain eight fractions (Fr. C1–C8). Fraction C4 (9.7 g) was further chromatographed over a silica gel column, eluted with petroleum ether/acetone (100:1-0:1, v/v), to obtain six fractions (Fr. C4.1-C4.6). Sephadex LH-20 was applied to afford three fractions (Fr. C4.5.1-C4.5.3) from Fr. C4.5 (740 mg). Compounds **1** (1.2 mg, t_R = 9.93 min, 85% MeOH) and **2** (1.2 mg, t_R = 8.90 min, 85% MeOH), and compound **8** (1.7 mg, t_R = 10.80 min, 80% MeOH) were purified from Fr. C4.5.3 (140 mg) and Fr. C4.5.2 (480 mg), respectively, by preparative HPLC. Fr. C5.4 (37.9 mg) was separated by preparative HPLC to give compound **3** (1.6 mg, t_R = 5.63 min, 85% MeOH).

SI-2. Physical data of the new compounds.

Ascynol A (1): colorless needle crystals; mp 127–129 °C; $[\alpha]^{21}\text{D} -42.6$ (*c* 0.06, MeOH); UV (MeOH) λ_{\max} (log ε) 204 (4.20), 257 (3.95), 294 (3.19) nm; IR (KBr) ν_{\max} 3423, 2956, 2929, 2876, 1714, 1644, 1595, 1239, 764 cm^{-1} ; ECD (MeOH) λ_{\max} ($\Delta\varepsilon$) 377 (−0.1), 337 (−6.7), 292 (+1.3), 255 (+10.3), 222 (−4.1), 206 (+21.2); ^1H and ^{13}C NMR data, see [Table S1](#); HRESIMS *m/z* 405.2404 [M + Na]⁺ (calcd for C₂₅H₃₄O₃Na, 405.2406).

Ascynol B (2): colorless needle crystals; mp 115–117 °C; $[\alpha]^{21}\text{D} +17$ (*c* 0.1, MeOH); UV (MeOH) λ_{\max} (log ε) 202 (4.13), 245 (3.85), 279 (2.88), 326 (2.44) nm; IR (KBr) ν_{\max} 3442, 2968, 2929, 1713, 1670, 1446, 1416, 1366, 1215, 698 cm^{-1} ; ECD (MeOH) λ_{\max} ($\Delta\varepsilon$) 307 (+0.1), 280 (−0.7), 243 (+3.9), 211 (−3.3); ^1H and ^{13}C NMR data, see [Table S1](#); HRESIMS *m/z* 407.2559 [M + Na]⁺ (calcd for C₂₅H₃₆O₃Na, 407.2562).

Ascynol C (3): colorless gum; $[\alpha]^{20}\text{D} -82$ (*c* 0.06, MeOH); UV (MeOH) λ_{\max} (log ε) 196 (3.58), 260 (2.14) nm; IR (KBr) ν_{\max} 2920, 1754, 1714, 1272 cm^{-1} ; ECD (MeOH) λ_{\max} ($\Delta\varepsilon$) 279 (−0.1), 235 (+0.1), 209 (−0.6), 193 (−0.6); ^1H and ^{13}C NMR data, see [Table S1](#); HRESIMS *m/z* 307.2283 [M + H]⁺ (calcd for C₁₉H₃₀O₃Na, 307.2268).

Ascynol D (4): colourless gum; $[\alpha]^{19}\text{D} -31$ (*c* 0.1, MeOH); UV (MeOH) λ_{\max} (log ε) 201 (4.40), 228 (4.43), 271 (3.22) nm; IR (KBr) ν_{\max} 3454, 2969, 2934, 2879, 1706, 1678, 1451, 1381, 1287, 1115 cm^{-1} ; ECD (MeOH) λ_{\max} ($\Delta\varepsilon$) 240 (−5.2), 200 (+15.9), 196 (−45.2); ^1H and ^{13}C data, see [Table S2](#); HRESIMS *m/z* 435.2517 [M + Na]⁺ (calcd for C₂₆H₃₆O₄Na, 435.2506).

Ascynol E (5): colorless gum; $[\alpha]^{20}\text{D} -39$ (*c* 0.2, MeOH); UV (MeOH) λ_{\max} (log ε) 203 (3.90), 270 (3.38), 378 (1.77) nm; IR (KBr) ν_{\max} 2960, 2873, 1692, 1629, 1466, 1384, 1366 cm^{-1} ; ^1H and ^{13}C data, see [Table S2](#); ESIMS *m/z* 359 [M + H]⁺; HRESIMS *m/z* 359.2944 [M + H]⁺ (calcd for C₂₄H₃₉O₂, 359.2945).

Ascynol F (8): colorless gum; $[\alpha]^{18}\text{D} +22$ (*c* 0.1, MeOH); UV (MeOH) λ_{\max} (log ε) 245 (4.11), 199 (4.52), 221 (3.69) nm; IR (KBr) ν_{\max} 3435, 2969, 2928, 1712, 1686, 1597, 1448, 1376, 1181, 688 cm^{-1} ; ECD (MeOH) λ_{\max} ($\Delta\varepsilon$) 337 (+1.3), 317 (+0.6), 284 (+2.9), 252 (−5.7), 220 (−3.7), 200 (+16.1), 195 (+8.5); ^1H and ^{13}C NMR data, see [Table](#)

S2; HRESIMS m/z 419.2559 [M + Na]⁺ (calcd for C₂₆H₃₆O₃Na, 419.2557).

Ascynol G (9): colourless oil; $[\alpha]^{20}_{\text{D}} +78$ (c 0.1, MeOH); UV (MeOH) λ_{\max} (log ε) 204 (4.04), 291 (2.54) nm; IR (KBr) ν_{\max} 3437, 2969, 2930, 2873, 1770, 1726, 1628, 1453, 1381, 1221 cm⁻¹; ECD (MeOH) λ_{\max} ($\Delta\varepsilon$) 342 (+0.4), 301 (+6.7), 243 (-1.7), 196 (-8.4); ¹H and ¹³C data, see [Table S3](#); HRESIMS m/z 523.3402[M + Na]⁺ (calcd for C₃₁H₄₈O₅Na, 523.3394).

Ascynol H (10): colourless crystals; $[\alpha]^{20}_{\text{D}} -22$ (c 0.3, MeOH); UV (MeOH) λ_{\max} (log ε) 203 (4.39), 246 (3.45) nm; IR (KBr) ν_{\max} 2968, 1743, 1630, 1448, 1379, 1233, 1133, 764 cm⁻¹; ECD (MeOH) λ_{\max} ($\Delta\varepsilon$) 308 (-4.5), 248 (+4.7), 212 (-8.2), 201 (+2.6), 197 (-8.5); ¹H and ¹³C data, see [Tables S4 and S5](#); HRESIMS m/z 553.2917 [M + Na]⁺ (calcd for C₃₄H₄₂O₅Na, 553.2924).

Ascynol I (11): colourless gum; $[\alpha]^{24}_{\text{D}} -149$ (c 0.1, MeOH); UV (MeOH) λ_{\max} (log ε) 338 (3.35), 251 (4.11), 203 (4.45) nm; IR (KBr) ν_{\max} 3419, 2969, 2933, 1723, 1703, 1673, 1386, 1215, 692 cm⁻¹; ¹H and ¹³C data, see [Tables S4 and S5](#); HRESIMS m/z 545.3242 [M + Na]⁺ (calcd for C₃₃H₄₆O₅Na, 545.3243).

Ascynol J (12): colourless gum; $[\alpha]^{21}_{\text{D}} -30$ (c 0.1, MeOH); UV (MeOH) λ_{\max} (log ε) 202 (3.86), 220 (3.57), 268 (3.02), 320 (2.70) nm; IR (KBr) ν_{\max} 3435, 2972, 2930, 1712, 1694, 1630, 1461, 1383 cm⁻¹; ECD (MeOH) λ_{\max} ($\Delta\varepsilon$) 332 (-1.5), 229 (-2.9), 206 (-0.8), 196 (-13.6); ¹H and ¹³C data, see [Tables S4 and S5](#); HRESIMS m/z 511.3405 [M + Na]⁺ (calcd for C₃₀H₄₈O₅Na, 511.3394).

Ascynol K (13): colourless gum; $[\alpha]^{22}_{\text{D}} -24$ (c 0.1, MeOH); UV (MeOH) λ_{\max} (log ε) 202 (3.98) nm; IR (KBr) ν_{\max} 3435, 2972, 2932, 1713, 1691, 1462, 1384 cm⁻¹; ECD (MeOH) λ_{\max} ($\Delta\varepsilon$) 333 (-1.8), 304 (+1.1), 229 (-4.0), 202 (+0.9), 196 (-19.4); ¹H and ¹³C data, see [Tables S4 and S5](#); HRESIMS m/z 525.3565 [M + Na]⁺ (calcd for C₃₁H₅₀O₅Na, 525.3550).

Ascynol L (14): colourless gum; $[\alpha]^{21}_{\text{D}} +20$ (c 0.1, MeOH); UV (MeOH) λ_{\max} (log ε) 280 (4.07), 202 (4.16) nm; IR (KBr) ν_{\max} 3430, 2961, 2928, 1726, 1619, 1384, 1245 cm⁻¹; ECD (MeOH) λ_{\max} ($\Delta\varepsilon$) 306 (-20.9), 278 (+37.3), 243 (+5.9), 233 (+7.8), 209 (-16.3); ¹H and ¹³C data, see [Tables S6 and S7](#); HRESIMS m/z 535.3407 [M + Na]⁺ (calcd for C₃₂H₄₈O₅Na, 535.3394).

Ascynol M (15): colourless gum; $[\alpha]^{21}_D -15$ (*c* 0.21, MeOH); UV (MeOH) λ_{\max} (log ε) 449 (1.55), 280 (3.98), 203 (4.02) nm; IR (KBr) ν_{\max} 3430, 2961, 2928, 2859, 1726, 1619, 1451, 1384, 1245 cm⁻¹; ¹H and ¹³C data, see [Tables S6 and S7](#); HRESIMS *m/z* 535.3397 [M + Na]⁺ (calcd for C₃₂H₄₈O₅Na, 535.3399).

Ascynol N (17): colourless gum; $[\alpha]^{22}_D +44$ (*c* 0.2, MeOH); UV (MeOH) λ_{\max} (log ε) 202 (4.15), 281 (4.07) nm; IR (KBr) ν_{\max} 3432, 2973, 2934, 2873, 1727, 1622, 1458, 1383, 1173 cm⁻¹; ECD (MeOH) λ_{\max} ($\Delta\varepsilon$) 305 (-18.9), 277 (+24.3), 244 (-7.3), 216 (+5.2), 196 (-25.3); ¹H and ¹³C data, see [Tables S6 and S7](#); HRESIMS *m/z* 535.3404 [M + Na]⁺ (calcd for C₃₂H₄₈O₅Na, 535.3394).

Ascynol O (18): colourless oil; $[\alpha]^{27}_D -55$ (*c* 0.1, MeOH); UV (MeOH) λ_{\max} (log ε) 196 (4.28), 248 (3.63), 280 (3.97) nm; IR (KBr) ν_{\max} 3430, 1728, 1618, 1384, 1172 cm⁻¹; ECD (MeOH) λ_{\max} ($\Delta\varepsilon$) 331 (+1.0), 303 (-11.9), 276 (+11.0), 248 (-6.9), 212 (+4.5); ¹H and ¹³C data, see [Tables S6 and S7](#); HRESIMS *m/z* 535.3402 [M + Na]⁺ (calcd for C₃₂H₄₈O₅Na, 535.3394).

Ascynol P (20): colourless gum; $[\alpha]^{20}_D -130$ (*c* 0.1, MeOH); UV (MeOH) λ_{\max} (log ε) 203 (4.33), 247 (4.06), 276 (3.82), 513 (2.49), 549 (2.51) nm; IR (KBr) ν_{\max} 2973, 2931, 1724, 1696, 1631, 1449, 1382, 1223 cm⁻¹; ECD (MeOH) λ_{\max} ($\Delta\varepsilon$) 354 (-3.8), 326 (-8.7), 247 (+11.3), 216 (-13.9), 201 (+11.2); ¹H and ¹³C data, see [Table S8](#); HRESIMS *m/z* 537.2995 [M + Na]⁺ (calcd for C₃₄H₄₂O₆Na, 537.2975).

Ascynol Q (21): colourless gum; $[\alpha]^{21}_D -112$ (*c* 0.1, MeOH); UV (MeOH) λ_{\max} (log ε) 247 (4.22), 202 (4.47) nm; IR (KBr) ν_{\max} 3444, 2974, 2922, 1723, 1697, 1663, 1626, 1447, 1377, 1221, 985, 688 cm⁻¹; ECD (MeOH) λ_{\max} ($\Delta\varepsilon$) 328 (-3.9), 291 (+1.9), 265 (-6.9), 244 (+10.0), 215 (-24.7), 195 (+7.5); ¹H and ¹³C data, see [Table S8](#); HRESIMS *m/z* 555.3082 [M + Na]⁺ (calcd for C₃₄H₄₄O₅Na, 555.3086).

SI-3. Structure elucidation of new compounds.

Ascynol D (**4**) had a molecular formula of C₂₆H₃₆O₄ (*m/z* 435.2517 [M + Na]⁺, calcd 435.2506), indicating 9 indices of hydrogen deficiency (IHCs). Its ¹H NMR spectrum illustrated one monosubstituted benzene ring (δ_{H} 7.88, d, H-12/16; 7.39, t, H-13/15; 7.50, t, H-14; *J* = 7.2 Hz), an olefinic proton (δ_{H} 5.11, t, *J* = 6.6 Hz), a doublet methyl (δ_{H} 0.88, d, *J* = 6.0 Hz), five singlet methyls and a hydroxyl (δ_{H} 4.05, s). The ¹³C NMR and HSQC spectra showed the presence of 26 carbon signals attributable to a phenyl, a prenyl group, one nonconjugated (δ_{C} 216.5) and one esterified (δ_{C} 166.2) carbonyls, three quaternary carbons, three methines, three methylenes, and four methyls. Despite 7 IHCs accounted to the phenyl and prenyl groups and two carbonyls, the 2 remaining IHCs inferred that **4** should feature a bicyclic system.

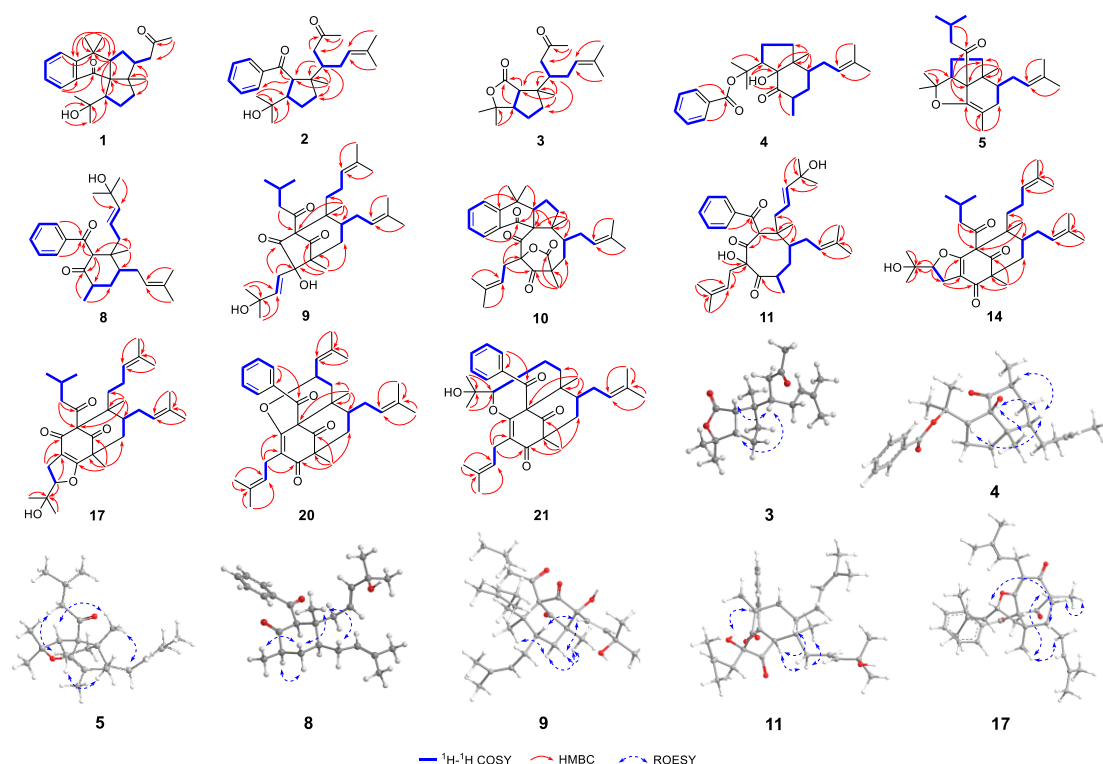


Fig. S1. ¹H-¹H COSY (bold), selected HMBC (arrow) and key NOESY (double arrow) of new compounds.

The ¹H-¹H COSY correlations of Me-22/H-5/H₂-6/H-7 and H₂-29/H₂-30/H-31, together with the HMBC correlations from Me-22 to C-1/C-9, from Me-28 to C-1/C-7/C-8, and from H-31 to C-1/C-9 established a 5/6 ring system. A prenyl group was attached to C-7 by the ¹H-¹H COSY correlations of H-7/H-23/H-24 and HMBC correlations from Me-26/27 to C-24. The quaternary carbon at δ_{C} 88.6 (C-1) was oxygenated by a hydroxyl, which was supported by the HMBC correlations from OH-

1 to C-1/C-8/C-9. In addition, the HMBC correlations from a *gem*-dimethyl at Me-33/34 to C-31/C-32 indicated the existence of an isopropyl moiety at C-31. Then, another oxygenated quaternary carbon at δ_{C} 86.3 (C-32) was attached by a phenyl ester side group, which was deduced by the HMBC correlations from H-9/13 to C-10. This deduction was consistent with the molecular formula and chemical shifts as well. In the ROESY spectrum, the cross-peaks of Me-28/OH-1, OH-1/H-7, H-7/H-5, H-7/H-31 suggested the α -configuration of Me-28, OH-1, H-5, H-7, and H-31. Hence, the structure of **4** was elucidated as shown.

The molecular formula of ascynol E (**5**) was deduced as $\text{C}_{24}\text{H}_{38}\text{O}_2$ on the basis of its ^{13}C NMR and (+)-HRESIMS data (m/z 359.2944 [$\text{M} + \text{H}$] $^+$, calcd 359.2945), which suggested that **5** had 12 more molecular weight than hypermogin A (**6**) [1]. The 1D and 2D NMR spectra of **5** and **6** implied the presence of *sec*-butyl group in **5** instead of an isopropyl group in **6**. Meanwhile, compounds **5** and **6** shared the same skeletons and configurations by detailed comparison of their 1D and 2D NMR data.

Ascynol F (**8**) was assigned the molecular formula $\text{C}_{26}\text{H}_{36}\text{O}_3$ on the basis of its HRESIMS (m/z 419.2559 [$\text{M} + \text{Na}$] $^+$ calcd 419.2562) and ^{13}C NMR data (Table S2). Extensive analysis of both 1D and 2D NMR data pointed that compound **8** shared a similar carbon skeleton and relative configuration with norascyonone C [2], the known analogue previously obtained from *H. ascyon* Linn. as well. The structural novelty involves a 2-methylbut-3-en-2-ol side chain at C-29 in **8** instead of a prenyl group as confirmed by the HMBC correlations of Me-33 and Me-34 with C-31, as well as the ^1H - ^1H COSY cross-peaks of H₂-29/H-30/H-31 (Fig. S1).

The molecular formula of ascynol G (**9**) was determined as $\text{C}_{31}\text{H}_{48}\text{O}_5$ by a sodium adduct ion at m/z 523.3402 [$\text{M} + \text{Na}$] $^+$ (calcd 523.3394) in the HRESIMS spectrum, which was consistent with its ^{13}C NMR and DEPT data. The IR spectrum displayed absorption bands due to carbonyls (1770 and 1726 cm^{-1}) and hydroxyl (3437 cm^{-1}) functionalities. ^1H NMR resonances of **9** revealed the presence of four olefinic protons, two doublet methyls, and seven singlet methyls. The ^{13}C and NMR spectra showed 31 carbon signals corresponding to ten quaternary carbons (including three carbonyls and two oxygenated), five methines, five methylenes, and nine methyls, 15 of which were attributable to an isovaleryl and two prenyl groups. The characteristic signals of three carbonyls at δ_{C} 208.5 (C-2), 208.9 (C-9), and 201.4 (C-10), three quaternary carbons at δ_{C} 78.8 (C-1), 56.7 (C-5), and 55.7 (C-8), one methine at δ_{C} 43.3 (C-7), and one methylene at δ_{C} 41.5 (C-6) indicated that **9** should be a PPAP-type natural product.

Comparison of its 1D NMR data with those of garcinielliptone G [3], a known BPAP with bicyclo[3.3.1]nonane-2,4,9-trinone core, revealed some significant similarities, especially for the signals of C-1, C-2, C-5, C-6, C-7, C-8, C-9 and corresponding substituents at C-5, C-7 and C-8. However, the isobutyryl group at C-1 in garcinielliptone G was replaced by the isovaleryl group in **9**, which was supported by the ^1H - ^1H cosy correlations of Me-13(14)/H-12/H₂-11 and the HMBC cross-peaks of H₂-11 to C-1/C-10. Furthermore, the signal for olefinic carbon C-3 and carbonyl C-4 in hyperibine J was absent in **9**, while an oxygenated quaternary carbon at δ_{C} 82.0 was present. The oxygenated carbon of **9** should be ascribed to C-4 and connected with C-2 on the basis of HMBC correlations from H₂-6 and Me-22 to δ_{C} 82.0 and from Me-22 to C-2. Subsequently, a 2-methylbut-3-en-2-ol side chain, together with a hydroxyl, was deduced at C-3 by the HMBC correlations of Me-20 and Me-21 with C-19, H-17/18 and C-3, as well as the ^1H - ^1H COSY cross-peaks of H-17/H-18. Therefore, the structure of **9** was elucidated as a 3-*nor*-BPAP with bicyclo[3.2.1]octane-2,9-bione core. The cross-peaks of H-7/H-17, H-17/H-6a, H-6b/Me-28, and H₂-6/Me-22 in the ROESY spectrum suggested the α -orientations of H-7 and β -orientations of Me-28, Me-22, OH-4, and isobutyryl group at C-1.

Ascynol H (**10**), obtained as colorless crystals, possessed a molecular formula C₃₄H₄₂O₅ by analyzing its HRESIMS (m/z 553.2931 [M + Na]⁺, calcd 553.2924) and NMR spectroscopic data. The ^1H NMR spectrum of **10** showed the presence of an *ortho*-disubstituted benzene ring, two olefinic protons, and eight singlet methyls. The ^{13}C and DEPT NMR spectra revealed 34 carbon signals corresponding to nine quaternary carbons, two methines, three methylenes, four methyls, and sixteen other signals assignable to a benzene and two prenyl groups. These data suggested that **10** was highly similar to hyphenrone D [4], a known PPAP comprising a 6/6/5/8/5 fused ring system. Analysis of the NMR spectroscopic data of **10** and hyphenrone D indicated that a prenyl group in hyphenrone D was replaced by a methyl in **10**. This deduction was confirmed by correlations from Me-22 to C-4/C-5/C-6 in the HMBC spectrum. Other parts of **10** were identical to those of hyphenrone D by detailed analysis of 2D NMR spectroscopic data. In ROESY spectrum, the correlations of H-6a/Me-28, Me-28/H₂-23, Me-28/H-31, and H-17/Me-22 determined that Me-28, H-31 and the prenyl group at C-7 were β -oriented, while the prenyl group at C-3 and Me-22 were α -oriented. The definition of the C-1 configuration was problematic. Fortunately, quality crystals of **10** were obtained in methanol and its absolute configuration was unambiguously assigned to be 1*R*,3*S*,5*R*,7*S*,8*R*,31*S* via the single-crystal X-ray diffraction analysis

[Flack parameter = 0.08(6), CCDC 2359944].

The molecular formula of ascynol I (**11**) was deduced as C₃₃H₄₆O₅ based on its ¹³C NMR and HRESIMS data, which was 16 mass units more than that of ascyonone C [5], a known 9-nor-PPAP derivative isolated from *H. ascyonon* as well. A 2-methylbut-3-en-2-ol side chain at C-29 in **11** instead of a prenyl group was evidenced by the HMBC correlations of Me-33 and Me-34 with C-31 and the ¹H-¹H COSY cross-peaks of H₂-29/H-30/H-31. The ROESY correlations of Me-28/H₂-23, H-7/H-1, H-1/H₂-17, and OH-3/H-5 determined the relative configuration of **11** to be the same as that of ascyonone C. Based on the MS and NMR data of ascynols J and K (**12** and **13**), they had the same carbon skeletons and configurations as those of **11**. Differently, the existence of a phenyl group in **11** at C-10 was replaced by a isopropyl group in **12** and a sec-butyl group in **13**, respectively.

The molecular formulas of ascynols N and O (**17** and **18**) were confirmed as C₃₂H₄₈O₅ via the sodium-added molecules at *m/z* 535.3404 [M + Na]⁺ (calcd 535.3394) and *m/z* 535.3402 [M + Na]⁺ (calcd. 535.3394) in the HRESIMS spectra of **17** and **18**, respectively. Comparative analyses of their NMR data revealed the commonality of a isobutyl group, a dihydrofuran ring and two prenyl groups in their structures. The substituents at C-1 were confirmed by HMBC correlations from H₂-11 to C-1/C-10 and ¹H-¹H COSY cross peaks of Me-13/14/H-12/H₂-11, which implied that the benzoyl groups in compounds hyperascyrins A and B [6] were replaced by the isovaleryl groups in **17** and **18**, respectively. Differences in their structures were established by NOESY experiments, in which the correlations of H-7/H-29b, H-29a/Me-28, Me-28/H-6b, H₂-6/Me-22 revealed the same orientations of H-7, Me-22, and Me-28 in both structures. The α -orientation of H-18 in **17** was deduced by the correlations of Me-20/Me-26, while the β -orientation of H-18 in **18** was based on the correlations of Me-20/H-6a.

The molecular formulas of ascynols L and M (**14** and **15**) were identified as C₃₂H₄₈O₅, in accordance with compound **18** (ascynol O), from their ¹³C NMR and HRESIMS data (**15**: *m/z* 535.3397 [M + Na]⁺, calcd 535.3399; **14**: *m/z* 535.3407 [M + Na]⁺, calcd 535.3394). Comparative analyses of their NMR data suggested that compounds compounds **14** and **15** shared the same skeleton as well as the isovaleryl group, the dihydrofuran ring, and two prenyl groups in their structures, which were similar to those of **18**. However, their chemical shifts of C-2 (**15**: δ_{C} 171.8; **14**: δ_{C} 171.5; **18**: δ_{C} 188.2) and C-4 (**15**: δ_{C} 190.1; **14**: δ_{C} 190.7; **18**: δ_{C} 177.0) implied that the dihydrofuran rings

in compounds **14** and **15** were linked to C-2 and C-3 instead of C-3 and C-4 as in **17** and **18**. In the NOESY spectra of **14** and **15**, correlations were evident among H-6a, Me-28, and H₂-23, as well as between Me-28 and H-12, suggesting that the relative configurations of C-1, C-5, C-7 and C-8 were identical to those of **18**. Furthermore, the ROESY correlation of H-12/Me-20 in the spectrum of **14** indicated the α -orientation of H-18. In contrast, the correlations of H-12/H-18 and Me-20/H-31 were found in the ROESY spectrum of **15**. Therefore, compounds **14** and **15** were established as pairs of epimers at C-18. Finally, the absolute configuration of **14** was determined as 1*S*,5*R*,7*S*,8*R*,18*S* by the X-ray diffraction data [Flack parameter = 0.07(4), CCDC 2359945] unequivocally.

Ascynol P (**20**) was obtained as colourless gum. Its molecular formula C₃₄H₄₂O₄ was deduced on the basis of the positive HRESIMS peak at *m/z* 537.2995 [M + Na]⁺ (calcd 537.2975). Distinct signals for a monosubstituted benzene moiety, three olefinic protons, and seven methyl singlets were discovered in the ¹H NMR spectrum. The ¹³C NMR data displayed characteristic resonances for three carbonyls and an epoxane. Compared 1D data for **20** with those of hypercohone D [7], they shared the bicyclo[3,3,1]nonane-2,4,9-trinone core fused a furan ring because of the prenyl side chain at C-8 and O-2 cyclization, except for the signals of its acyl group and the loss of one olefinic proton specific for prenyl group in **20**. The presence of a benzoyl group at C-1 in **20** was determined by the ¹H-¹H COSY correlations of H-12/16/H-13/15/H-14 and the HMBC cross-peaks of H-12/16 to C-1/C-10. The correlations from Me-22 to C-4/C-5/C-6/C-9 in the HMBC spectrum confirmed the decorated methyl at C-5. In the ROESY spectrum, cross-peaks of Me-22/H-6a, H-6b/Me-28, Me-28/H-23, and H-7/H-30 determined that H-7 and H-30 were α -oriented, while Me-28, Me-22, and benzoyl group at C-1 were β -orientated.

Ascynol Q (**21**) had the same molecular formula, C₃₃H₄₄O₅, as hyperascyrin H (**22**) [6] according to the HRESIMS (*m/z* 555.3082 [M + Na]⁺, calcd 555.3086) and ¹³C NMR data. The ¹H and ¹³C NMR data of **22** and those of **21**, while differences were observed for the chemical shifts of H-31, implying that **21** was a stereoisomer of **22** at C-31. The deduction was further identified by the NOE contacts of H-31/H-18, Me-23a/Me-28, Me-28/H-6b, and H-6a/Me-22.

In addition, hypermogin A (**6**) [1], yezo'otogirin C (**7**) [8], hypermongone A (**16**) [9], hypermongone F (**19**) [9], hyperascyrin H (**22**) [6], hyperelatone A (**23**) [10],

longistylione B (**24**) [11], longistylione A (**25**) [11], longistylione C (**26**) [11], and longistylione D (**27**) [11] were carefully identified by comparison of their spectroscopic data with literature values. Meanwhile, crystals of longistylione C (**26**) [11] was obtained. And the absolute configuration of **26** was the first time to be confirmed as $1R,5R,7R,8S,31R$ via single-crystal X-ray crystallography with a Flack parameter = 0.06(5) (CCDC 2359946).

- [1] Y. Zeng, J. Yang, Y. Li, W. Gu, L. Huang, P. Yi, C. Yuan, X. Hao, Hypermogins A–D, four highly modified polycyclic polyprenylated acylphloroglucinols from *Hypericum monogynum*. *Tetrahedron Lett.* 64 (2021) 152733.
- [2] Y.-L. Hu, K. Hu, L.-M. Kong, F. Xia, X.-W. Yang, G. Xu, Norascyrionones A and B, 2,3,4-nor-polycyclic polyprenylated acylphloroglucinols from *Hypericum ascyron*. *Org. Lett.* 21 (2019) 1007-1010.
- [3] J.-R. Weng, C.-N. Lin, L.-T Tsao, J.-P. Wang, Terpenoids with a new skeleton and novel triterpenoids with anti-inflammatory effects from *Garcinia subelliptica*. *Chem. Eur. J.* 9 (2003) 5520-5527.
- [4] X.-W. Yang, Y. Ding, J.-J. Zhang, X. Liu, L.-X. Yang, X.-N. Li, D. Ferreira, L.A. Walker, G. Xu, New acylphloroglucinol derivatives with diverse architectures from *Hypericum henryi*, *Org. Lett.* 16 (2014) 2434-2437.
- [5] L.-M. Kong, X.-W. Long, X.-W. Yang, F. Xia, A. Khan, H. Yan, J. Deng, X. Li, G. Xu, seco-polycyclic polyprenylated acylphloroglucinols with unusual carbon skeletons from *Hypericum ascyron*, *Tetrahedron Lett.* 58 (2017) 2113-2117.
- [6] J.-W. Hu, M.-J. Shi, J.-J. Wang, L. Li, J.-D. Jiang, T.-F. Ji, Methylated polycyclic polyprenylated acylphloroglucinol derivatives from *Hypericum ascyron*, *J. Nat. Prod.* 81 (2018) 2348-2356.
- [7] J.-J. Zhang, X.-W. Yang, J.-Z. Ma, X. Liu, L.-X. Yang, S.-C. Yang, G. Xu, Hypercohones D-G, new polycyclic polyprenylated acylphloroglucinols type natural products from *Hypericum cohaerens*, *Nat. Prod. Bioprospect.* 4 (2014) 73-79.
- [8] N. Tanaka, Y. Kakuguchi, H. Ishiyama, T. Kubota, J. Kobayashi. Yezo'otogirins A–C, new tricyclic terpenoids from *Hypericum yezoense*, *Tetrahedron Lett.* 50 (2009) 4747-4750.
- [9] W.-J. Xu, M.-D. Zhu, X.-B. Wang, M.-H. Yang, J. Luo, L.-Y. Kong, Hypermongones A–J, rare methylated polycyclic polyprenylated acylphloroglucinols from the flowers of *Hypericum monogynum*, *J. Nat. Prod.* 78 (2015) 1093-1100.
- [10] X.-T. Yan, Z. An, Y. Huangfu, Y.-T. Zhang, C.-H. Li, X. Chen, P.-L. Liu, J.-M. Gao, Polycyclic polyprenylated acylphloroglucinol and phenolic metabolites from the aerial parts of *Hypericum elatoides* and their neuroprotective and anti-neuroinflammatory activities, *Phytochemistry*, 159 (2016) 65-74.
- [11] X. Cao, X. Yang, P. Wang, Y. Liang, F. Liu, M. Tuerhong, D.-Q. Jin, J. Xu, D. Lee, Y. Ohizumi, Y. Guo, Polycyclic phloroglucinols as PTP1B inhibitors from *Hypericum longistylum*: Structures, PTP1B inhibitory activities, and interactions with PTP1B, *Bioorg. Chem.* 75 (2017) 139-148.

SI-4. Biological assays.

Materials and regents. The chemicals used in electrophysiology including NaCl, KCl, CsCl, CaCl₂, MgCl₂, HEPES, Glucose, TEA-Cl, NaOH, KOH, EGTA, CsCH₃SO₃, Na₂-ATP were purchased Sangon Biotech unless otherwise noted. Carrageenan were purchased from SlarbiO.

Cell culture and transfection. HEK 293T cells (American Type Culture Collection (ATCC)) were grown in DMEM (HyClone, SH30243.01), with 10% fetal bovine serum (Gibco, 2424346) and 1% penicillin (10,000 U/ml)/streptomycin (10 mg/ml) (VivaCell Biosciences, 2233204). HEK 293T cells were transiently transfected with human pCDNA3.1-Ca_v3.2 with pCDNA3.1-EGFP plasmids together using Lipofectamine 3000 (Invitrogen, CN2465613) and used within 48 h.

All the cell were cultured in the incubator with 5% CO₂ atmosphere at 37°C.

Patch-clamp electrophysiology. Double IPA (Sutter Instrument, USA), which is an integrated patch clamp amplifier with data acquisition system, was used for cell electrical signal amplification. Currents were low-pass filtered at 2 kHz and sampled at 10 kHz. SutterPatch2.1 software (Sutter Instrument) was used for data acquisition and analysis. All experiments were performed at room temperature (approximately 23°C). For patch-clamp recordings, pipettes were fabricated from borosilicate glass (Sutter Instrument, 2605321) using a micropipette puller (P-1000, Sutter Instrument), and were fire-polished to resistances of 4-6 MΩ for whole-cell recording.

For LVGCCs (hCa_v3.1-3.3) current measurements, the extracellular solution contained (in mM): 105 CsCl, 40 TEA-Cl, 10 Glucose, 10 HEPES, 2 CaCl₂ and 1 MgCl₂ (pH 7.4 adjusted with CsOH). The intracellular solution contained (in mM): 130 CsCH₃SO₃, 10 TEA-Cl, 10 HEPES, 5 MgCl₂, 5 EGTA, 5 Na₂-ATP (pH 7.4 adjusted with CsOH). Peak currents of LVGCCs were elicited by 300-ms (hCa_v3.1 and hCa_v3.2)/600-ms (hCa_v3.3) depolarizations to -40 mV at 3-s intervals from a holding potential (HP) of -100 mV. For studying state-dependent of hCa_v3.2, the HP was set to -100 mV and -75 mV, respectively. I-V curves of LVGCCs were evoked by 300-ms (hCa_v3.1 and hCa_v3.2)/600-ms (hCa_v3.3) depolarizations from -80 mV to +50 mV in 5-

mV increments with a 3-s interval from a HP of -100 mV.

Animals. All the procedures and care and handling of the animals were approved by the Animal Care and Use Committee at Kunming Institute of Botany, Chinese Academy of Sciences and the principles of laboratory animal care (NIH publication No. 86-23, revised 1985) were followed.

Experiments were performed on 18-22 g and aged 6-8 weeks Wilde type C57BL/6J mice (SKbex Biotechnology Co., Ltd.). Mice were housed in a temperature-and humidity-controlled environment and maintained in a 12 h light-dark cycle, and food and water were available *ad libitum*. All efforts were made to minimize both the suffering and number of animals used.

Acetic acid induced writhing test in mice. Before the measurement of acetic acid (AA)-induced writhing test, mice were acclimated to a plexiglas chamber for at least 1 hour to adapt to the experimental environment. AA was diluted with 0.9% (*v/v*) normal saline to 0.6% for modeling. Vehicle for compound **23** and Z944 is 20% (*v/v*) β -cyclodextrin and 0.4% DMSO in normal saline (same vehicle was used in following experiments). After 30 minutes of intraperitoneal injection of **23** (5, 15, 30 mg/kg) and Z944 (10 mg/kg) into mice, 0.6% (*v/v*) AA was i.p. injection at a volume of 10 ml/kg. During 20 minutes after i.p. administrating 0.6% (*v/v*) AA, the number of abdominal writhes was recorded for each group of mice. The definition of a writhing is a contraction of the abdominal muscles followed by body elongation and hind limb extension.

The above behavioral experiment was conducted in a double blind setting. Other behavioral tests in this study also followed this procedure.

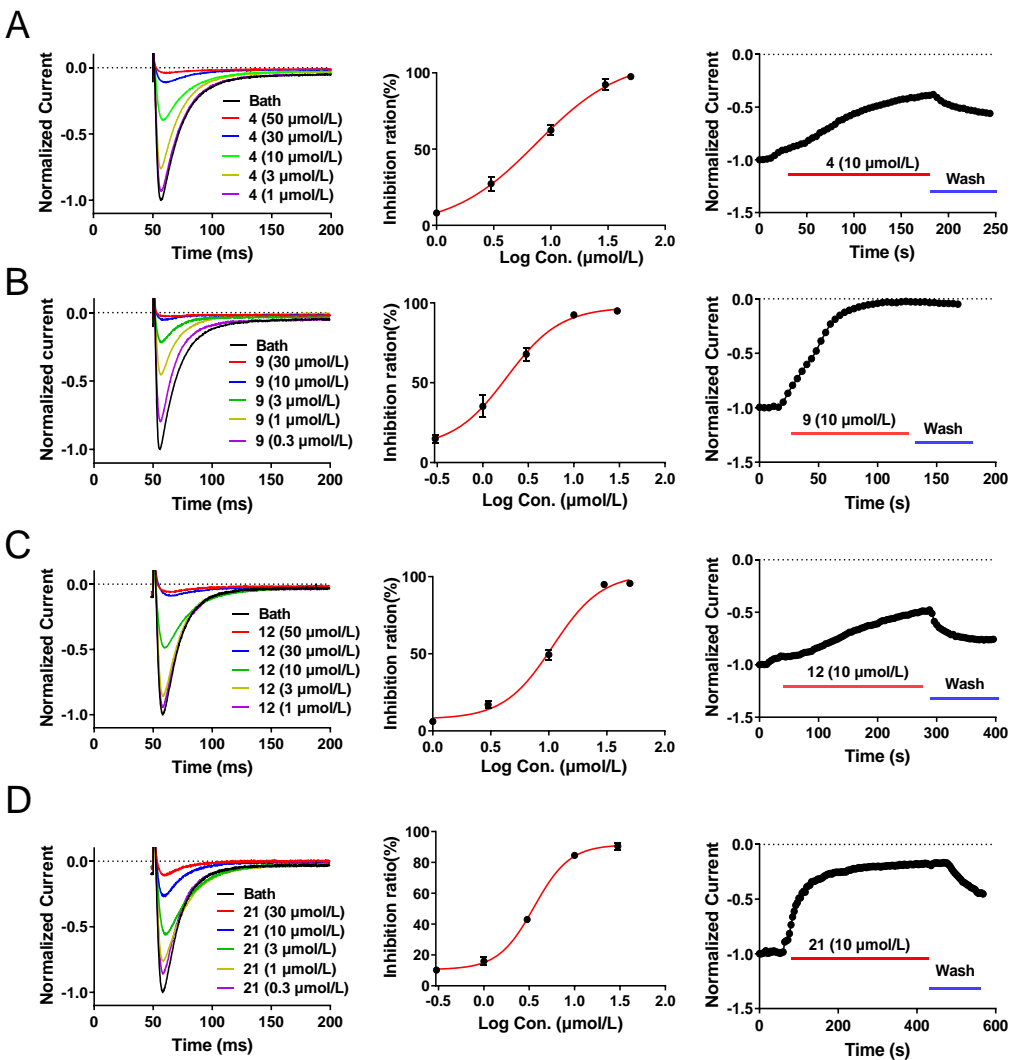


Fig. S2. Inhibitory effect of compounds **4** (A), **9** (B), **12** (C), **21** (D) on Ca_v3.1. The first column: representative Ca_v3.1 peak current traces were elicited by 200 ms depolarization to -40 mV at 4 s intervals from a holding potential (HP) of -100 mV in the absence (Bath) and presence of various concentrations of indicated compounds. The second column: Dose-response curve of peak current inhibition by indicated compounds. Solid curve represents fit to the Hill equation. Data are represented as mean \pm SEM ($n \geq 3$). The third column: time course of peak current inhibition by indicated compounds at 10 μ mol/L. Ordinate axis, peak current during exposure to testing compounds, which normalized by the peak current before drug exposure. The IC₅₀ of compounds **4**, **9**, **12**, **21** are 7.51, 1.84, 10.81, 3.57 μ mol/L, respectively.

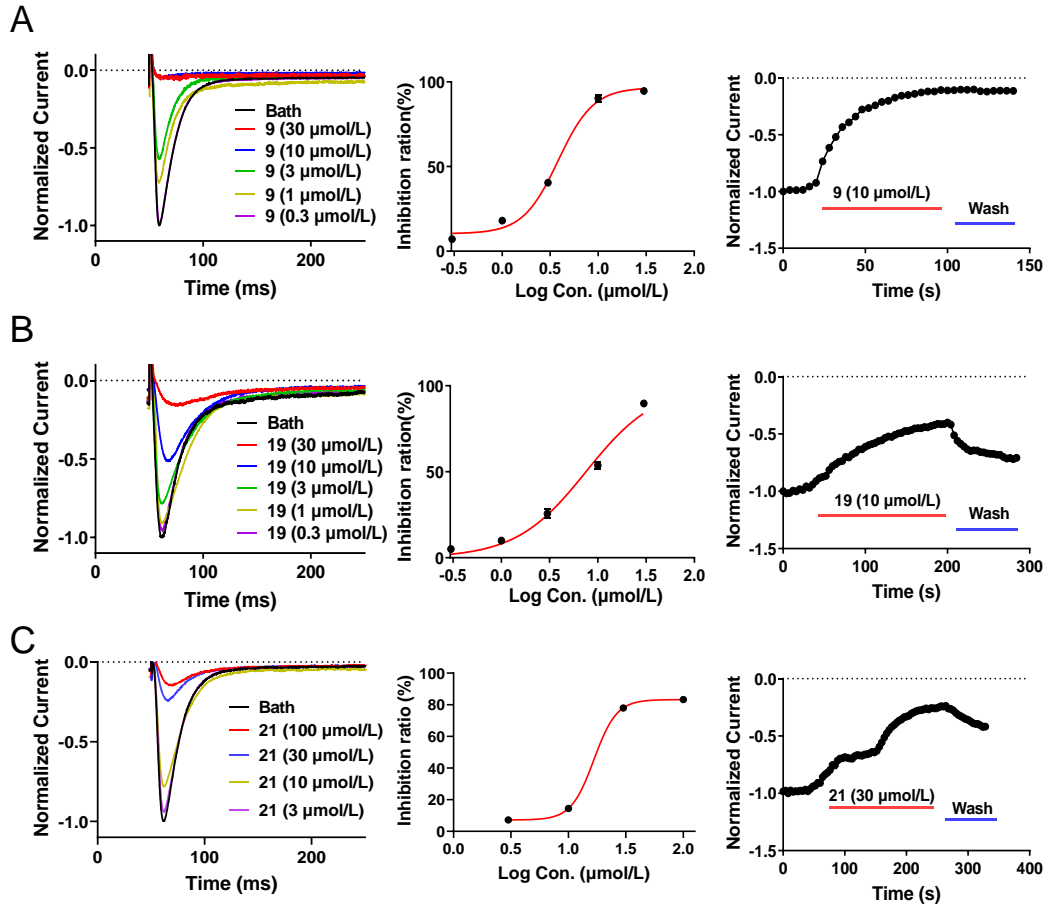


Fig. S3. Inhibitory effect of compounds **9** (A), **19** (B), **21** (C) on Ca_v3.2. The first column: representative Ca_v3.2 peak current traces were elicited by 300 ms depolarization to -40 mV at 4 s intervals from a holding potential (HP) of -100 mV in the absence (Bath) and presence of various concentrations of indicated compounds. The second column: Dose-response curve of peak current inhibition by indicated compounds. Solid curve represents fit to the Hill equation. Data are represented as mean \pm SEM ($n \geq 3$). The third column: time course of peak current inhibition by indicated compounds at 10 μ mol/L or 30 μ mol/L. Ordinate axis, peak current during exposure to testing compounds, which normalized by the peak current before drug exposure. The IC₅₀ of compounds **9**, **19**, **21** are 3.83, 7.53, 3.57 μ mol/L, respectively.

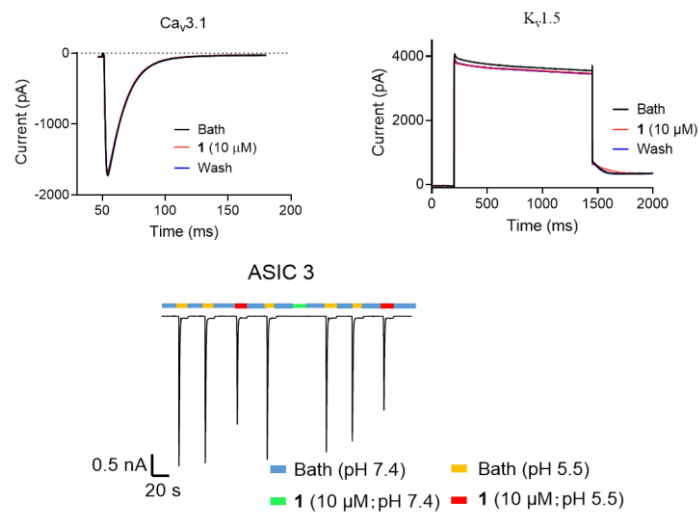


Figure S3-1. The activity of compound **1** was tested on Ca_V3.1, K_v1.5, and ASIC3 channels.

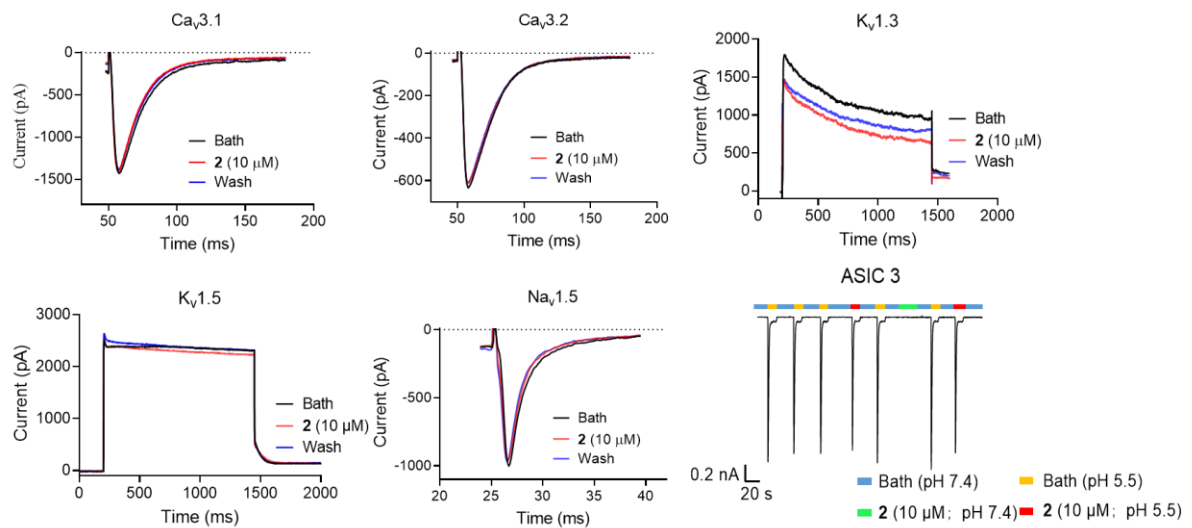


Figure S3-2. The activity of compound **2** on Ca_V3.1, Ca_V3.2, K_v1.3, K_v1.5, Na_v1.5, and ASIC3 channels.

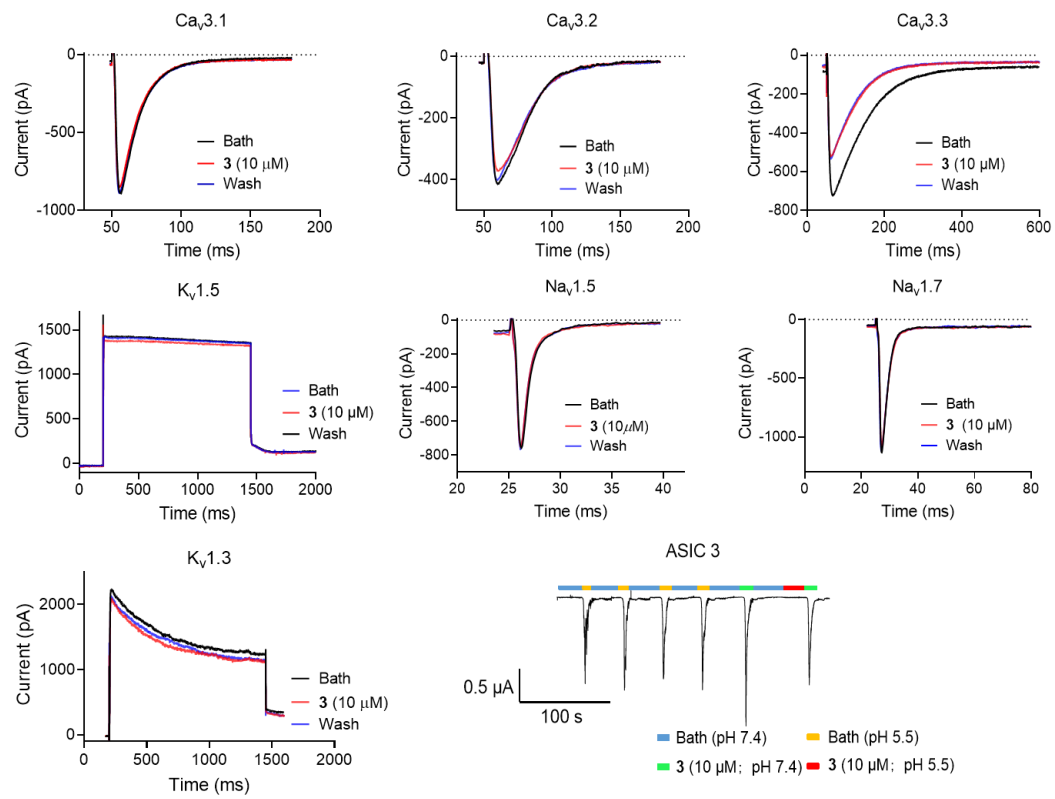


Figure S3-3. The activity of compound **3** was assessed on channels including Ca_v3.1, Ca_v3.2, Ca_v3.3, K_v1.3, K_v1.5, Na_v1.5, Na_v1.7, and ASIC3.

SI-5. The NMR spectroscopic data of new compounds.

Table S1 ^1H (600 MHz) and ^{13}C NMR (150 MHz) spectroscopic data of **1–3** (in CDCl_3).

	1		2		3	
no.	δ_{C}	δ_{H} (J in Hz)	δ_{C}	δ_{H} (J in Hz)	δ_{C}	δ_{H} (J in Hz)
1	70.1		54.5	3.72, d (9.0)	55.3	2.84, d (10.3)
5	208.4		208.7		209.2	
6	45.8	α : 2.38, dd (16.0, 3.3) β : 2.06, dd (16.0, 10.8)	46.0	2.01, m	45.9	β : 2.76, dd (17.8, 2.8) α : 2.33, dd (17.8, 7.5)
7	42.9	1.42, m	42.0	2.19, m	45.8	2.12, m
8	63.6		51.8		49.2	
9						
10	205.1		204.8		177.2	
11	134.4		139.3			
12	128.0	7.83, d (7.8)	128.7	7.82, d (7.7)		
13	126.7	7.27, t (7.8)	128.2	7.37, t (7.7)		
14	134.0	7.48, t (7.8)	132.5	7.45, t (7.7)		
15	125.2	7.30, d (7.8)	128.2	7.37, t (7.7)		
16	150.7		128.7	7.82, d (7.7)		
22	30.0	1.91, s	29.9	1.75, s	30.6	2.04, s
23	34.5	1.57, m	30.0	α : 2.04, m β : 1.71, m	30.1	β : 1.93, m α : 1.83, m
24	58.4	2.23, overlap	123.6	4.79, t (7.3)	123.5	4.86, t (6.6)
25	37.8		132.7		132.7	
26	34.9	1.32, s	25.7	1.54, s	25.7	1.57, s
27	27.3	1.35, s	17.7	1.45, s	17.8	1.54, s
28	21.3	1.01, s	18.8	0.74, s	18.0	0.92, s
29	33.9	β : 1.66, m α : 1.26, dd (12.2, 7.6)	38.5	β : 1.73, overlap α : 1.49, m	42.3	α : 1.62, m β : 1.47, m
30	27.8	α : 2.26, overlap β : 1.97, m	25.2	α : 1.82, m β : 1.58, m	27.1	β : 1.67, m α : 1.58, overlap
31	64.4	2.42, br t (8.8)	55.3	2.82, q (9.0)	51.5	2.58, m
32	71.9		72.5		83.0	
33	31.2	1.13, s	30.3	1.09, s	30.5	1.28, s
34	30.3	1.08, s	26.3	1.16, s	23.5	1.30, s
OH-32		5.18, s				

Table S2 ^1H (600 MHz) and ^{13}C NMR (150 MHz) spectroscopic data of **4**, **5**, and **8** (in CDCl_3).

no.	4		5		8	
	δ_{H} (J in Hz)	δ_{C} , type	δ_{H} (J in Hz)	δ_{C} , type	δ_{H} (J in Hz)	δ_{C} , type
1		88.6, C		72.7, C	4.36, s	63.9, CH
5	3.09, m	39.7, CH		107.4, C	2.55, m	45.3, CH
6	2.04, m	39.4, CH_2	1.82, m	32.3, CH_2	2.13, m	37.3, CH_2
	1.15, q (13.2)				1.25, q (12.6)	
7	1.83, m	41.7, CH	1.20, m	47.1, CH	1.87, br t (12.6)	43.0, CH
8		60.2, C		48.2, C		47.5, C
9		216.5, C		149.4, C		210.0, C
10		166.2, C		212.9, C		197.1, C
11		131.6, C	2.57, dd (6.0, 18.0)	48.8, CH_2		138.4, C
			2.20, dd (6.0, 18.0)			
12	7.88, d (7.2)	129.4, CH	2.04, m	24.0, CH	7.68, d (7.8)	127.5, CH
13	7.39, t (7.2)	128.2, CH	0.87, d (6.9)	22.9, CH_3	7.34, t (7.8)	128.6, CH
14	7.50, t (7.2)	132.6, CH	0.86, d (6.9)	22.7, CH_3	7.44, t (7.8)	132.7, CH
15	7.39, t (7.2)	128.2, CH			7.34, t (7.8)	128.6, CH
16	7.88, d (7.2)	129.4, CH			7.68, d (7.8)	127.5, CH
22	0.88, d (6.0)	14.3, CH_3	1.68, s	16.2, CH_3	0.98, d (6.6)	14.4, CH_3
23	2.07, m	29.5, CH_2	1.91, m	29.6, CH_2	2.20, m	27.1, CH_2
	1.60, m		1.79, m		1.72, m	122.9, CH
24	5.11, t, (6.6)	123.5, CH	5.09, t (7.2)	124.2, CH	5.09, t (7.2)	133.1, C
25		132.9, C		132.4, C		25.9, CH_3
26	1.70, s	25.9, CH_3	1.70, s	25.9, CH_3	1.69, s	18.0, CH_3
27	1.57, s	17.8, CH_3	1.58, s	17.9, CH_3	1.58, s	16.9, CH_3
28	0.70, s	12.7, CH_3	0.76 s	19.2, CH_3	1.13, s	39.1, CH_2
29	1.89, m	34.6, CH_2	1.73, m	41.7, CH_2	2.28, dd (14.6, 5.6)	34.6, CH_2
	1.64, m		1.36, m		2.22, overlap	
30	1.98, m	24.5, CH_2	1.52, m	25.5, CH_2	5.56, m	121.0, CH
31	3.85, t (9.6)	53.2, CH	3.07, dd (7.2, 11.4)	56.0, CH	5.22, d (15.4)	142.6, CH
32		86.3, C		83.2, C		70.5, C
33	1.58, s	26.5, CH_3	1.12, s	29.7, CH_3	1.01, s	29.8, CH_3
34	1.54 s	25.0, CH_3	1.16, s	25.2, CH_3	0.89, s	29.4, CH_3
OH-1	4.05, s					

Table S3 ^1H (600 MHz) and ^{13}C NMR (150 MHz) spectroscopic data of **9** (in CDCl_3).

no	9			
	δ_{H} (<i>J</i> in Hz)	δ_{C} , type	δ_{H} (<i>J</i> in Hz)	δ_{C} , type
1		78.8, C	20	1.36, s
2		208.5, C	21	1.35, s
4		82.0, C	22	1.06, s
5		56.7, C	23	2.09, m
6	1.91, m	41.5, CH_2		1.60, m
	1.49, m		24	4.92, t (7.2)
7	1.51, m	43.3, CH	25	
8		55.7, C	26	1.64, s
9		208.9, C	27	1.50, s
10		201.4, C	28	1.11, s
11	2.29, m	51.1, CH_2	29	1.76, m
	2.11, m			1.58, m
12	2.12, m	23.4, CH	30	2.02, m
13	0.83, overlap	22.5, CH_3	31	5.01, t (7.2)
14	0.82, overlap	22.2, CH_3	32	
17	5.82, d (15.6)	118.6, CH	33	1.54, s
18	6.32, d (15.6)	144.6, CH	34	1.64, s
19		70.9, C		

Table S4 ^1H (600 MHz) spectroscopic data of **10–13** (in CDCl_3).

no	10	11	12	13
1		4.97, s	4.08, s	4.05, s
2				
3				
4				
5		3.44, m	3.46, m	3.46, m
6	3.27, dd (7.2, 15.6)	H _a , 1.73, m	H _a , 1.60, m	H _a , 1.59, m
	1.48, d (15.6)	H _b , 1.32, dd (17.3, 4.2)	H _b , 1.18, m	H _b , 1.18, m
7	0.99, m	1.37, m	1.22, m	1.22, m
8				
9				
10				
11			2.89, m	2.67, m
12		7.93, d (7.4)	0.98, d (6.6)	1.00, d (6.6)
13	7.32, overlap	7.43, t (7.4)	1.01, d (6.6)	H _a , 1.49, m H _b , 1.21, overlap
14	7.49, t (7.2)	7.52, t (7.4)		0.87, s
15	7.35, overlap	7.43, d (7.4)		
16	8.02, d (7.2)	7.93, d (7.4)		
17	2.64, dd (7.8, 15.0)	H _a , 2.46, dd (15.3, 7.6)	H _a , 2.71, dd (7.2, 15.6)	H _a , 2.72, dd (6.6, 15.6)
	2.21, dd (5.4, 15.0)	H _b , 2.09, dd (15.3, 7.6)	H _b , 2.40, dd (7.2, 15.6)	H _b , 2.18, dd (6.6, 15.6)
18	3.96, t (7.2)	4.39, t (6.0)	4.75, t (6.6)	4.78, t (6.6)
19				
20	1.34, s	1.43, s	1.56, s	1.56, s
21	1.28, s	1.21, s	1.62, s	1.63, s
22	1.14, s	0.93, d (6.9)	0.85, d (6.6)	0.86, s
23	1.82, m	H _a , 1.98, overlap H _b , 1.71, m	H _a , 1.97, m H _b , 1.71, m	H _a , 1.98, overlap H _b , 1.71, m
24	4.84, t (7.2)	4.91, t (6.0)	4.88, m	4.89, m
25				
26	1.71, s	1.65, s	1.66, s	1.66, s
27	1.55, s	1.53, s	1.56, s	1.54, s
28	1.30, s	1.24, s	1.15, s	1.14, s
29	1.80, m	H _a , 2.13, m H _b , 2.01, m	H _a , 2.18, m H _b , 1.92, dd (5.4, 15.6)	H _a , 2.17, m H _b , 1.98, m
30	2.33, m 1.76, m	5.38, m	5.58, m	5.57, m
31	2.82, t (10.5)	5.23, d (15.5)	5.62, m	5.62, m
32				
33	1.24, s	1.10, s	1.33, s	1.33, s
34	1.19, s	1.12, s	1.35, s	1.34, s
OH-3			4.27, s	4.28, s

Table S5 ^{13}C NMR (150 MHz) spectroscopic data of **10–13** (in CDCl_3).

no	10	11	12	13
1	71.8, C	57.1, CH	64.2, CH	64.2, CH
2	202.4, C	200.8, C	203.0, C	203.2, C
3	100.2, C	88.1, C	88.0, C	88.0, C
4	203.1, C	212.5, C	210.8, C	210.9, C
5	49.5, C	41.2, CH	40.7, CH	40.6, CH
6	39.7, CH_2	31.4, CH_2	30.9, CH_2	30.9, CH_2
7	45.7, CH	39.9, CH	38.9, CH	38.9, CH
8	55.3, C	50.2, C	49.0, C	49.0, C
9	174.3, C			
10	195.6, C	192.4, C	208.2, C	207.6, C
11	135.5, C	137.5, C	41.2, CH	47.6, CH
12	151.3, C	128.9, CH	19.7, CH_3	15.5, CH_3
13	126.1 CH	129.0, CH	19.2, CH_3	26.1, CH_2
14	133.0, CH	133.9, CH		11.3, CH_3
15	126.5, CH	129.0, CH		
16	130.0, CH	128.9, CH		
17	32.8, CH_2	33.4, CH_2	33.2, CH_2	33.3, CH_2
18	114.2, CH	115.2, CH	115.5, CH	115.6, CH
19	137.7, C	137.0, C	137.1, C	136.9, C
20	17.8, CH_3	25.8, CH_3	18.2, CH_3	18.2, CH_3
21	25.9, CH_3	17.8, CH_3	25.9, CH_3	25.9, CH_3
22	17.6, CH_3	13.3, CH_3	13.6, CH_3	13.6, CH_3
23	31.8, CH_2	29.8, CH_3	29.8, CH_2	29.8, CH_2
24	122.6, CH	123.1, CH	123.2, CH	123.2, CH
25	134.6, C	133.1, C	132.9, C	132.9, C
26	25.8, CH_3	25.9, CH_3	26.0, CH_3	25.9, CH_3
27	18.1, CH_3	18.0, CH_3	18.0, CH_3	18.0, CH_3
28	20.4, CH_3	16.4, CH_3	16.2, CH_3	16.3, CH_3
29	39.7, CH_2	40.8, CH_3	41.0, CH_2	40.8, CH_2
30	21.0, CH_2	120.9, CH	120.2, CH	120.4, CH
31	54.6, CH	142.4, CH	142.8, CH	142.7, CH
32	38.1, C	70.5, C	70.7, C	70.7, C
33	34.4, CH_3	29.7, CH_3	29.8, CH_3	29.8, CH_3
34	23.5, CH_3	29.4, CH_3	29.9, CH_3	29.9, CH_3

Table S6 ^1H (600 MHz) spectroscopic data of **14**, **15**, **17**, and **18** (in CDCl_3).

no.	14	15	17	18
6	1.91, m 1.26, m	1.88, dd (13.7, 4.4) 1.22, br t (13.7)	1.93, dd (4.2, 13.8) 1.39, br t (13.2)	1.90, m 1.41, m
7	1.69, m	1.56, m	1.63, m	1.57, m
11	1.37, dd (6.0, 18.0) 2.50, m	2.26, dd (17.0, 6.1) 2.05, m	2.01, dd (3.0, 6.6)	2.05, dd (3.0, 6.6)
12	2.20, m	2.21, m	2.18, m	2.18, m
13	0.91, d (6.0)	0.82, d (6.6)	0.85, d (6.6)	0.88, d (6.6)
14	0.90, d (6.0)	0.88, d (6.6)	0.89, d (6.6)	0.86, d (6.6)
17	2.99, m 2.93, m	2.99, dd (15.0, 9.5) 2.85, dd (15.0, 9.5)	3.00, dd (10.8, 15.0) 2.87, dd (7.8, 15.0)	2.97, dd (10.2, 15.0) 2.83, dd (7.8, 15.0)
18	4.74, t (9.6)	4.62, t (9.9)	4.75, dd (7.8, 10.8)	4.75, dd (7.8, 10.4)
20	1.33, s	1.26, s	1.28, s	1.24, s
21	1.26, s	1.17, s	1.19, s	1.18, s
22	1.19, s	1.16, s	1.30, s	1.29, s
23	2.05, m 1.69, m	2.02, m 1.63, m	2.10, m 1.76, m	2.10, m 1.72, m
24	4.92, t (6.0)	4.86, t (6.3)	4.93, t (7.2)	4.89, t (7.2)
26	1.68, s	1.61, s	1.68, s	1.63, s
27	1.58, s	1.47, s	1.55, s	1.53, s
28	1.09, s	1.03, s	1.01, s	1.01, s
29	1.70, m 1.61, m	2.17, m 1.61, m	1.86, m 1.45, m	1.88, overlap 1.37, m
30	2.01, m 1.92, overlap	2.01, m 1.94, m	2.08, m 1.87, overlap	2.08, m 1.87, overlap
31	4.97, t (6.0)	4.94, t (6.3)	5.01, t (7.2)	5.02, t (7.2)
33	1.55, s	1.59, s	1.57, s	1.57, s
34	1.63, s	1.54, s	1.63, s	1.61, s

Table S7 ^{13}C NMR (150 MHz) spectroscopic data of **14**, **15**, **17**, and **18** (in CDCl_3).

No.	14	15	17	18
1	72.2, C	73.3, C	82.2, C	82.1, C
2	171.5, C	171.8, C	188.2, C	188.2, C
3	119.9, C	119.9, C	117.7, C	117.5, C
4	190.7, C	191.0, C	177.0, C	176.8, C
5	60.0, C	59.8, C	50.5, C	50.5, C
6	41.3, CH_2	41.5, CH_2	39.5, CH_2	39.2, CH_2
7	42.0, CH	44.3, CH	42.8, CH	43.3, CH
8	46.9, C	46.6, C	47.6, C	47.7, C
9	207.0, C	206.6, C	206.7, C	206.6, C
10	202.5, C	202.5, C	203.6, C	203.7, CH
11	51.0, CH_2	50.6, CH_2	51.1, CH_2	51.1, CH_2
12	23.8, CH	24.1, CH	24.1, CH	24.0, CH
13	22.9, CH_3	22.6, CH_3	22.6, CH_3	22.7, CH_3
14	22.4, CH_3	22.5, CH_3	22.5, CH_3	22.5, CH_3
17	26.9, CH_2	26.8, CH_2	27.4, CH_2	27.6, CH_2
18	93.0, CH	93.5, CH	93.1, CH	92.5, CH
19	71.6, C	71.3, C	72.0, C	72.1, C
20	26.5, CH_3	26.4, CH_3	25.4, CH_3	24.8, CH_3
21	25.5, CH_3	24.8, CH_3	23.8, CH_3	23.4, CH_3
22	16.0, CH_3	15.9, CH_3	15.3, CH_3	15.3, CH_3
23	27.9, CH_2	27.8, CH_2	27.2, CH_2	26.9, CH_2
24	122.2, CH	122.2, CH	122.3, CH	122.4, CH
25	133.5, C	133.5, C	133.5, C	133.6, C
26	25.9, CH_3	25.8, CH_3	25.9, CH_3	25.8, CH_3
27	18.0, CH_3	17.9, CH_3	18.0, CH_3	17.8, CH_3
28	14.5, CH_3	12.6, CH_3	13.7, CH_3	13.5, CH_3
29	37.7, CH_2	25.3, CH_2	36.4, CH_2	36.5, CH_2
30	24.3, CH_2	39.0, CH_2	24.9, CH_2	24.9, CH_2
31	124.3, CH	124.2, CH	124.5, CH	124.5, CH
32	131.6, C	132.2, C	131.2, C	131.2, C
33	17.7, CH_3	17.8, CH_3	17.7, CH_3	17.7, CH_3
34	25.7, CH_3	25.6, CH_3	25.7, CH_3	25.7, CH_3

Table S8 ^1H (600 MHz) and ^{13}C NMR (150 MHz) spectroscopic data of **20** and **21** (in CDCl_3).

no	20		21	
	δ_{H} (<i>J</i> in Hz)	δ_{C} , type	δ_{H} (<i>J</i> in Hz)	δ_{C} , type
1		69.9, C		73.8, C
2		169.4, C		166.7, C
3		128.7, C		131.1, C
4		196.4, C		197.6, C
5		62.8, C		62.3, C
6	2.03, dd (13.6, 5.0) 1.45, brt (13.2)	43.0, CH ₂	2.01, dd (12.9, 4.8) 1.41, brt (12.9)	43.3, CH ₂
7	2.32, m	38.1, CH	2.11, m	36.7, CH
8		49.4, C		46.3, C
9		207.5, C		208.3, C
10		195.0, C		194.3, C
11		137.2, C		137.6, C
12	7.52, d (7.2)	128.5, CH	7.51, d (7.8)	128.2, CH
13	7.23, t (7.2)	128.0, CH	7.22, t (7.8)	128.1, CH
14	7.39, t (7.2)	132.2, CH	7.38, t (7.8)	132.2, CH
15	7.23, t (7.2)	128.0, CH	7.22, t (7.8)	128.1, CH
16	7.52, d (7.2)	128.5, CH	7.51, d (7.8)	128.2, CH
17	3.07, d (7.2)	22.4, CH ₂	3.03, m	22.9, CH ₂
18	4.97, m	120.2, CH	4.92, t (6.9)	119.5, CH
19		133.3, C		138.7, C
20	1.57, s	17.7, CH ₃	1.61, s	25.7, CH ₃
21	1.62, s	25.7, CH ₃	1.55, s	18.1, CH ₃
22	1.30, s	15.8, CH ₃	1.25, s	15.9, CH ₃
23	2.01, m	28.2, CH ₂	1.89, m	26.9, CH ₂
	1.64, overlap		1.59, m	
24	4.98, m	121.9, CH	4.89, t (6.8)	121.8, CH
25		133.8, C		133.8, C
26	1.66, s	25.7, CH ₃	1.63, s	25.8, CH ₃
27	1.55, s	17.8, CH ₃	1.50, s	18.0, CH ₃
28	1.26, s	15.2, CH ₃	1.20, s	15.8, CH ₃
29	2.44, dd (12.0, 15.0) 1.69, overlap	36.3, CH ₂	2.74, m 1.66, overlap	31.4, CH ₂
30	4.91, m	79.6, CH	1.79, m	22.7, CH ₂
31	5.19, d (8.4)	123.8, CH	4.02, t (4.8)	87.2, CH
32		138.2, C		73.5, C
33	1.63, s	18.2, CH ₃	0.99, s	25.9, CH ₃
34	1.70, s	25.8, CH ₃	1.01, s	25.2, CH ₃

SI-6. The original NMR and MS spectra of new compounds.

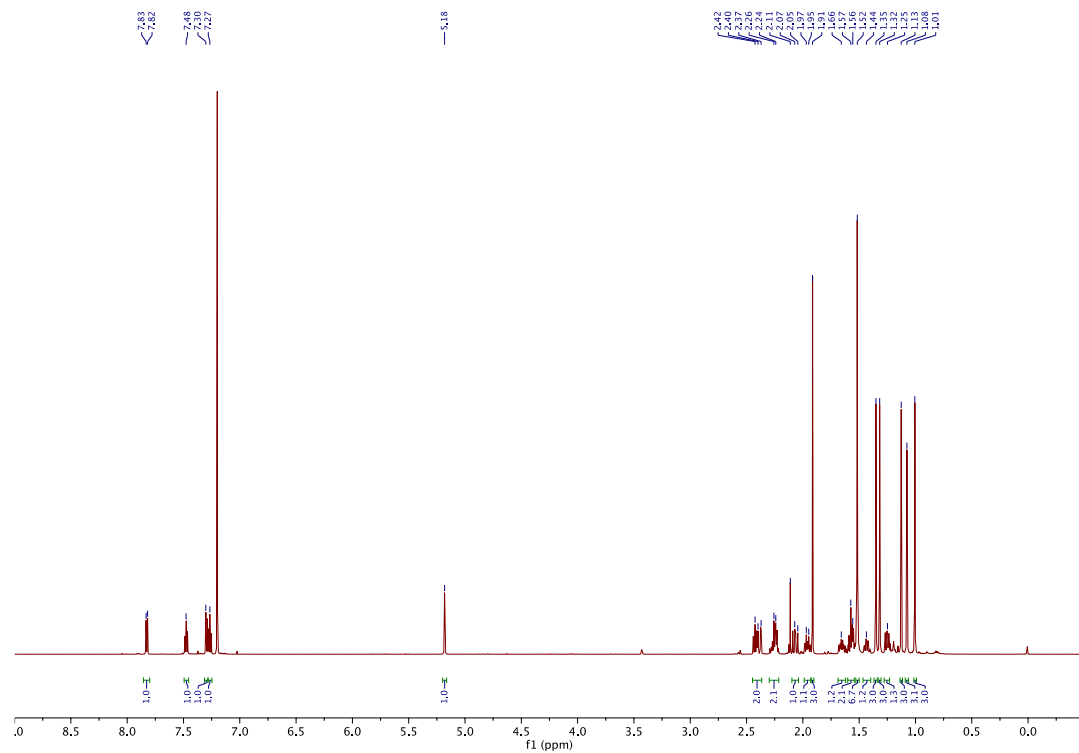


Figure S1. ¹H (in CDCl_3) spectrum of ascynol A (1).

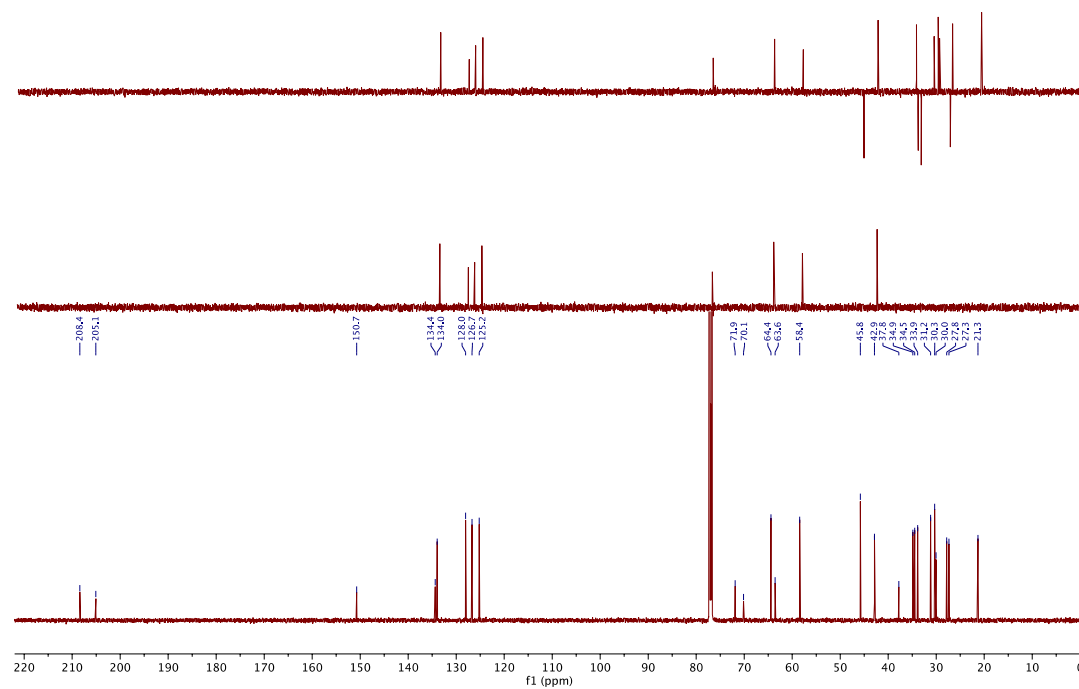


Figure S2. ¹³C and DEPT (in CDCl_3) spectrum of ascynol A (1).

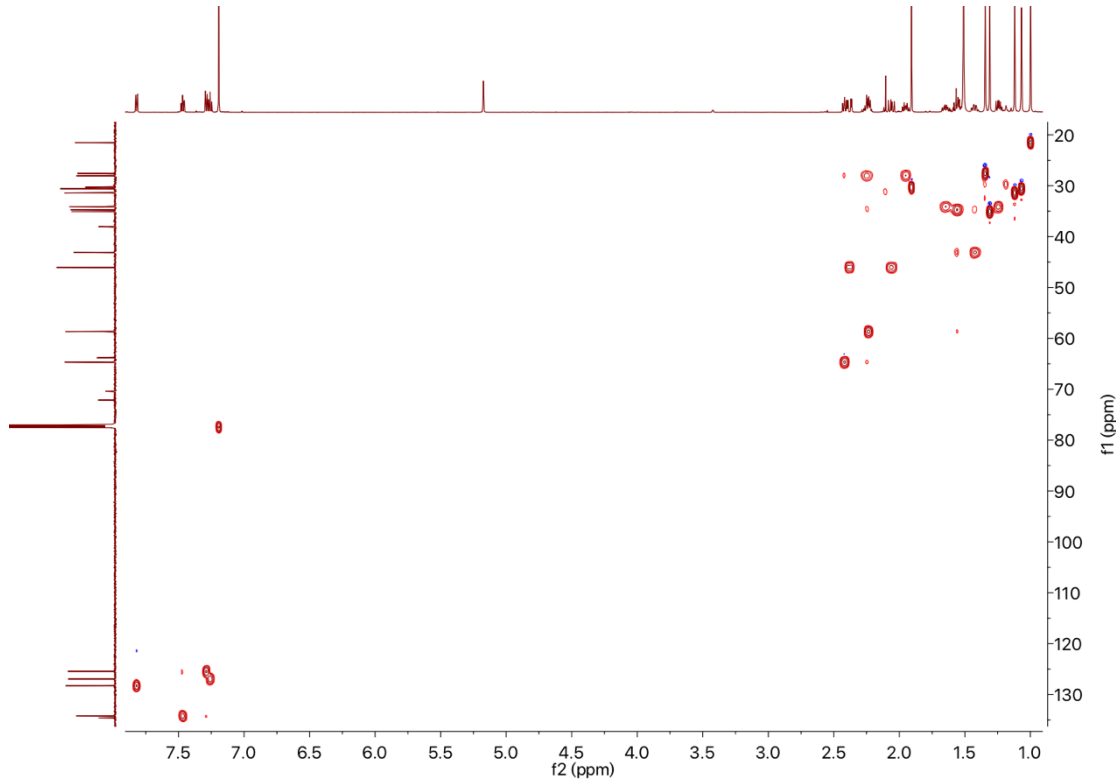


Figure S3. HSQC spectrum of ascynol A (**1**).

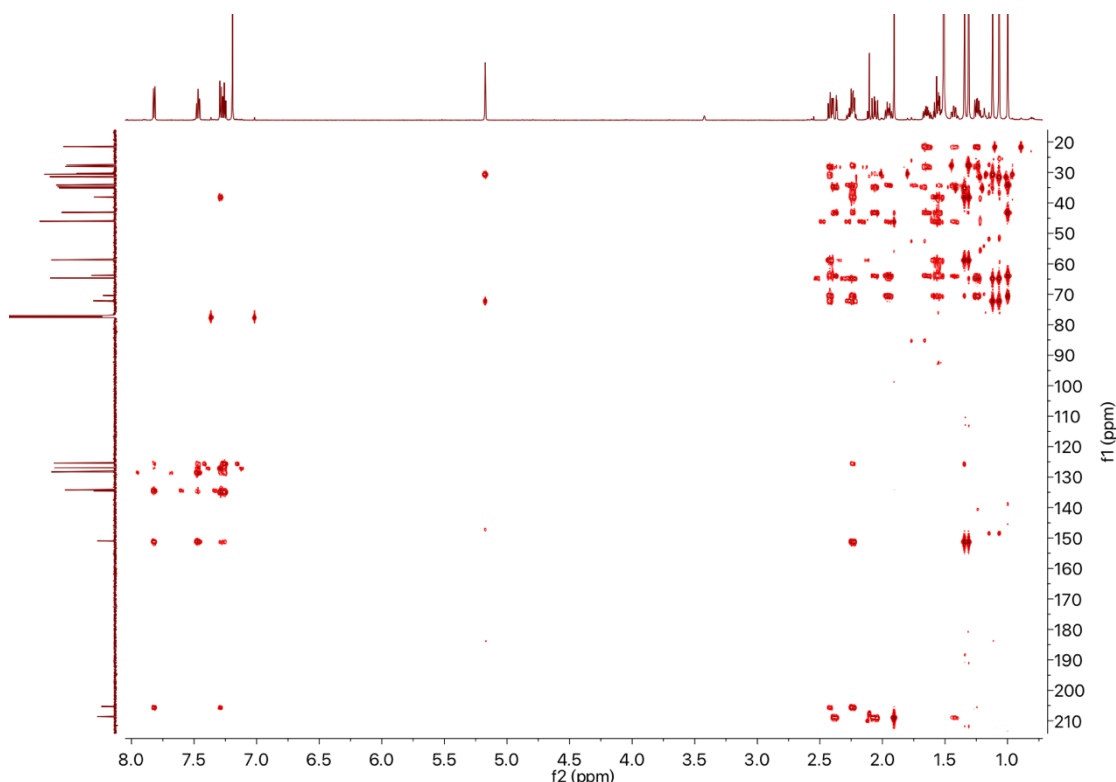


Figure S4. HMBC spectrum of ascynol A (**1**).

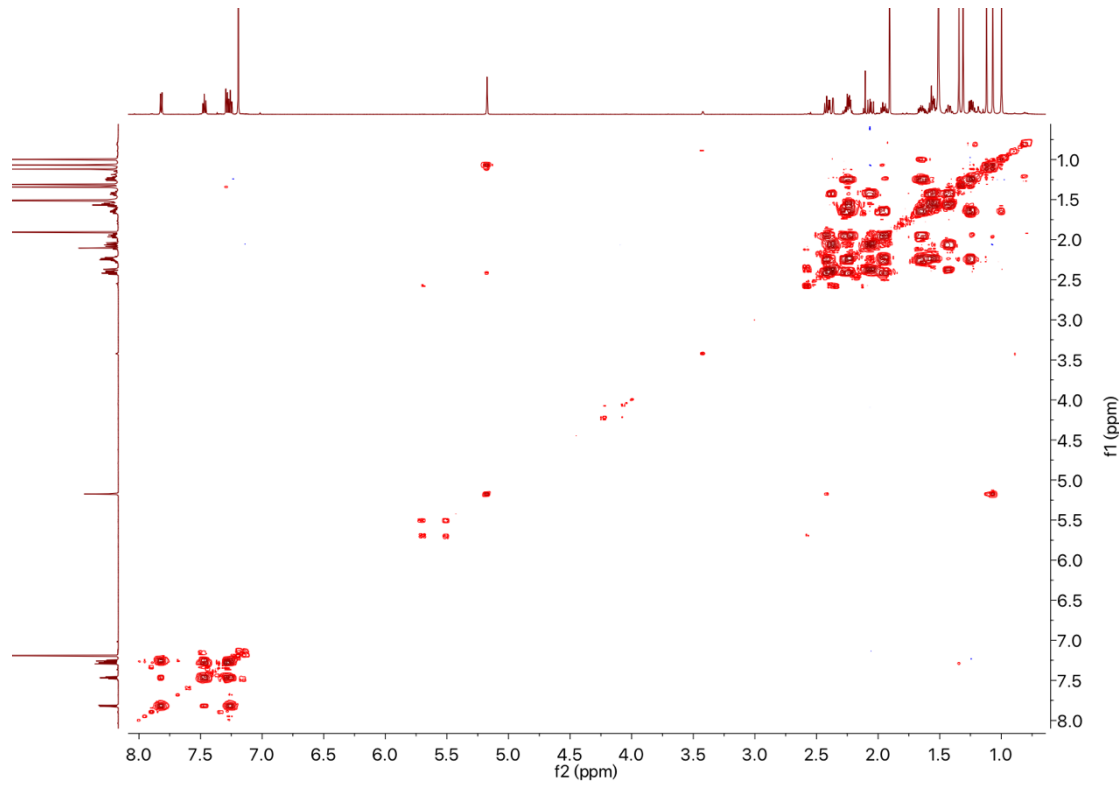


Figure S5. ^1H - ^1H COSY spectrum of ascynol A (**1**).

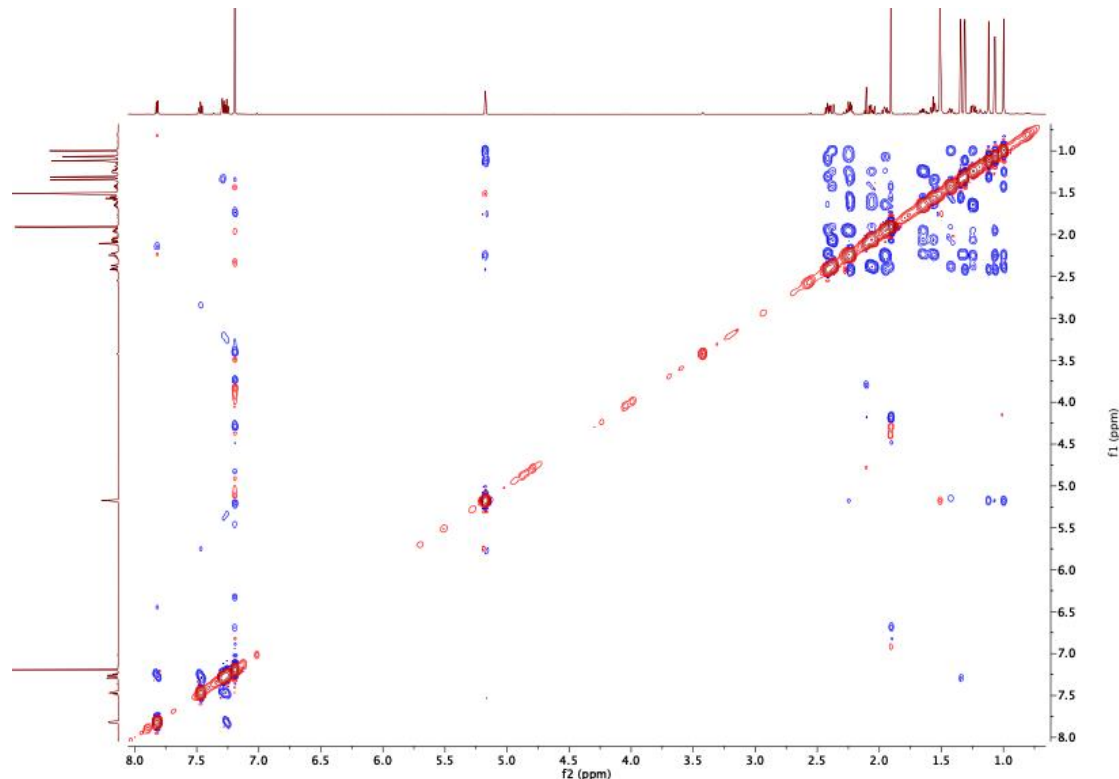


Figure S6. ROESY spectrum of ascynol A (**1**).

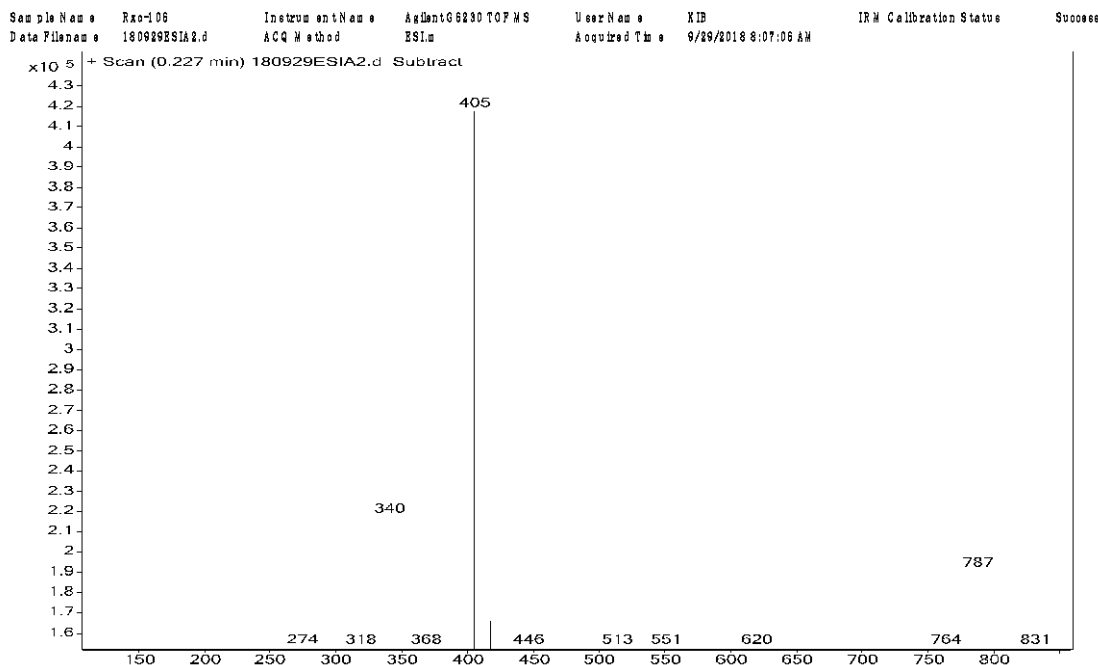
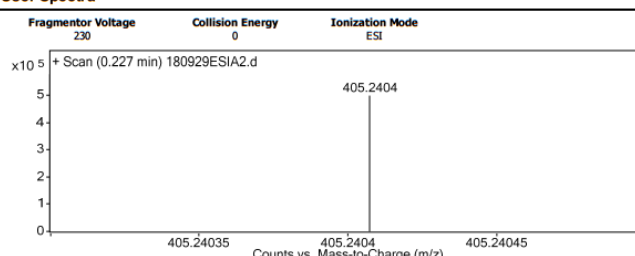


Figure S7. ESIMS spectrum of ascynol A (**1**).

Qualitative Analysis Report

Data File Name	180929ESIA2.d	Sample Name	Rxo-106
Sample Type	Sample	Position	
Instrument Name	Agilent G6230 TOF MS	User Name	KIB
Acq Method	ESI.m	Acquired Time	9/29/2018 8:07:06 AM
IRM Calibration Status	Success	DA Method	ESI.m
Comment			
Sample Group		Info.	
Acquisition SW	6200 series TOF/6500 series		
Version	Q-TOF B.05.01 (B5125.2)		

User Spectra



Peak List

m/z	z	Abund	Formula	Ion
274.2739	1	165193.3		
340.2822	1	247044.78		
368.3134	1	137664.69		
384.3083	1	136040.77		
405.2404	1	498246.03	C25 H34 Na O3	M+
417.24	1	202750.58		
437.1942	1	142429.13		
446.2666	1	157387.67		
787.4904	1	231141.08		
922.0098	1	152511.94		

Formula Calculator Element Limits

Element	Min	Max
C	0	200
H	0	400
O	0	10
Na	1	1

Formula Calculator Results

Formula	Calculated Mass	Mz	Dif.(mDa)	Dif. (ppm)	DBE
C25 H34 Na O3	405.2406	405.2404	0.2	0.4	8.5

--- End Of Report ---

Figure S8. HRESIMS spectrum of ascynol A (**1**).

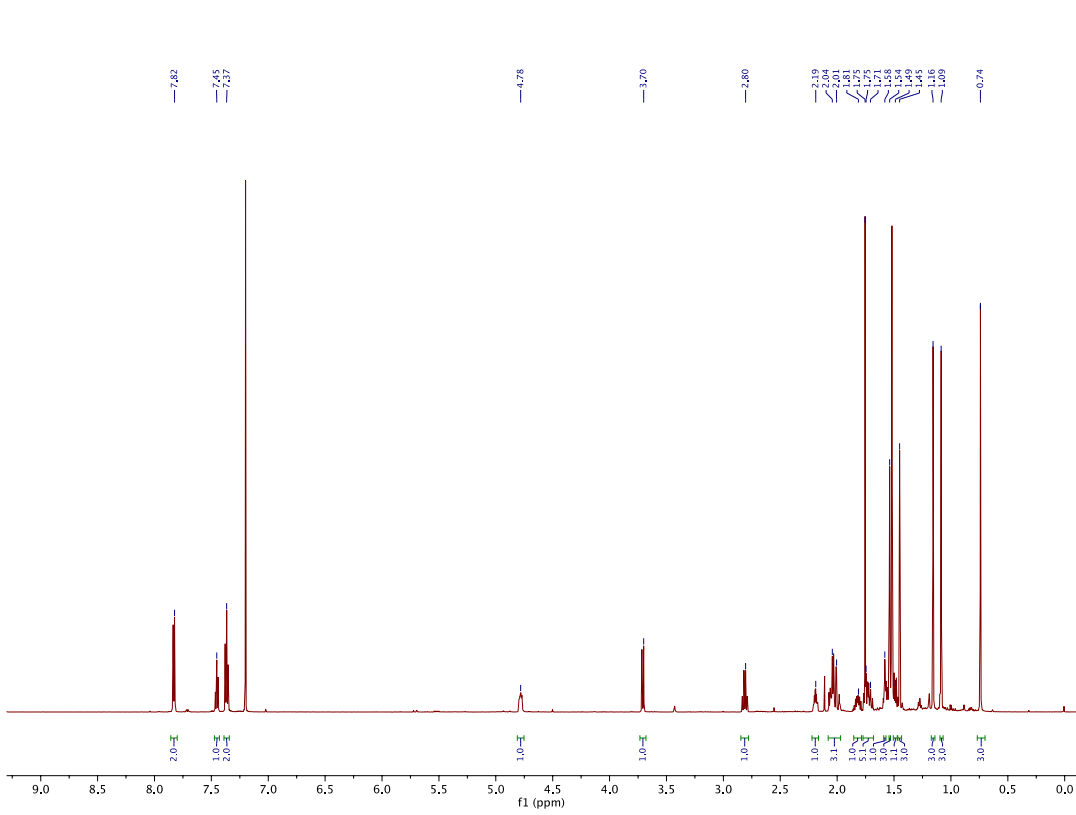


Figure S9. ^1H (in CDCl_3) spectrum of ascynol B (2).

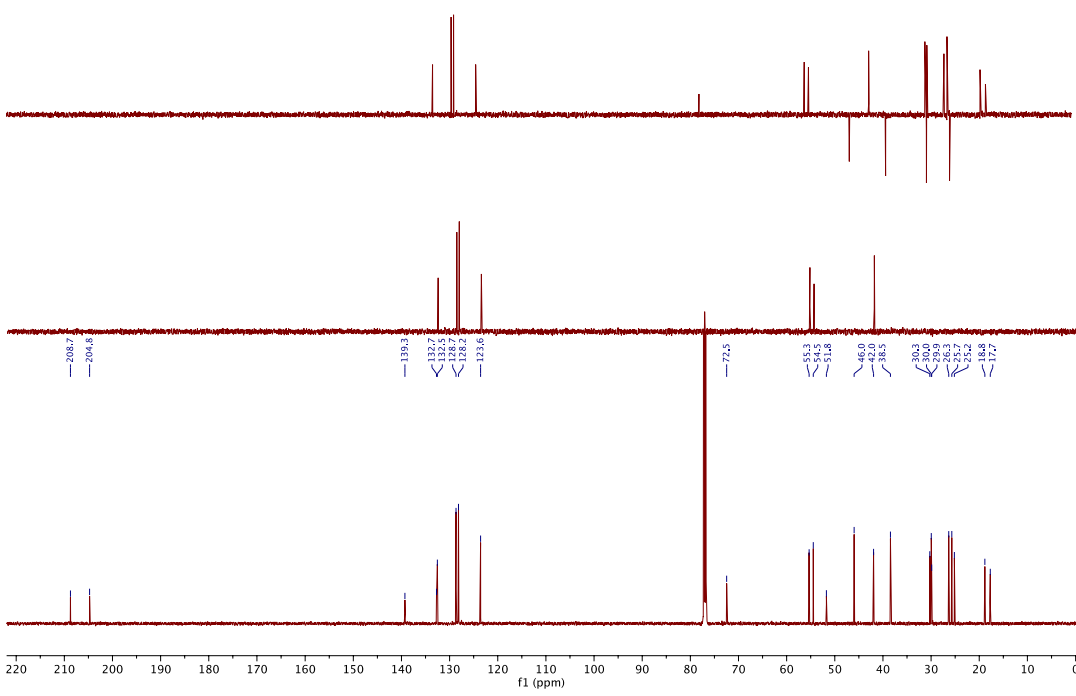


Figure S10. ^{13}C and DEPT (in CDCl_3) spectrum of ascynol B (2).

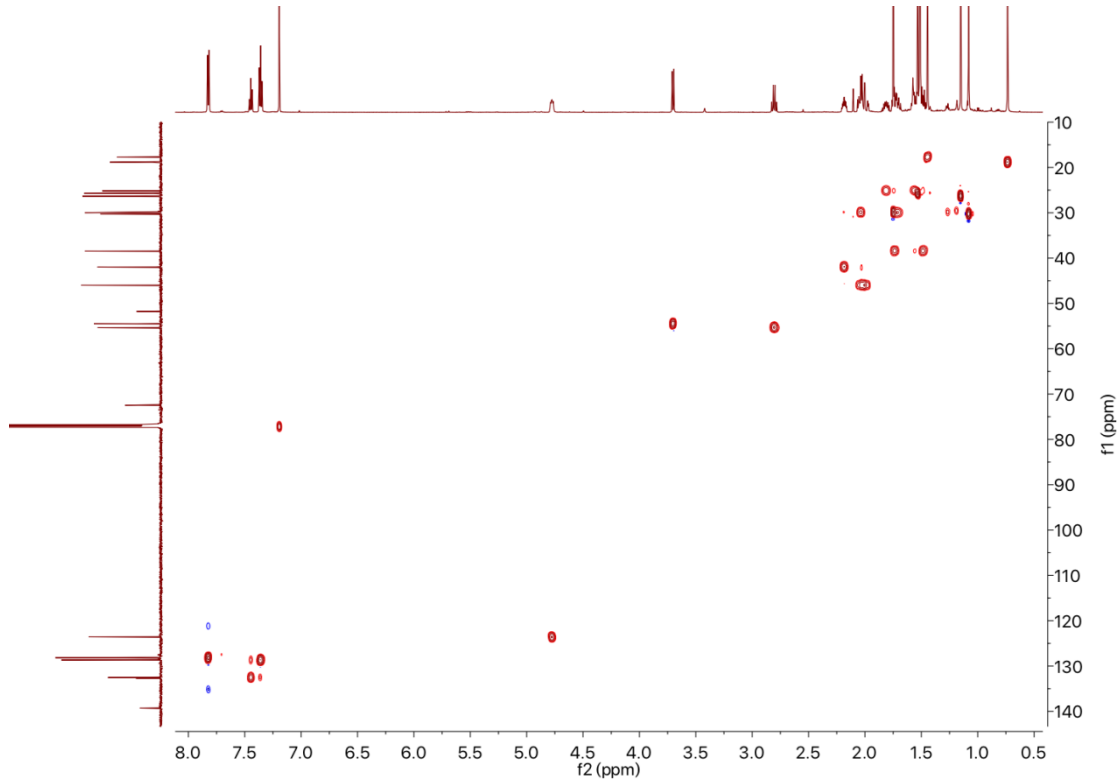


Figure S11. HSQC spectrum of ascynol B (2).

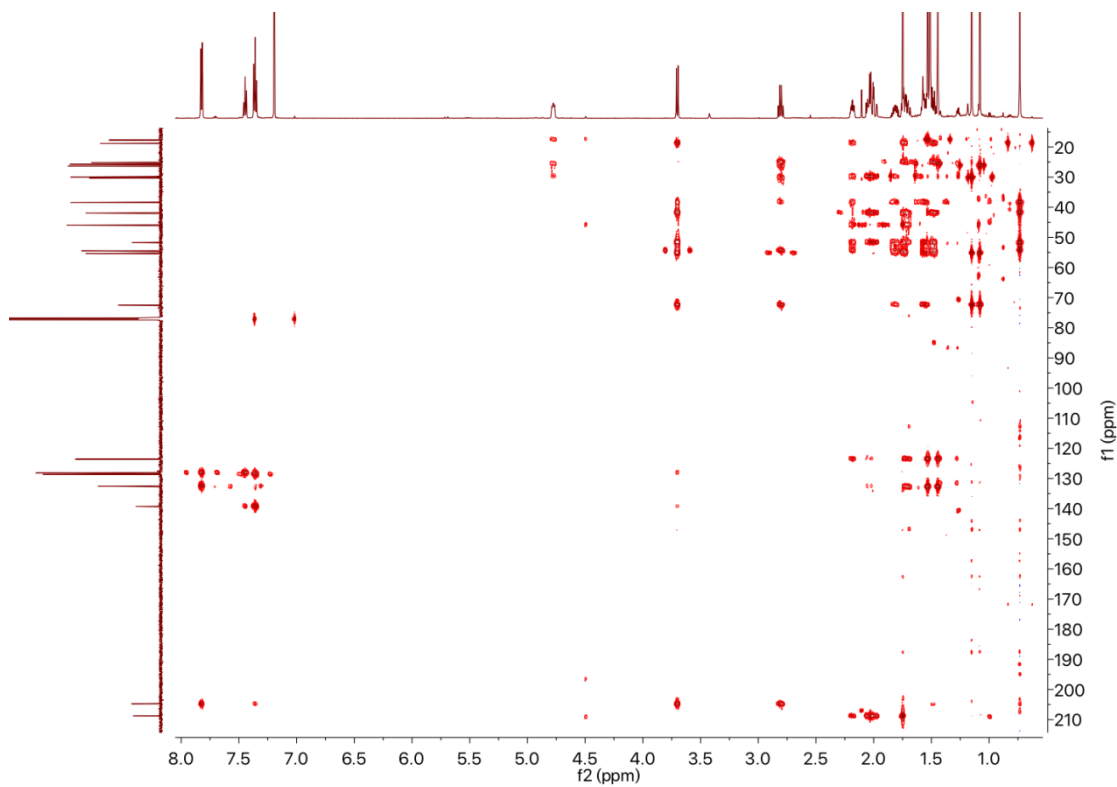


Figure S12. HMBC spectrum of ascynol B (2).

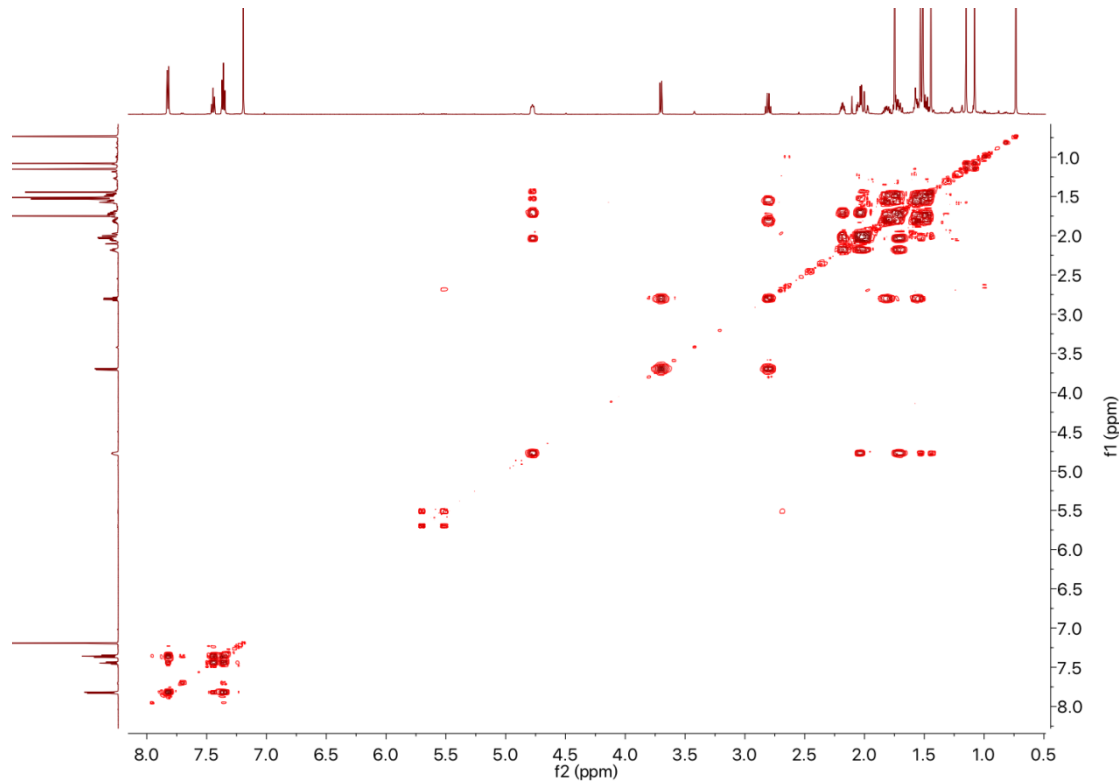


Figure S13. ^1H - ^1H COSY spectrum of ascynol B (2).

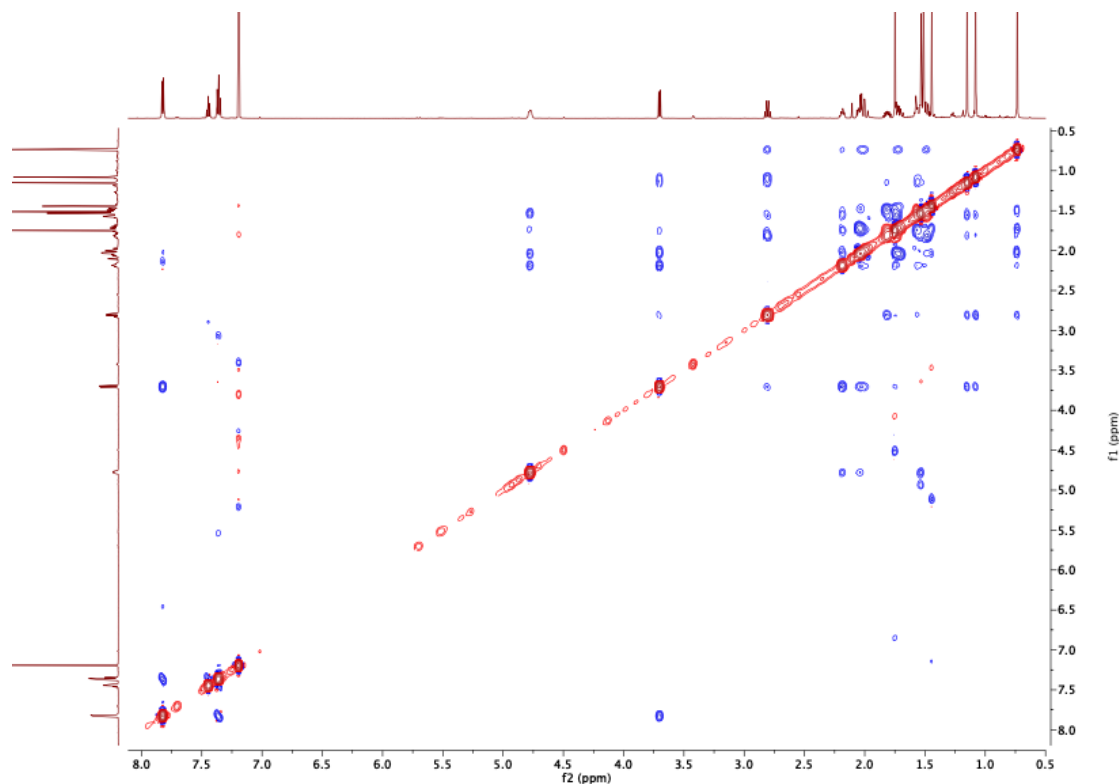


Figure S14. ROESY spectrum of ascynol B (2).

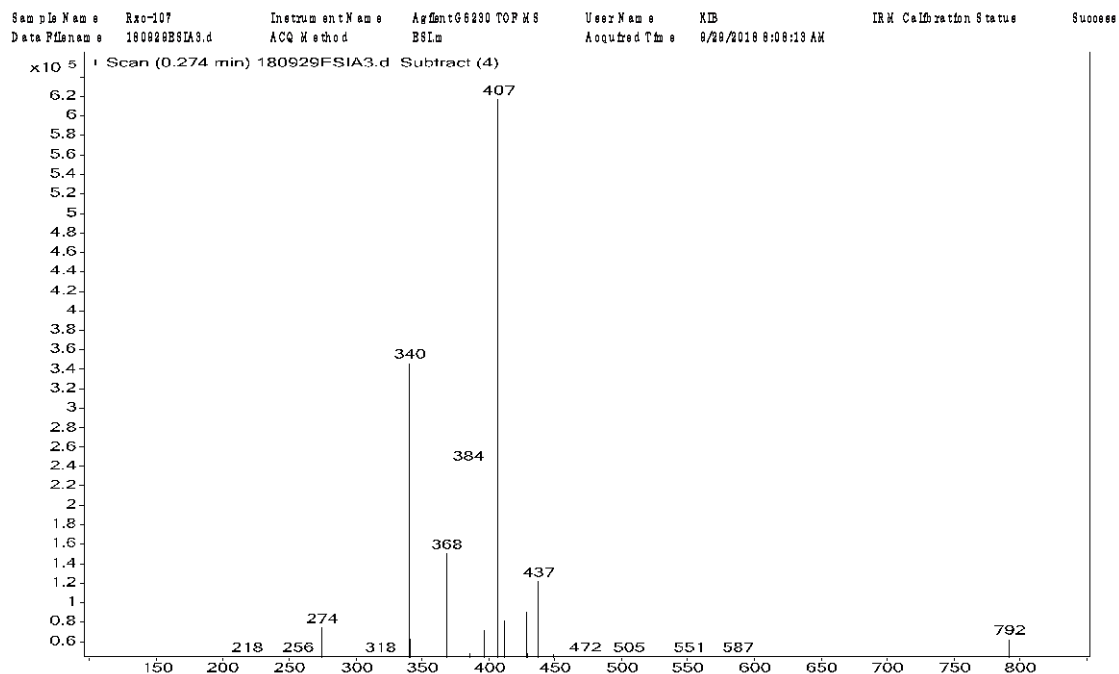
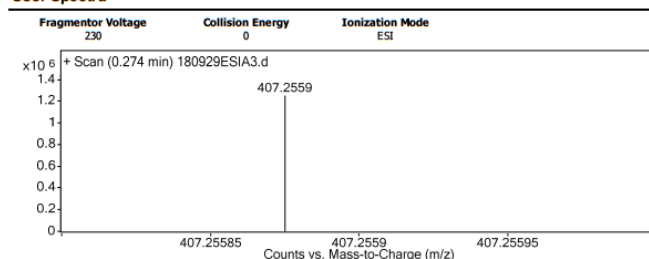


Figure S15. ESIMS spectrum of ascynol B (2).

Qualitative Analysis Report

Data Filename	180929ESIA3.d	Sample Name	Rxo-107
Sample Type	Sample	Position	
Instrument Name	Agilent G6230 TOF MS	User Name	KIB
Acq Method	ESI.m	Acquired Time	9/29/2018 8:08:13 AM
IRW Calibration Status	Success	DA Method	ESI.m
Comment			
Sample Group	Info.		
Acquisition SW	6200 series TOF/6500 series		
Version	Q-TOF B.05.01 (B5125.2)		

User Spectra



Peak List

m/z	z	Abund	Formula	Ion
274.2742	1	407154.44		
302.3053	1	125415.61		
318.3003	1	149270.95		
340.2824	1	475497.56		
368.3138	1	207587.17		
384.3085	1	321241.19		
407.2559	1	1249257.63	C25 H36 Na O3	M+
408.2593	1	322602.66	C25 H36 Na O3	M+
437.1944	1	230929.36		
791.5216	1	166142.97		

Formula Calculator Element Limits

Element	Min	Max
C	0	200
H	0	400
O	0	10
Na	1	1

Formula Calculator Results

Formula	Calculated Mass	Mz	Dif. (mDa)	Dif. (ppm)	DBE
C25 H36 Na O3	407.2562	407.2559	0.3	0.8	7.5

--- End Of Report ---

Figure S16. HRESIMS spectrum of ascynol B (2).

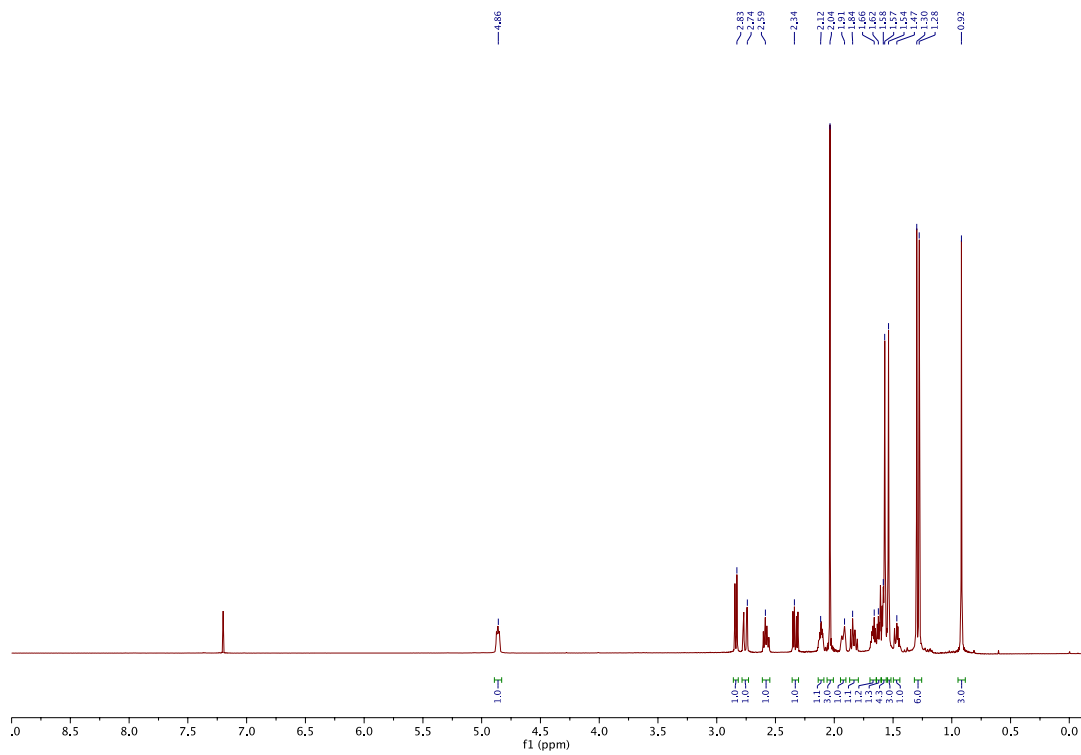


Figure S17. ^1H (in CDCl_3) spectrum of ascynol C (3).

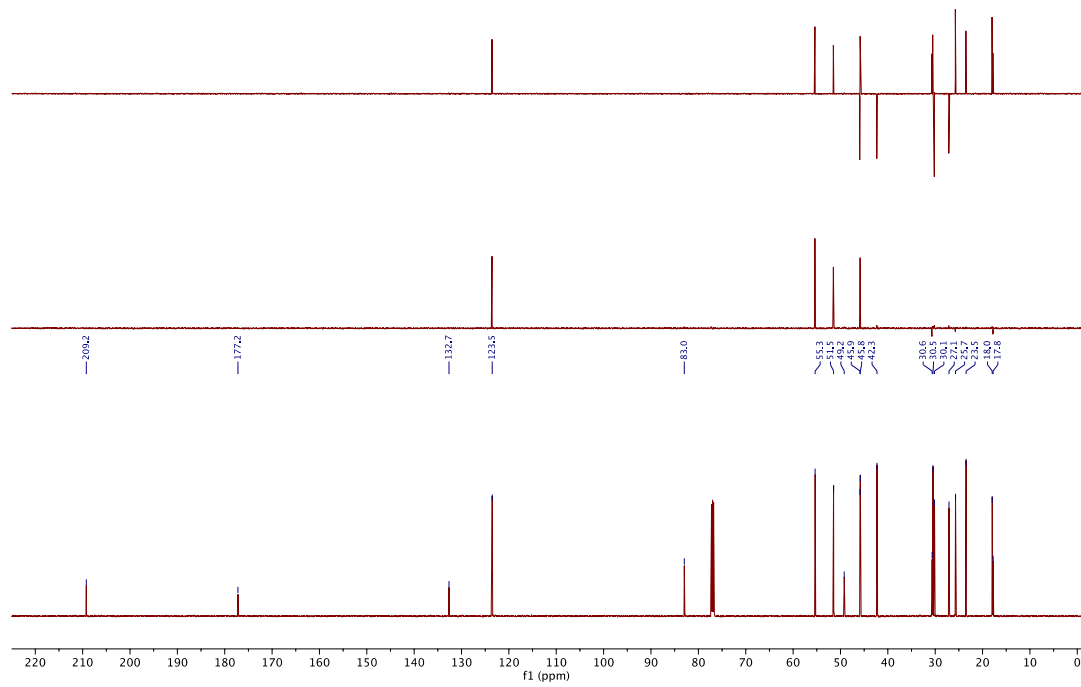


Figure S18. ^{13}C and DEPT (in CDCl_3) spectrum of ascynol C (3).

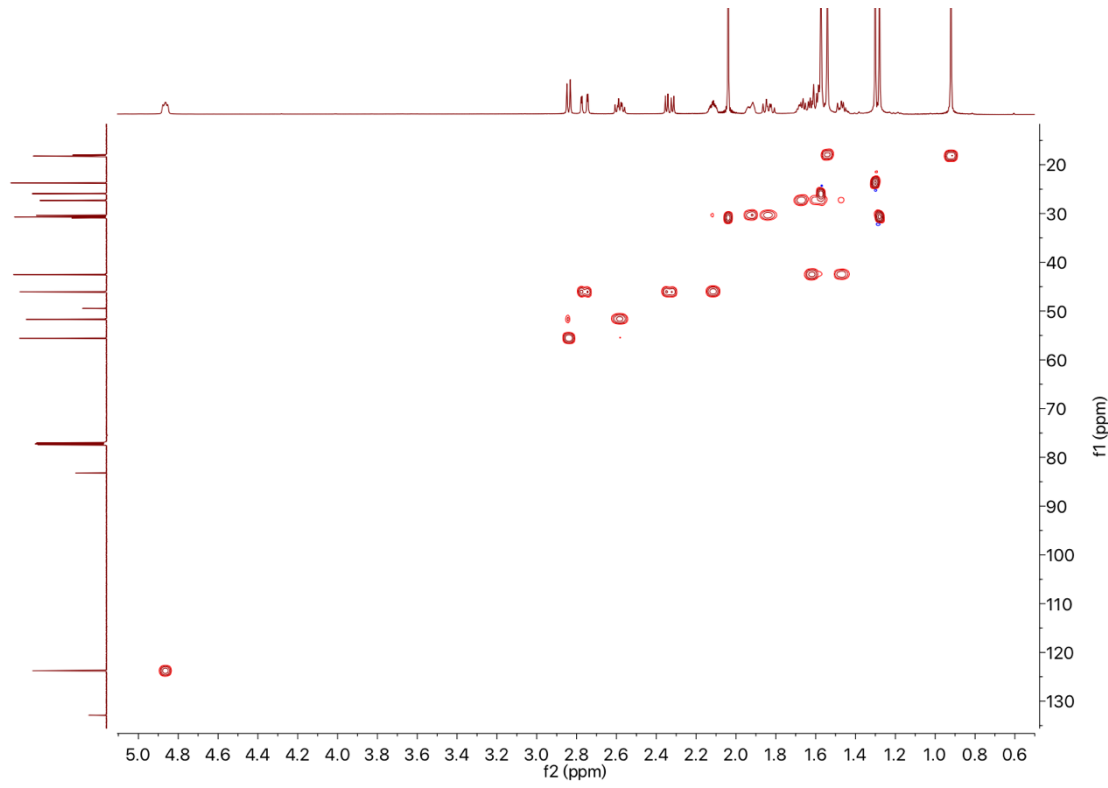


Figure S19. HSQC spectrum of ascynol C (3).

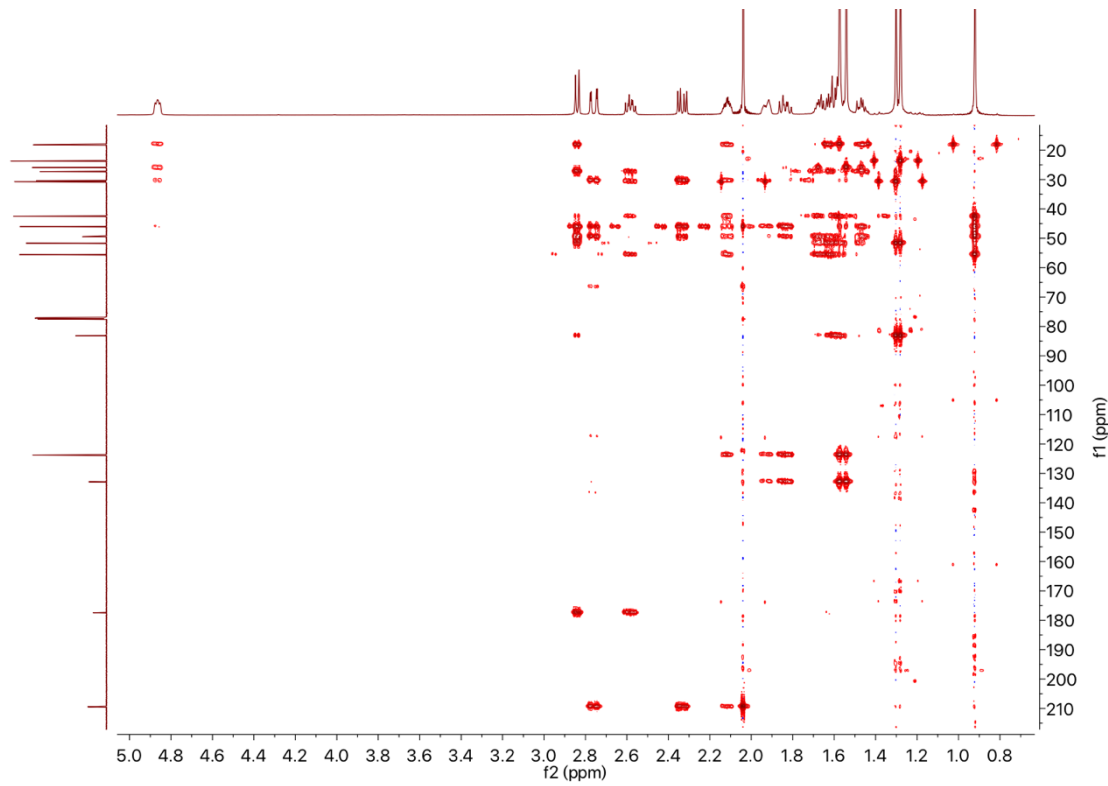


Figure S20. HMBC spectrum of ascynol C (3).

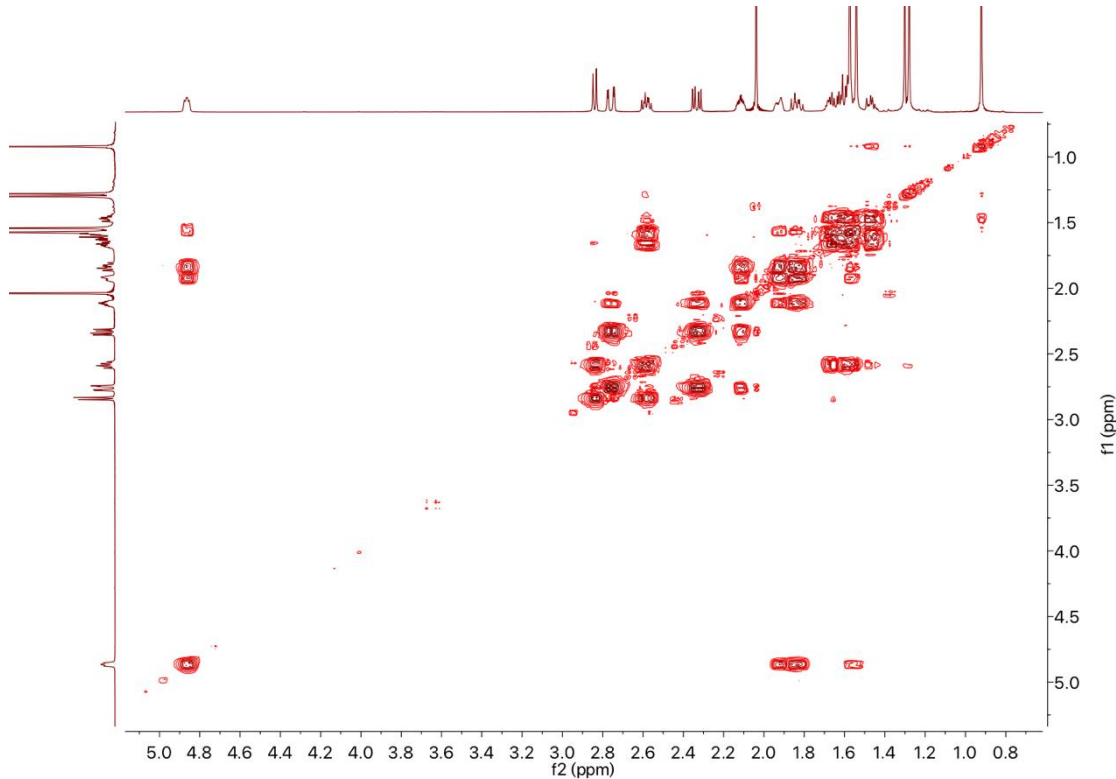


Figure S21. ^1H - ^1H COSY spectrum of ascynol C (3).

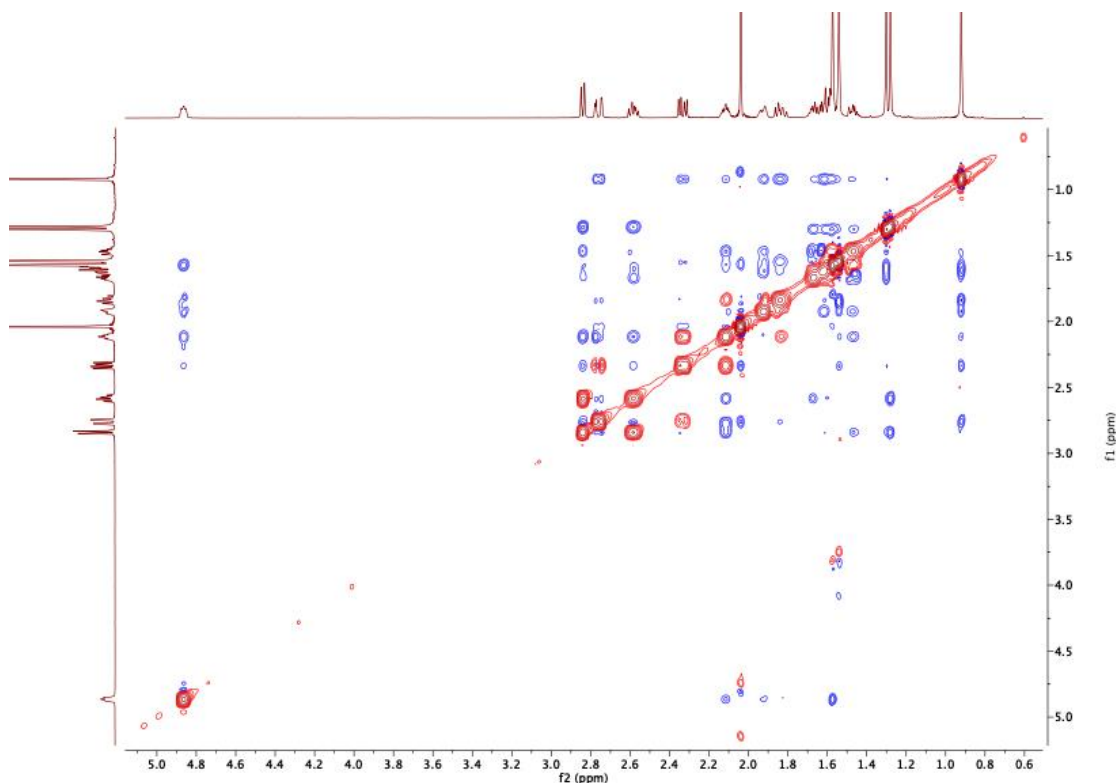


Figure S22. ROESY spectrum of ascynol C (3).

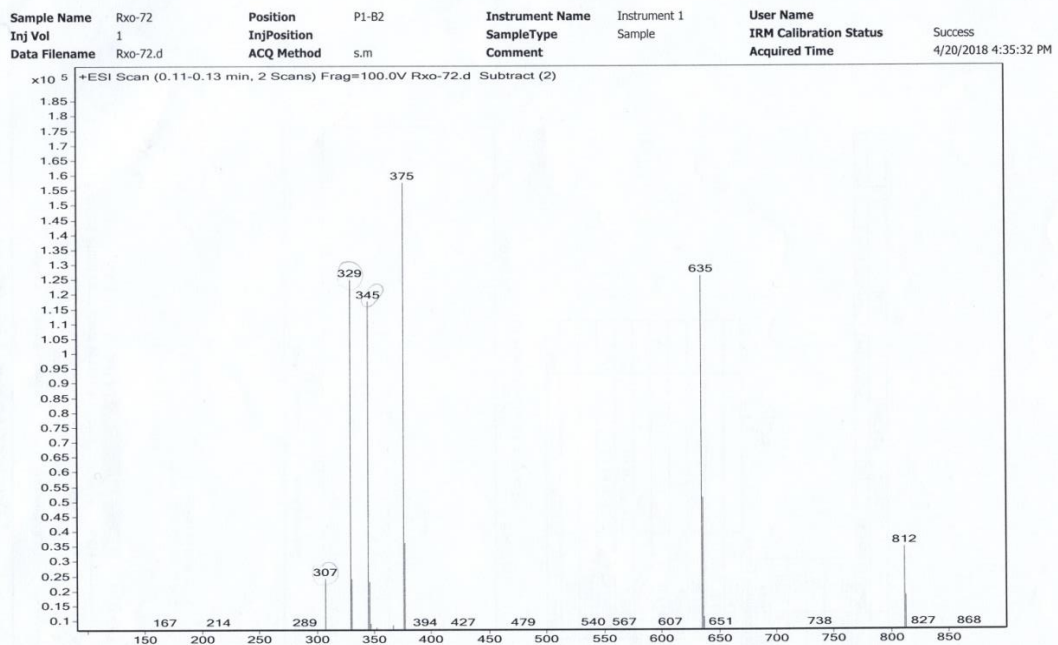
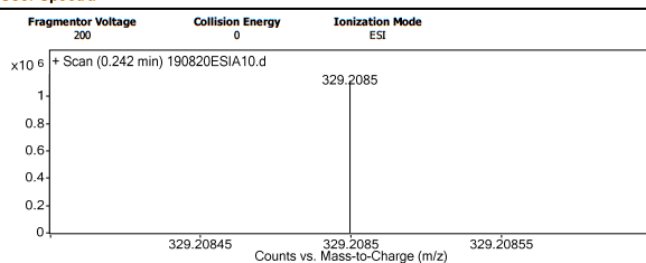


Figure S23. ESIMS spectrum of ascynol C (3).

Qualitative Analysis Report

Data Filename	190820ESIA10.d	Sample Name	Rxo-72
Sample Type	Sample	Position	
Instrument Name	Agilent G6230 TOF MS	User Name	KIB
Acq Method	ESI.m	Acquired Time	8/12/2019 2:43:31 PM
IRM Calibration Status	Success	DA Method	ESI.m
Comment			
Sample Group	Info.		
Acquisition SW	6200 series TOF/6500 series		
Version	Q-TOF B.05.01 (B5125.2)		

User Spectra



Peak List

m/z	z	Abund	Formula	Ion
121.0509	1	341921.66		
274.2735	1	96157.55		
329.2085	1	1108491.63	C19 H30 Na O3	M+
330.2116	1	205249.2	C19 H30 Na O3	M+
370.2346	1	67572.31		
635.4284	1	428913.16		
636.4316	1	174744.2		
683.4124	1	177994.56		
684.4162	1	71644.5		
922.0098	1	112179.77		

Formula Calculator Element Limits

Element	Min	Max
C	0	200
H	0	400
O	0	10
Na	1	1

Formula Calculator Results

Formula	CalculatedMass	Mz	Dif.(mDa)	Dif. (ppm)	DBE
C19 H30 Na O3	329.2093	329.2085	0.8	2.3	4.5

--- End Of Report ---

Figure S24. HRESIMS spectrum of ascynol C (3).

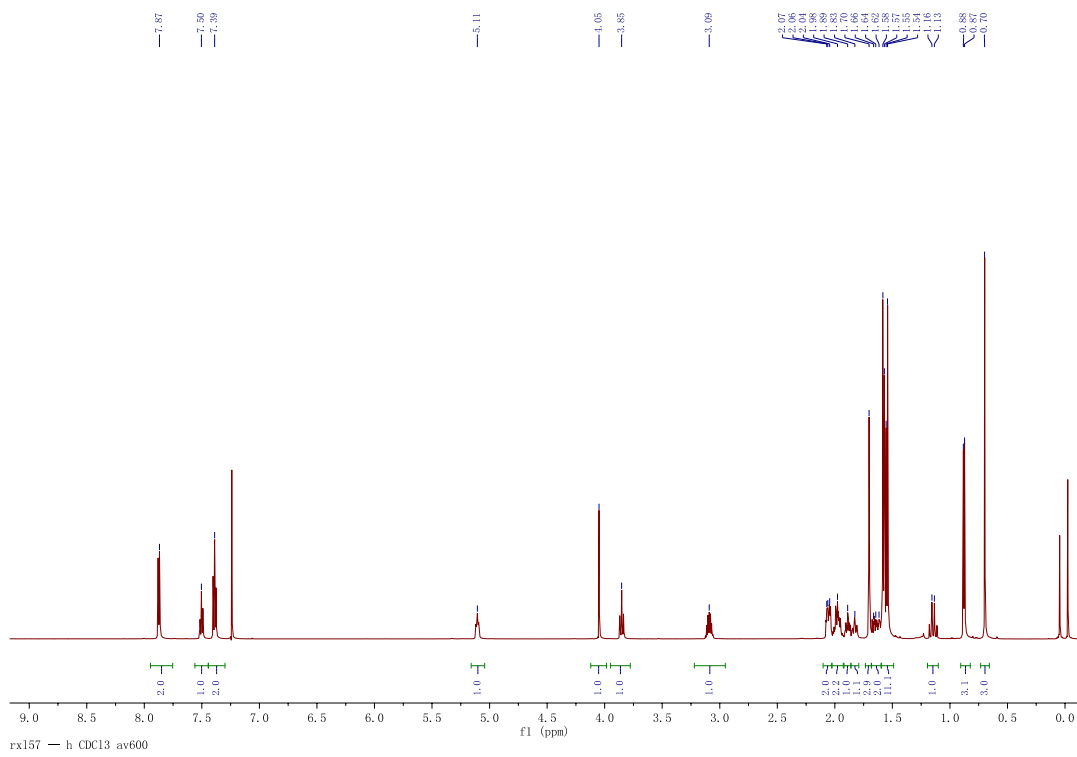


Figure S25. ^1H (in CDCl_3) spectrum of ascynol D (**4**).

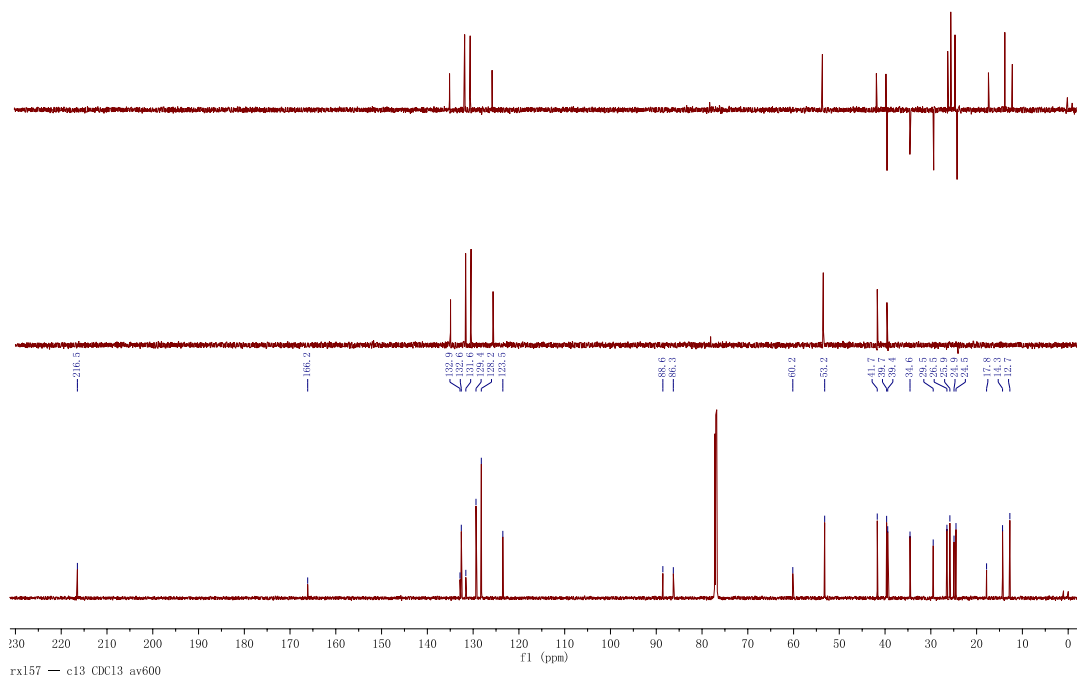


Figure S25. ^{13}C (in CDCl_3) spectrum of ascynol D (**4**).

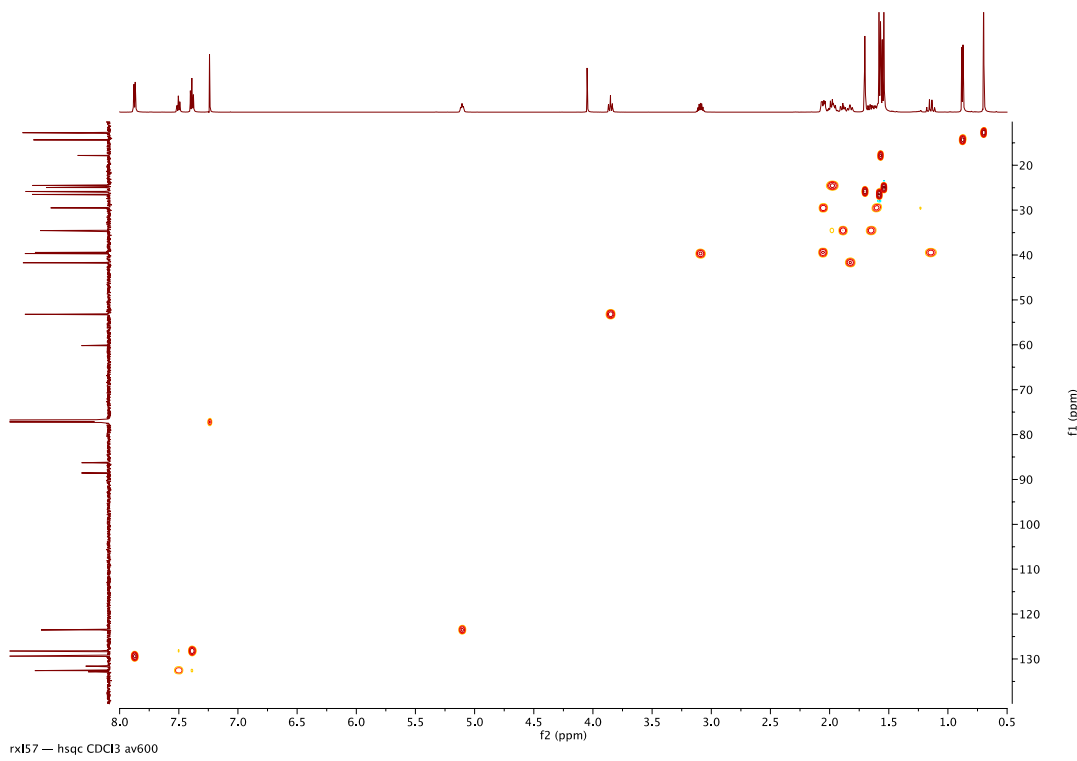


Figure S27. HSQC spectrum of ascynol D (**4**).

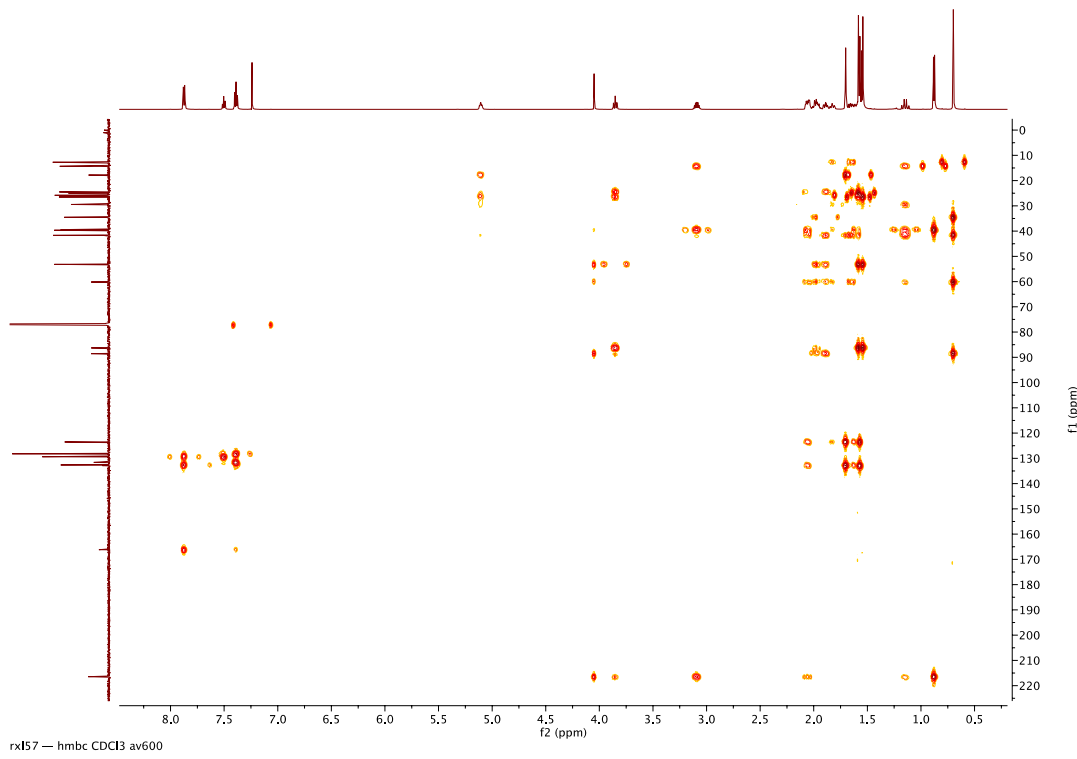


Figure S28. HMBC spectrum of ascynol D (**4**).

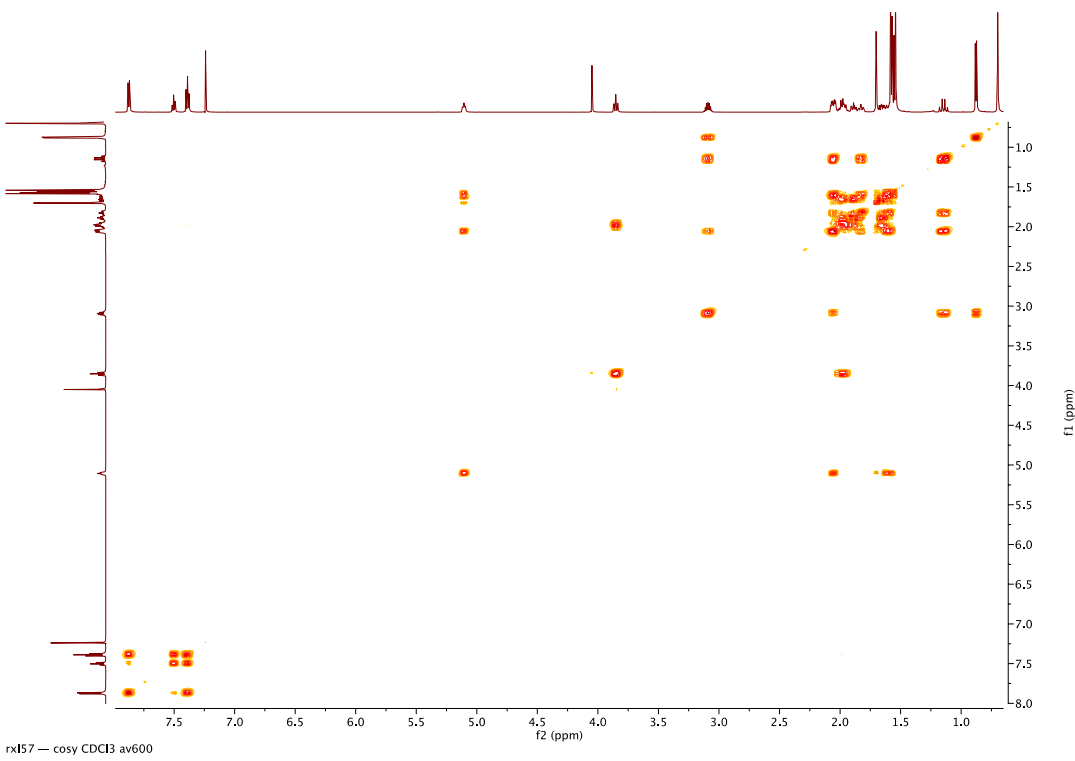


Figure S29. ^1H - ^1H COSY spectrum of ascynol D (**4**).

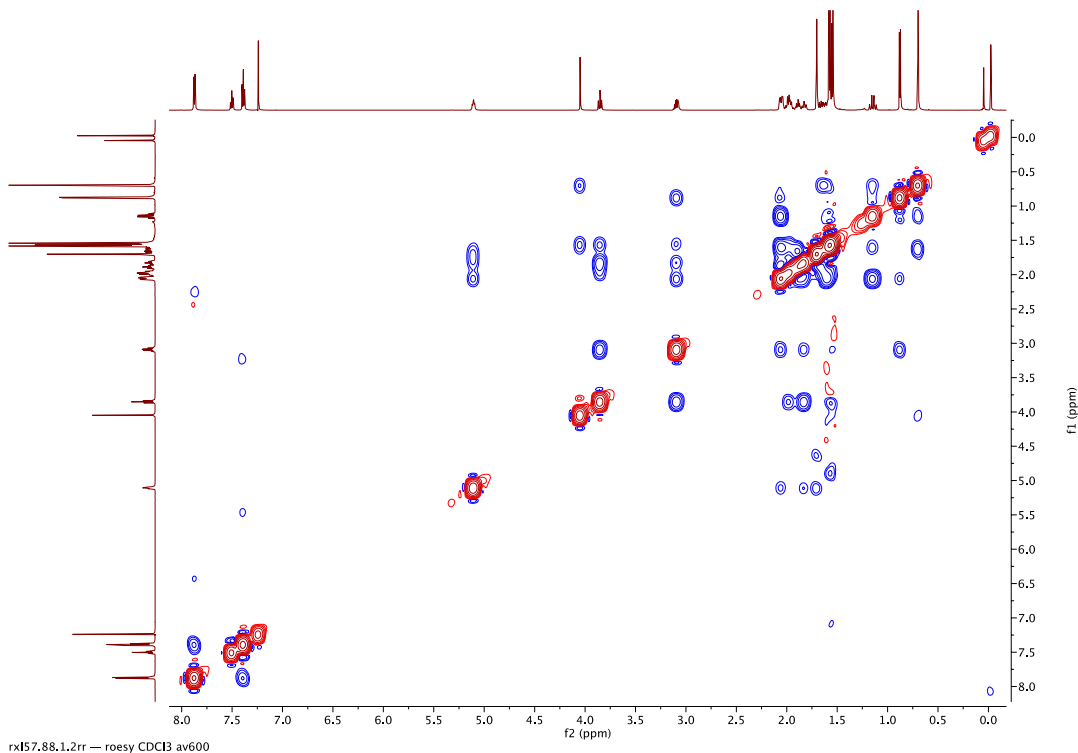


Figure S30. ROESY spectrum of ascynol D (**4**).

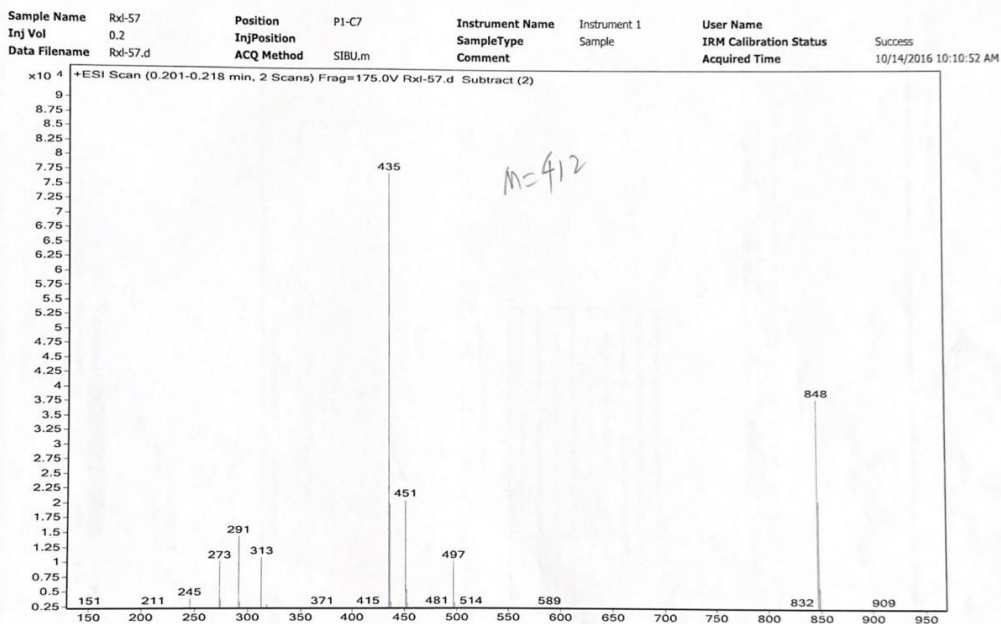


Figure S31. ESIMS spectrum of ascynol D (4).

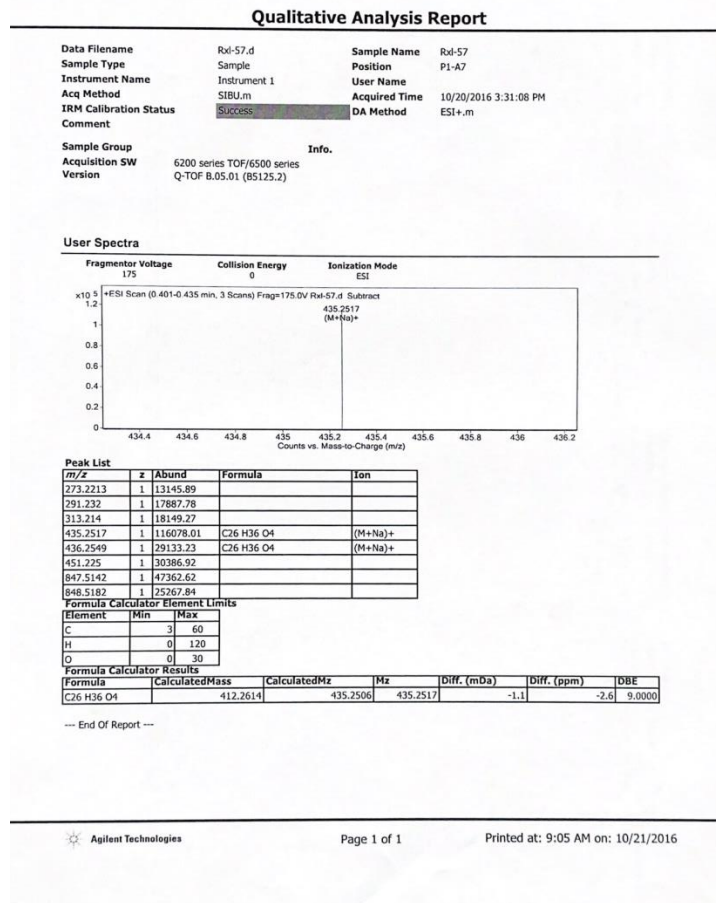


Figure S32. HRESIMS spectrum of ascynol D (4).

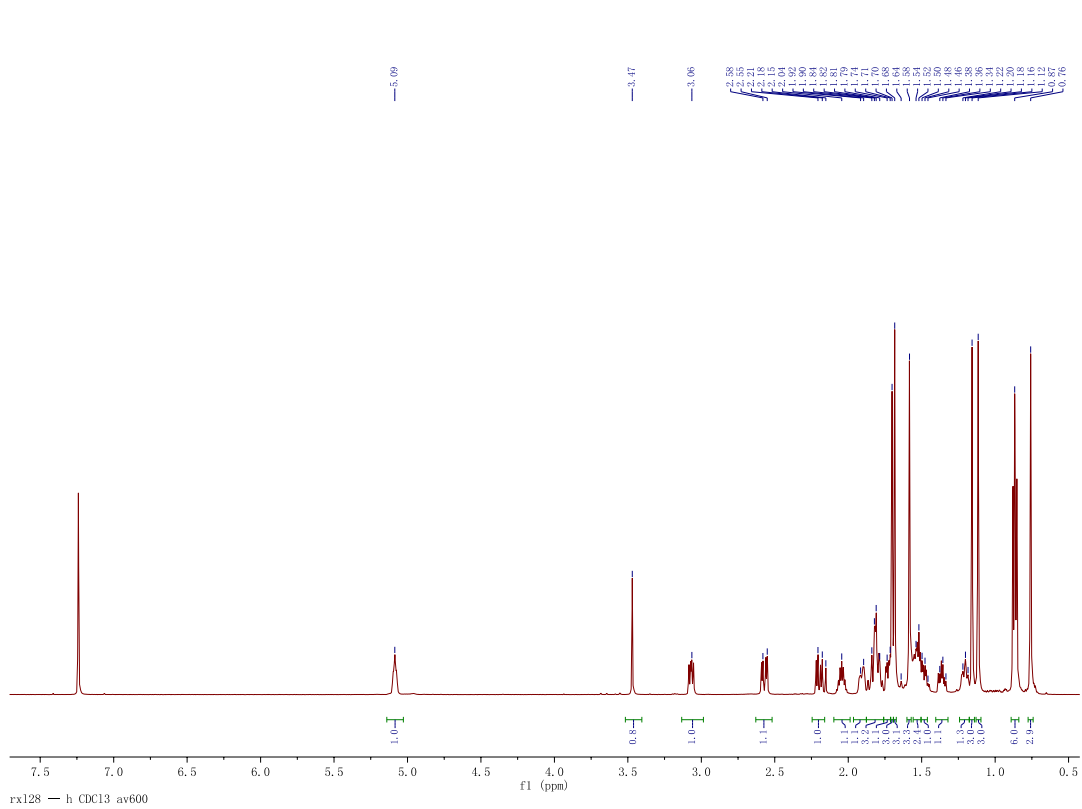


Figure S25. ¹H (in CDCl₃) spectrum of ascynol E (**5**).

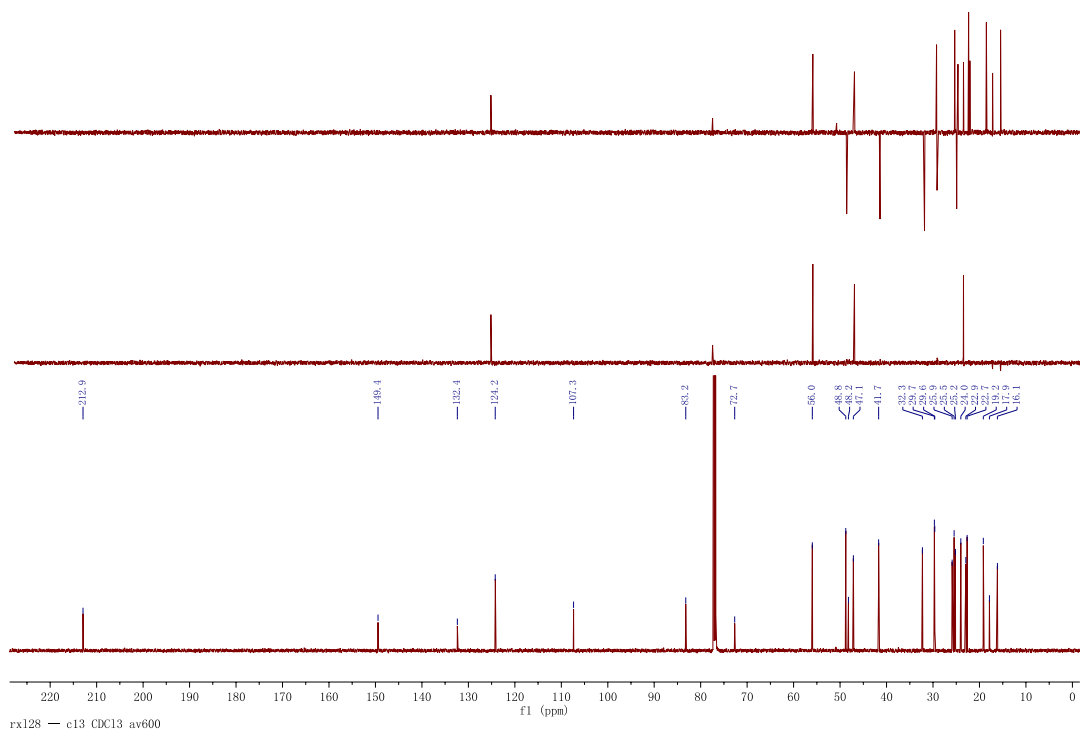


Figure S26. ¹³C (in CDCl₃) spectrum of ascynol E (**5**).

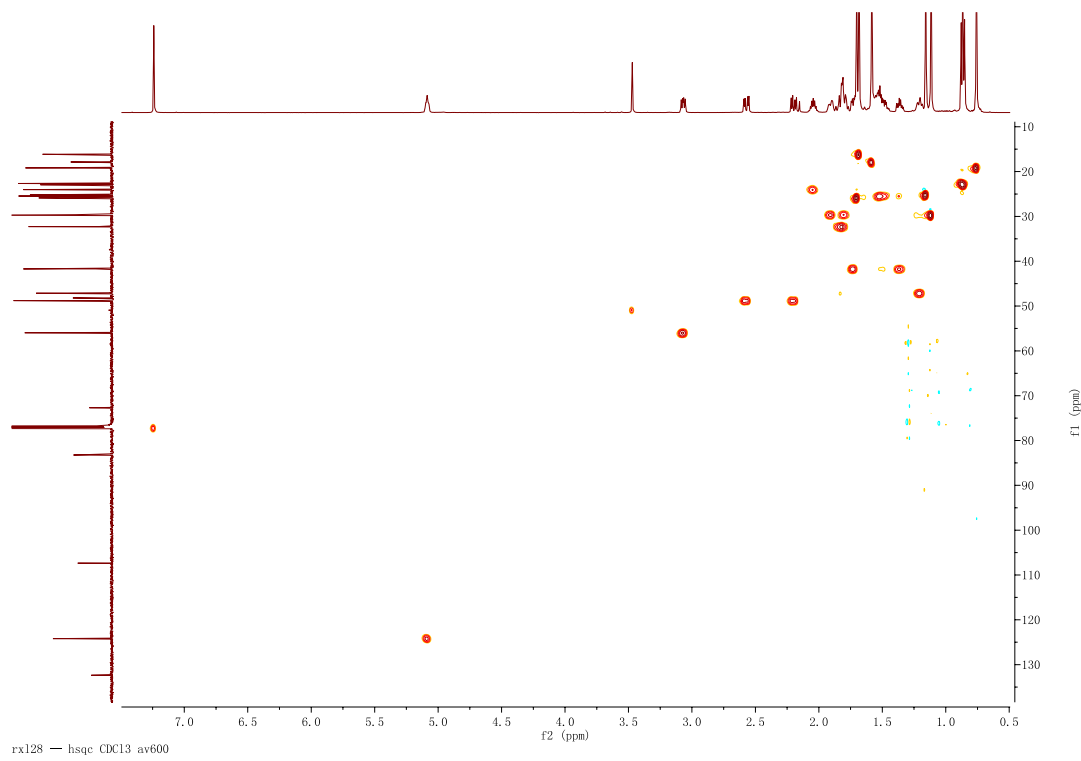


Figure S27. HSQC spectrum of ascynol E (5).

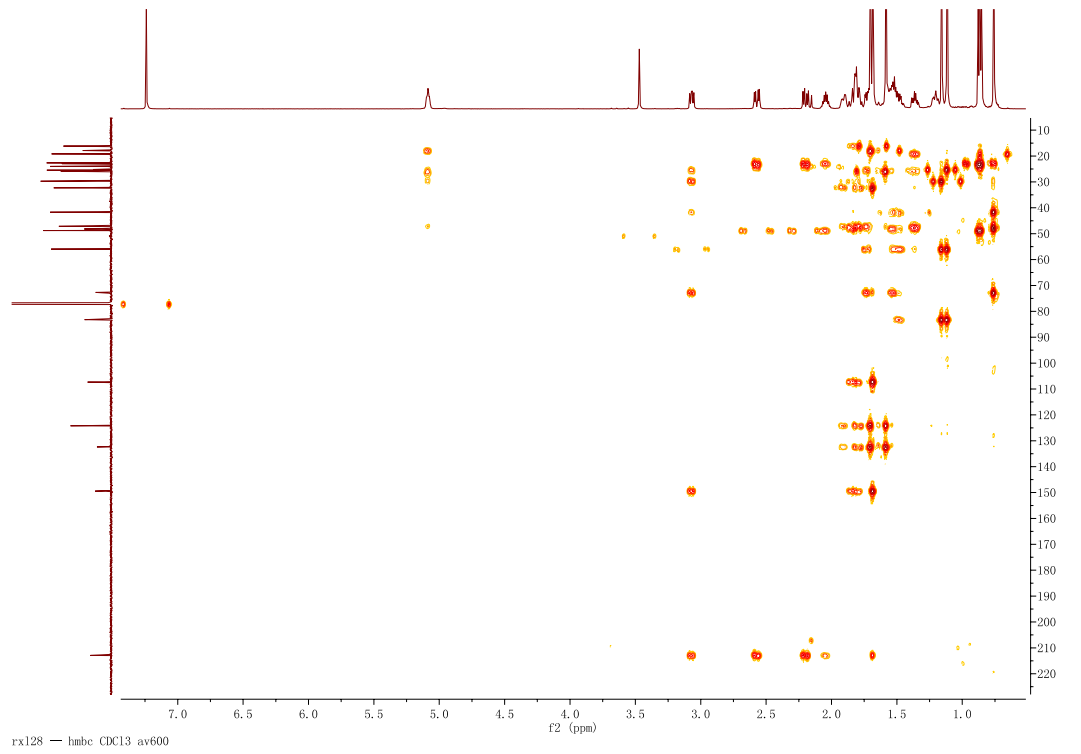


Figure S28. HMBC spectrum of ascynol E (5).

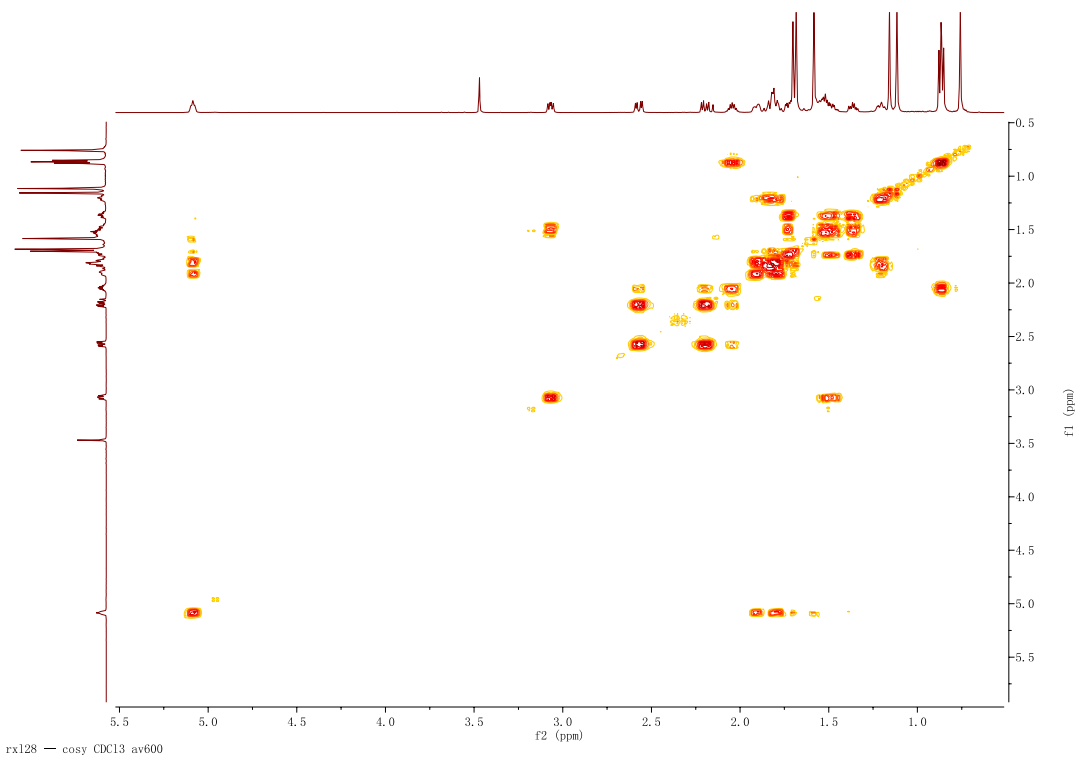


Figure S29. ^1H - ^1H COSY spectrum of ascynol E (**5**).

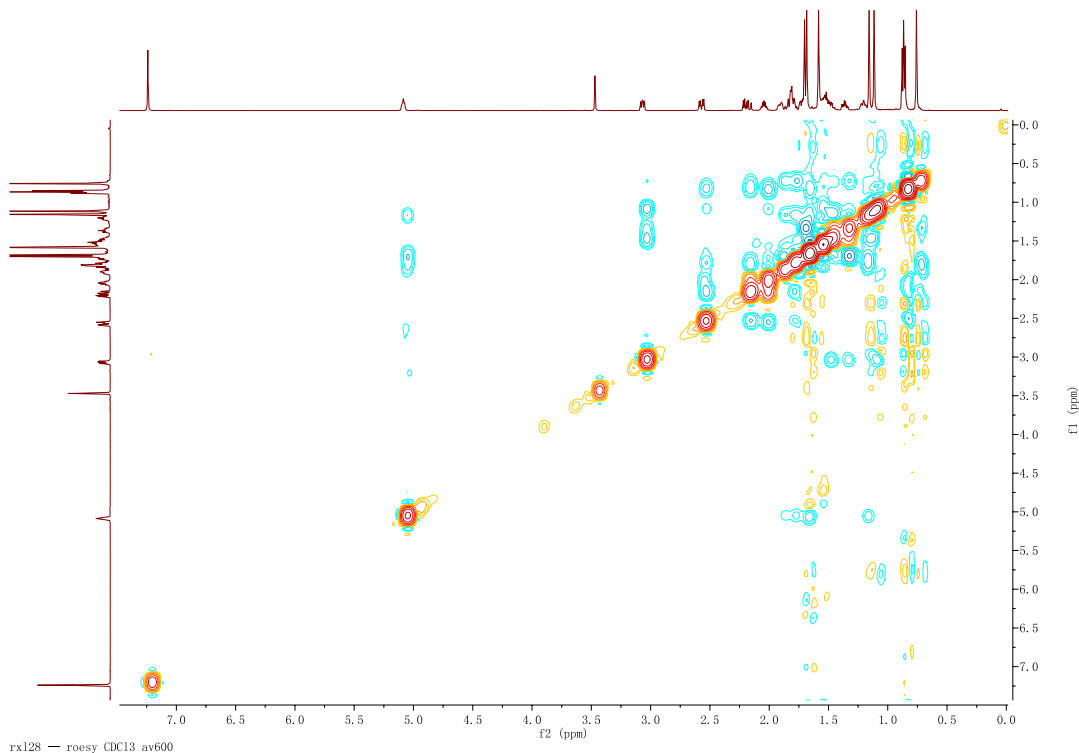


Figure S30. ROESY spectrum of ascynol E (**5**).

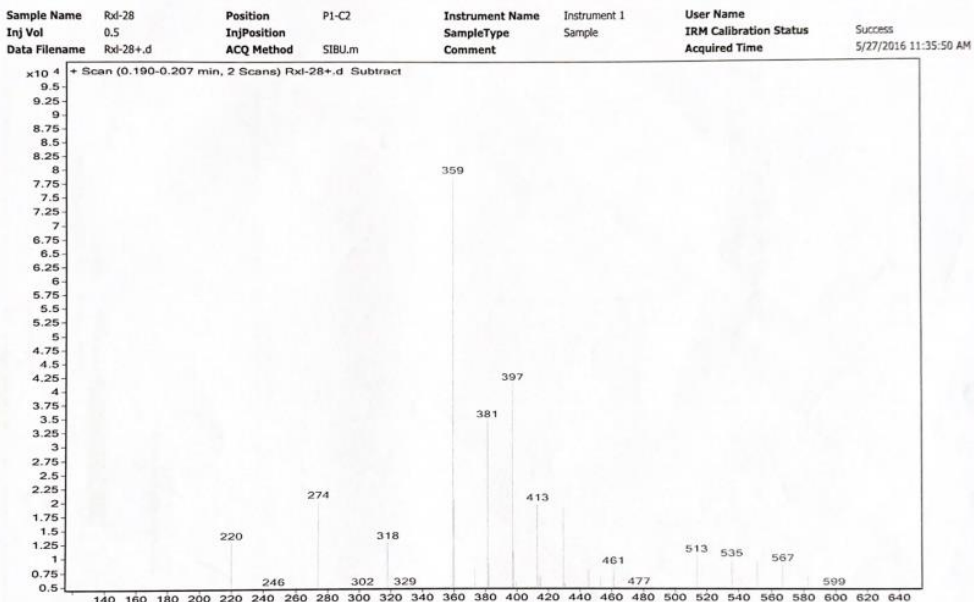


Figure S31. ESIMS spectrum of ascynol E (5).

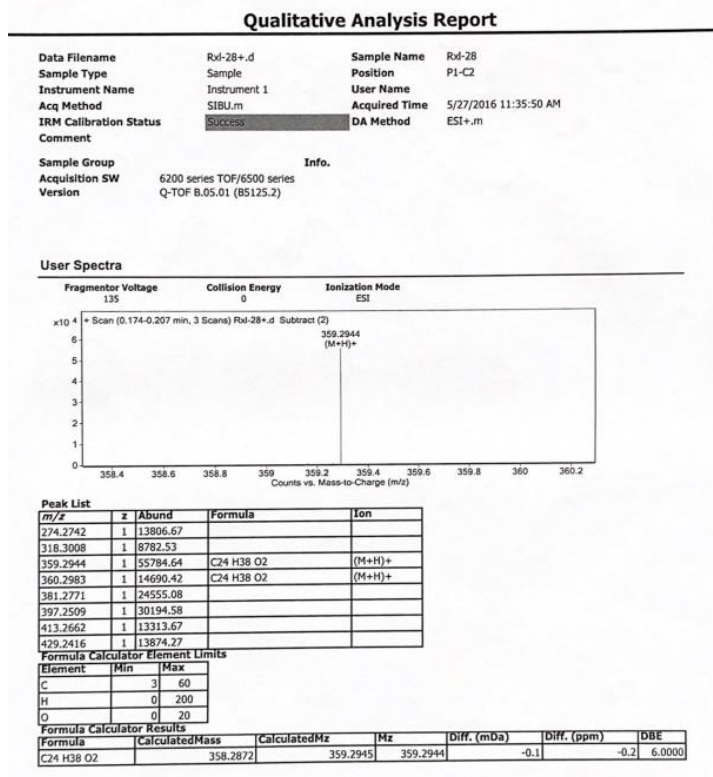


Figure S32. HRESIMS spectrum of ascynol E (5).

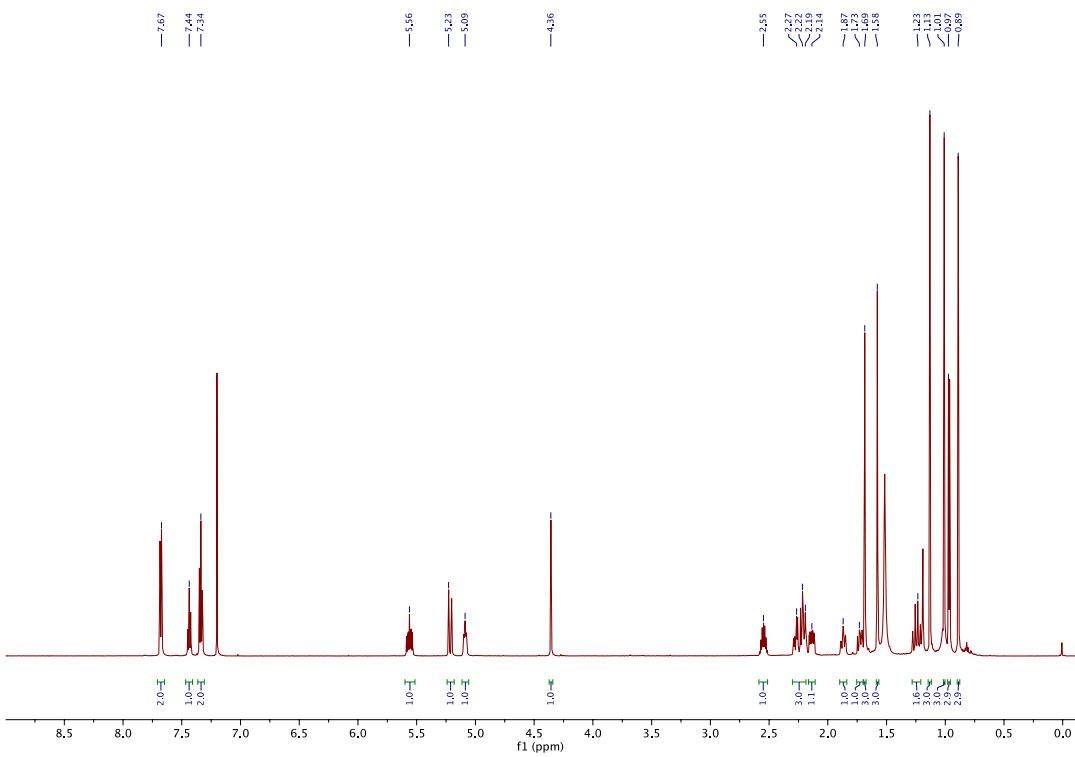


Figure S25. ^1H (in CDCl_3) spectrum of ascynol F (**8**).

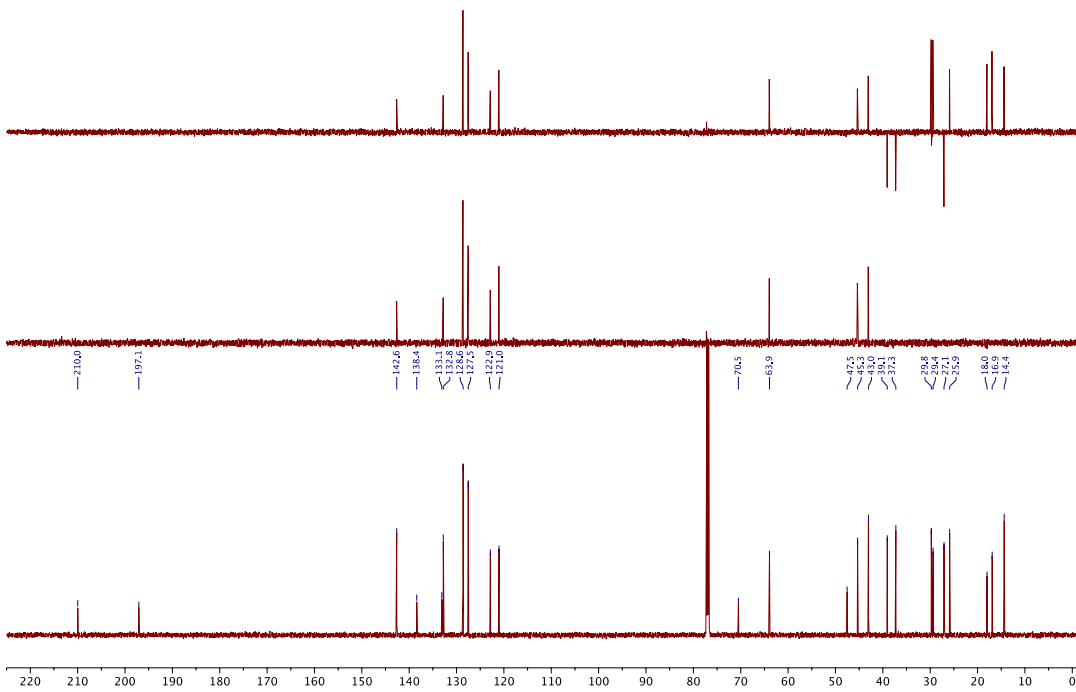


Figure S26. ^{13}C and DEPT (in CDCl_3) spectrum of ascynol F (**8**).

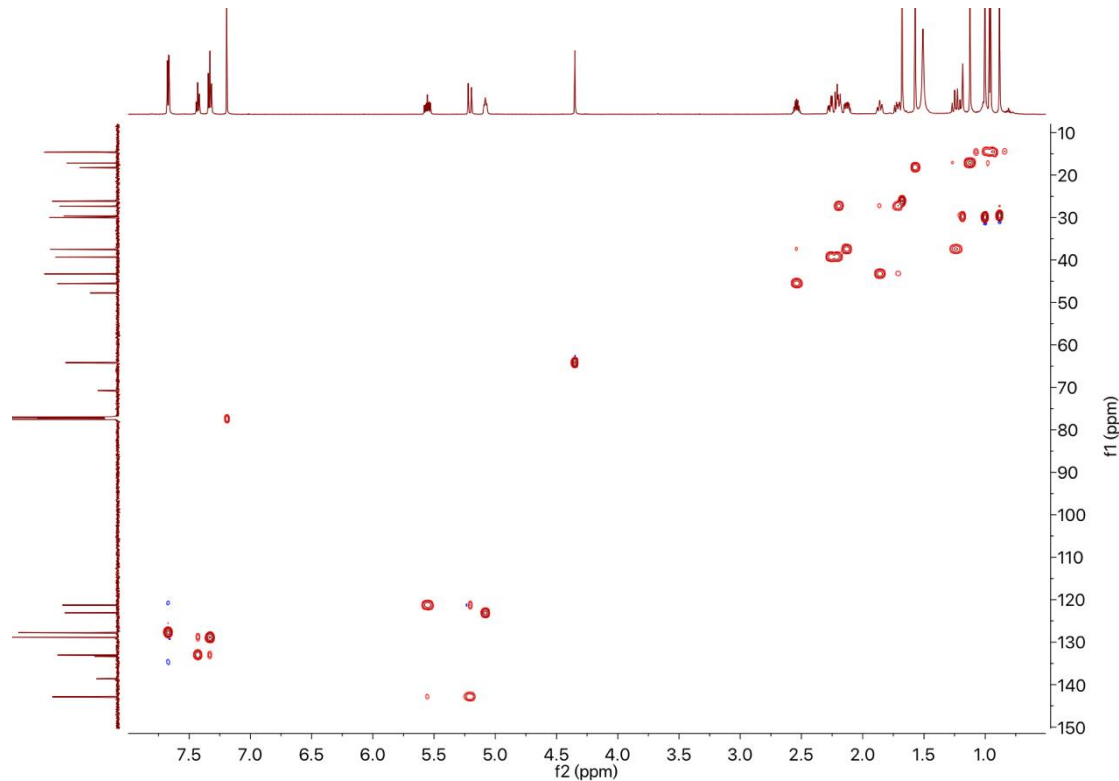


Figure S27. HSQC spectrum of ascynol F (8).

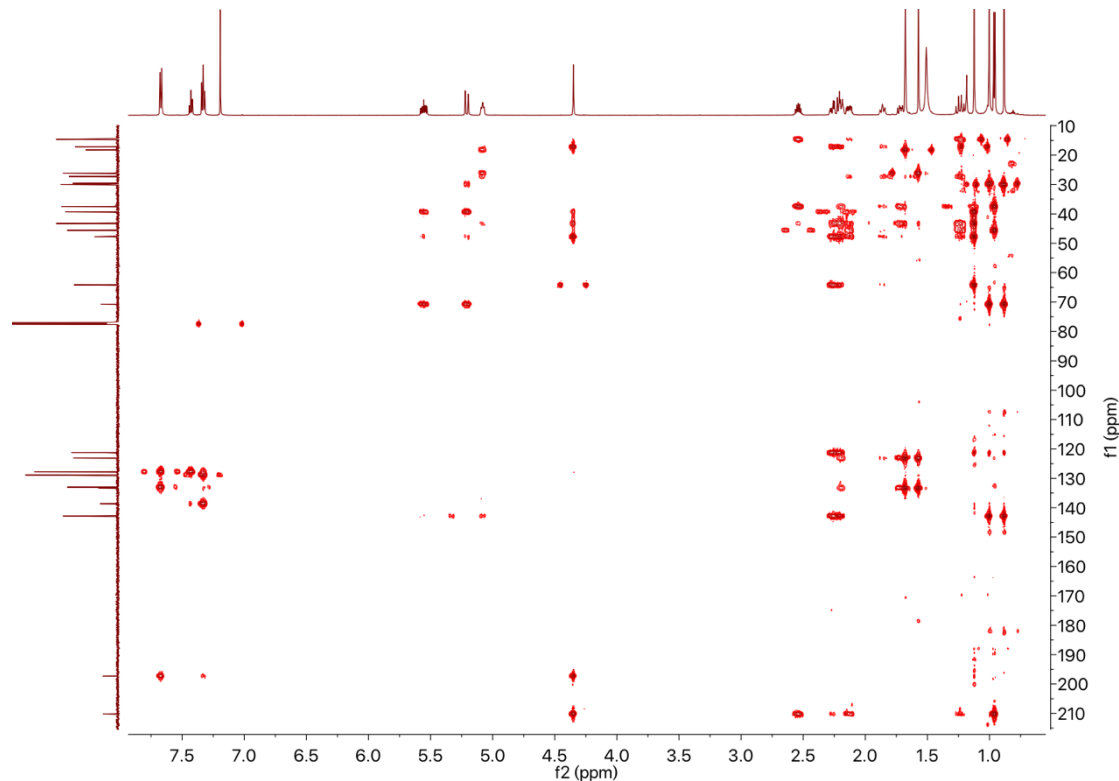


Figure S28. HMBC spectrum of ascynol F (8).

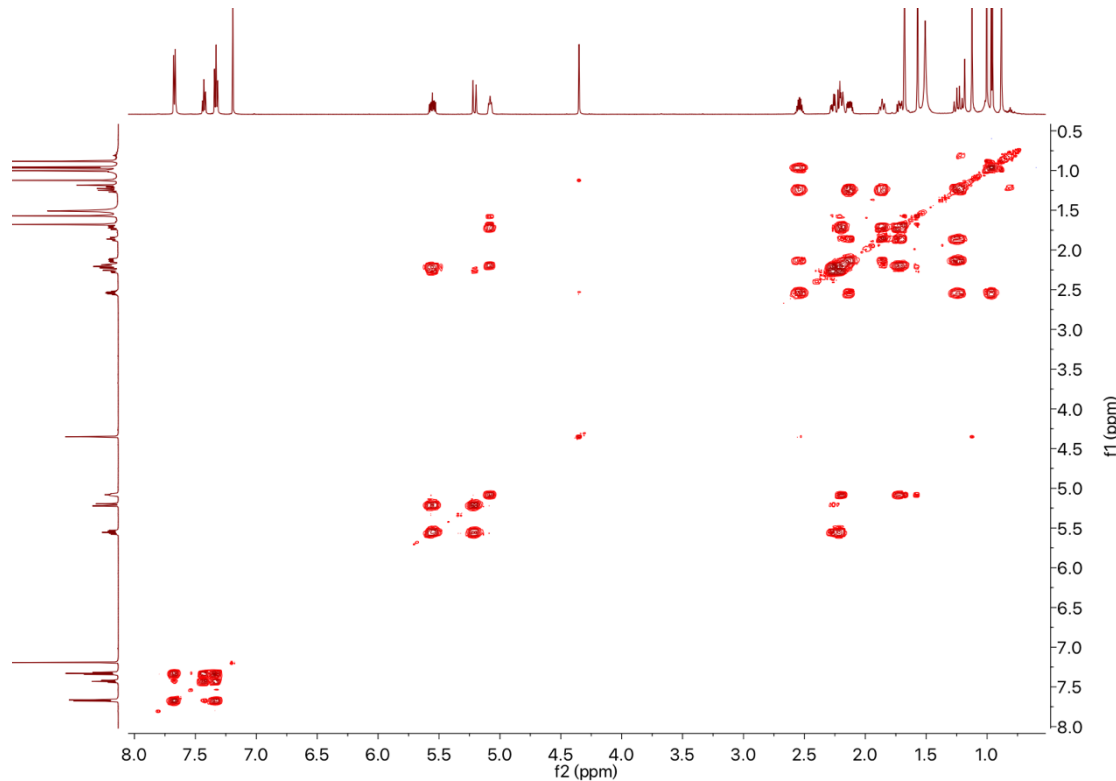


Figure S29. ^1H - ^1H COSY spectrum of ascynol F (8).

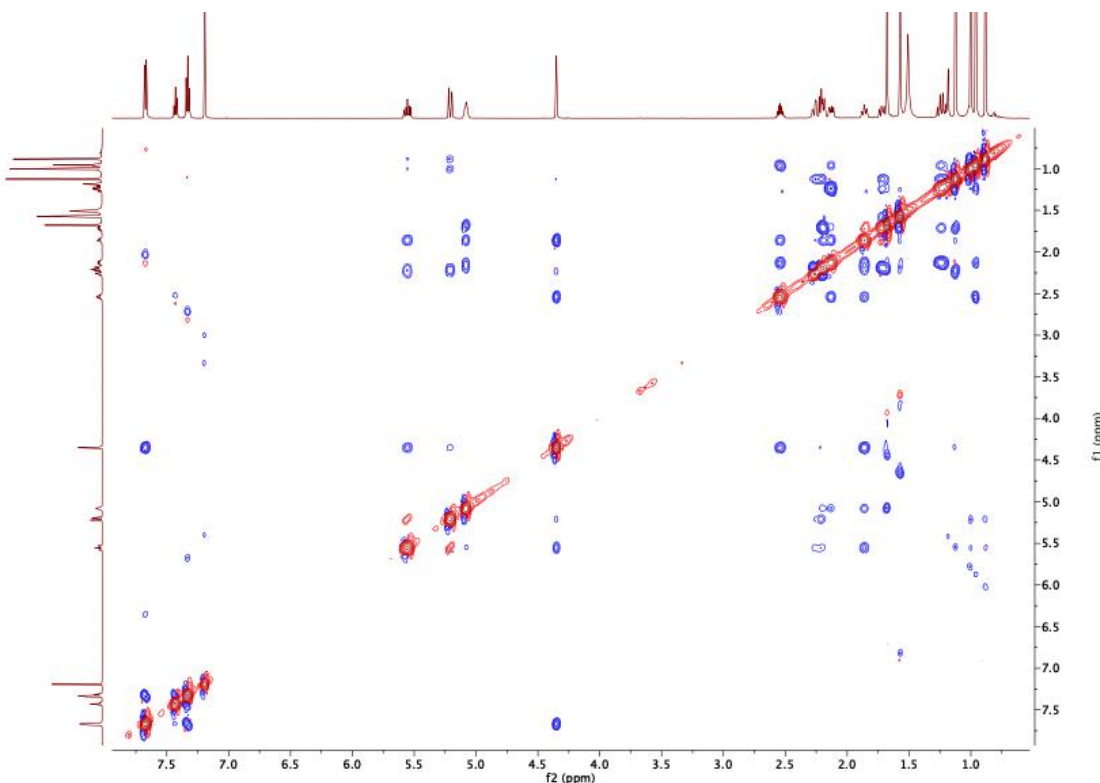


Figure S30. ROESY spectrum of ascynol F (8).

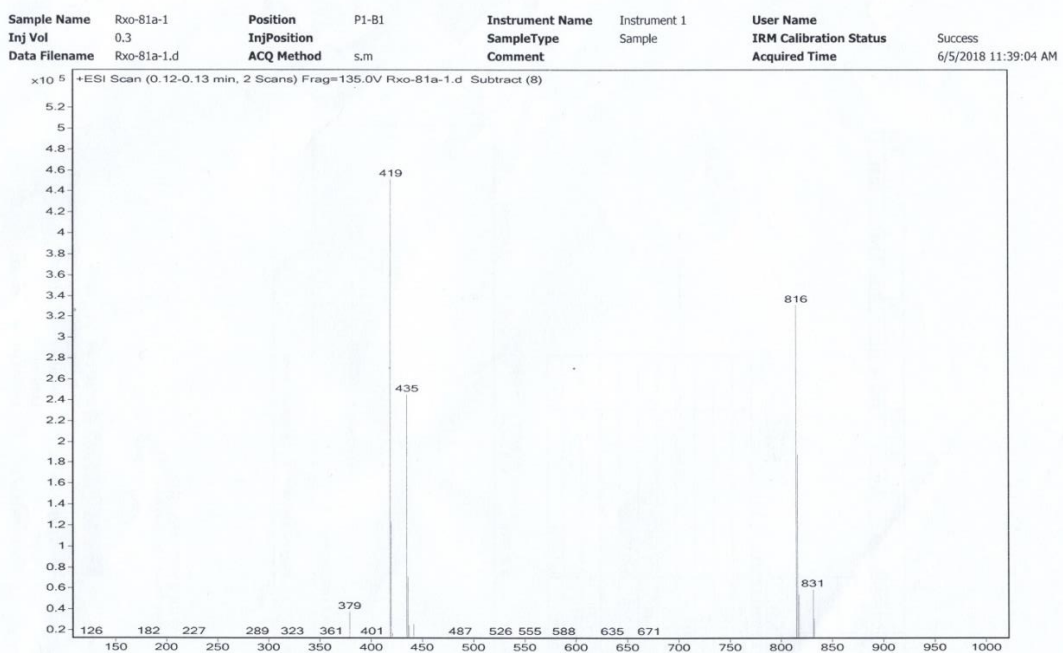
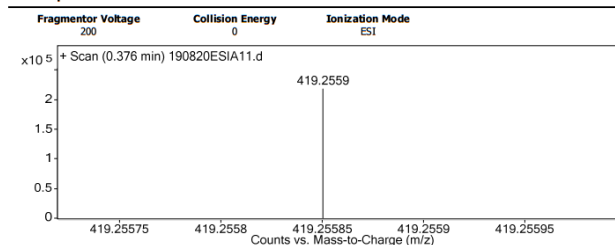


Figure S31. ESIMS spectrum of ascynol F (8).

Qualitative Analysis Report

Data Filename	190820ESIA11.d	Sample Name	Rxo-81
Sample Type	Sample	Position	
Instrument Name	Agilent G6230 TOF MS	User Name	KIB
Acq Method	ESI.m	Acquired Time	8/12/2019 2:44:42 PM
IRM Calibration Status	Success	DA Method	ESI.m
Comment			
Sample Group		Info.	
Acquisition SW	6200 series TOF/6500 series		
Version	Q-TOF B.05.01 (B5125.2)		

User Spectra



Peak List

m/z	z	Abund	Formula	Ion
121.0509	1	83430.25		
274.2734	1	71194.38		
379.2629	1	56187.67		
419.2559	1	218019.25	C26 H36 Na O3	M+
420.2587	1	60328.18	C26 H36 Na O3	M+
549.3187	1	54304.32		
815.5234	1	707915.06		
816.5265	1	396600		
817.5294	1	112899.1		
945.5849	1	64600.77		

Formula Calculator Element Limits

Element	Min	Max
C	0	200
H	0	400
O	0	10
Na	1	1

Formula Calculator Results

Formula	CalculatedMass	Mz	Diff.(mDa)	Diff. (ppm)	DBE
C26 H36 Na O3	419.2562	419.2559	0.3	0.7	8.5

--- End Of Report ---

Figure S32. HRESIMS spectrum of ascynol F (8).

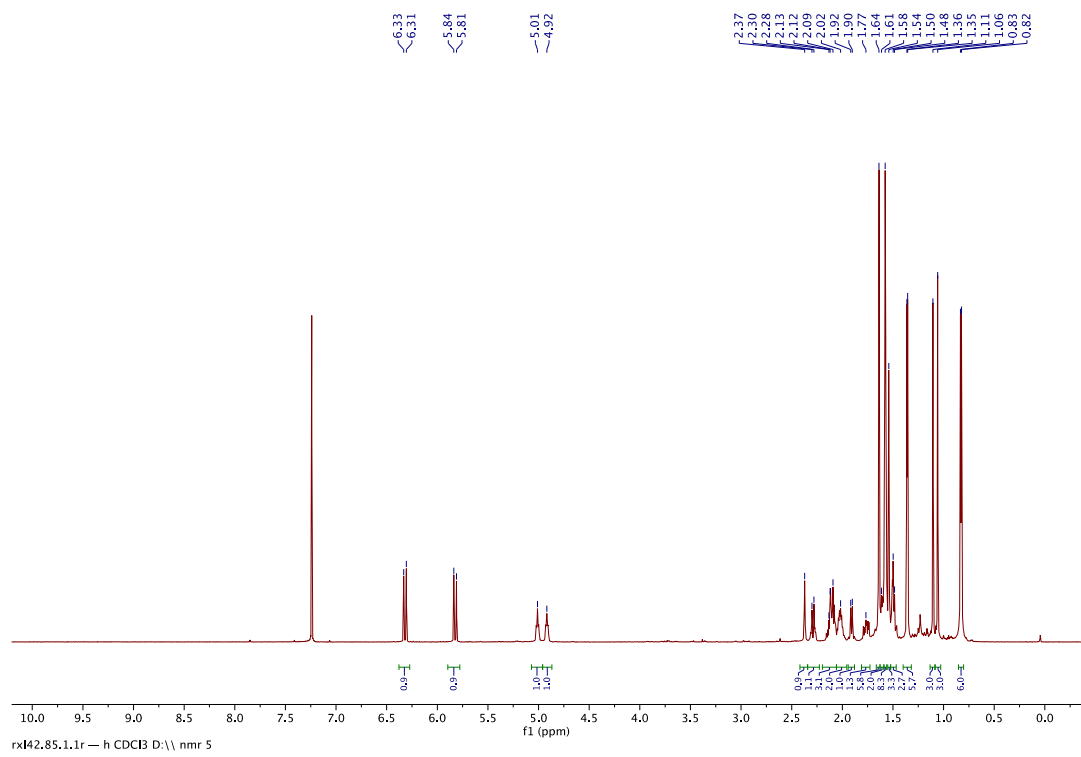


Figure S25. ¹H (in CDCl₃) spectrum of ascynol G (**9**).

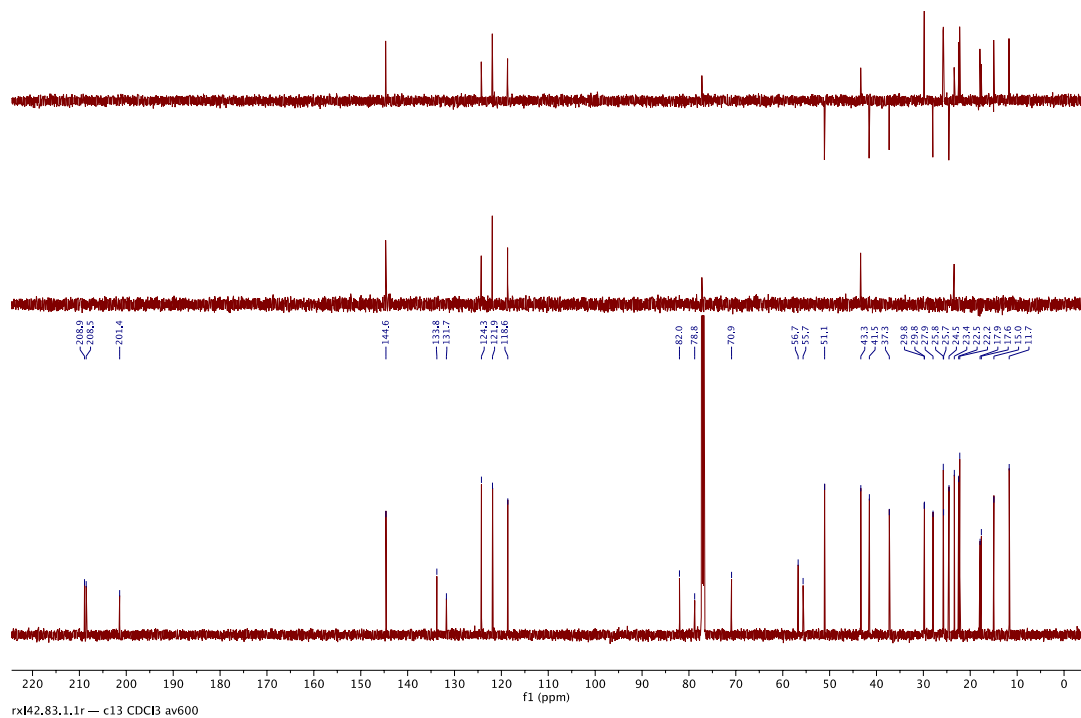


Figure S26. ¹³C (in CDCl₃) spectrum of ascynol G (**9**).

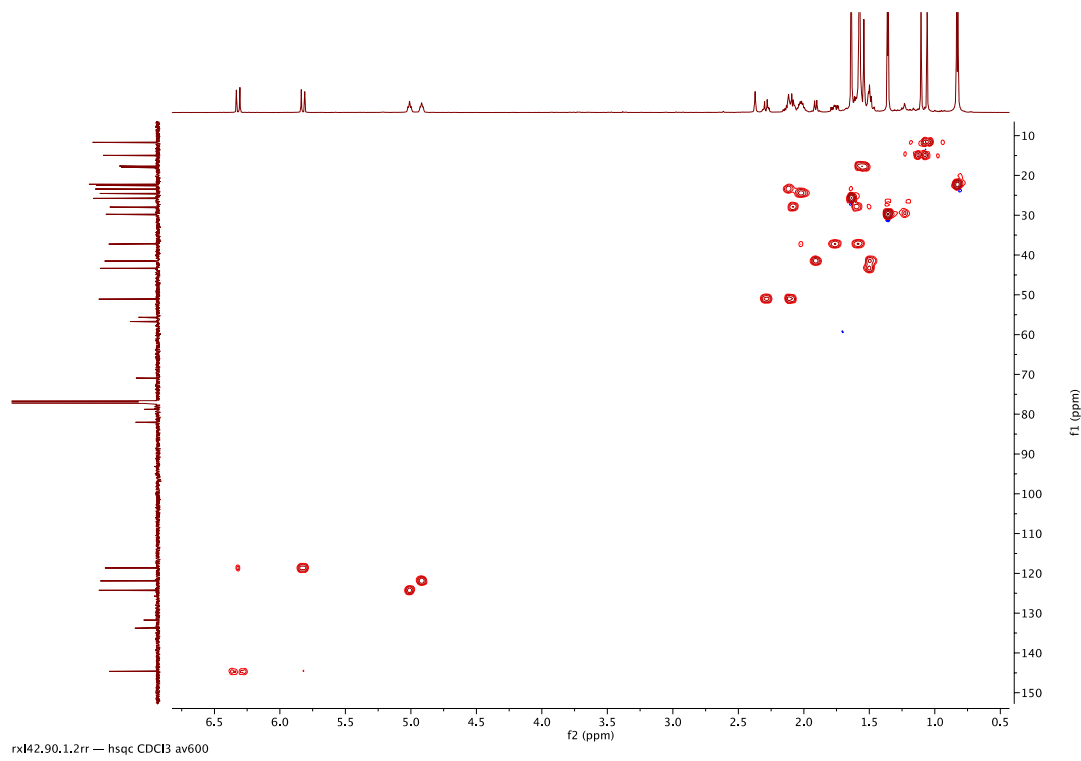


Figure S27. HSQC spectrum of ascynol G (**9**).

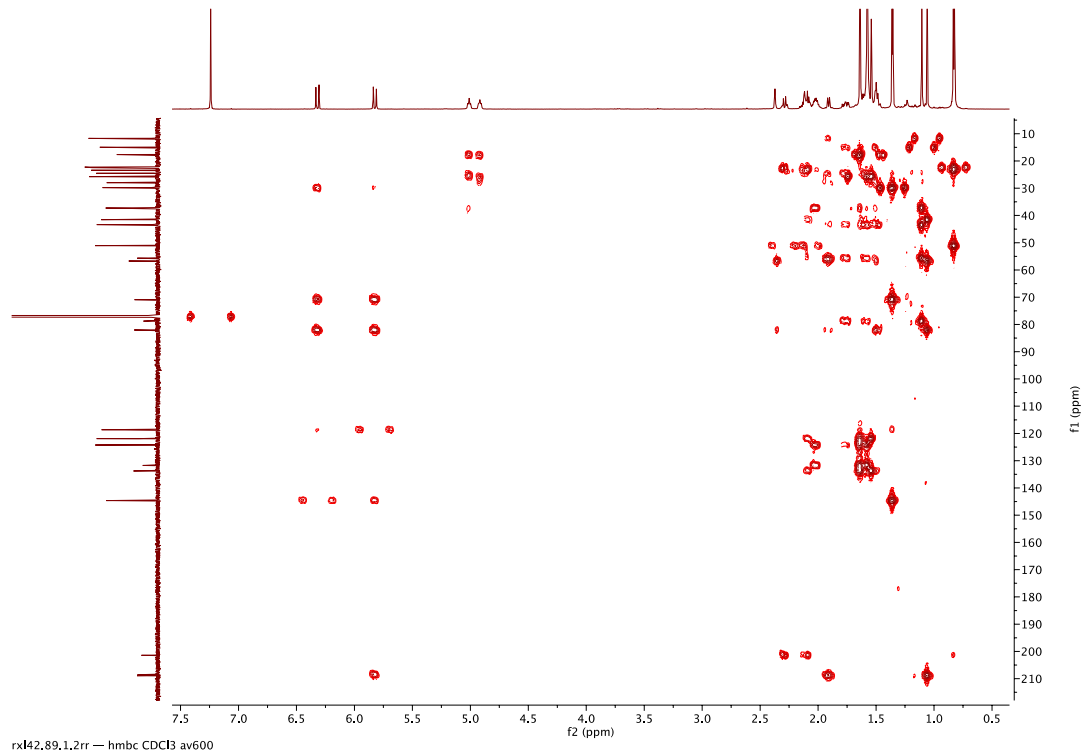


Figure S28. HMBC spectrum of ascynol G (**9**).

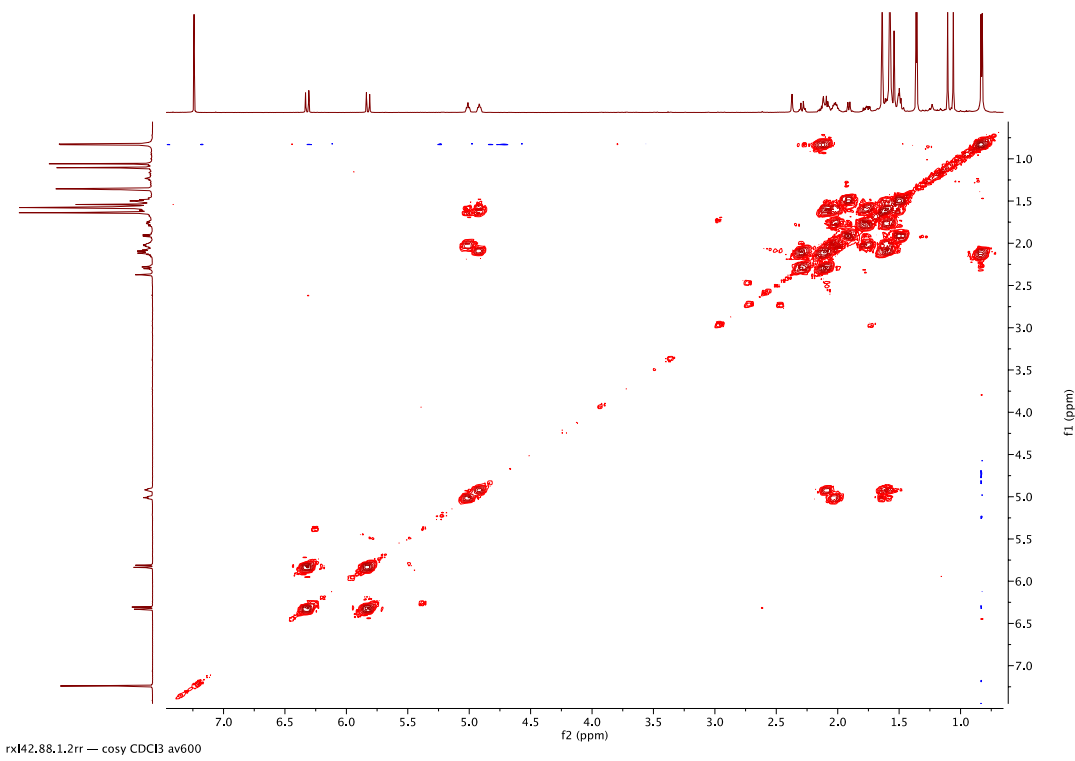


Figure S29. ^1H - ^1H COSY spectrum of ascynol G (9).

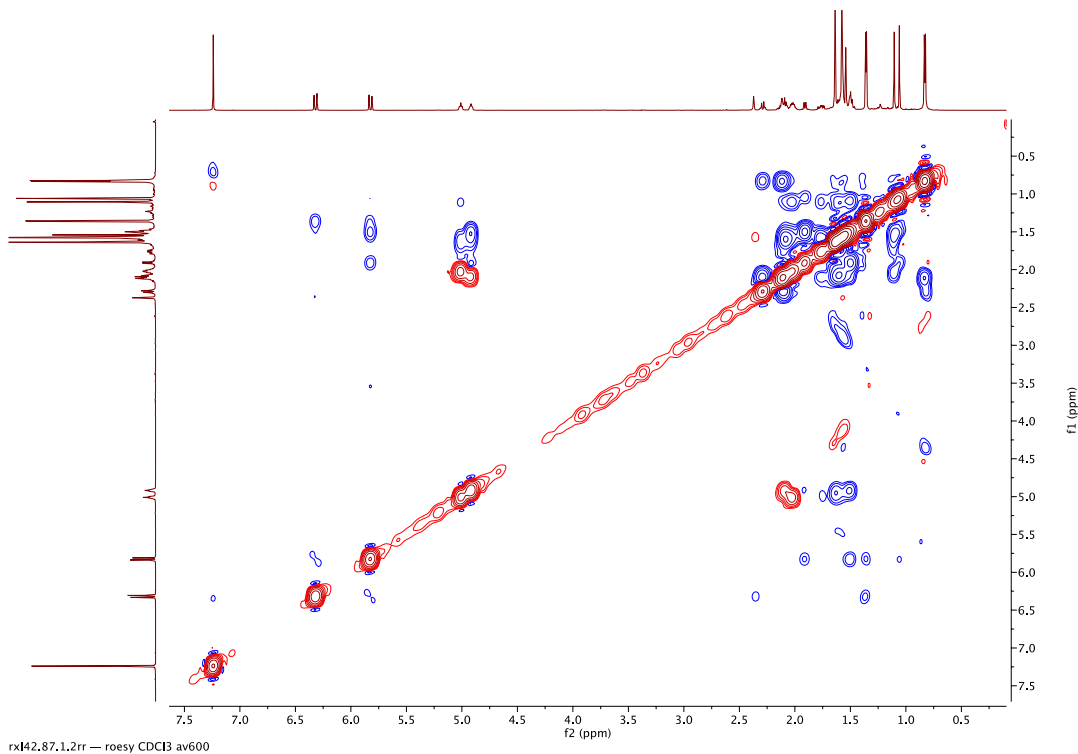


Figure S30. ROESY spectrum of ascynol G (9).

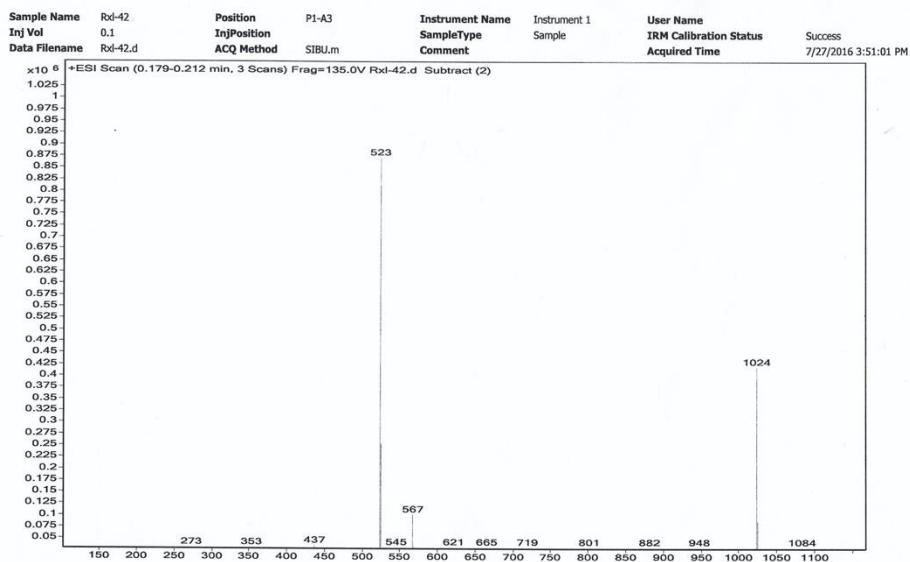


Figure S31. ESIMS spectrum of ascynol G (9).

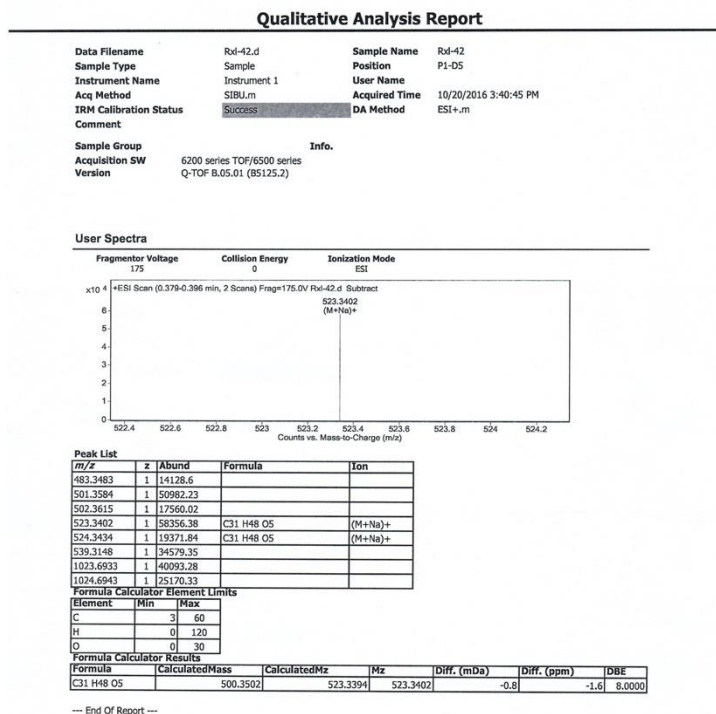


Figure S32. HRESIMS spectrum of ascynol G (9).

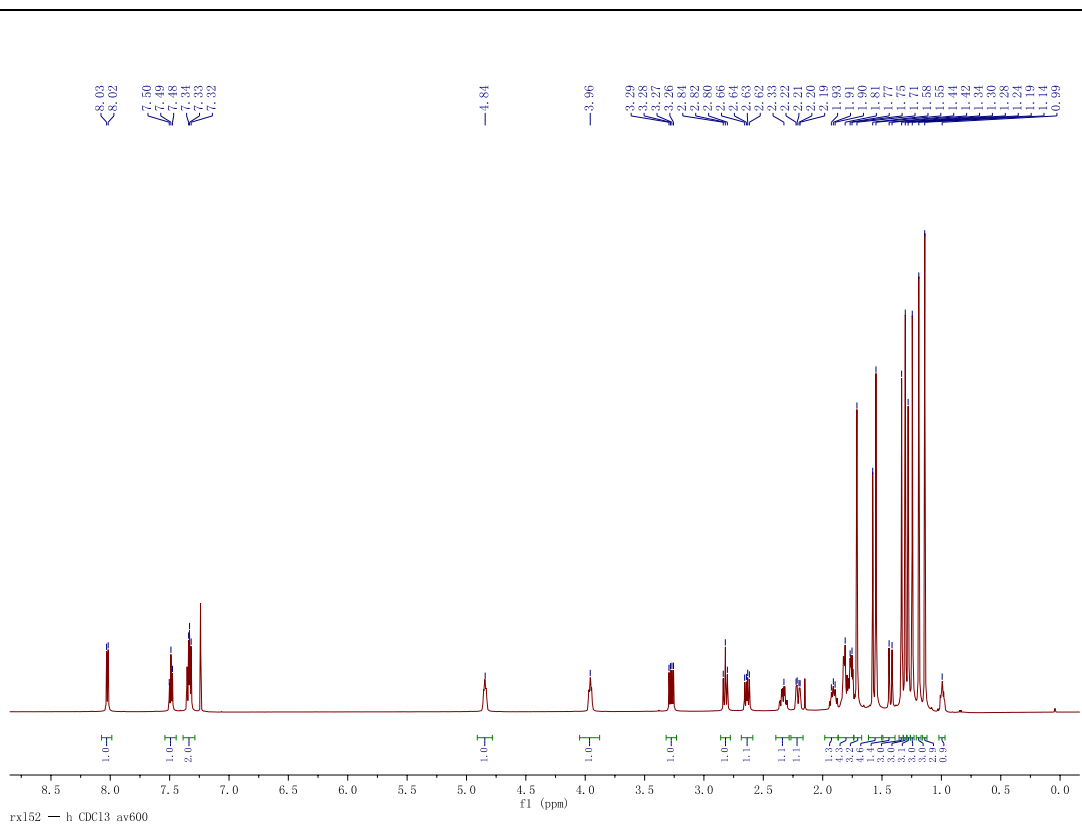


Figure S25. ^1H (in CDCl_3) spectrum of ascynol H (**10**).

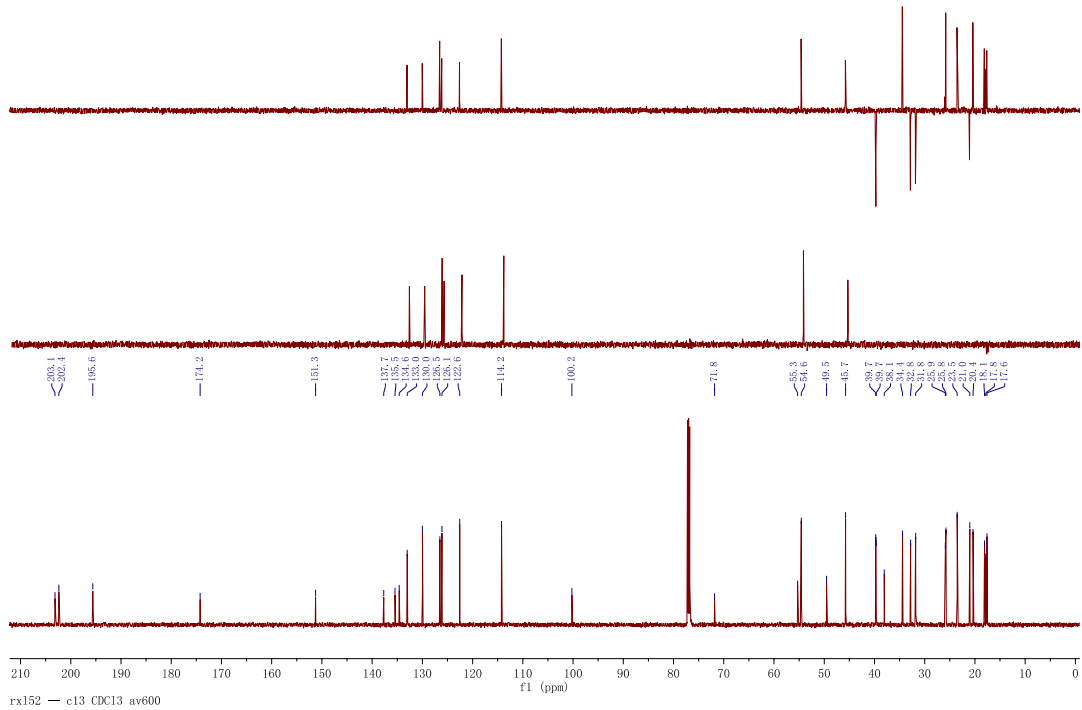


Figure S26. ^{13}C (in CDCl_3) spectrum of ascynol H (**10**).

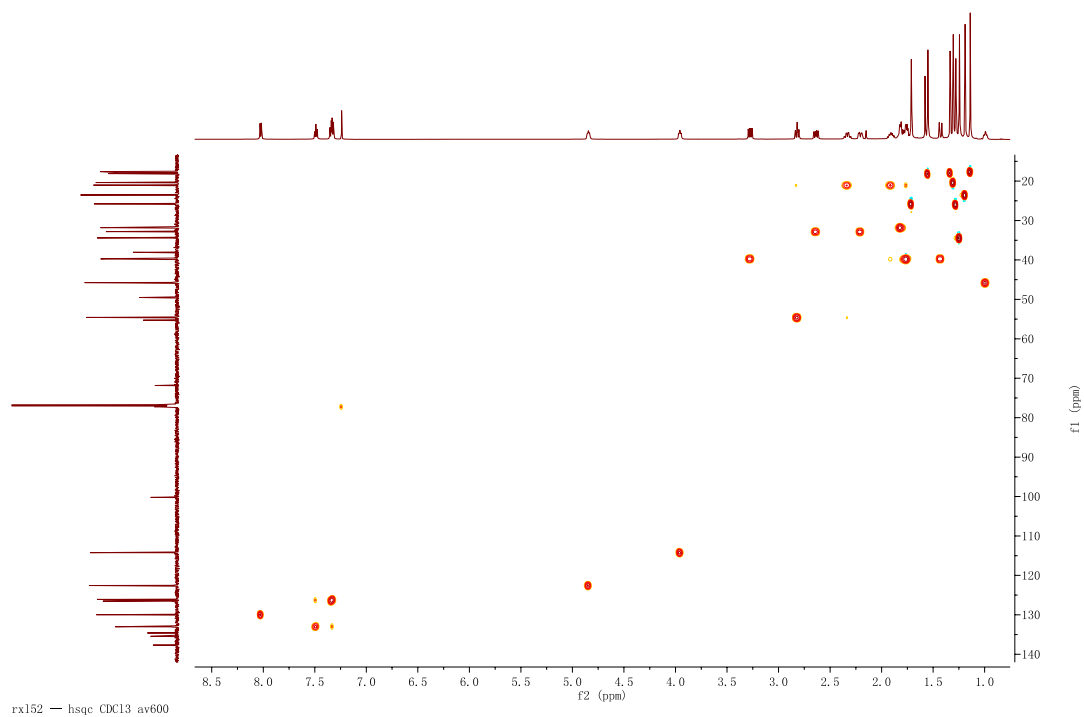


Figure S27. HSQC spectrum of ascynol H (**10**).

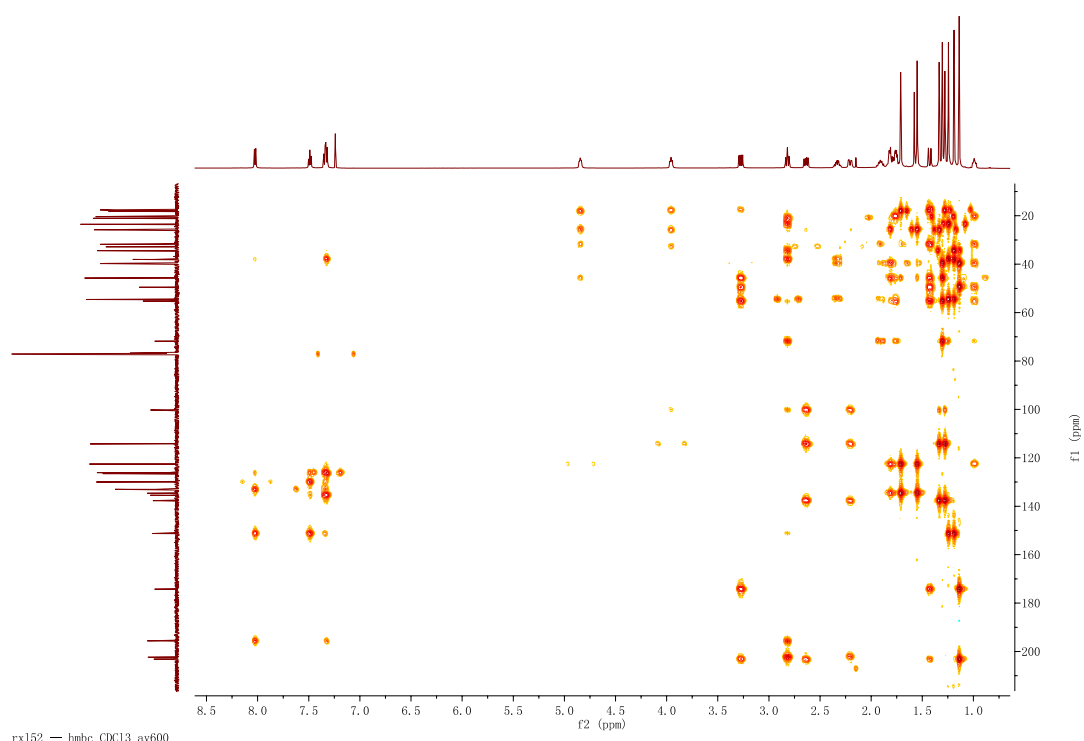


Figure S28. HMBC spectrum of ascynol H (**10**).

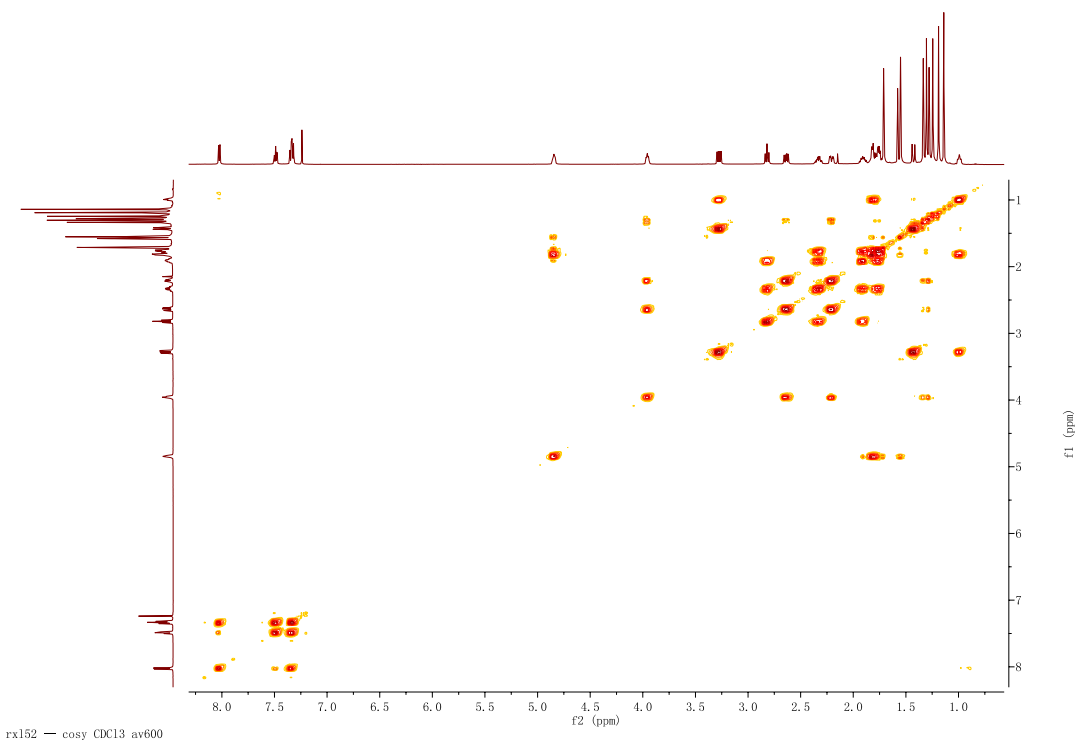


Figure S29 ¹H-¹H COSY spectrum of ascynol H (**10**).

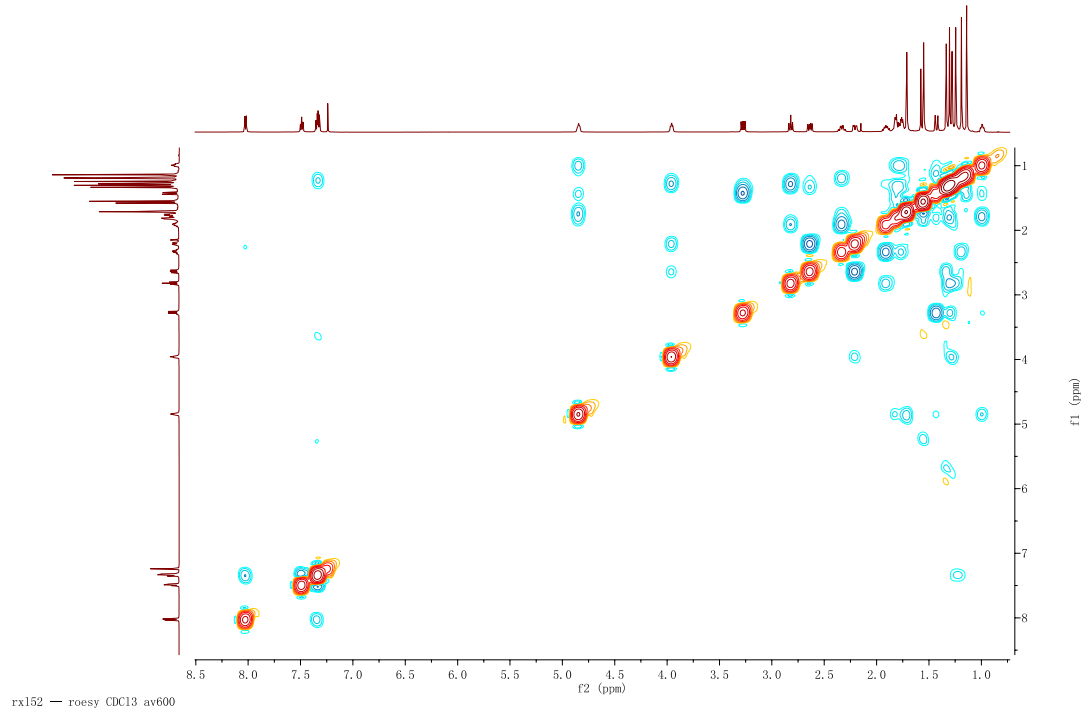


Figure S30. ROESY spectrum of ascynol H (**10**).

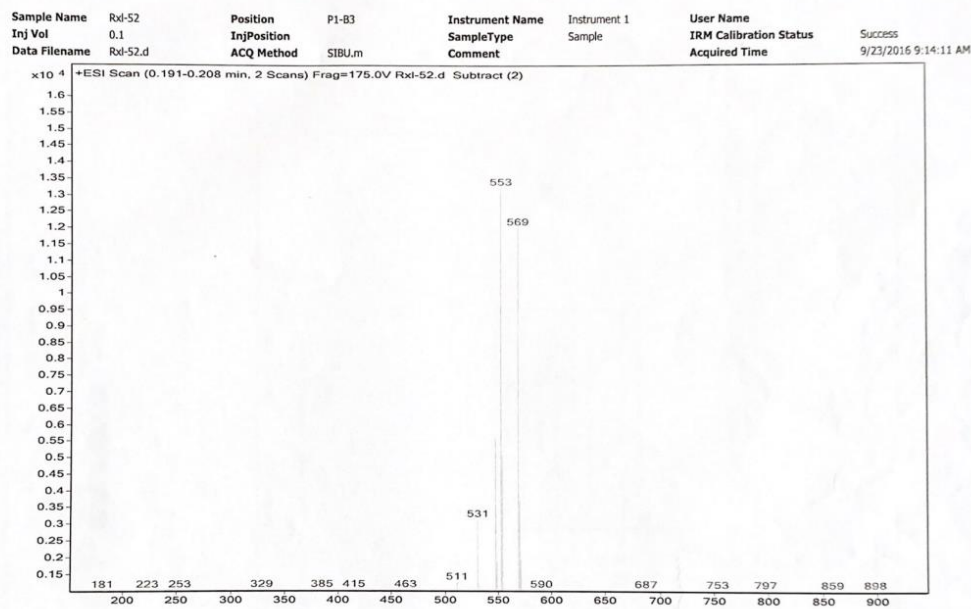


Figure S31. ESIMS spectrum of ascynol H (**10**).

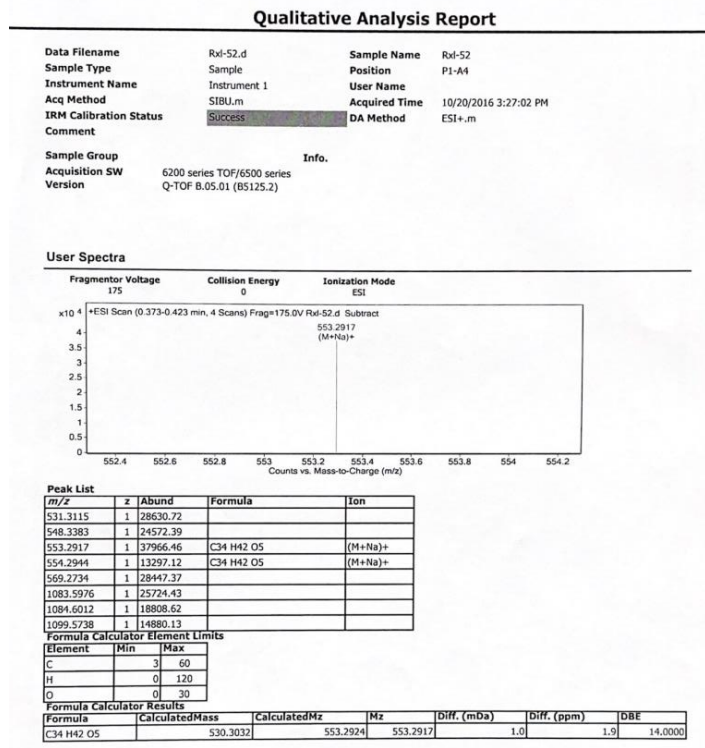


Figure S32. HRESIMS spectrum of ascynol H (**10**).

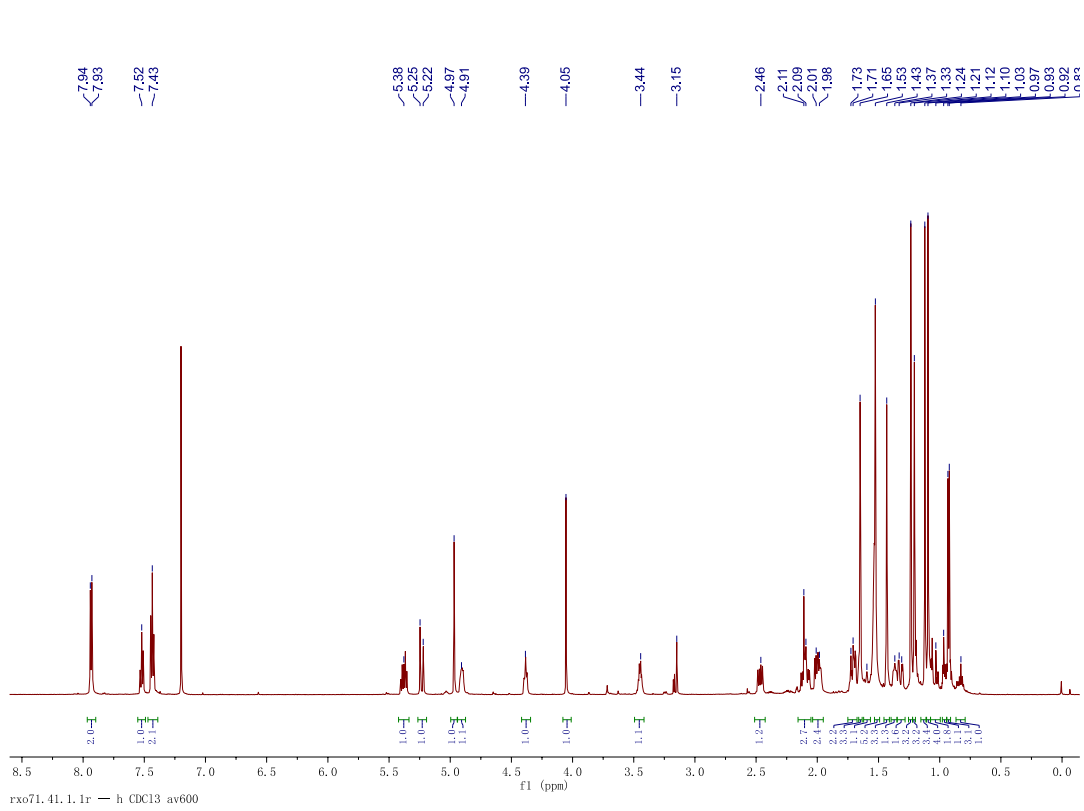


Figure S25. ^1H (in CDCl_3) spectrum of ascynol I (**11**).

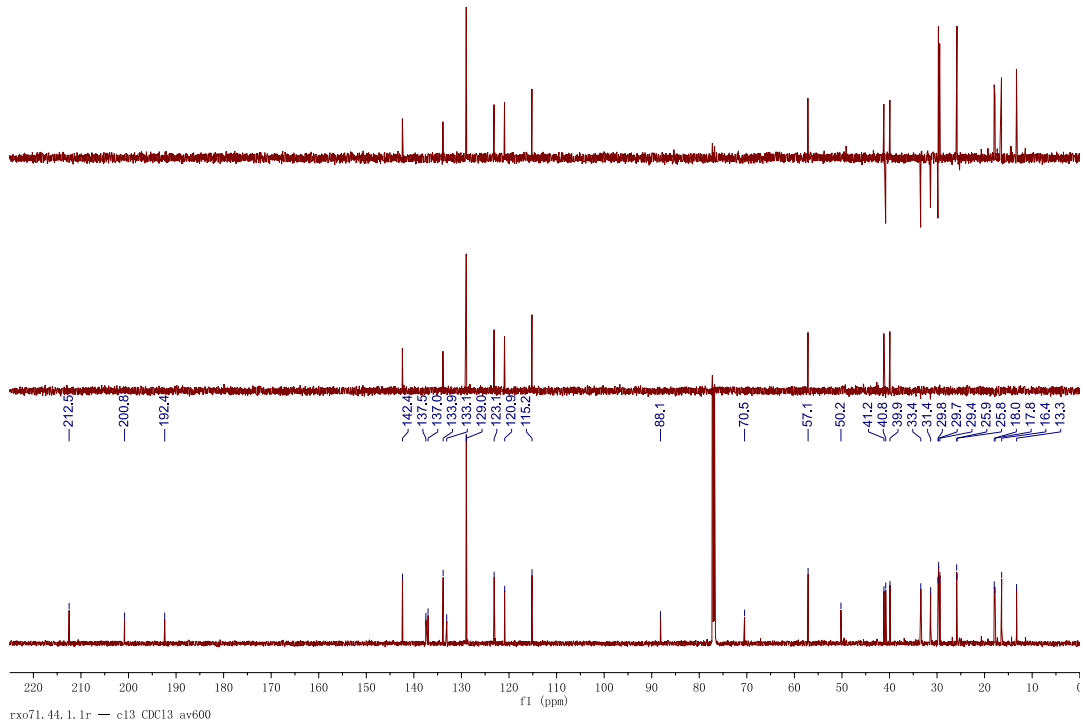


Figure S26. ^{13}C (in CDCl_3) spectrum of ascynol I (**11**).

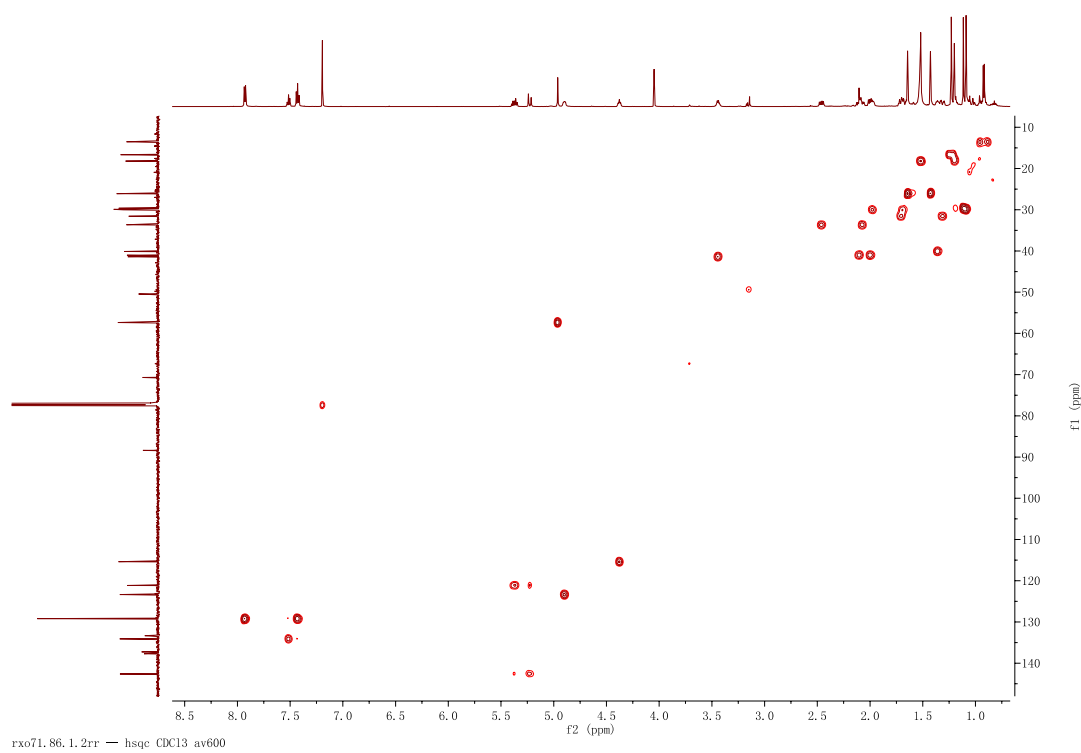


Figure S27. HSQC spectrum of ascynol I (**11**).

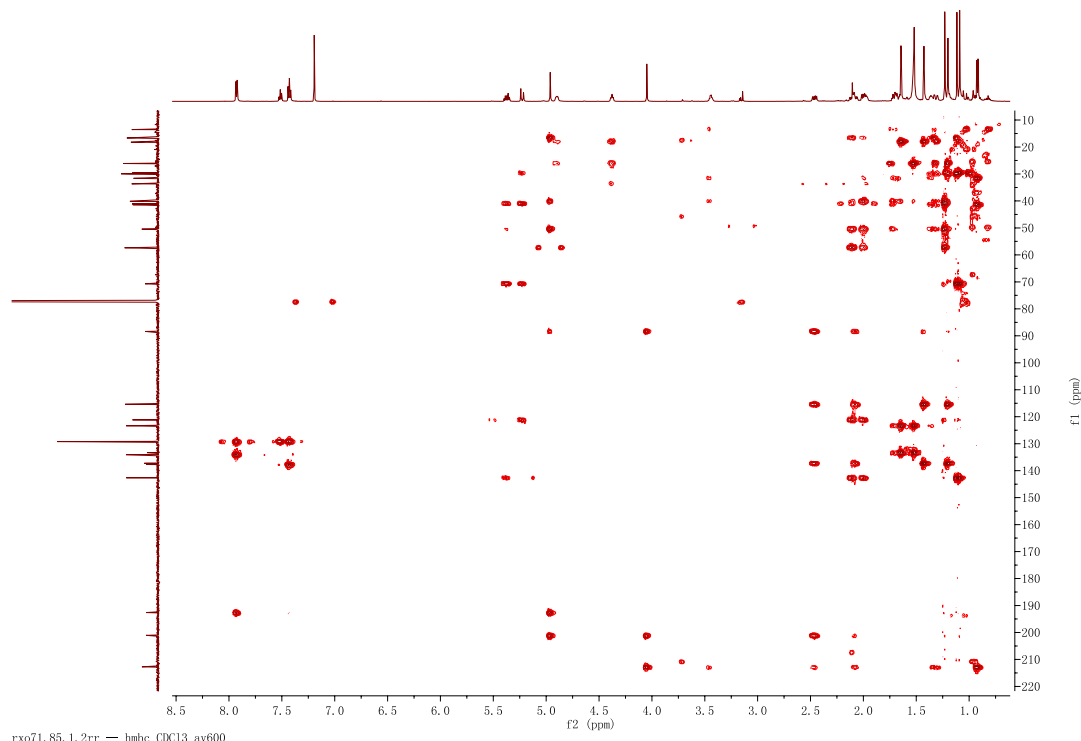


Figure S28. HMBC spectrum of ascynol I (**11**).

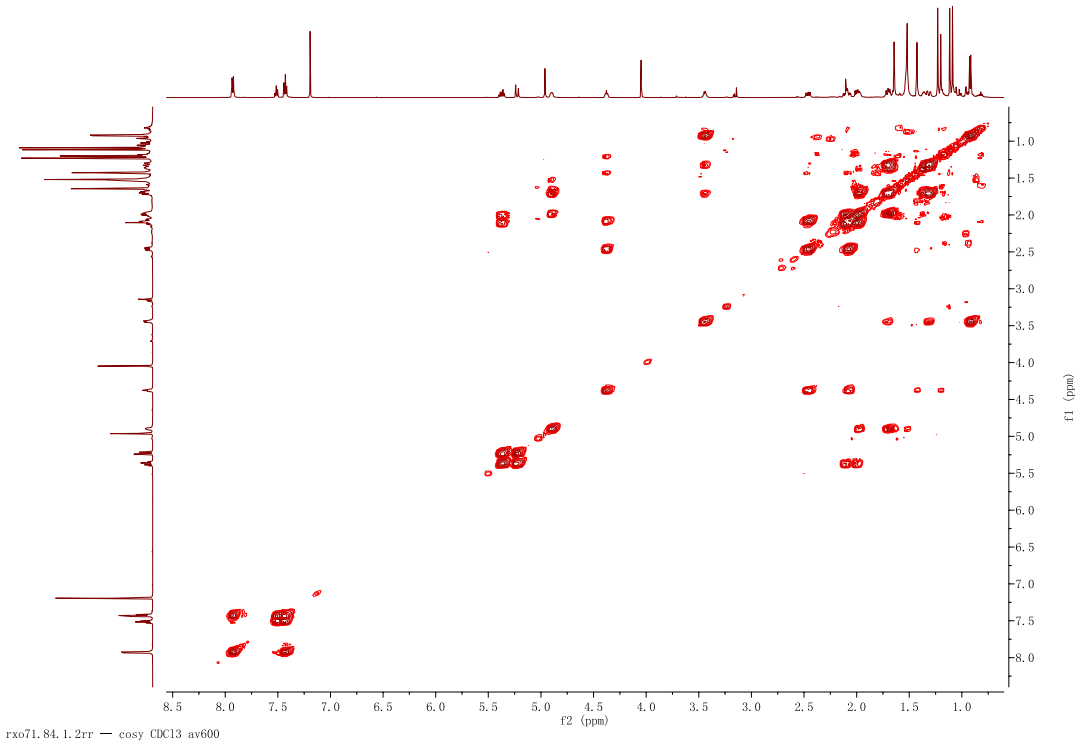


Figure S29 ¹H-¹H COSY spectrum of ascynol I (11).

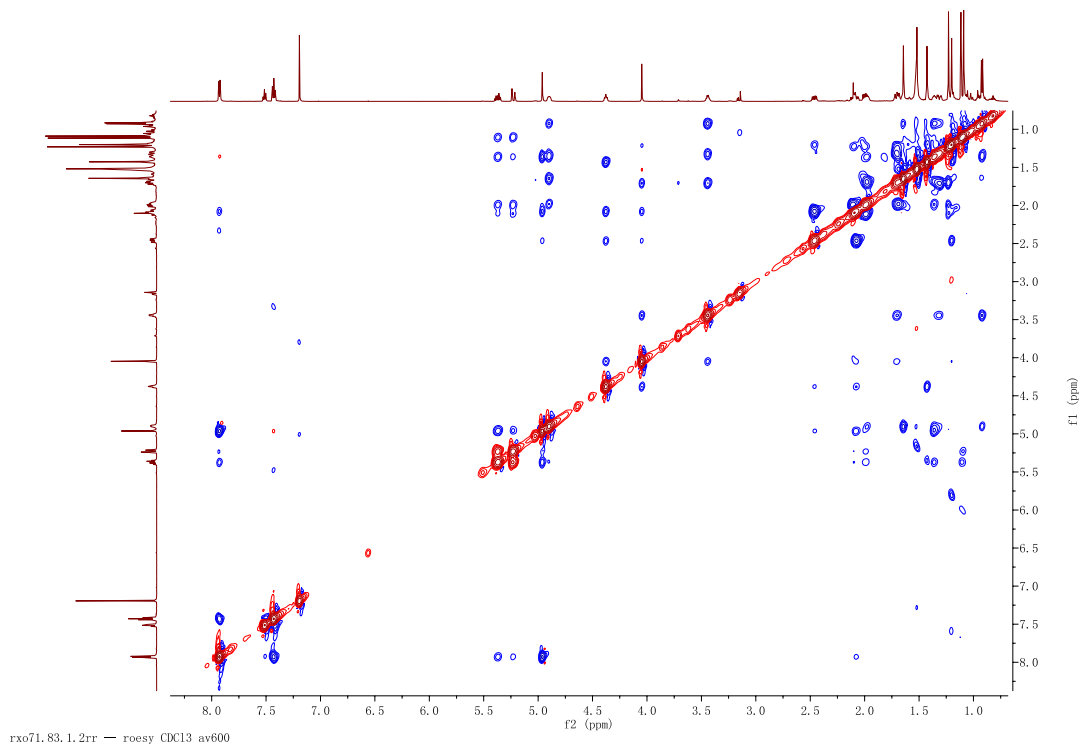


Figure S30. ROESY spectrum of ascynol I (11).

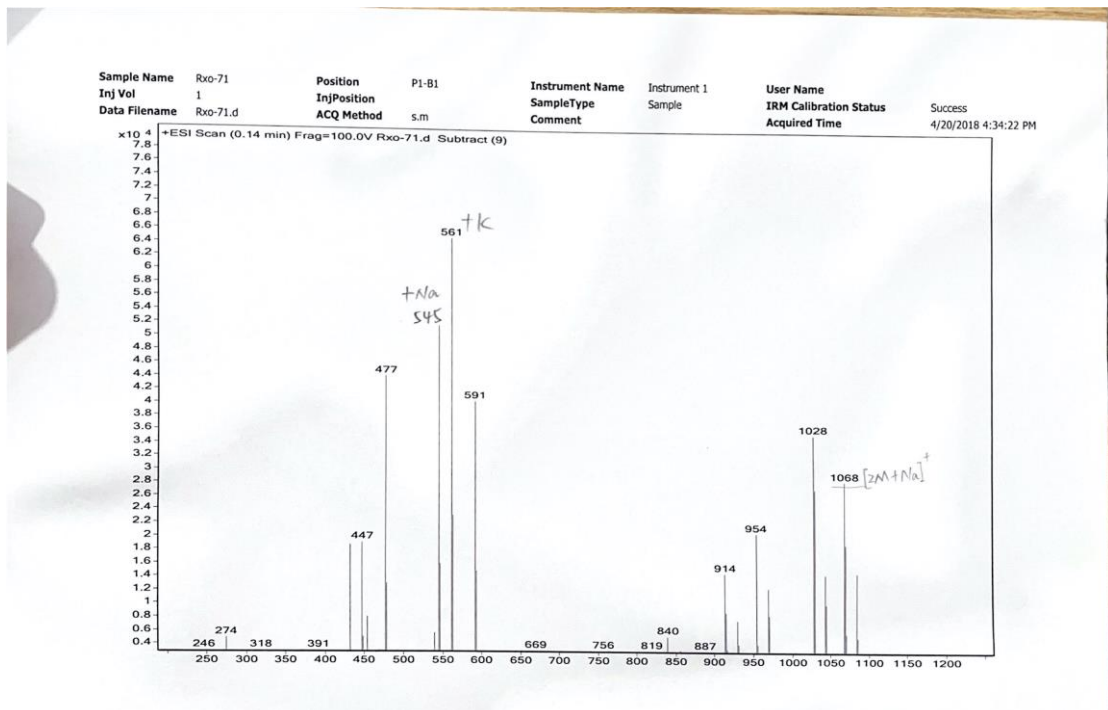


Figure S31. ESIMS spectrum of ascynol I (**11**).

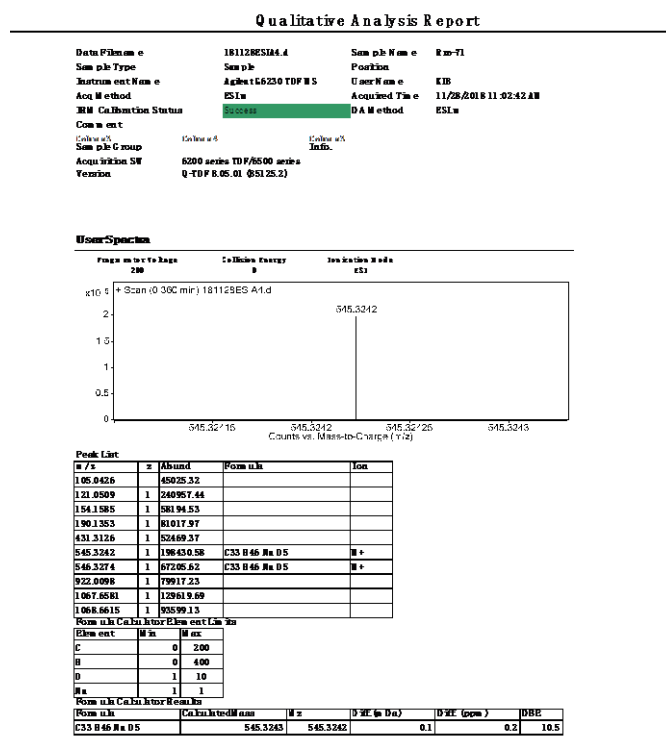


Figure S32. HRESIMS spectrum of ascynol I (**11**).

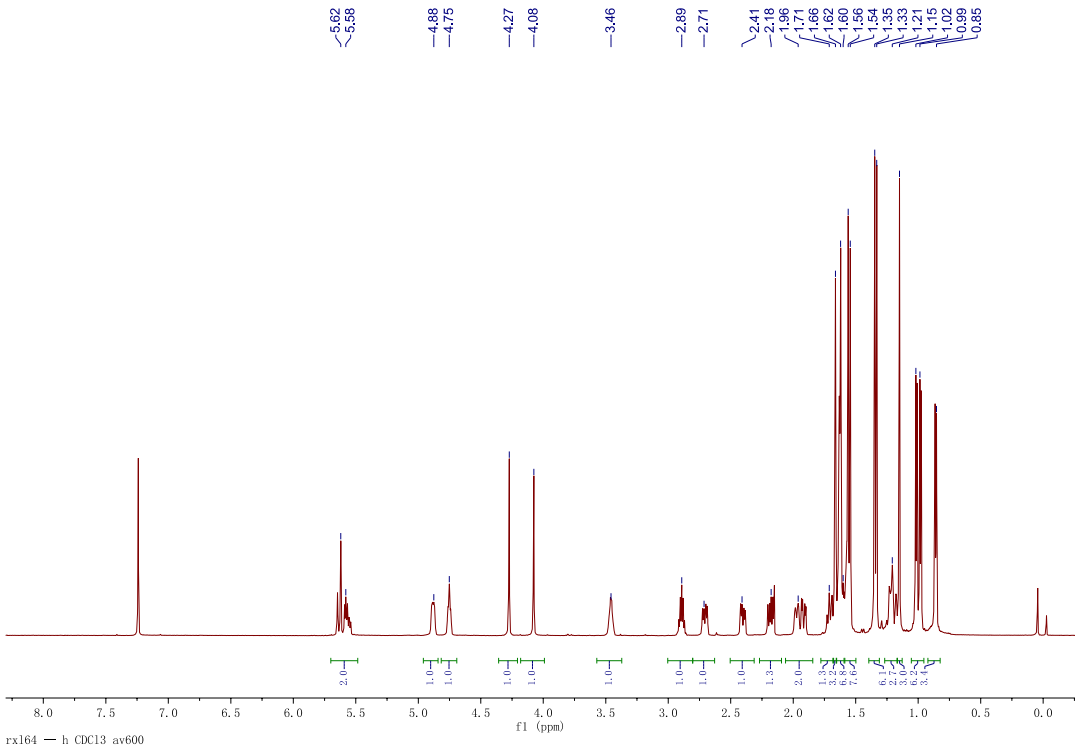


Figure S25. ¹H (in CDCl₃) spectrum of ascynol J (**12**).

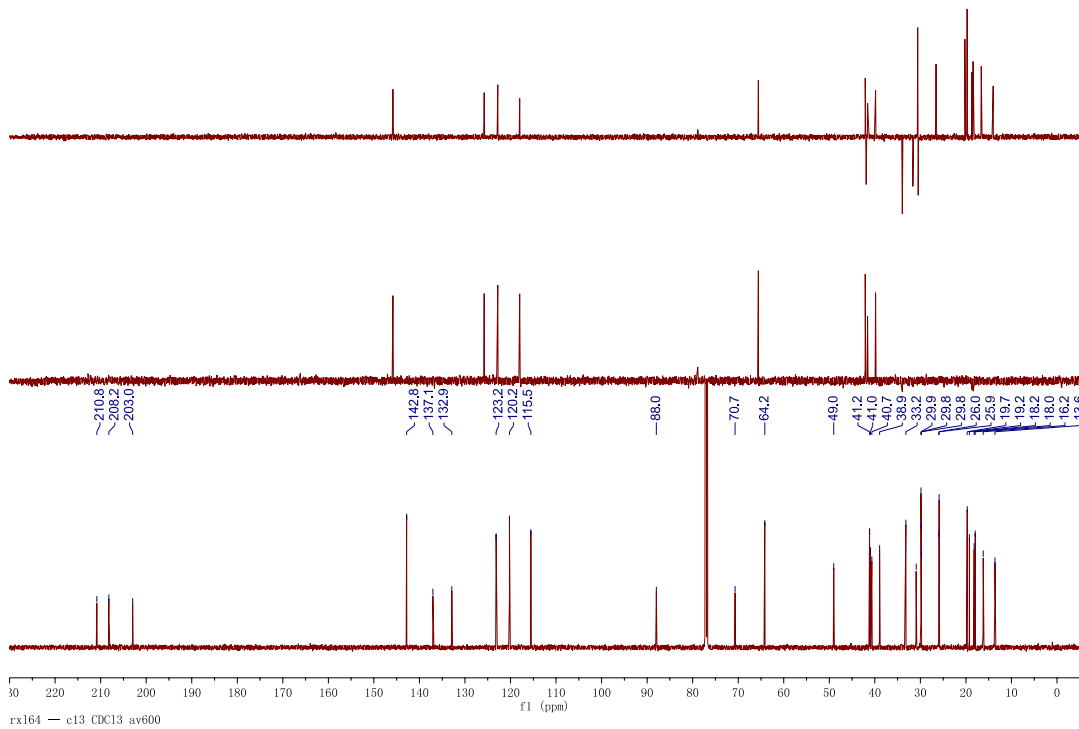


Figure S26. ¹³C (in CDCl₃) spectrum of ascynol J (**12**).

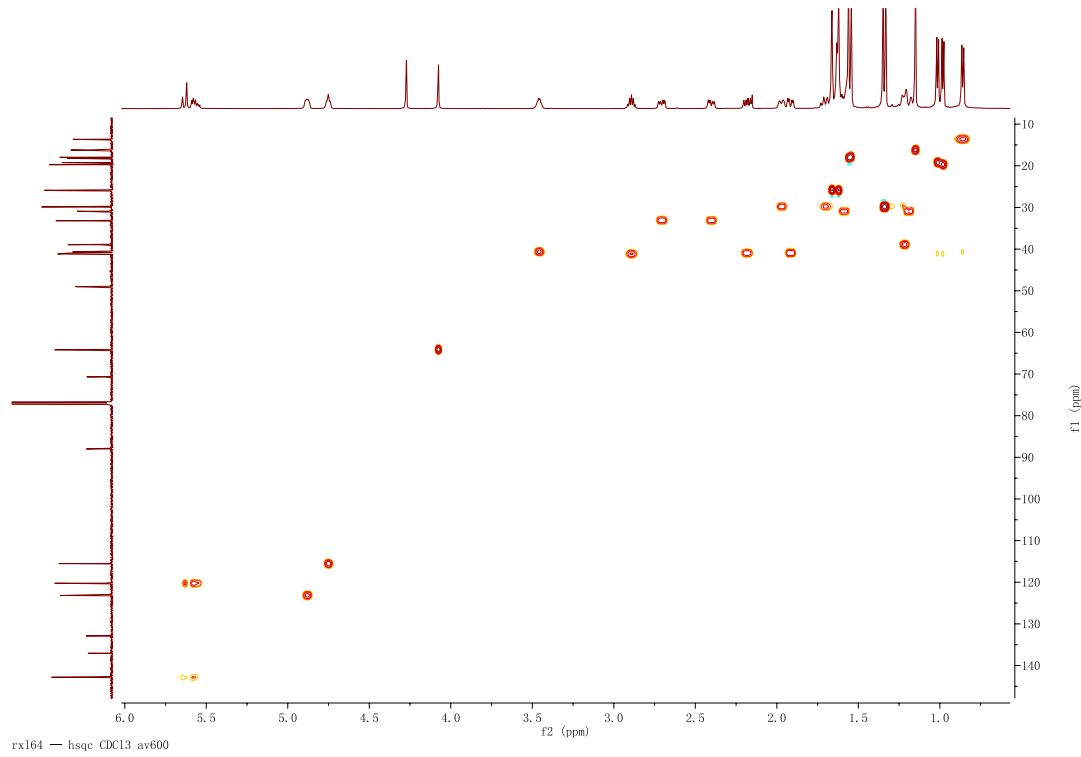


Figure S27. HSQC spectrum of ascynol J (**12**).

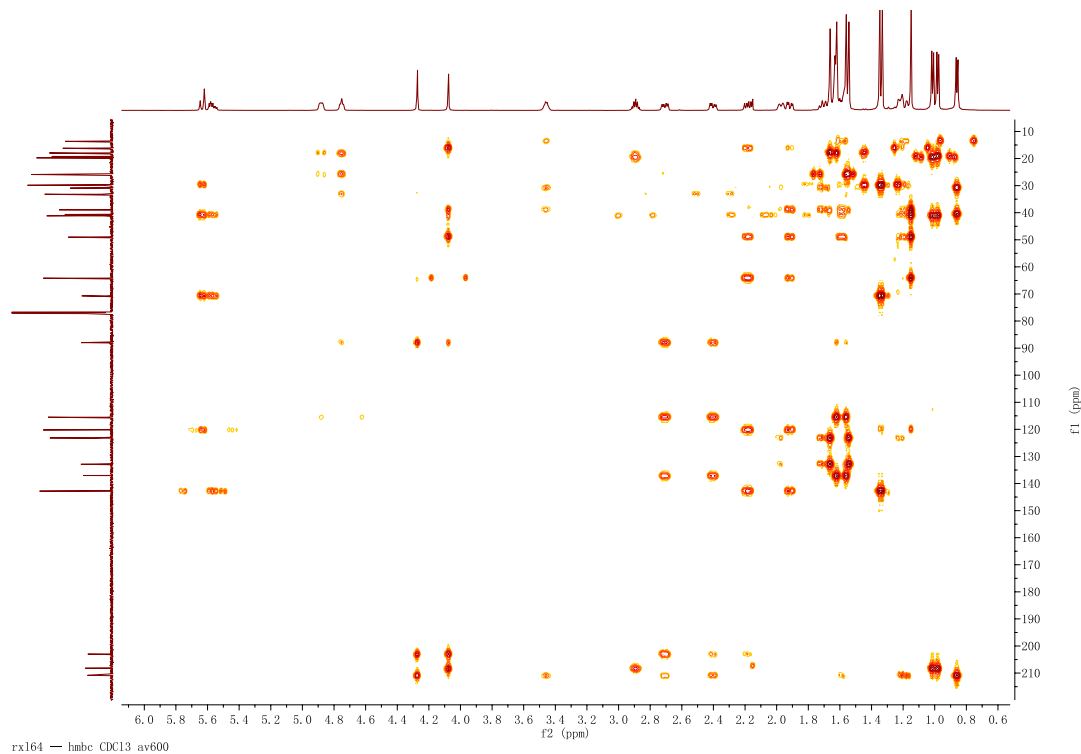


Figure S28. HMBC spectrum of ascynol J (**12**).

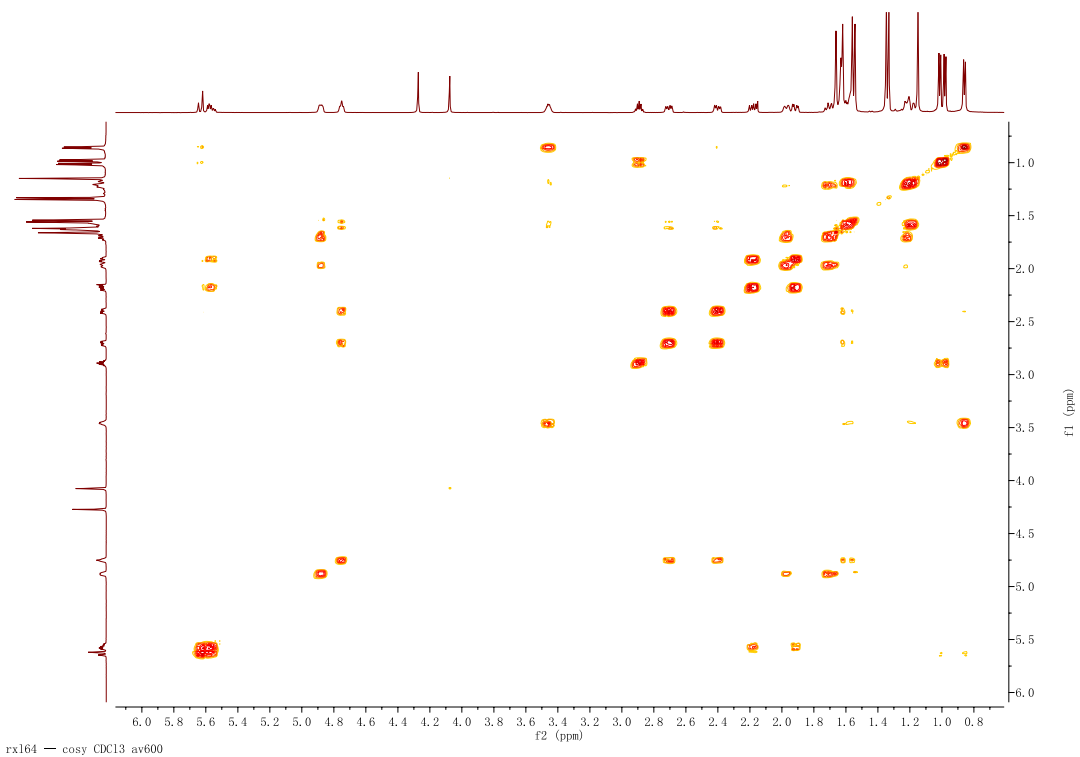


Figure S29 ^1H - ^1H COSY spectrum of ascynol J (**12**).

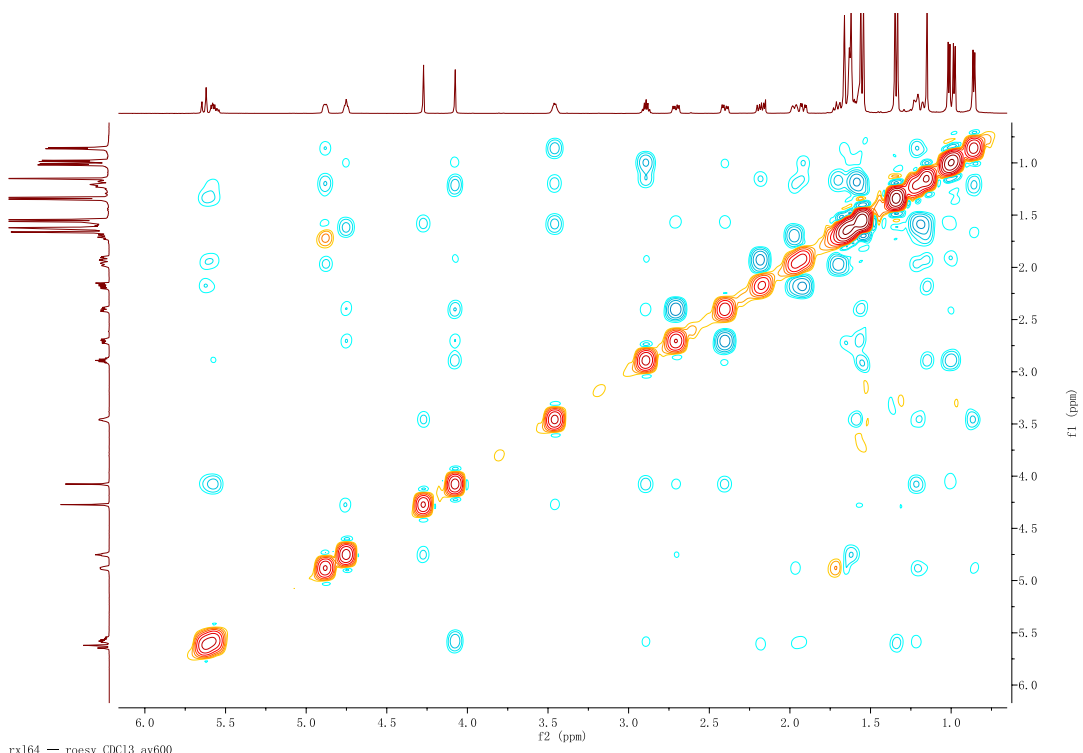


Figure S30. ROESY spectrum of ascynol J (**12**).

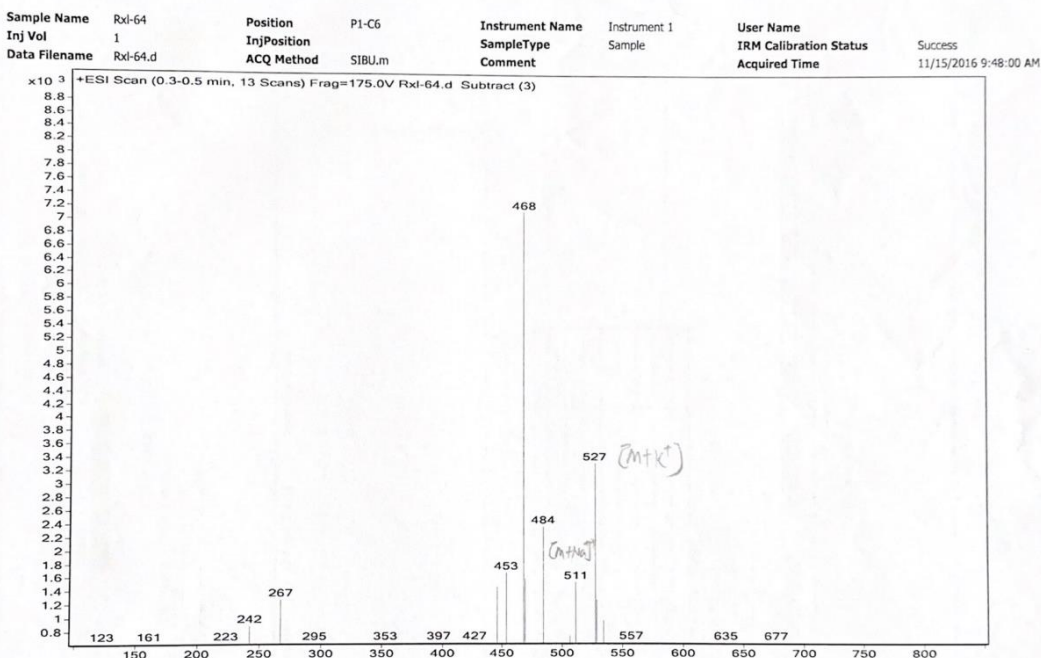


Figure S31. ESIMS spectrum of ascynol J (12).

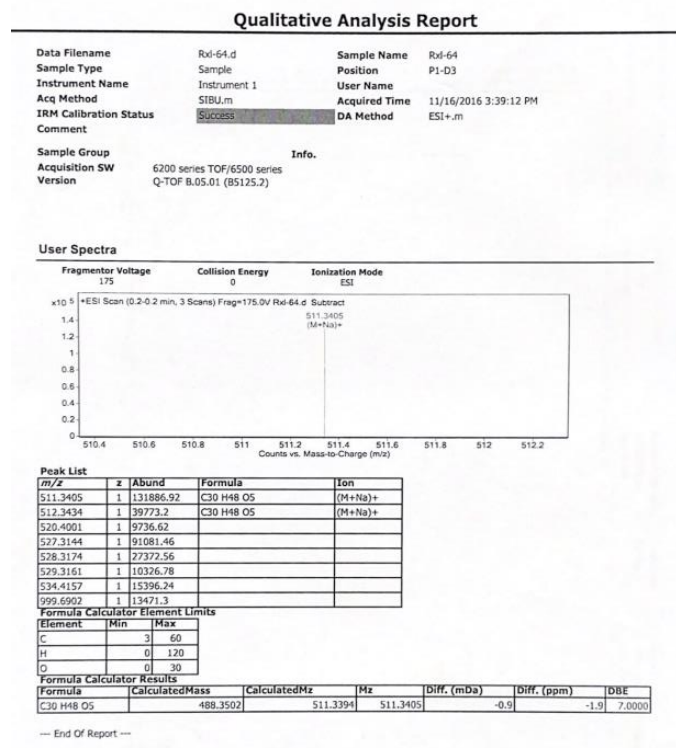


Figure S32. HRESIMS spectrum of ascynol J (12).

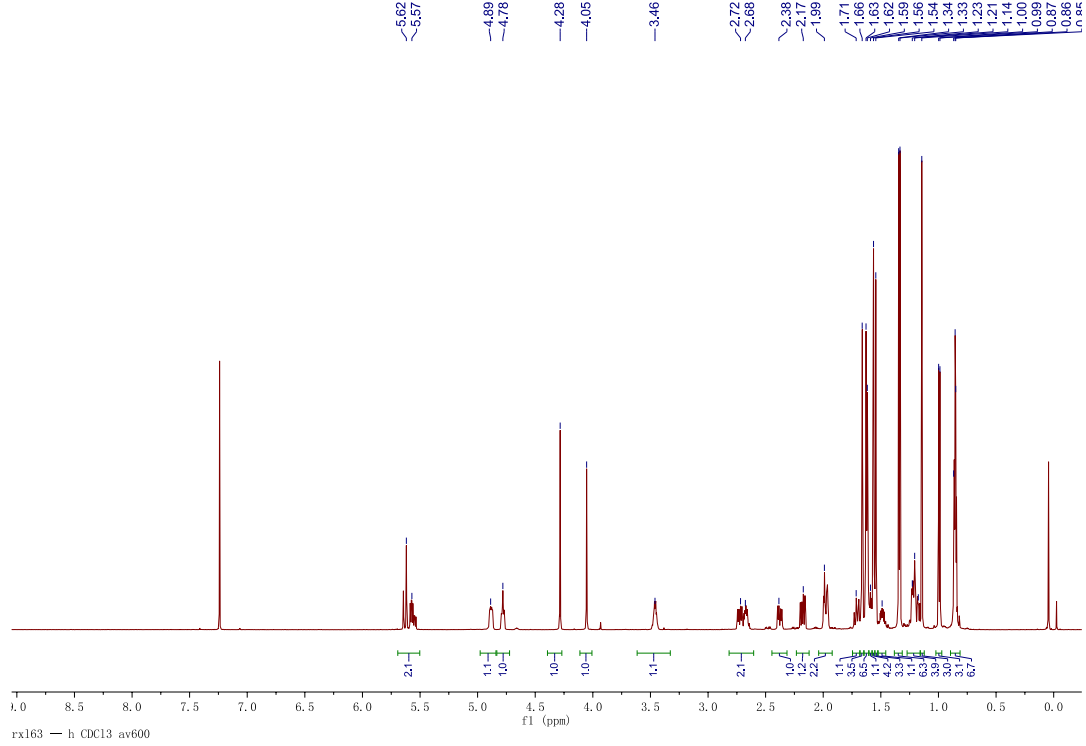


Figure S25. ¹H (in CDCl₃) spectrum of ascynol K (**13**).

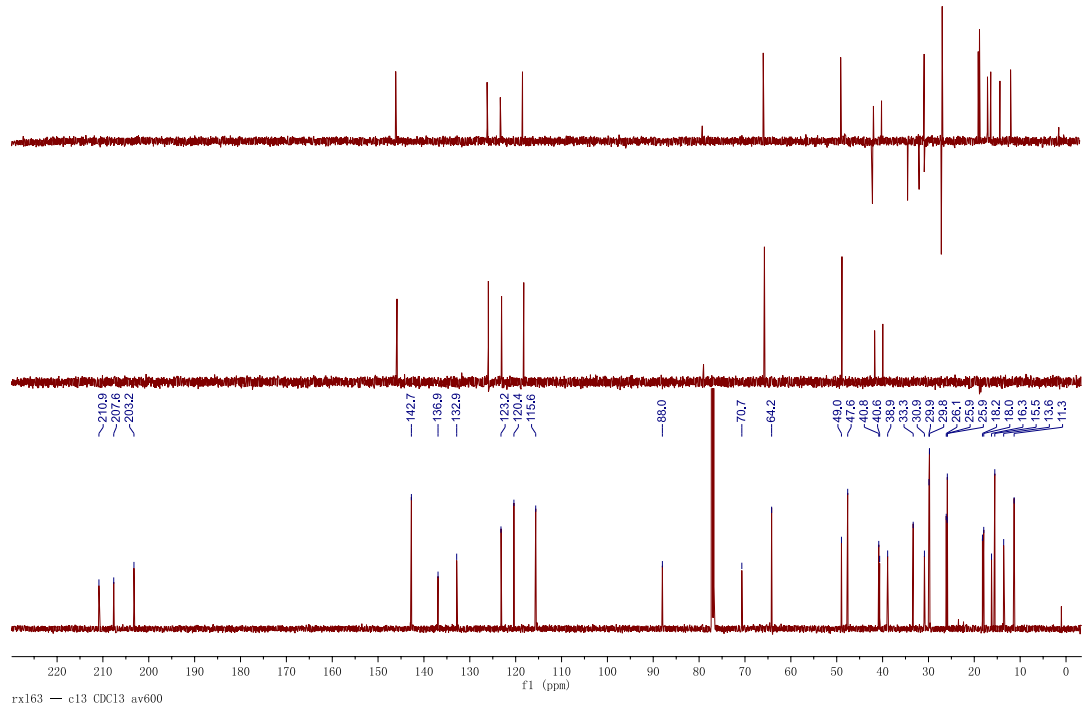


Figure S26. ¹³C (in CDCl₃) spectrum of ascynol K (**13**).

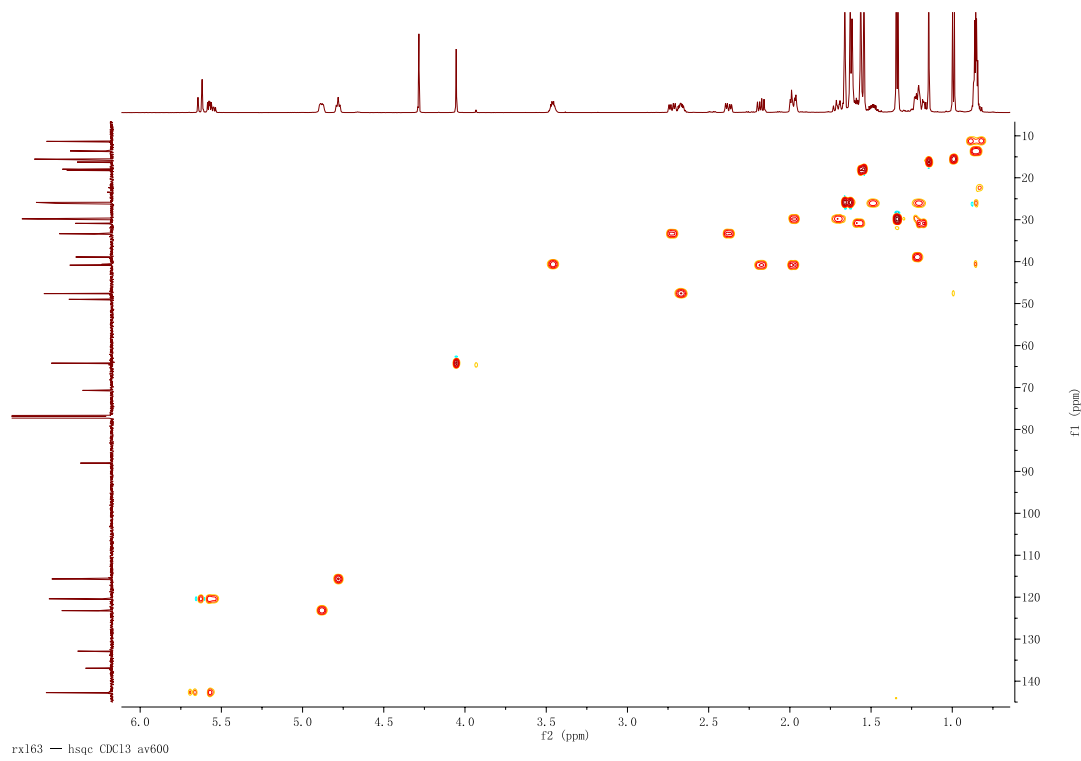


Figure S27. HSQC spectrum of ascynol K (**13**).

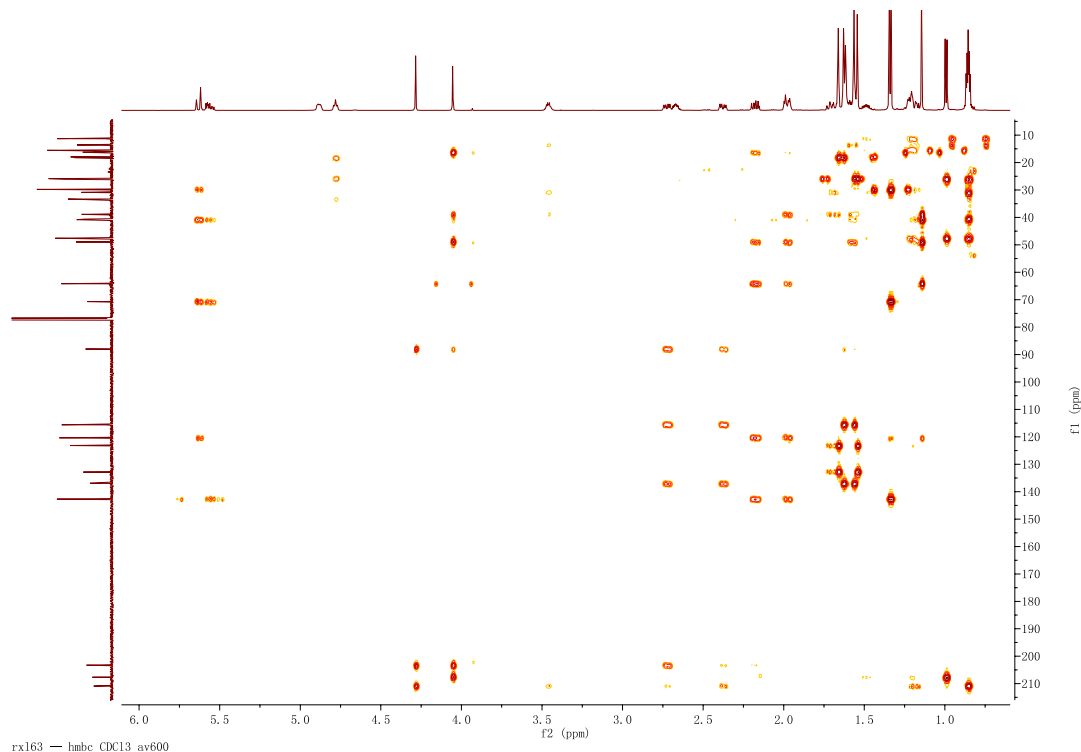


Figure S28. HMBC spectrum of ascynol K (**13**).

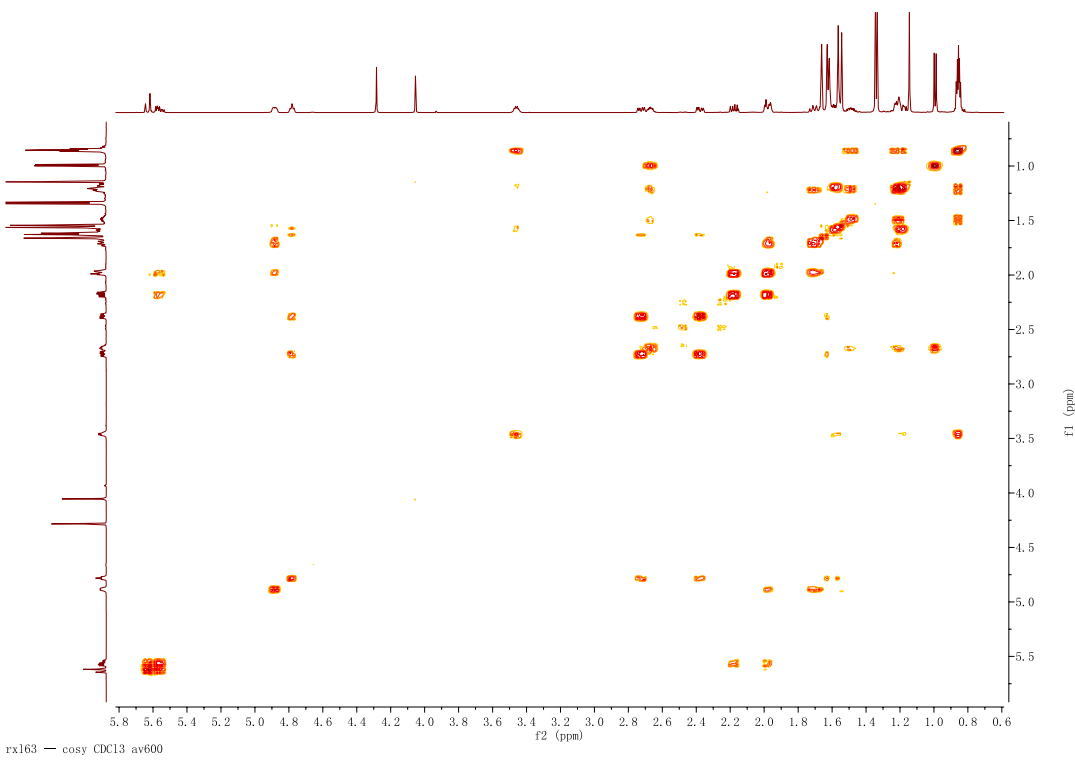


Figure S29 ^1H - ^1H COSY spectrum of ascynol K (**13**).

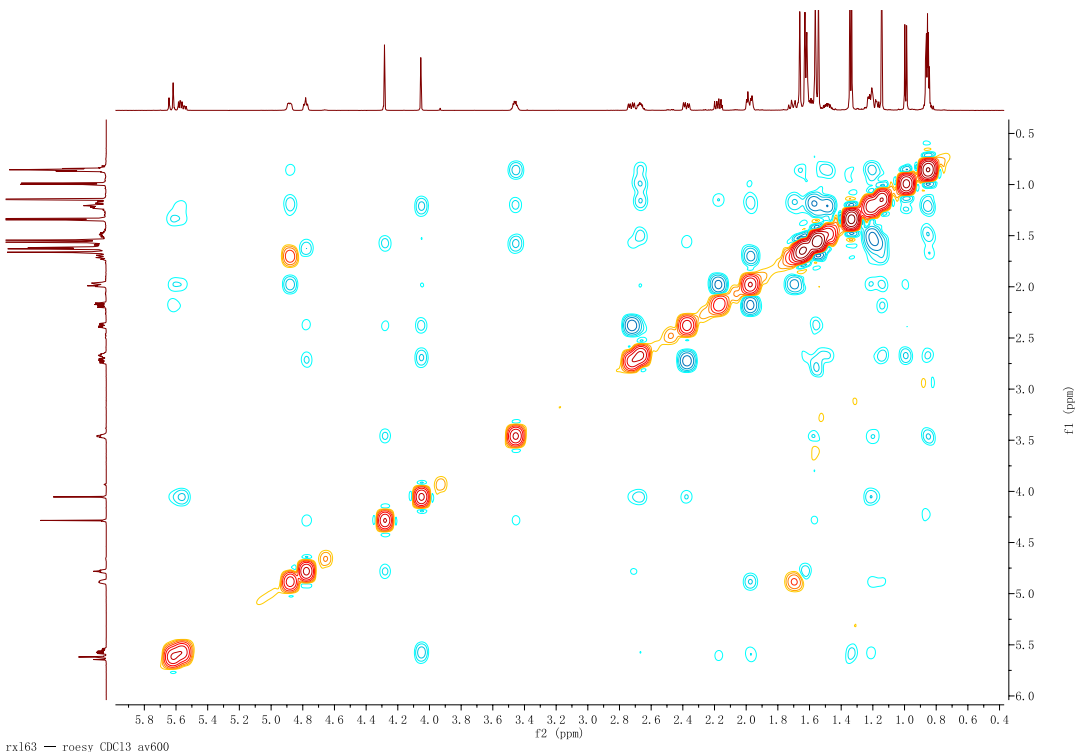


Figure S30. ROESY spectrum of ascynol K (**13**).

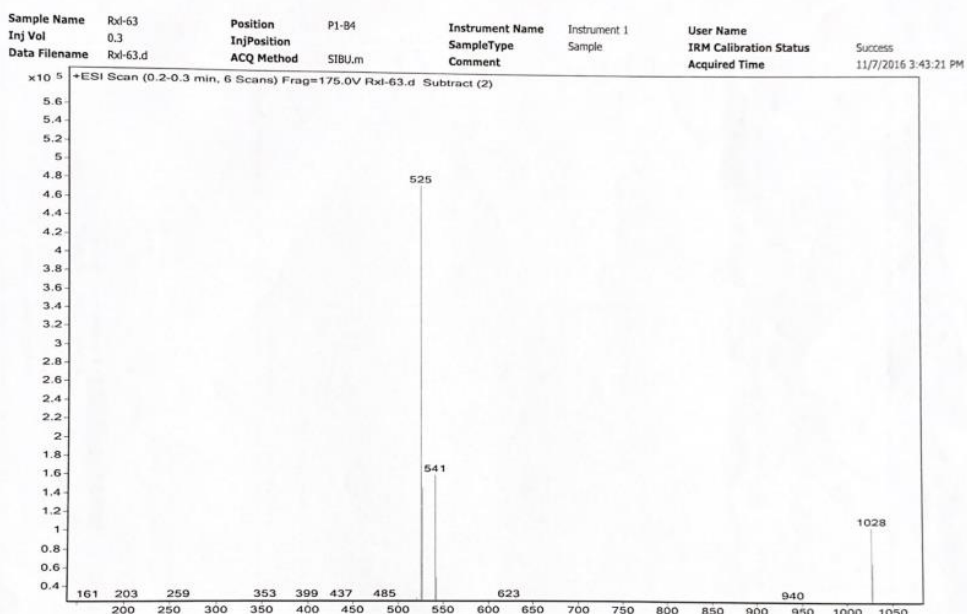
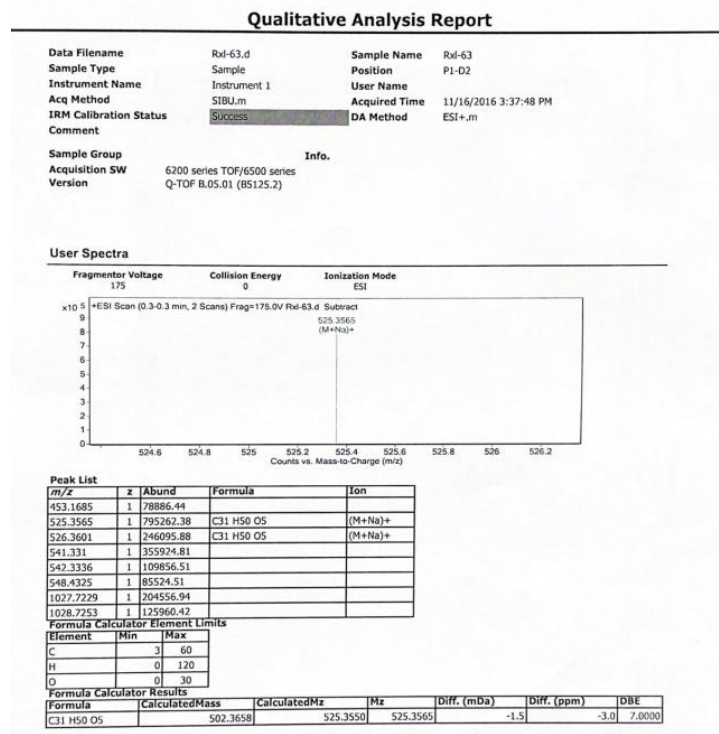


Figure S31. ESIMS spectrum of ascynol K (13).



Agilent Technologies Page 1 of 1 Printed at: 3:41 PM on: 11/16/2016

Figure S32. HRESIMS spectrum of ascynol K (13).

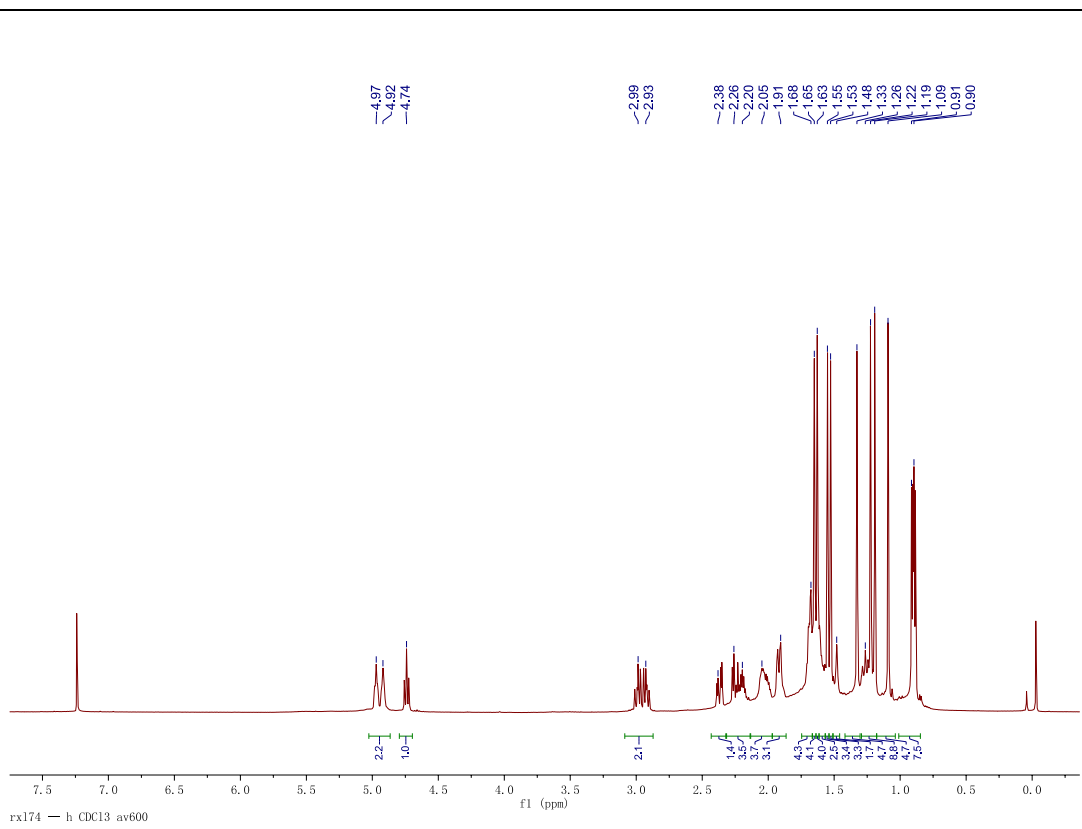


Figure S25. ¹H (in CDCl₃) spectrum of ascynol L (**14**).

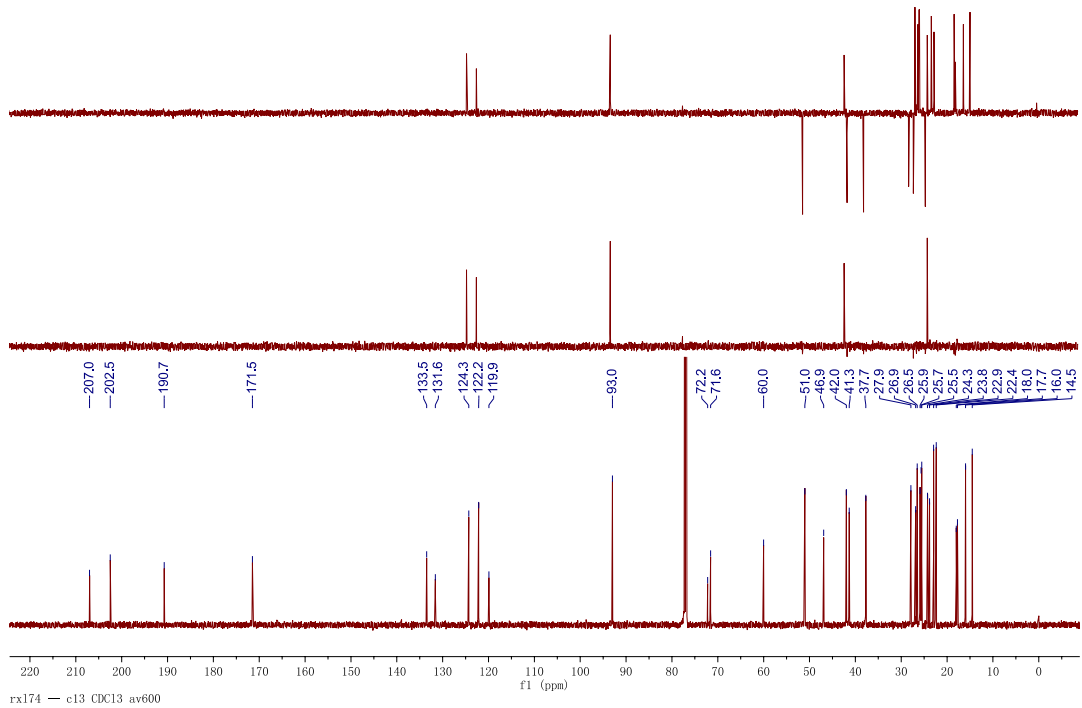


Figure S26. ¹³C (in CDCl₃) spectrum of ascynol L (**14**).

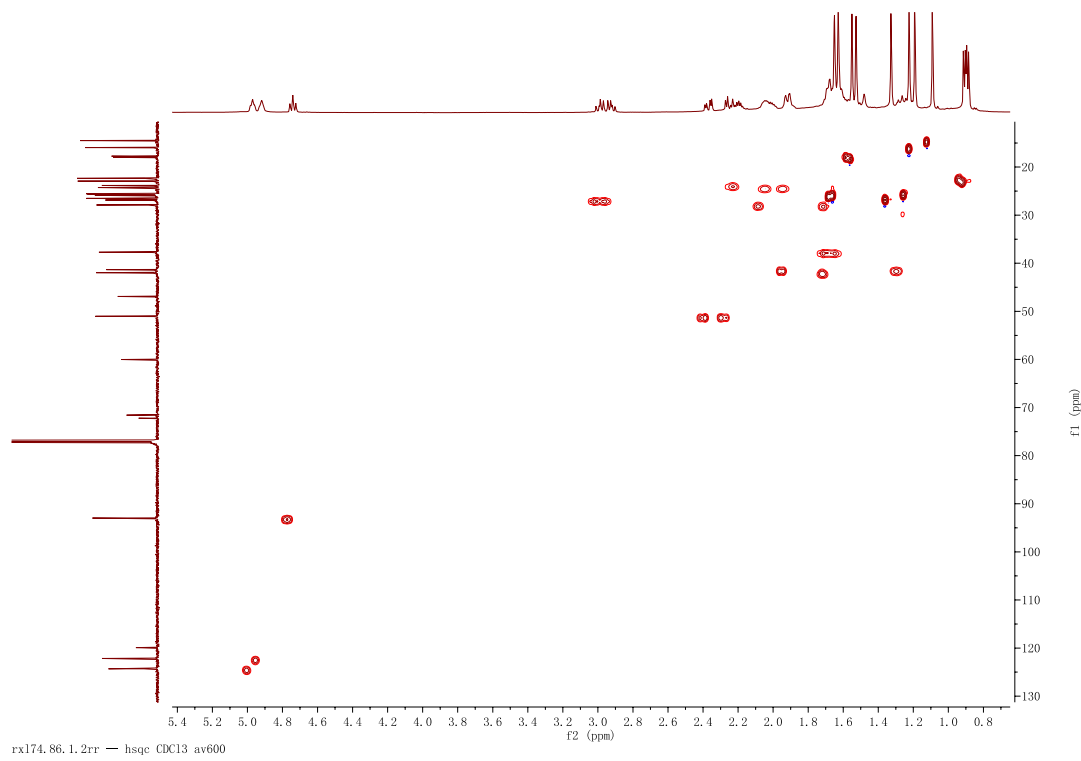


Figure S27. HSQC spectrum of ascynol L (**14**).

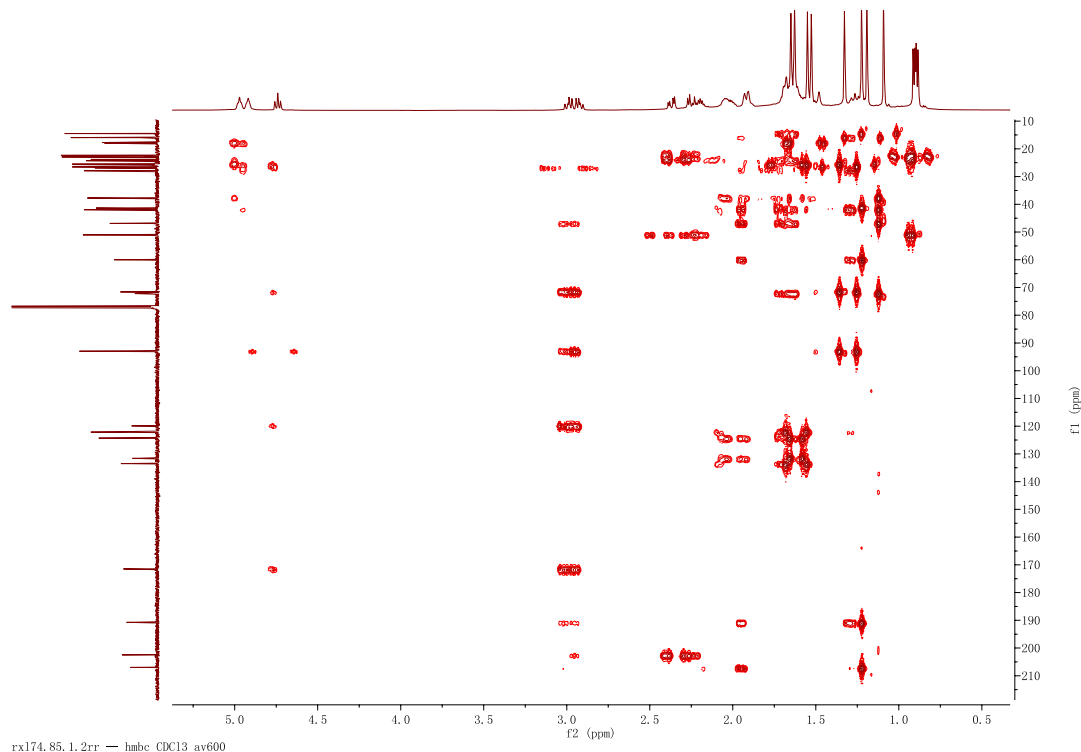


Figure S28. HMBC spectrum of ascynol L (**14**).

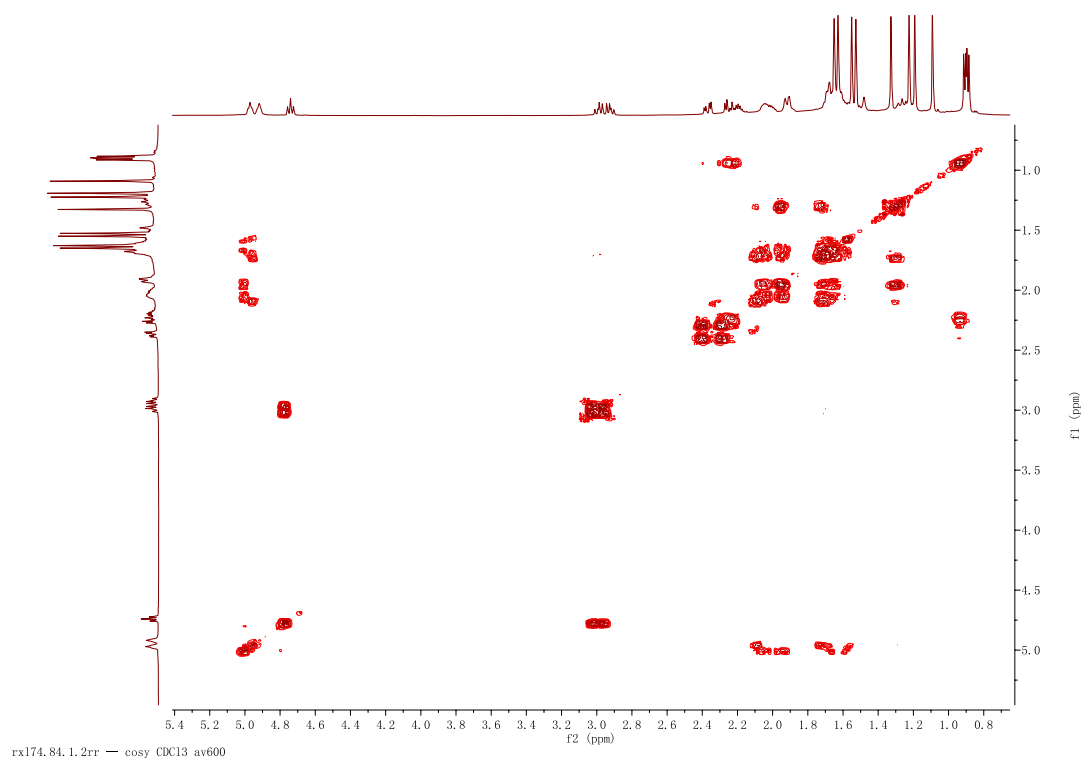


Figure S29 ¹H-¹H COSY spectrum of ascynol L (14).

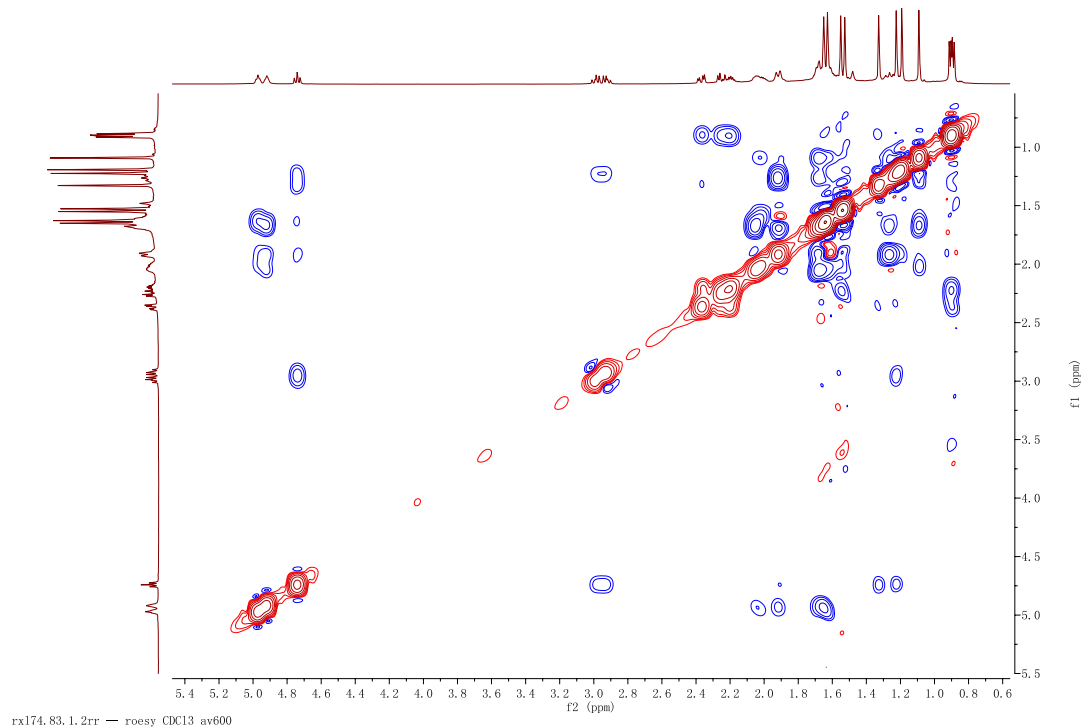


Figure S30. ROESY spectrum of ascynol L (14).

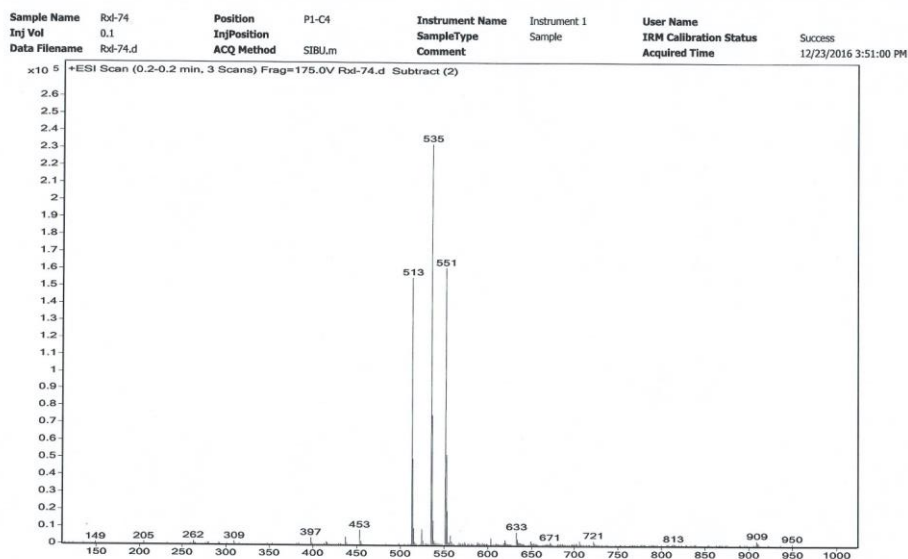


Figure S31. ESIMS spectrum of ascynol L (14).

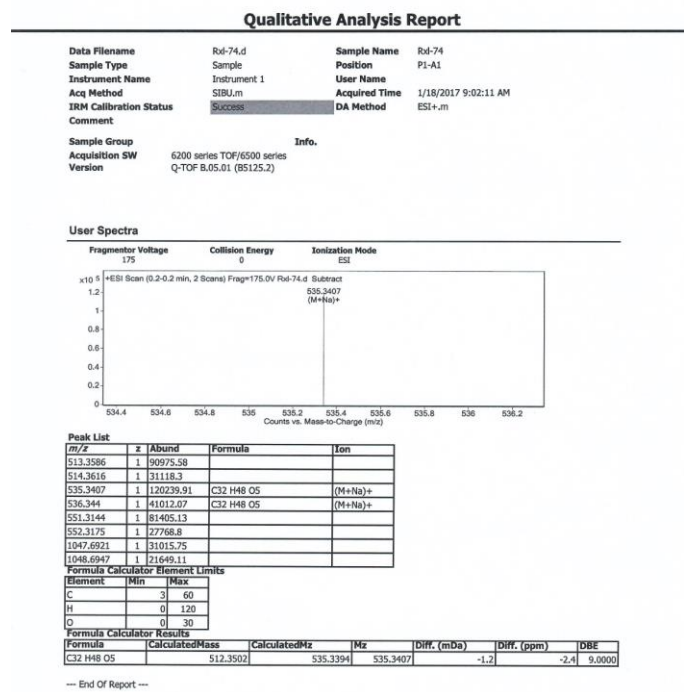


Figure S32. HRESIMS spectrum of ascynol L (14).

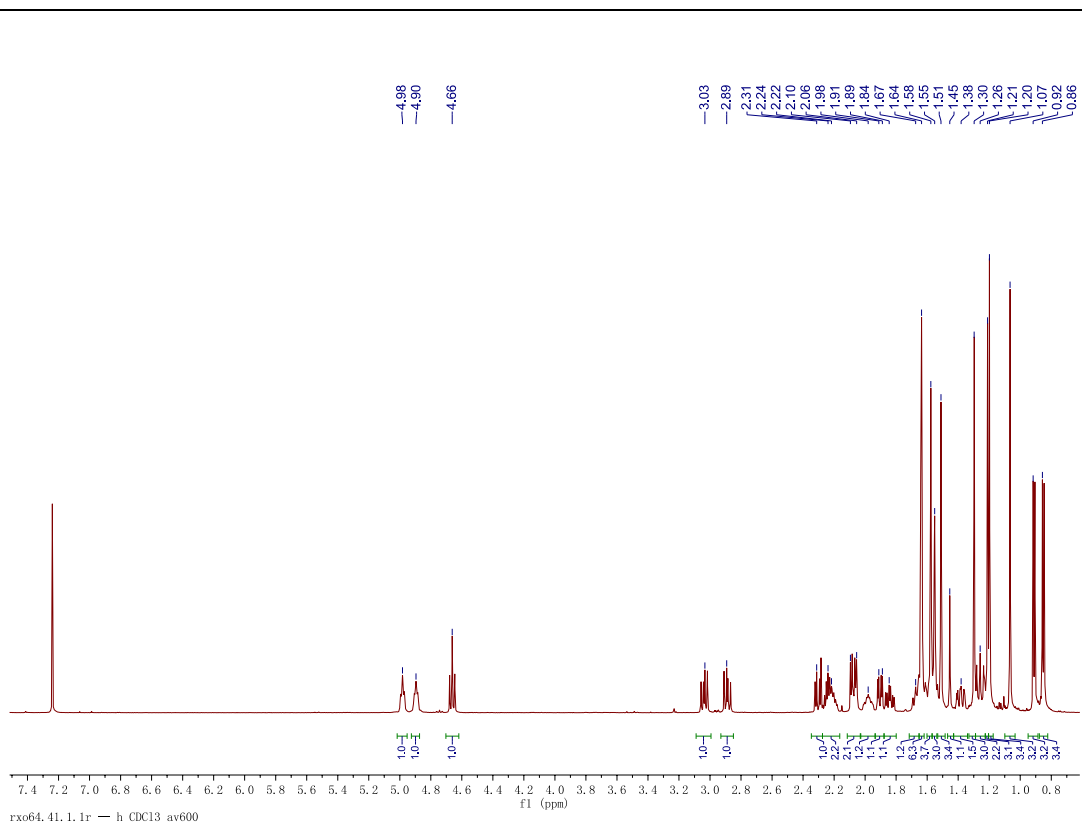


Figure S25. ¹H (in CDCl₃) spectrum of ascynol M (**15**).

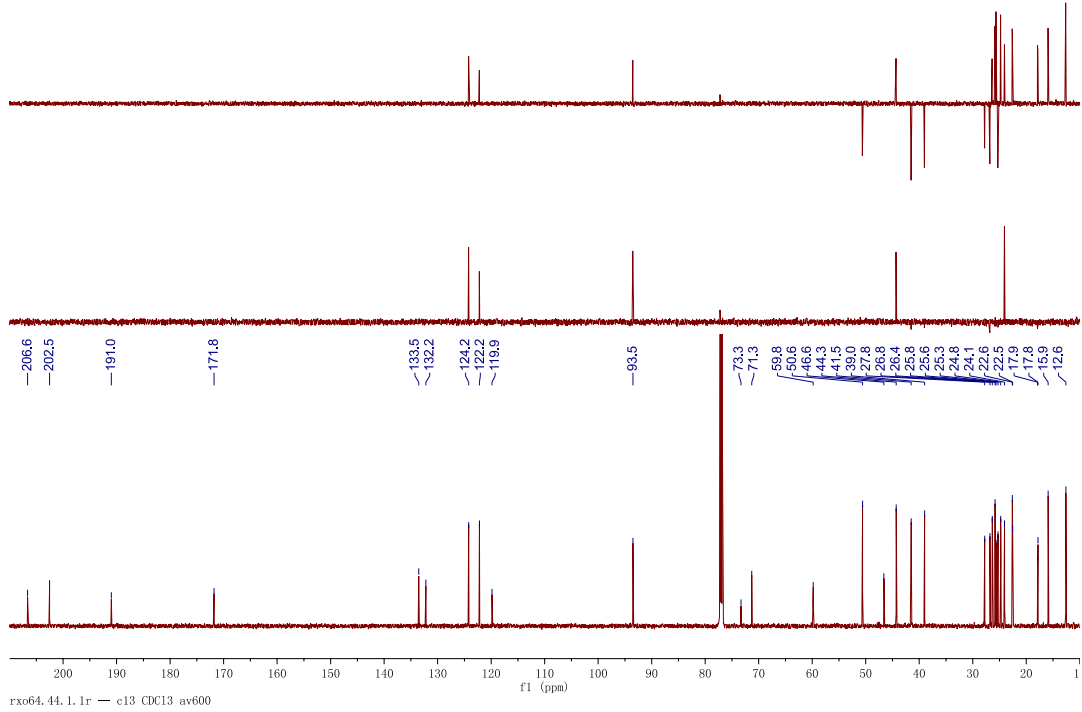


Figure S26. ¹³C (in CDCl₃) spectrum of ascynol M (**15**).

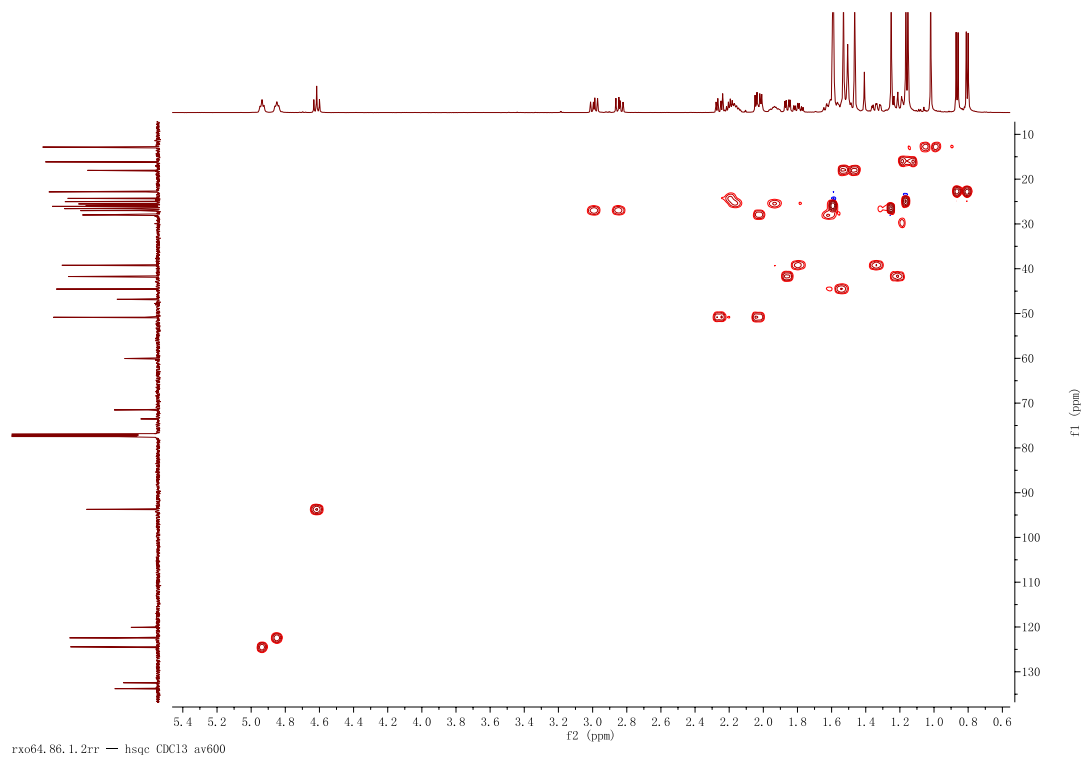


Figure S27. HSQC spectrum of ascynol M (**15**).

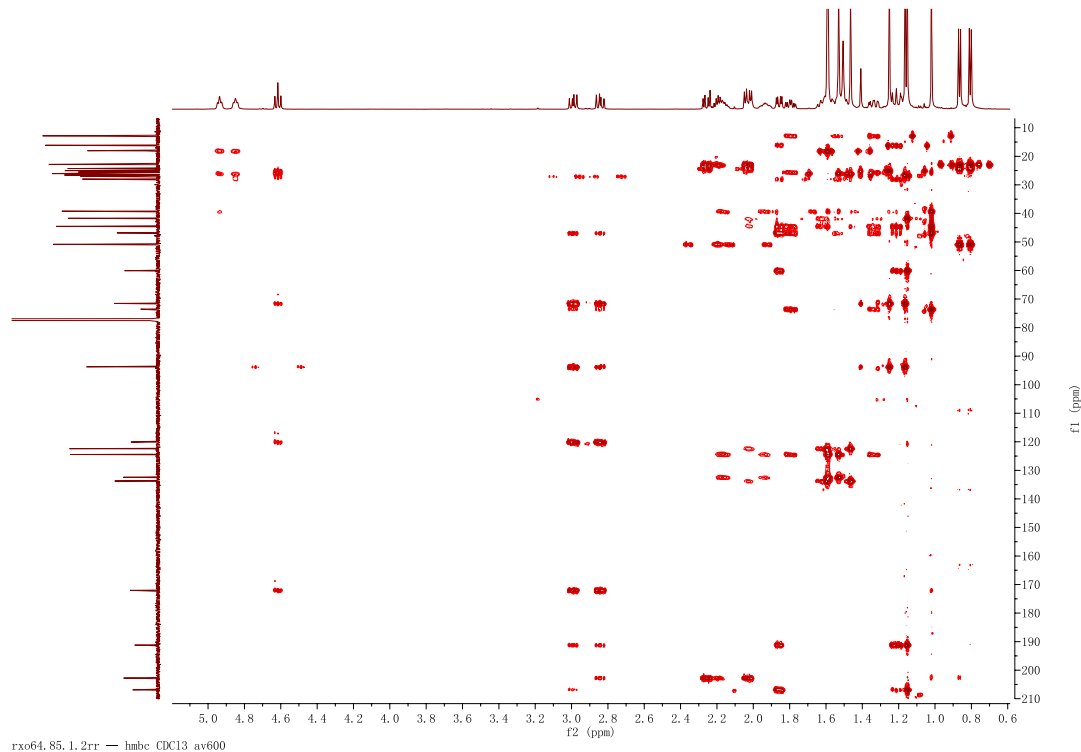


Figure S28. HMBC spectrum of ascynol M (**15**).

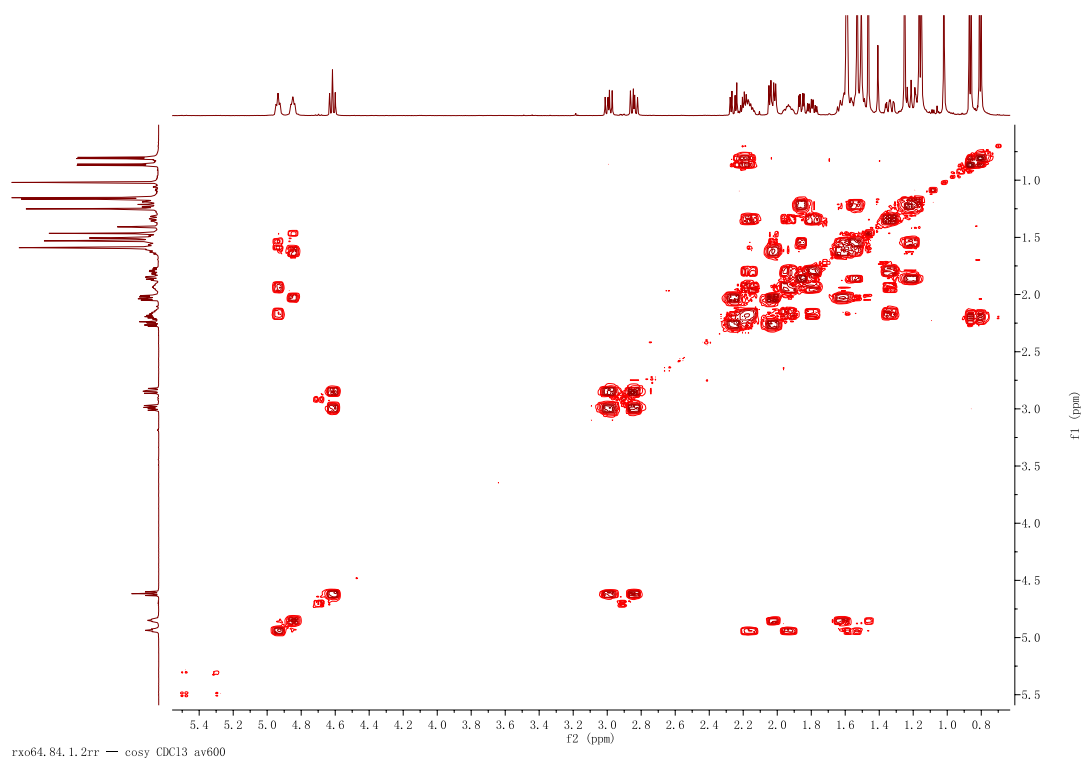


Figure S29 ¹H-¹H COSY spectrum of ascynol M (**15**).

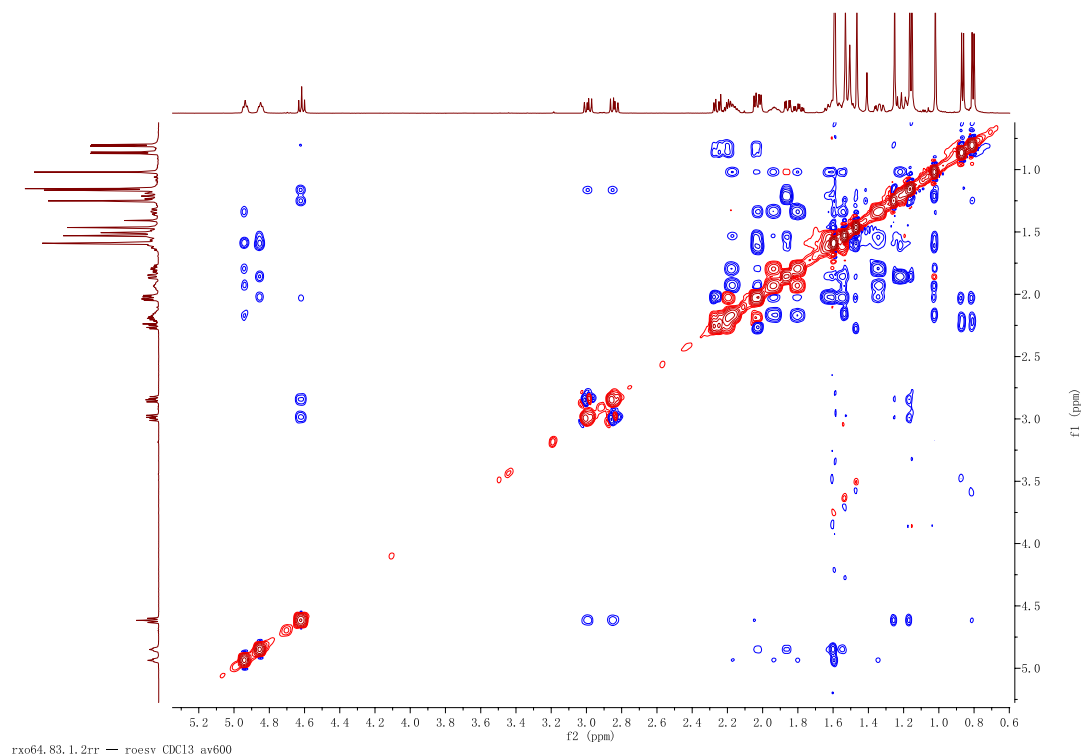


Figure S30. ROESY spectrum of ascynol M (**15**).

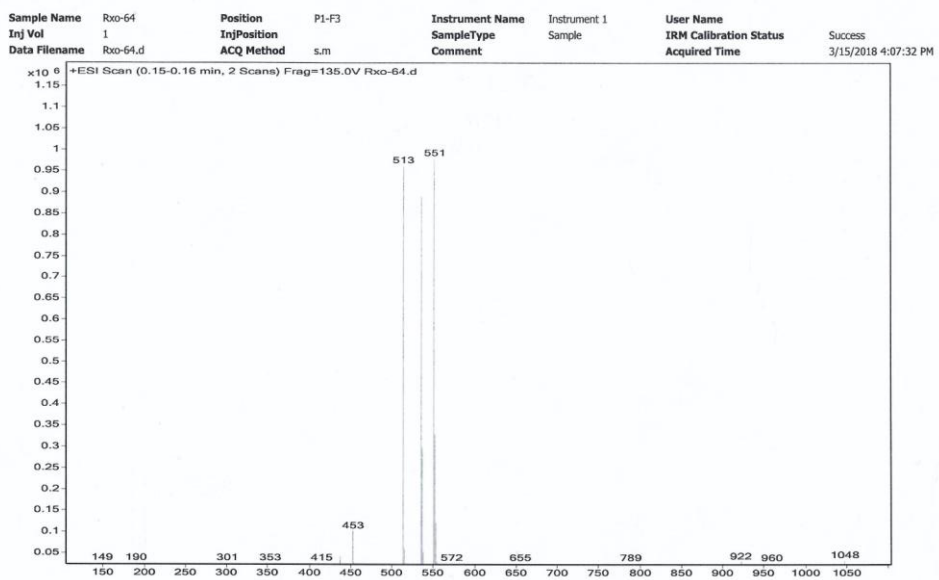


Figure S31. ESIMS spectrum of ascynol M (15).

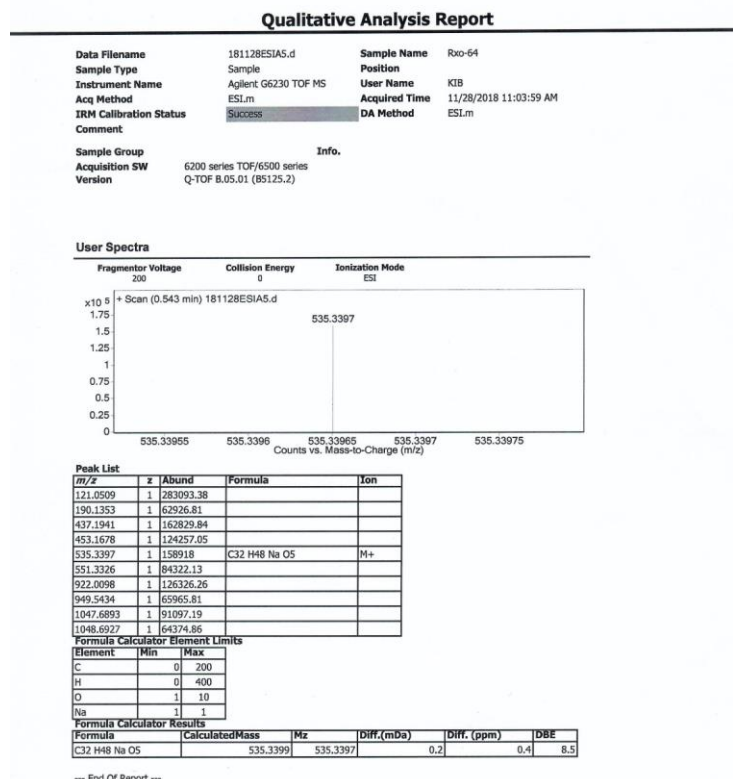


Figure S32. HRESIMS spectrum of ascynol M (15).

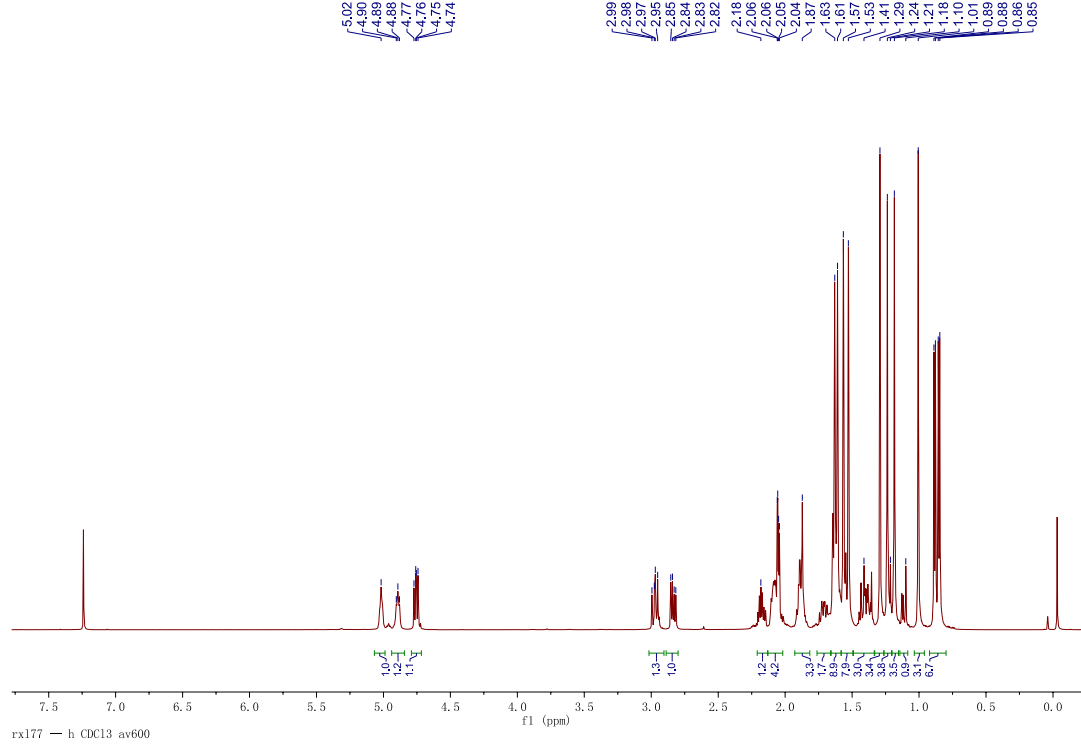


Figure S25. ¹H (in CDCl₃) spectrum of ascynol N (**17**).

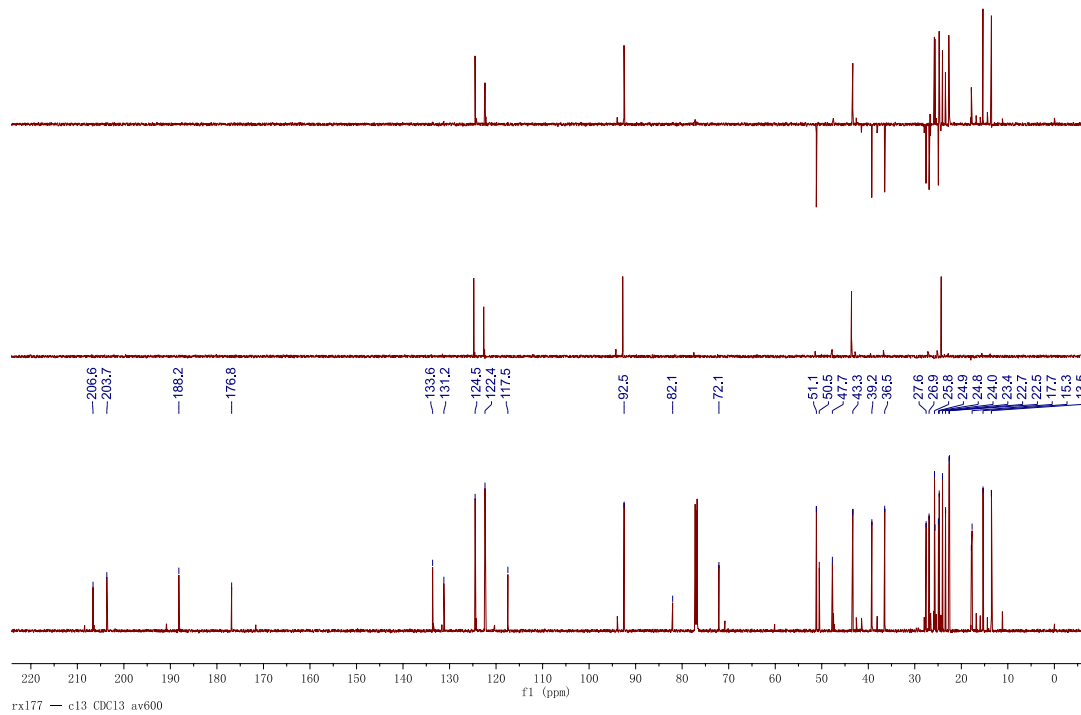


Figure S26. ¹³C (in CDCl₃) spectrum of ascynol N (**17**).

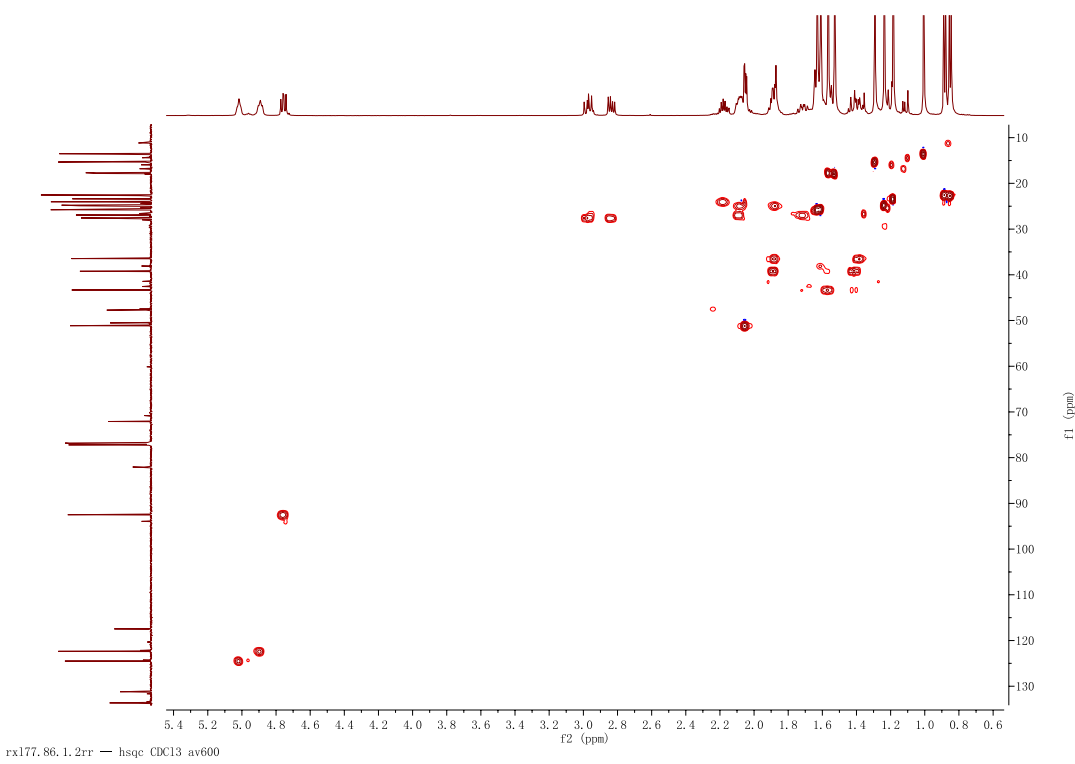


Figure S27. HSQC spectrum of ascynol N (17).

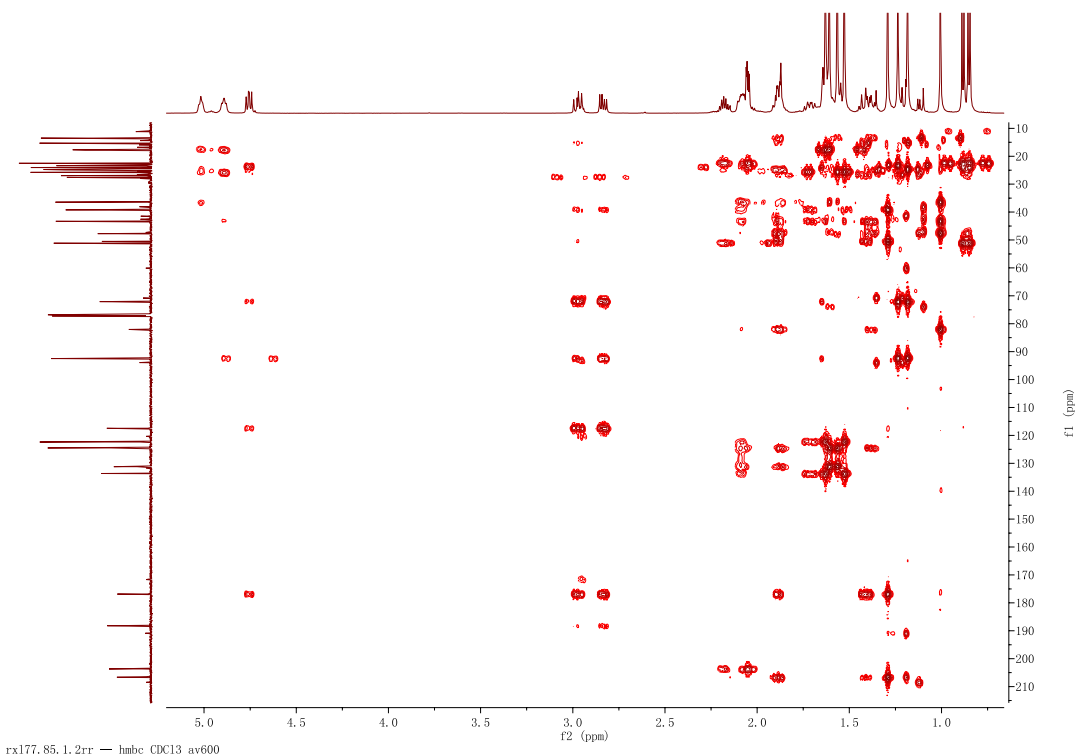


Figure S28. HMBC spectrum of ascynol N (17).

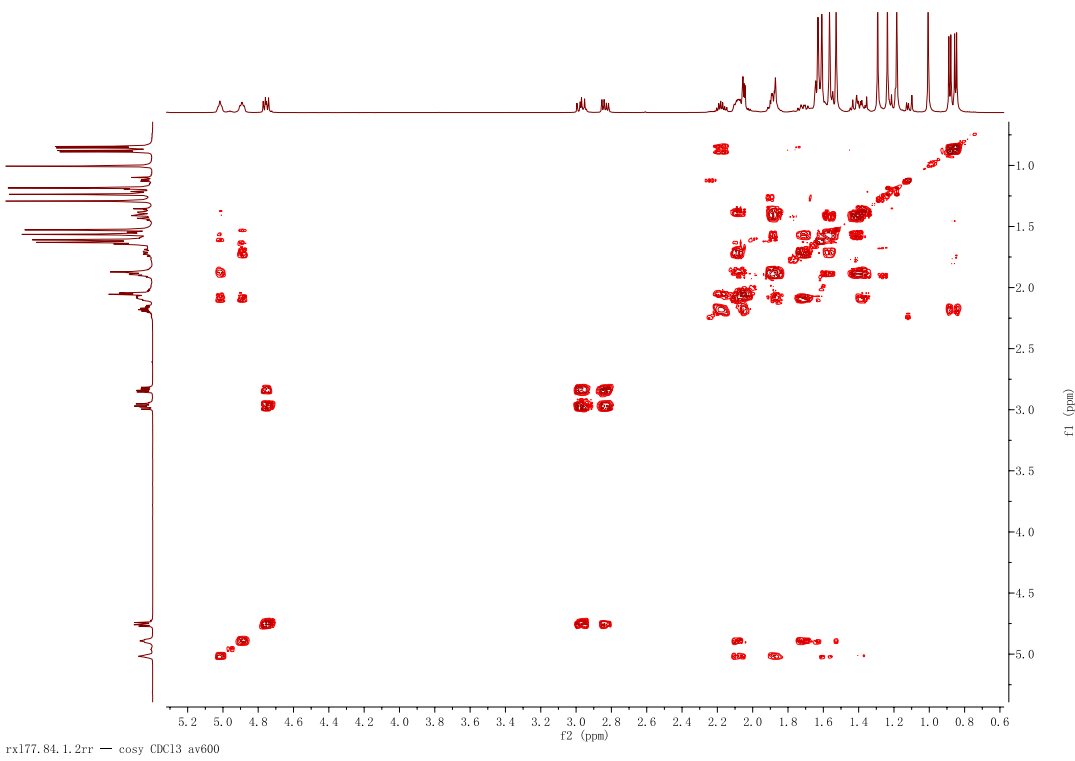


Figure S29 ¹H-¹H COSY spectrum of ascynol N (17).

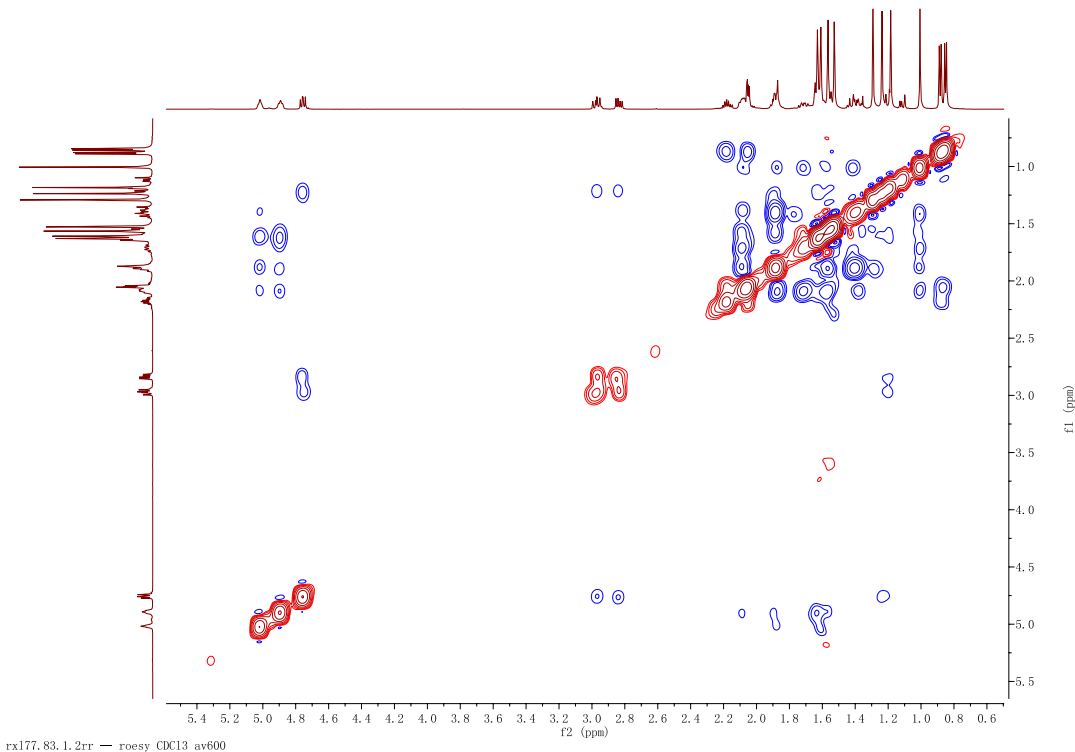


Figure S30. ROESY spectrum of ascynol N (17).

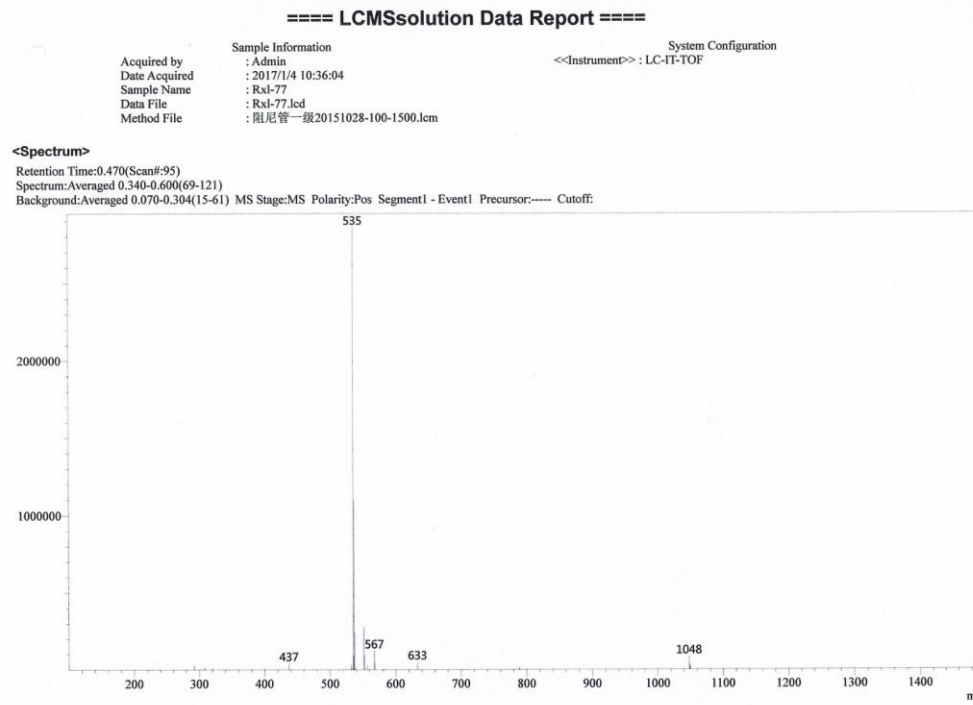
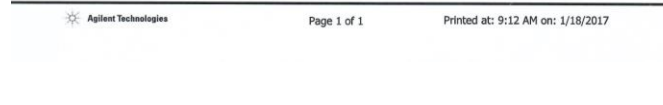
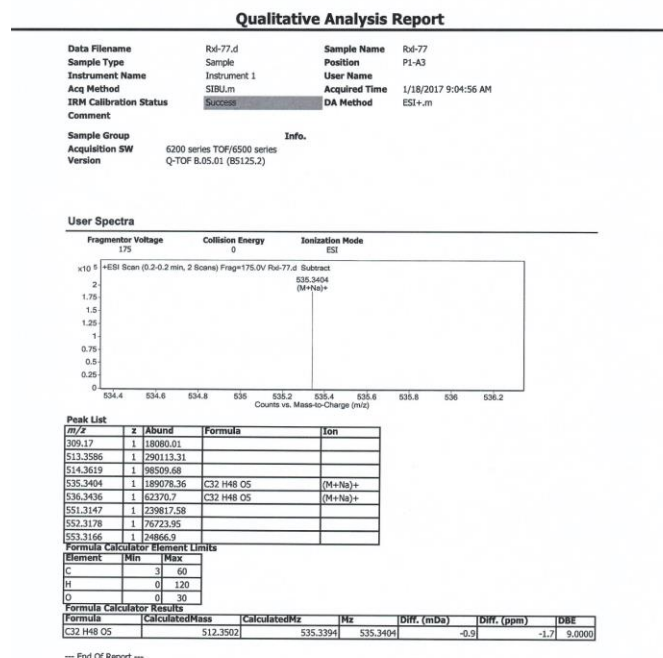


Figure S31. ESIMS spectrum of ascynol N (17).



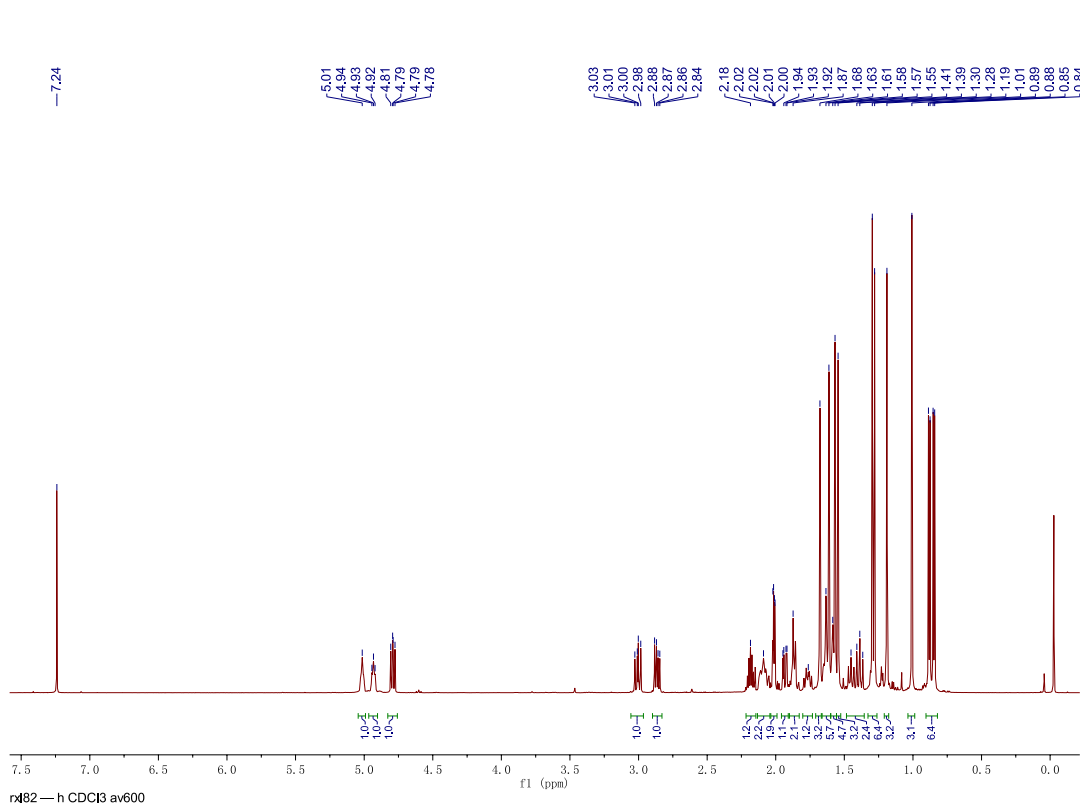


Figure S25. ¹H (in CDCl₃) spectrum of ascynol O (**18**).

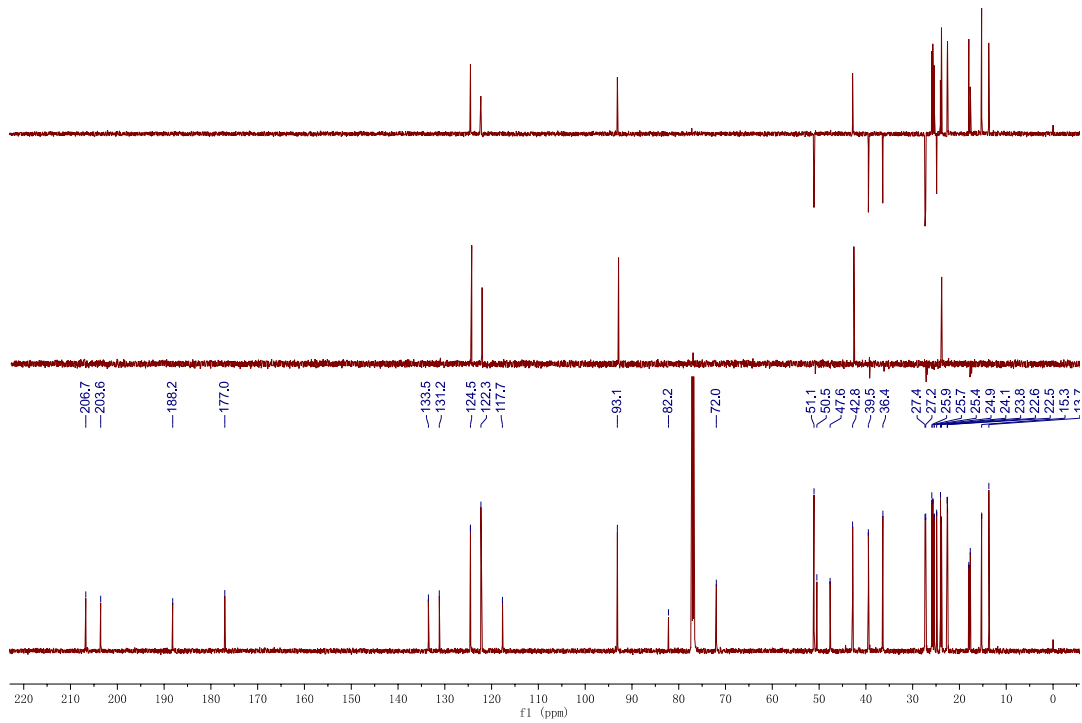


Figure S26. ¹³C (in CDCl₃) spectrum of ascynol O (**18**).

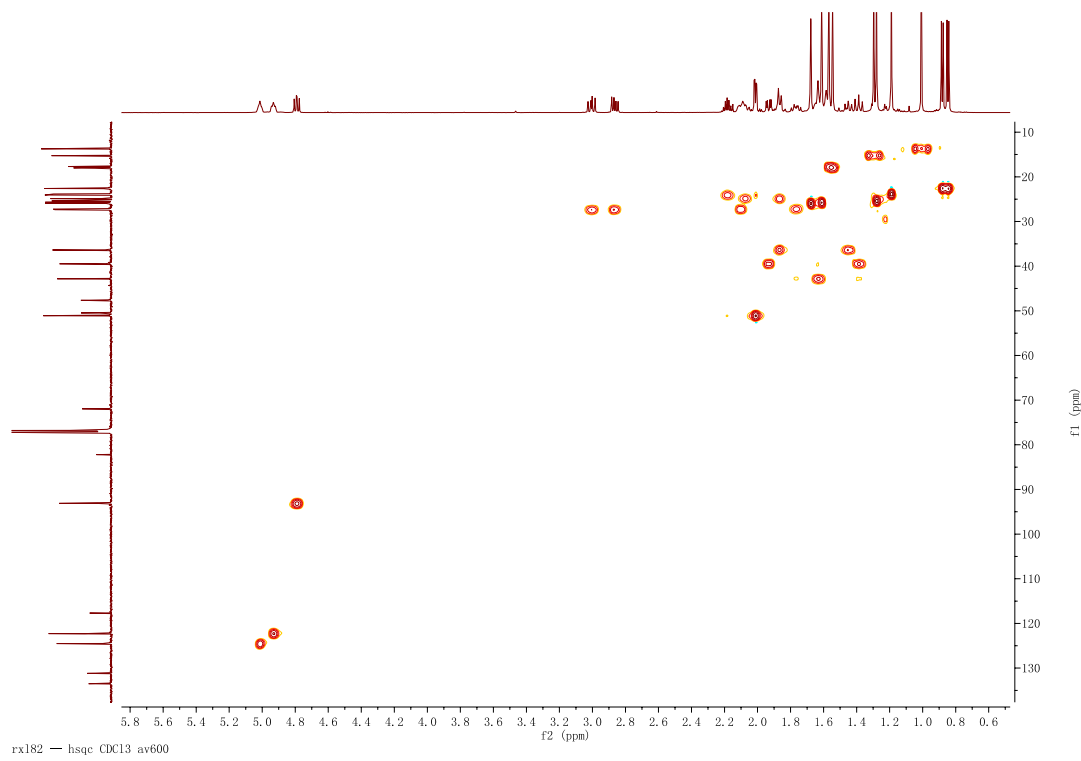


Figure S27. HSQC spectrum of ascynol O (18).

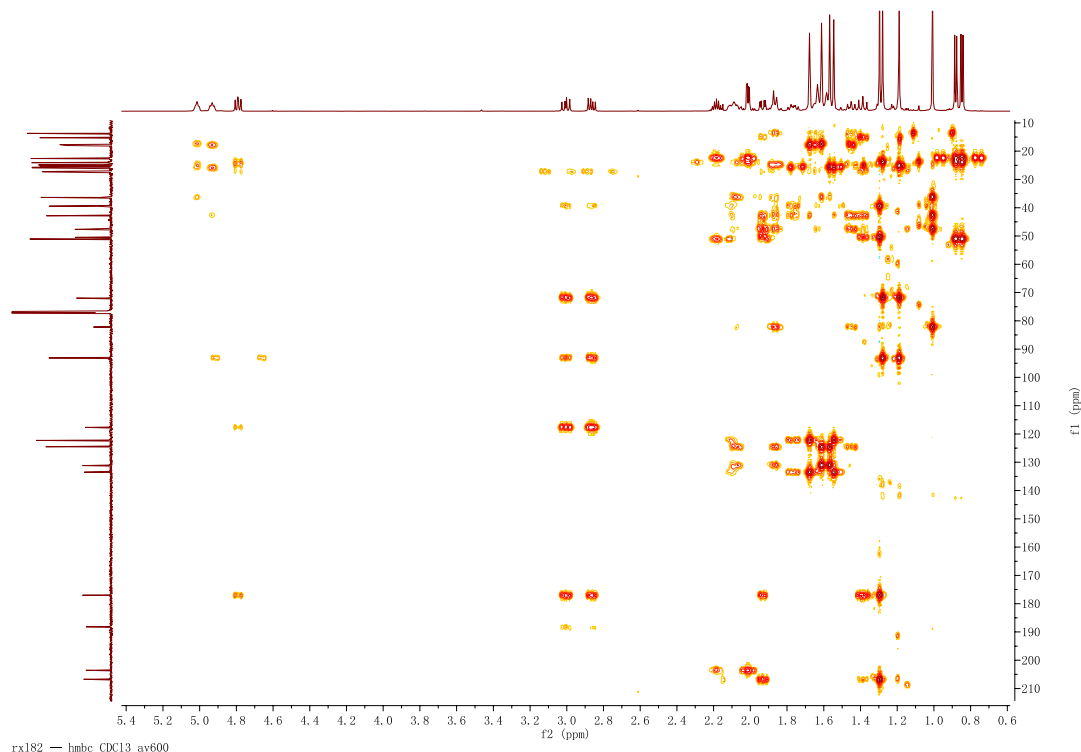


Figure S28. HMBC spectrum of ascynol O (18).

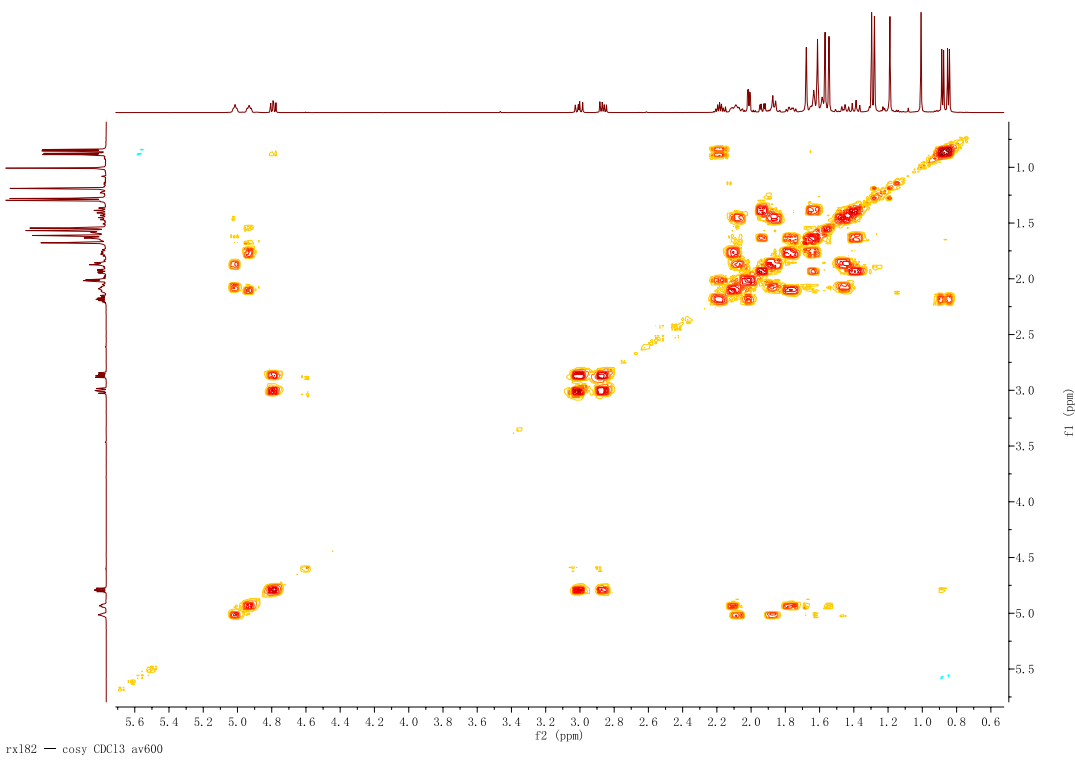


Figure S29 ^1H - ^1H COSY spectrum of ascynol O (18).

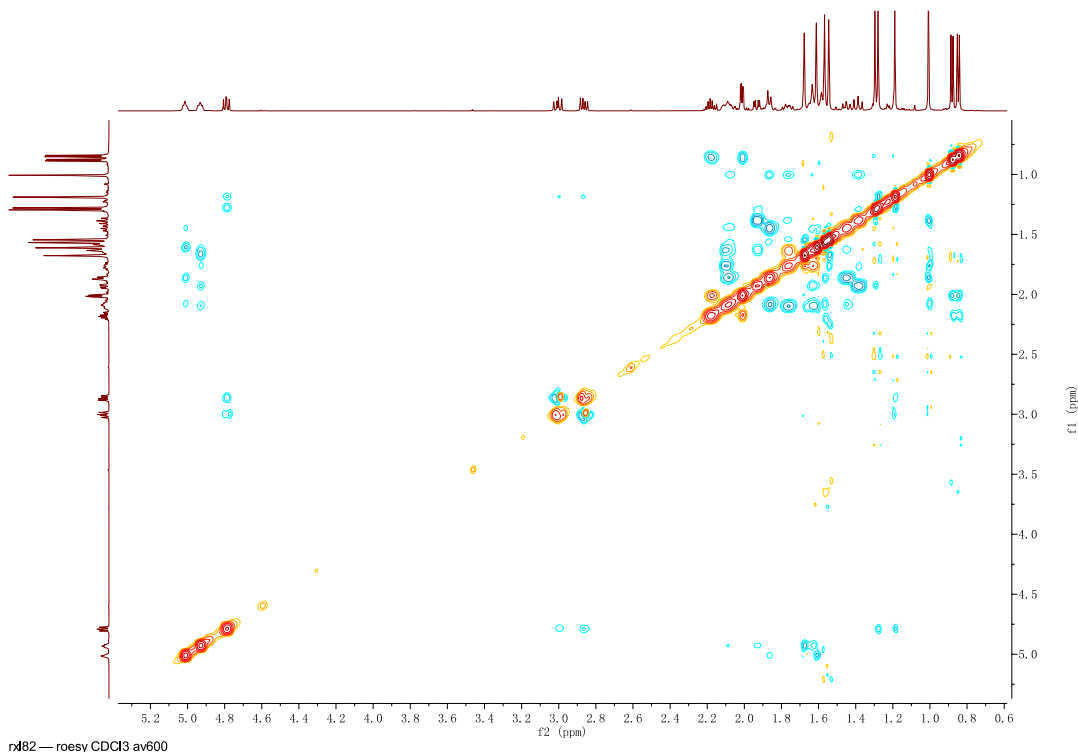


Figure S30. ROESY spectrum of ascynol O (18).

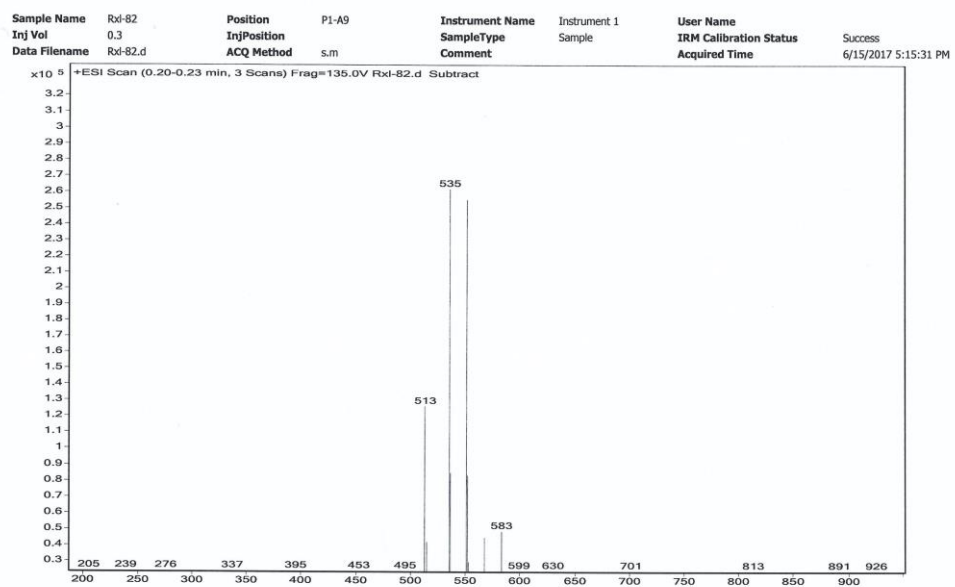


Figure S31. ESIMS spectrum of ascynol O (18).

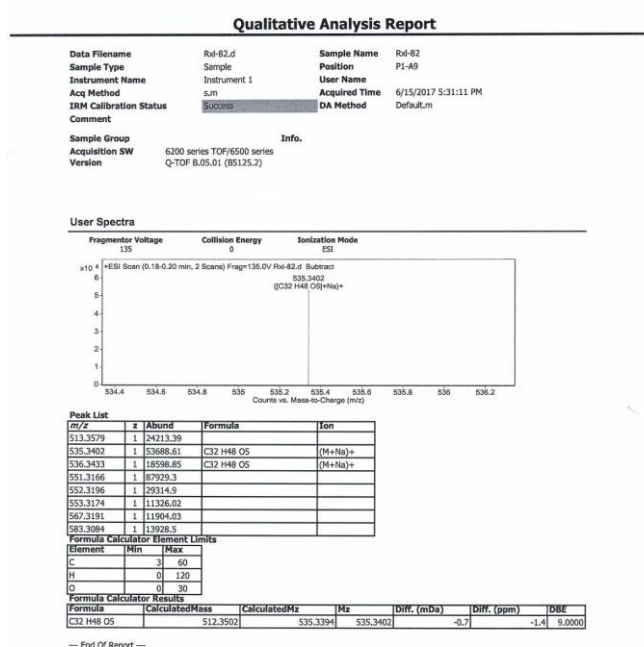


Figure S32. HRESIMS spectrum of ascynol O (18).

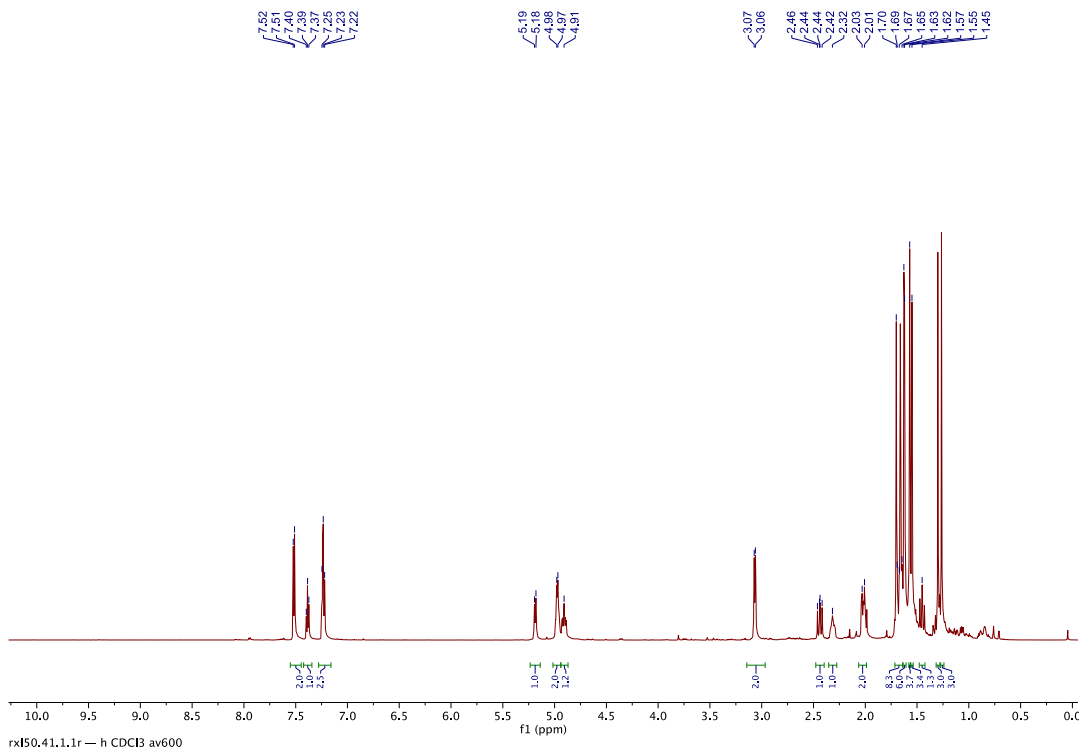


Figure S25. ^1H (in CDCl_3) spectrum of ascynol P (**20**).

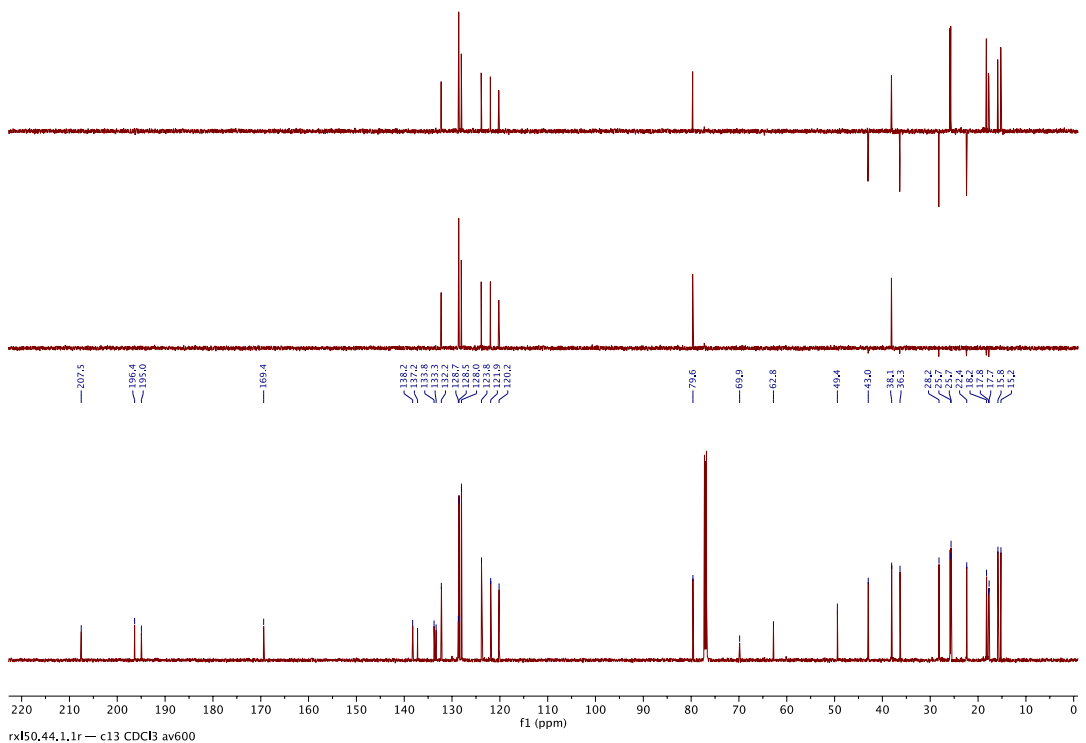


Figure S26. ^{13}C (in CDCl_3) spectrum of ascynol P (**20**).

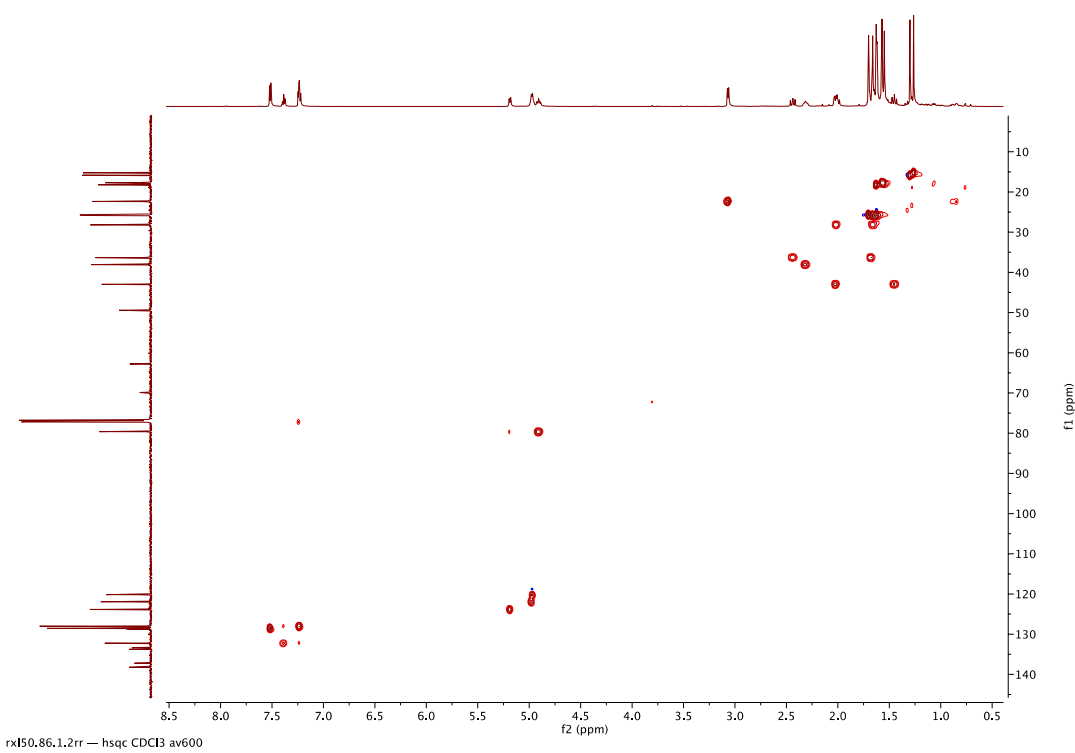


Figure S27. HSQC spectrum of ascynol P (**20**).

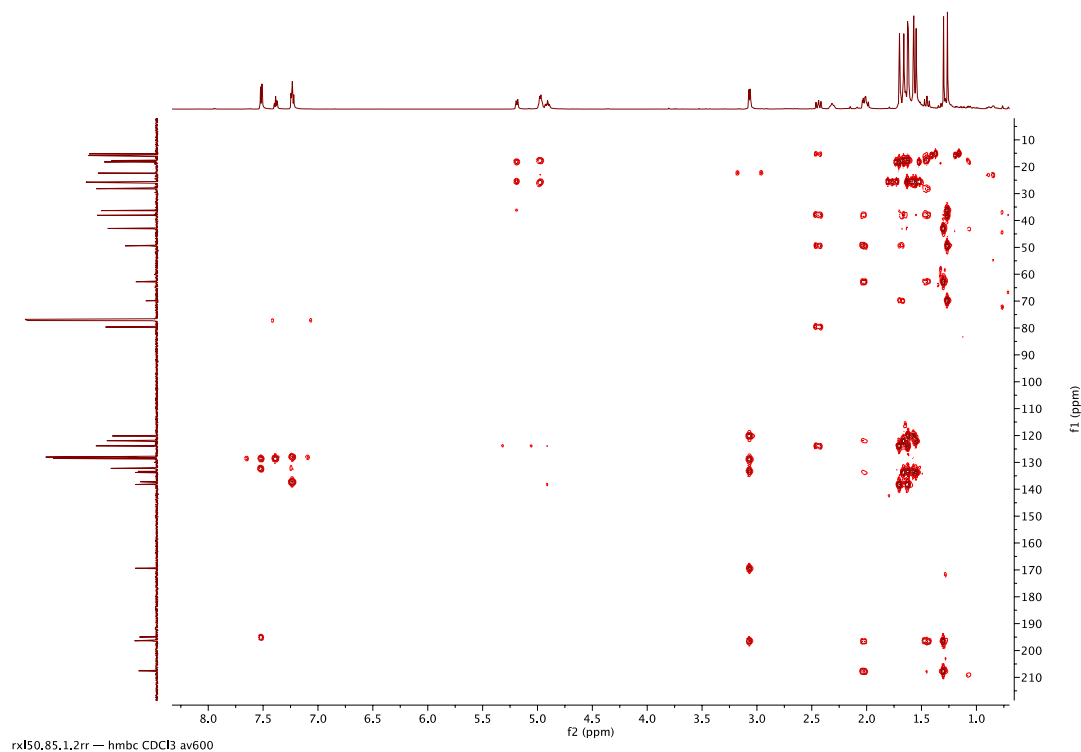


Figure S28. HMBC spectrum of ascynol P (**20**).

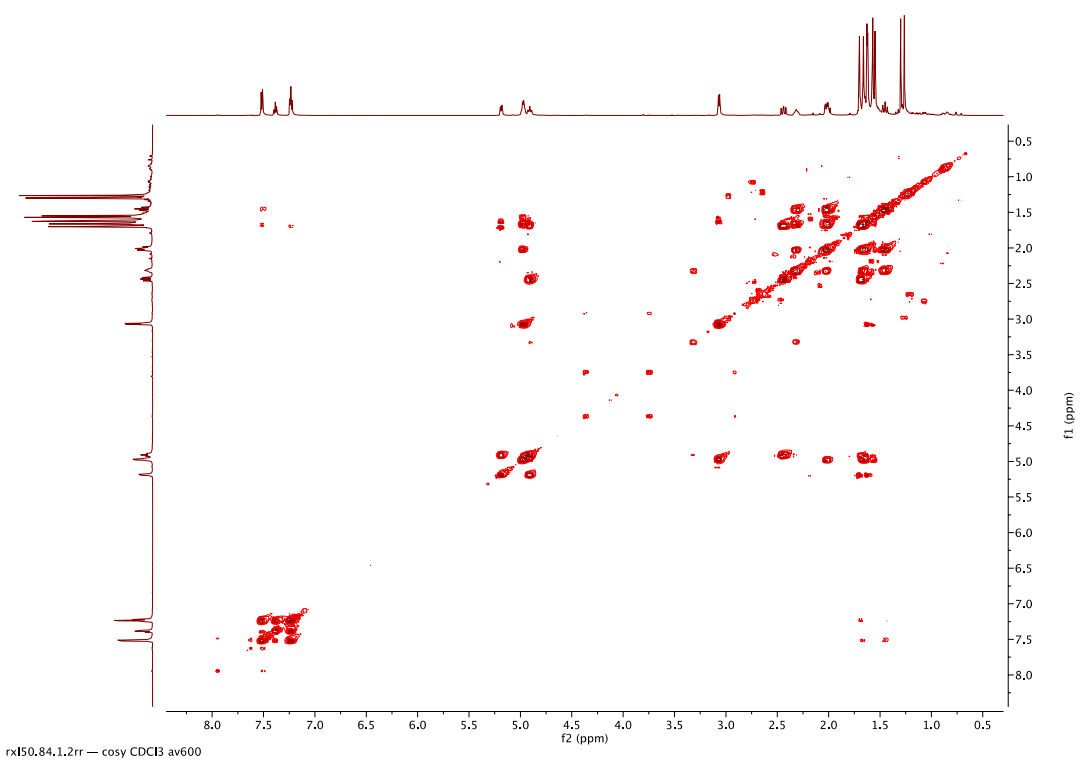


Figure S29 ¹H-¹H COSY spectrum of ascynol P (**20**).

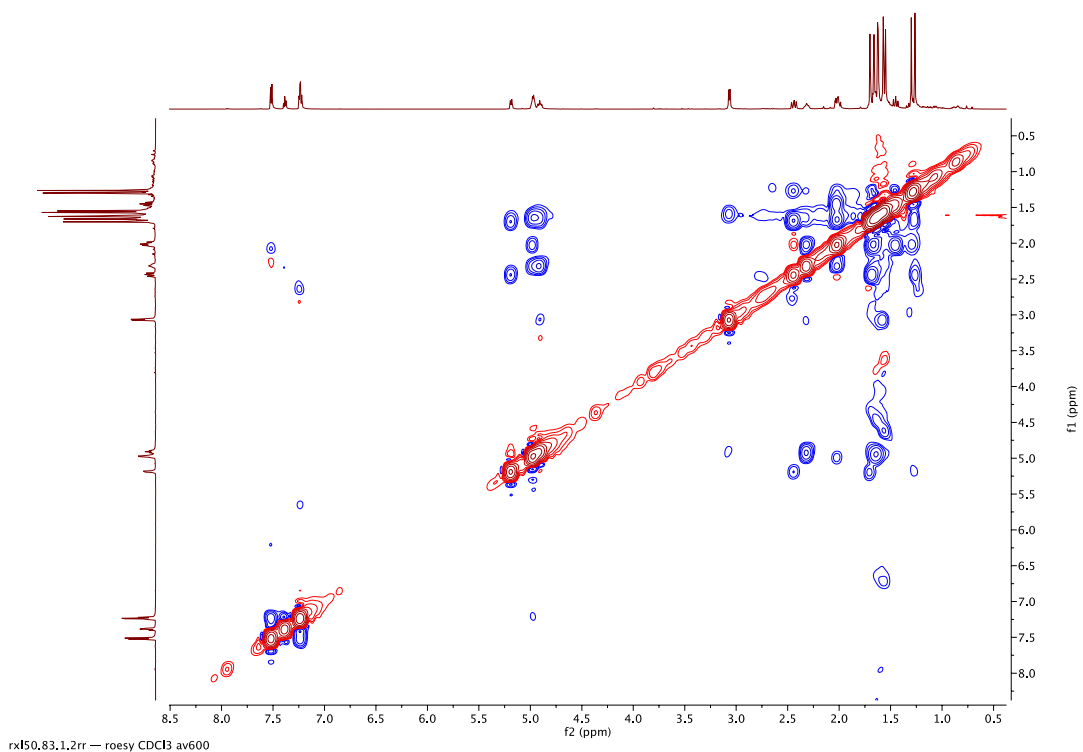


Figure S30. ROESY spectrum of ascynol P (**20**).

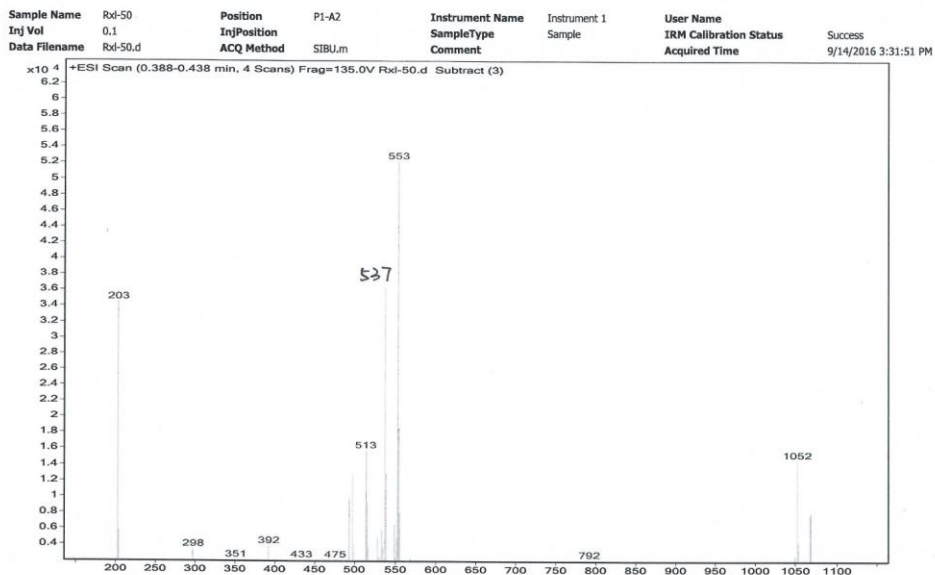


Figure S31. ESIMS spectrum of ascynol P (**20**).

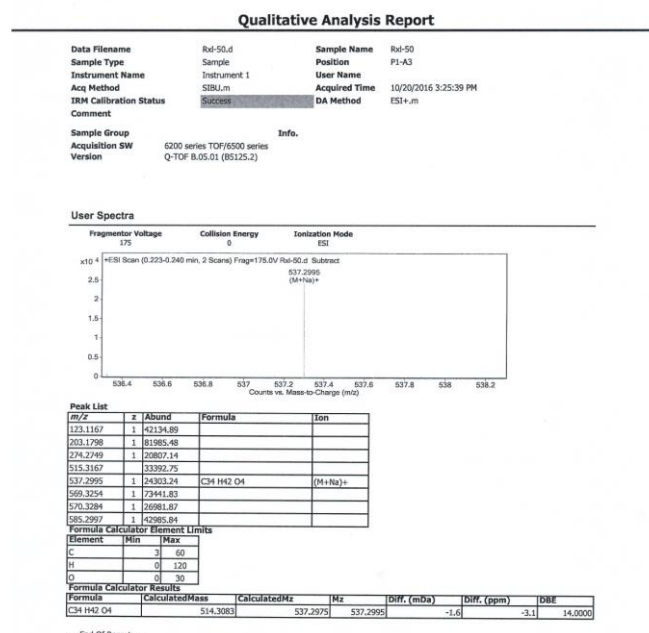


Figure S32. HRESIMS spectrum of ascynol P (**20**).

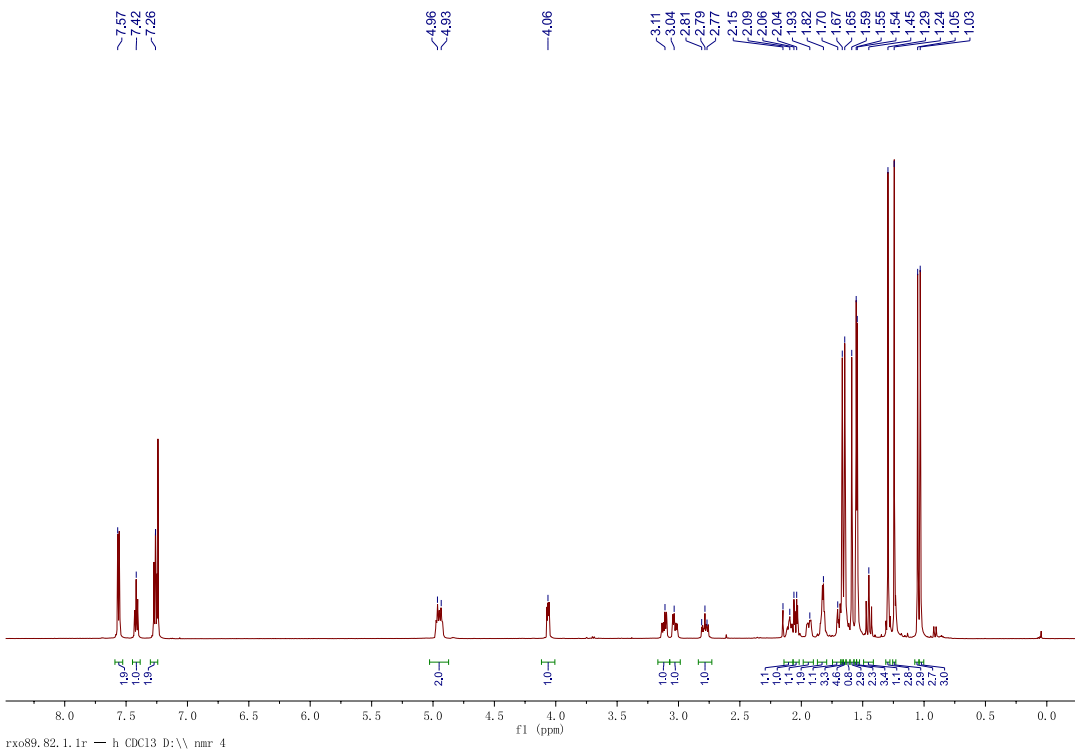


Figure S25. ¹H (in CDCl₃) spectrum of ascynol Q (**21**).

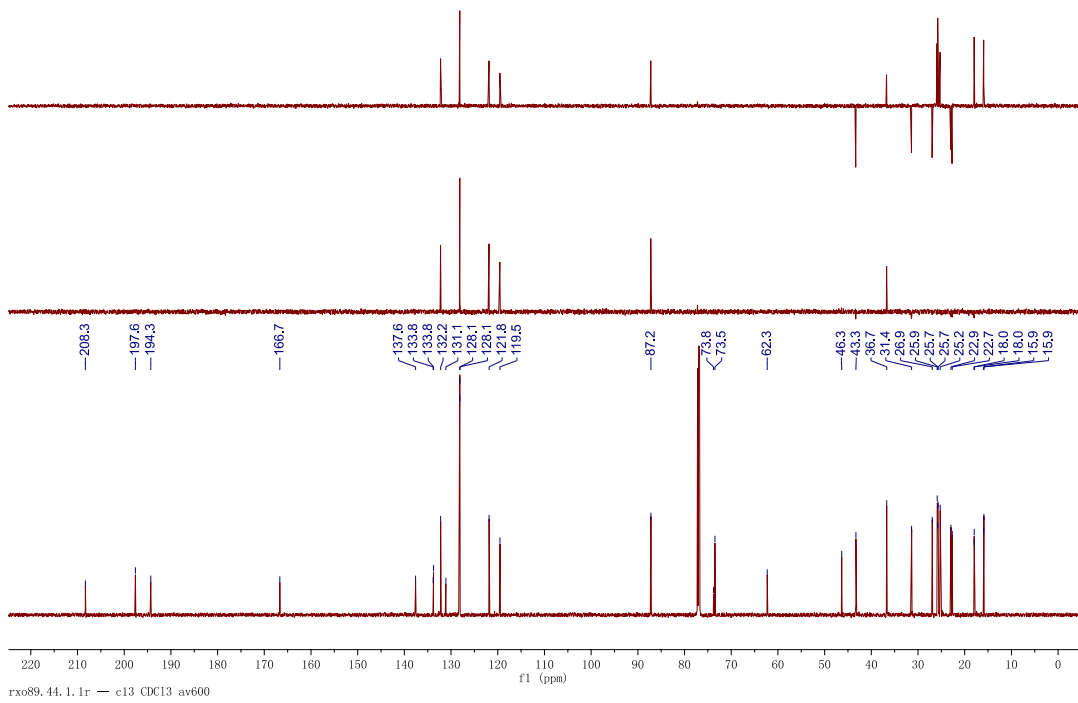


Figure S26. ¹³C (in CDCl₃) spectrum of ascynol Q (**21**).

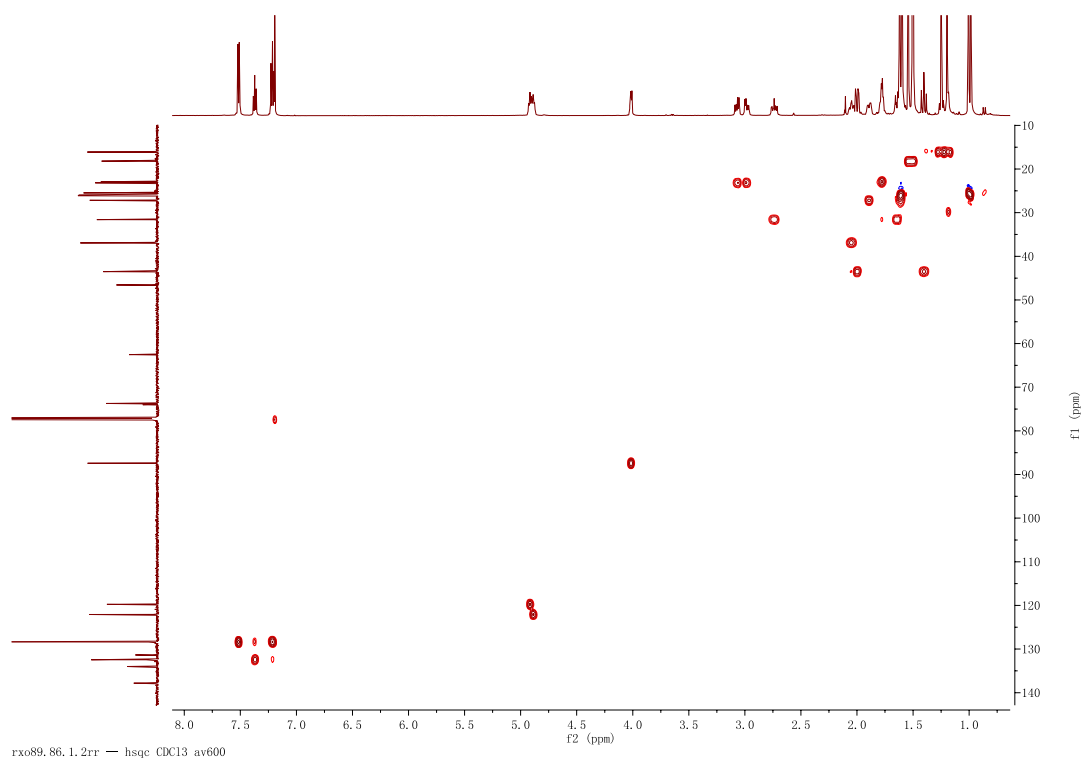


Figure S27. HSQC spectrum of ascynol Q (**21**).

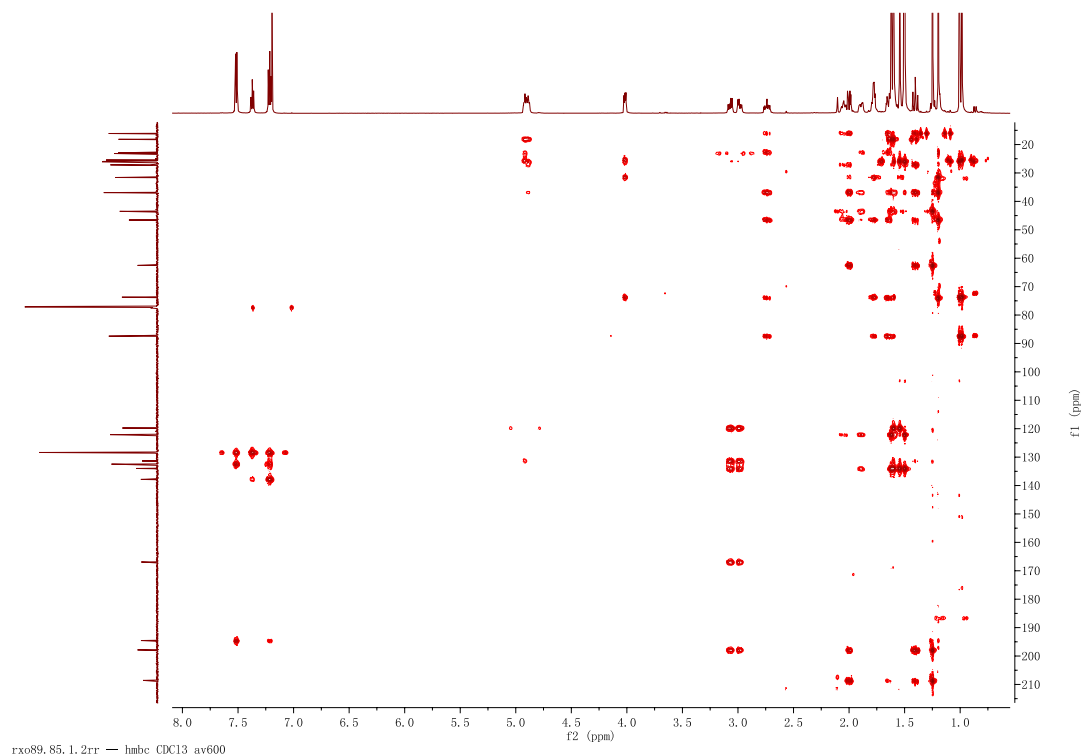


Figure S28. HMBC spectrum of ascynol Q (**21**).

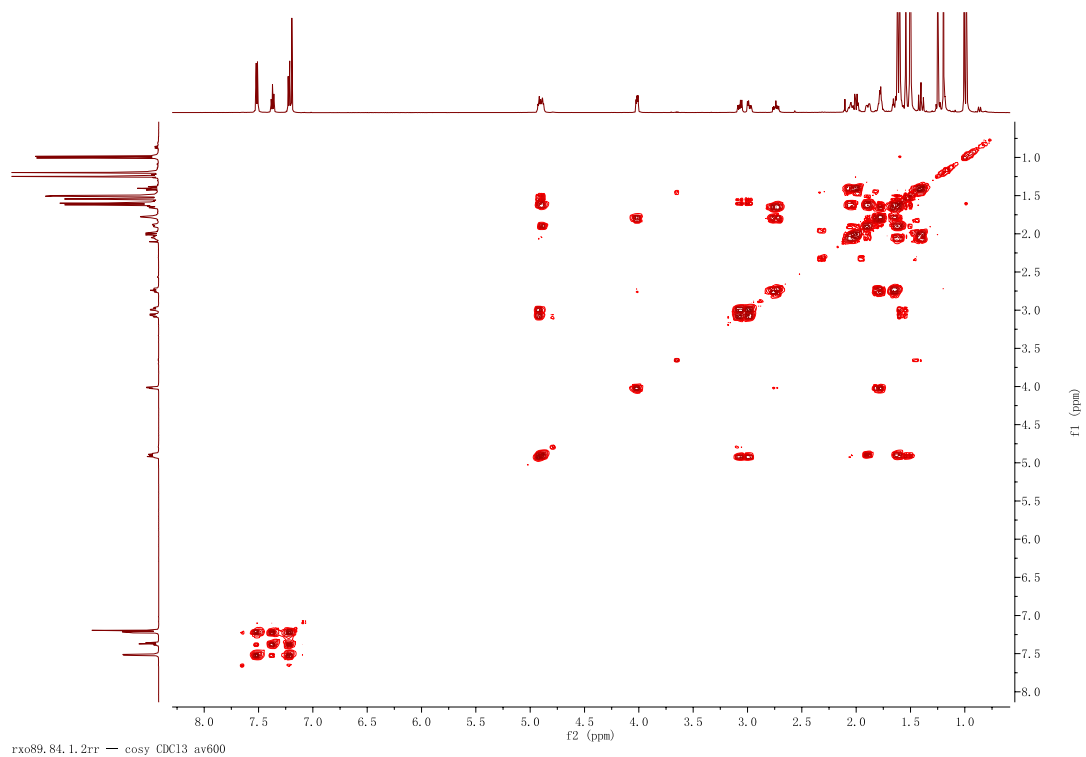


Figure S29 ¹H-¹H COSY spectrum of ascynol Q (21).

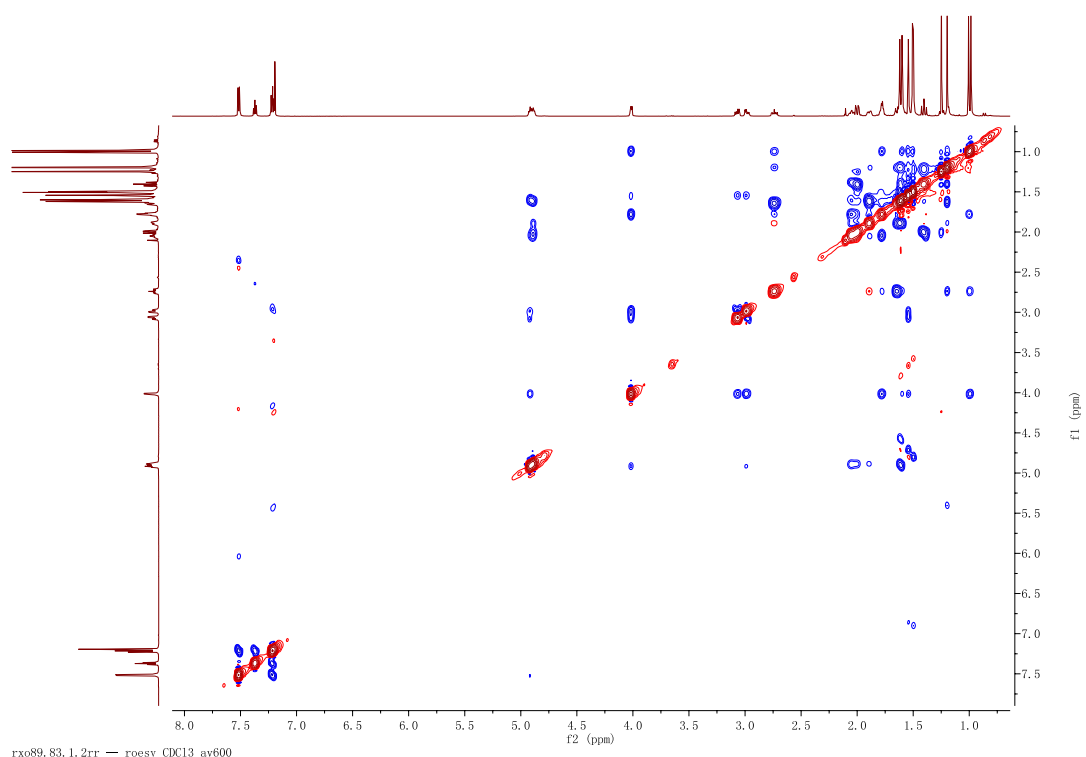


Figure S30. ROESY spectrum of ascynol Q (21).

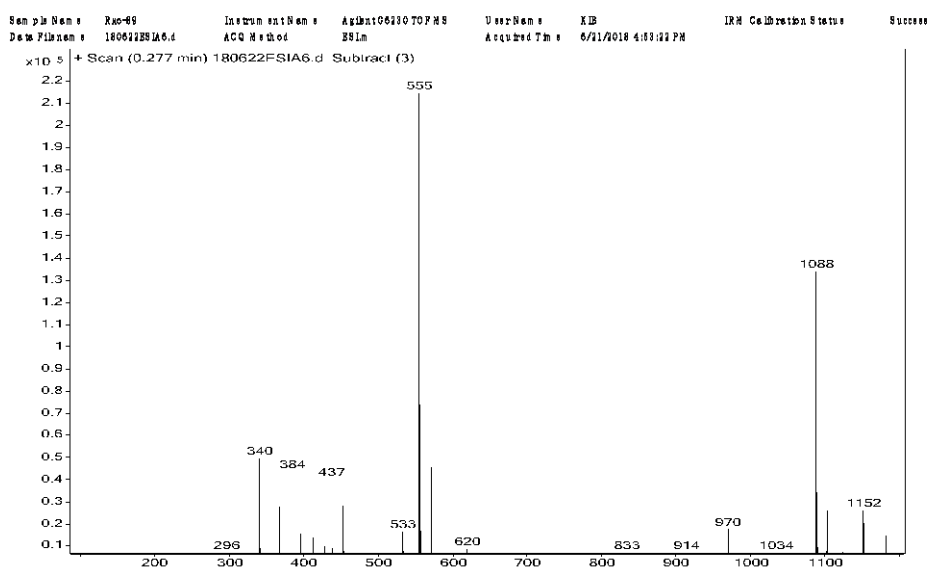
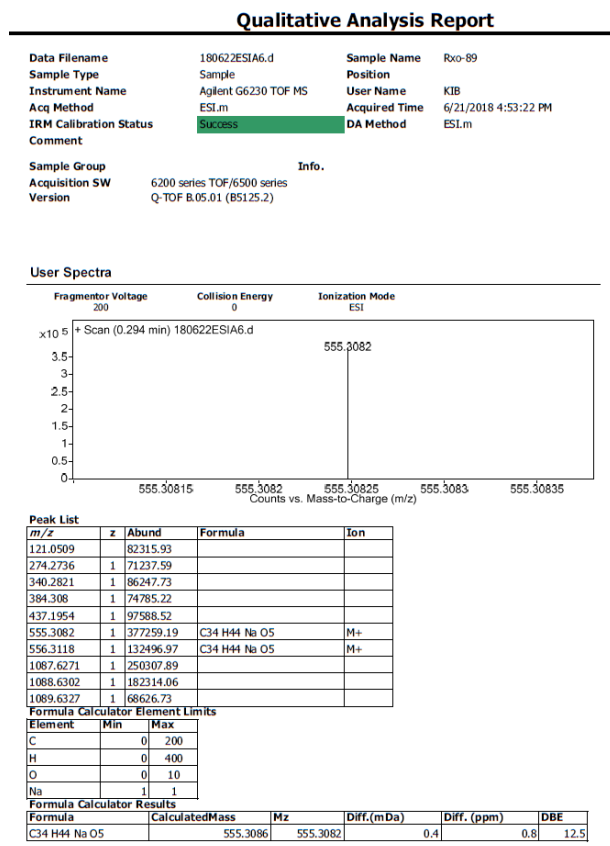


Figure S31. ESIMS spectrum of ascynol Q (21).



-- End Of Report --

Figure S31. ESIMS spectrum of ascynol Q (21).

SI-7. Computational data of compound 3

4.1 Methods for NMR and ECD calculation

Conformational searching of **3a** and **3b** were performed with the Crest code (version 2.10) using the default iMTD-GC procedure [1]. The first 50 conformers of **3a** and **3b**, respectively, were subjected to DFT geometry optimizations at B3LYP-D3BJ/6-31G(d) level of theory in the gas phase. Frequency analyses of all optimized conformers were undertaken at the same level of theory to ensure that no imaginary frequency exists. More accurate energies of optimized conformers were evaluated at M06-2X-D3/6-311+G(2d,p) level of theory in the gas phase, and were then added to “thermal correction to Gibbs free energies” obtained by frequency analysis to get the Gibbs free energy of each conformer. Those two B3LYP geometries with RMSD below 0.15 Å and energy difference below 0.15 kcal were regarded as duplicate conformers, and the one with higher energy was removed. Subsequently, Room-temperature (298.15 K) equilibrium populations were calculated according to Boltzmann distribution law:

$$p_i = \frac{n_i}{\sum_j n_j} = \frac{e^{-\Delta G_i/RT}}{\sum_j e^{-\Delta G_j/RT}}$$

Where P_i is the population of the i^{th} conformer; n_i the number of molecules in i^{th} conformer; ΔG is the relative Gibbs free energy (kcal/mol); T is room temperature (298.15 K); R is the ideal gas constant (0.0019858995).

NMR shielding tensors of all dereplicated conformers were calculated with the GIAO method at mPW1PW91-SCRF/6-31+G(d,p) level (Chloroform, IEFPCM solvent model). For each possible candidate, the parameters a and b of the linear regression $\delta_{\text{cal}} = a\delta_{\text{exp}} + b$; the correlation coefficient, R^2 ; the mean absolute error (MAE) defined as $\Sigma n |\delta_{\text{cal}} - \delta_{\text{exp}}|/n$; the corrected mean absolute error, $CMAE$, defined as $\Sigma n |\delta_{\text{corr}} - \delta_{\text{exp}}|/n$, where $\delta_{\text{corr}} = (\delta_{\text{cal}} - b)/a$, were calculated. Then, DP4+ probability analysis based on random conformational amplitudes [2] were undertaken using the calculated NMR shielding tensors and scripts provided by Sarotti, *et al.*, and DP4+ probabilities of each structural candidates were obtained (Figures S33).

For ECD calculation, those conformers with a population over 2% were subjected to TDDFT calculations at CAM-B3LYP/6-311+G(d,p) level of theory (MeOH, IEFPCM

solvent model), and 36 excited states were calculated for each conformer. The calculated ECD curves were generated using the Multiwfn software (version 3.8) [3].

The geometry optimization, single-point energy calculation, NMR shielding constant calculation were all completed in Gaussian 09 program [4].

- [1] P. Pracht, F. Bohle, S. Grimme, Automated exploration of the low-energy chemical space with fast quantum chemical methods, *Phys. Chem. Chem. Phys.* 22 (2020) 7169–7192.
- [2] M.M. Zanardi, M.O. Marcarino, A.M. Sarotti, Redefining the impact of Boltzmann analysis in the stereochemical assignment of polar and flexible molecules by NMR calculations, *Org. Lett.* 22 (2020) 52–56.
- [3] T. Lu, F. Chen, Multiwfn: A multifunctional wavefunction analyzer, *J. Comput. Chem.* 33 (2012) 580–592.
- [4] M.J. Frisch, G.W. Trucks, H.B. Schlegel, G.E. Scuseria, M.A. Robb, J.R. Cheeseman, G. Scalmani, V. Barone, B. Mennucci, G.A. Petersson, H. Nakatsuji, M. Caricato, X. Li, H.P. Hratchian, A.F. Izmaylov, J. Bloino, G. Zheng, J.L. Sonnenberg, M. Hada, M. Ehara, K. Toyota, R. Fukuda, J. Hasegawa, M. Ishida, T. Nakajima, Y. Honda, O. Kitao, H. Nakai, T. Vreven, J.A. Montgomery, J.E.P. Jr., F. Ogliaro, M. Bearpark, J.J. Heyd, E. Brothers, K.N. Kudin, V.N. Staroverov, T. Keith, R. Kobayashi, J. Normand, K. Raghavachari, A. Rendell, J.C. Burant, S.S. Iyengar, J. Tomasi, M. Cossi, N. Rega, J.M. Millam, M. Klene, J.E. Knox, J.B. Cross, V. Bakken, C. Adamo, J. Jaramillo, R. Gomperts, R.E. Stratmann, O. Yazyev, A.J. Austin, R. Cammi, C. Pomelli, J.W. Ochterski, R.L. Martin, K. Morokuma, V.G. Zakrzewski, G.A. Voth, P. Salvador, J.J. Dannenberg, S. Dapprich, A.D. Daniels, O. Farkas, J.B. Foresman, J.V. Ortiz, J. Cioslowski, D.J. Fox, Gaussian 09, Revision E.01; Gaussian, Inc., Wallingford CT: **2010**.

4.2 General results for NMR calculation

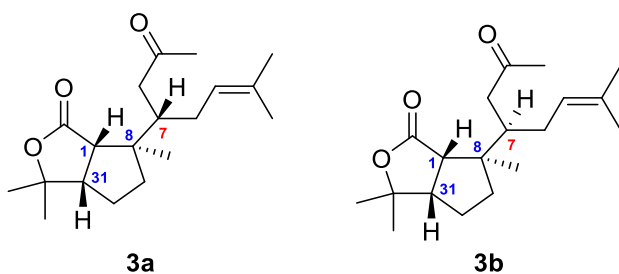


Figure S33. Structures of ($1S^*, 7S^*, 8R^*, 31S^*$)-3 (**3a**) and ($1S^*, 7R^*, 8R^*, 31S^*$)-3 (**3b**).

Table S9. Experimental and calculated ^{13}C NMR chemical shifts of **3a** and **3b**.

No.	$\delta_{\text{exptl.}}$ (ppm)	$\delta_{\text{calcd.}}$ (ppm)		No.	$\delta_{\text{exptl.}}$ (ppm)	$\delta_{\text{calcd.}}$ (ppm)	
		3a	3b			3a	3b
1	55.3	56.7	56.5	27	17.8	18.6	18.8
5	209.2	208.6	207.7	28	18.0	17.3	18.5
6	45.9	45.2	44.0	29	42.3	43.7	42.5
7	45.8	48.3	47.8	30	27.1	28.3	28.2
8	49.2	51.6	51.0	31	51.5	51.5	53.0
10	177.2	175.6	174.8	32	83.0	82.3	82.1
22	30.6	31.3	31.6	33	30.5	31.0	30.1
23	30.1	31.3	33.7	34	23.5	23.9	22.8
24	123.5	123.8	124.6	R²	-	0.9997	0.9994
25	132.7	133.9	133.9	MAE	-	1.0	1.3
26	25.7	26.7	27.0	CMAE	-	0.8	1.1

Table S10. Experimental and calculated ^1H NMR chemical shifts of **3a** and **3b**.

No.	$\delta_{\text{exptl.}}$ (ppm)	$\delta_{\text{calcd.}}$ (ppm)		No.	$\delta_{\text{exptl.}}$ (ppm)	$\delta_{\text{calcd.}}$ (ppm)	
		3a	3b			3a	3b
1	2.84	3.07	2.94	29a	1.62	1.44	1.36
6a	2.76	2.89	2.21	29b	1.47	1.36	1.21
6b	2.33	2.23	2.20	30a	1.67	1.70	1.60
7	2.12	2.26	2.10	30b	1.58	1.57	1.45
22	2.04	0.82	1.98	31	2.58	2.59	2.52
23a	1.93	1.99	2.24	33	1.28	1.13	1.15
23b	1.83	1.79	1.93	34	1.3	1.21	1.19
24	4.86	1.61	5.32				
26	1.57	5.20	1.54	R²	-	0.9911	0.9622
27	1.54	1.54	1.56	MAE	-	0.12	0.16
28	0.92	1.58	0.81	CMAE	-	0.07	0.11

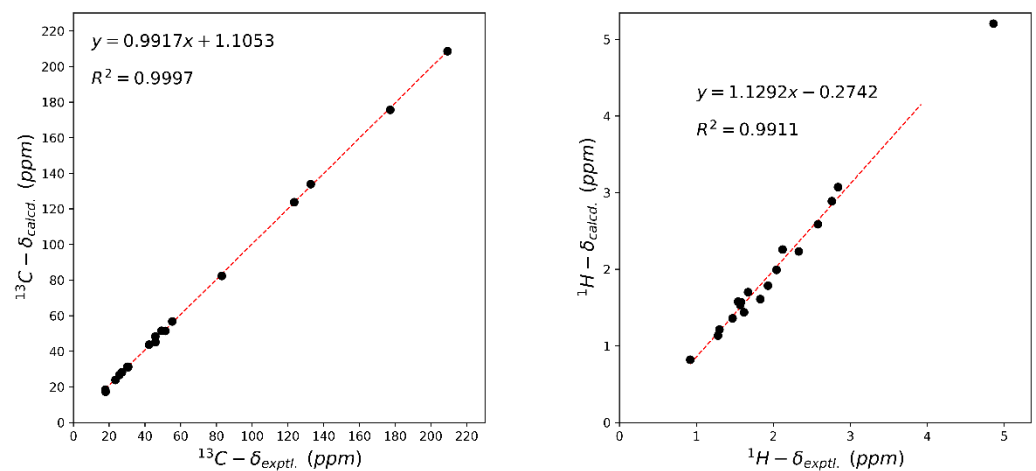


Figure S34. Linear regression analysis between the experimental and calculated NMR chemical shifts of **3a**.

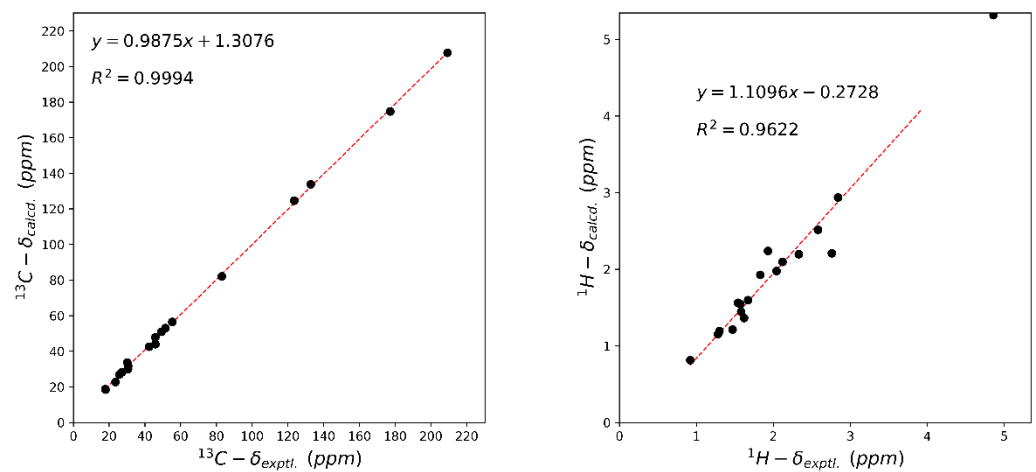


Figure S35. Linear regression analysis between the experimental and calculated NMR chemical shifts of **3b**.

DP4/DP4+ RANDOM CONFORMATIONAL AMPLITUDE CALCULATOR by Zanardi, Marcarino & Sarotti
Org. Lett. 2020, 22, 52-56

Select DP4 or DP4+ analysis (1 for DP4, 2 for DP4+): 2

You have chosen DP4+ analysis (see Grimblat, Zanardi & Sarotti, JOC 2015, 80, 12526)
Warning: the DP4+ parameters were taken at the PCM/mPW1PW91/6-31+G**//B3LYP/6-31G* level

Ensemble	Subset of conformers generated by random selection of...	E window (kcal/mol)
R1	Up to 100 conformations of the full set	3
R2	Up to 100 conformations of the full set	6
R3	Up to 100 conformations of the full set	9
R4	25% of the full set conformations	3
R5	25% of the full set conformations	6
R6	25% of the full set conformations	9
R7	50% of the full set conformations	3
R8	50% of the full set conformations	6
R9	50% of the full set conformations	9
R10	75% of the full set conformations	3
R11	75% of the full set conformations	6
R12	75% of the full set conformations	9
R13	Full set of conformations	3
R14	Full set of conformations	6
R15	Full set of conformations	9

Choose the strategy to generate the random amplitudes (type 0 for the full exploration): R0
Set the number of iterations (per R strategy): 10000

Averaged Probabilities with the R0 strategy after 10000 iterations

Isomer N°	Averaged Probability	Nº times ranked #1	Nº times ranked #2
1 (3a)	0.818	0.820	0.180
2 (3b)	0.182	0.180	0.820

The most likely isomer is N° 1, with an averaged probability of 81.76%

Normal termination. Thanks for using our method
For further inquiries, please contact Dr. A. Sarotti at sarotti@iquir-conicet.gov.ar
Cite this: Org. Lett. 2020, 22, 1, 52-56

Figure S36. DP4+ analysis of **3a** and **3b** based on random conformational amplitudes.

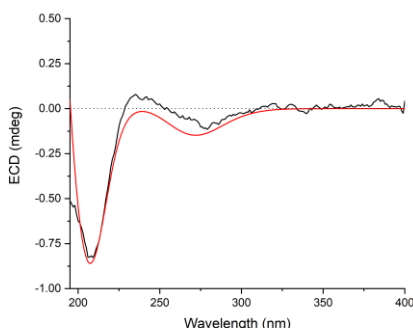


Figure S37. Experimental ECD spectrum of **3** (black). Calculated ECD spectra of (*1S,7S,8R,31S*)-**3** at CAM-B3LYP-SCRF/6-311+G(d,p) level of theory (red, shift = 4 nm).

4.3 Computational data of **3a**

Table S11. Conformational analysis of the B3LYP-D3BJ/6-31G(d) optimized conformers of **3a** in the gas phase (T=298.15 K)

Conformer	E (Hartree) ^a	C (Hartree) ^b	G (kcal/mol) ^c	ΔG (kcal/mol) ^d	Population ^e
3a-1	-967.654783	0.399582	-606952.638446	0.0	56.43%
3a-2	-967.653598	0.399411	-606952.002441	0.636005	19.28%
3a-3	-967.654537	0.400751	-606951.750408	0.888038	12.59%
3a-4	-967.652671	0.398955	-606951.70676	0.931686	11.70%

^aElectronic energy obtained at M06-2X-D3/6-311+G(2d,p) level of theory; ^bThermal correction to

Gibbs free energy obtained at B3LYP-D3BJ/6-31G(d) level of theory; ^cGibbs free energy (E + C);

^dThe relative Gibbs free energy; ^eThe Boltzmann distribution of each conformer.

Table S12. Atomic coordinates (\AA) of **3a-1** obtained at the B3LYP-D3BJ/6-31G(d) level of theory in the gas phase.

C	1.567789	0.219020	-0.190890	H	3.039772	-2.635893	-1.302781
C	-2.126595	1.809504	-0.418558	H	0.662805	-3.057413	-0.173266
C	-1.374286	0.846207	0.488113	H	0.649606	-2.048341	-1.625923
C	-0.895651	-0.420591	-0.244982	H	-1.992086	0.596570	1.358158
C	0.508861	-0.881770	0.212708	H	-0.522177	1.414736	0.889259
C	-3.174166	2.679844	0.243689	H	-2.104601	-1.836711	0.881430
C	-1.976665	-1.522698	-0.158904	H	-1.631289	-2.405910	-0.712482
C	-3.278444	-1.054739	-0.745775	H	-3.240911	-0.850159	-1.816032
C	-4.435133	-0.805327	-0.113746	H	-3.557021	3.416724	-0.464957
C	-4.671533	-0.997785	1.362846	H	-3.997237	2.048660	0.599055
C	-5.630359	-0.286556	-0.874532	H	-2.754406	3.185738	1.121805
C	0.536462	-1.214175	1.715745	H	-6.484047	-0.973185	-0.788630
C	1.015198	-2.109277	-0.591795	H	-5.967232	0.678557	-0.470193
C	2.541266	-1.979650	-0.582478	H	-5.406821	-0.147676	-1.936300
C	2.749502	-0.487762	-0.890212	H	-3.800119	-1.384793	1.894921
C	4.005606	0.227636	-0.329753	H	-4.959101	-0.048217	1.836031
C	4.433435	1.374706	-1.247077	H	-5.506538	-1.690840	1.533696
C	5.184190	-0.674156	0.009745	H	1.539343	-1.510041	2.042815
O	-1.866361	1.909655	-1.605227	H	0.238375	-0.361100	2.327373
O	1.656899	1.623973	1.818257	H	-0.136512	-2.050633	1.929153
O	3.558019	0.834387	0.925914	H	4.911354	-1.416621	0.763395
C	2.210186	0.975206	0.960435	H	5.528816	-1.198342	-0.887873
H	1.088700	0.961278	-0.837697	H	6.014403	-0.079030	0.402235
H	2.708267	-0.344271	-1.974720	H	4.845248	0.980796	-2.182620
H	-0.799136	-0.146726	-1.303439	H	3.580847	2.017277	-1.492791
H	2.928912	-2.232385	0.409952	H	5.196349	1.988014	-0.758614

Table S13. Atomic coordinates (Å) of **3a-2** obtained at the B3LYP-D3BJ/6-31G(d) level of theory in the gas phase.

C	1.394671	0.068607	-0.342035	H	2.602708	-2.970940	-1.221188
C	-1.051276	2.198524	-0.500086	H	0.187463	-3.094653	-0.099208
C	-1.513963	0.997527	0.309720	H	0.300423	-2.162927	-1.598591
C	-1.147283	-0.384740	-0.256319	H	-2.610192	1.087818	0.340319
C	0.257878	-0.893752	0.172481	H	-1.175893	1.128147	1.341786
C	-1.147359	3.536685	0.199080	H	-2.409437	-1.450428	1.165493
C	-2.266844	-1.403598	0.081542	H	-1.942762	-2.404547	-0.230647
C	-3.555601	-1.082260	-0.620293	H	-3.505541	-1.159143	-1.707854
C	-4.722663	-0.692448	-0.085705	H	-0.322709	3.591265	0.919389
C	-4.976556	-0.513704	1.390004	H	-1.054523	4.348518	-0.525159
C	-5.914203	-0.398152	-0.963133	H	-2.083995	3.631931	0.760091
C	0.343963	-1.126981	1.693562	H	-6.763211	-1.047157	-0.706795
C	0.643032	-2.210246	-0.555904	H	-6.260902	0.635345	-0.824487
C	2.175601	-2.251858	-0.515017	H	-5.684637	-0.540363	-2.023458
C	2.570103	-0.799467	-0.843710	H	-4.097569	-0.709833	2.007376
C	3.830542	-0.168452	-0.183295	H	-5.313470	0.510497	1.601044
C	4.574452	0.720551	-1.180546	H	-5.782280	-1.179862	1.727755
C	4.781178	-1.139674	0.503857	H	0.107840	-0.227212	2.264537
O	-0.642410	2.105023	-1.646282	H	-0.343848	-1.921272	1.999127
O	1.424300	1.796053	1.395055	H	1.351730	-1.434116	1.991846
O	3.315845	0.719982	0.861352	H	4.285317	-1.667453	1.322054
C	1.992776	0.968263	0.717828	H	5.155541	-1.878446	-0.212544
H	0.990954	0.702320	-1.133025	H	5.635653	-0.597497	0.920143
H	2.668890	-0.709053	-1.929693	H	5.037290	0.108587	-1.962650
H	-1.119184	-0.277917	-1.348875	H	3.885174	1.425015	-1.658722
H	2.511839	-2.547844	0.482823	H	5.356759	1.293814	-0.674086

Table S14. Atomic coordinates (\AA) of **3a-3** obtained at the B3LYP-D3BJ/6-31G(d) level of theory in the gas phase.

C	-1.415743	0.185087	0.156361	H	-2.728656	-2.932710	0.491165
C	2.244467	1.742743	0.311976	H	-0.600465	-2.861230	-1.114721
C	1.375869	1.114517	-0.768980	H	-0.309204	-2.390499	0.565143
C	0.999492	-0.345050	-0.439688	H	1.864283	1.194391	-1.746292
C	-0.473910	-0.676424	-0.774333	H	0.476936	1.744748	-0.833283
C	3.325300	2.699209	-0.143651	H	1.877796	-1.369432	-2.147058
C	2.021776	-1.326019	-1.061498	H	1.820620	-2.335972	-0.683173
C	3.452726	-0.930420	-0.778105	H	4.003990	-0.497842	-1.612805
C	4.078895	-1.006160	0.405429	H	3.807455	3.164656	0.718174
C	3.436274	-1.548972	1.654945	H	4.069697	2.150678	-0.732585
C	5.479812	-0.481229	0.582814	H	2.901756	3.471559	-0.797627
C	-0.779420	-0.485475	-2.270829	H	6.155165	-1.262395	0.957190
C	-0.854337	-2.120270	-0.349888	H	5.892606	-0.091892	-0.353405
C	-2.354238	-2.056259	-0.047158	H	5.494684	0.328322	1.325984
C	-2.472787	-0.758959	0.770469	H	4.141883	-2.170523	2.220192
C	-3.791079	0.054728	0.706642	H	3.130218	-0.720731	2.307734
C	-4.025643	0.811407	2.015529	H	2.547735	-2.149956	1.443260
C	-5.030799	-0.725912	0.292821	H	-0.565475	0.531684	-2.603600
O	2.041266	1.521491	1.494994	H	-0.185046	-1.181455	-2.870861
O	-1.822430	2.179530	-1.212679	H	-1.834207	-0.680769	-2.493134
O	-3.555938	1.062682	-0.328891	H	-4.912709	-1.159211	-0.703064
C	-2.231723	1.259228	-0.543056	H	-5.221336	-1.535417	1.005284
H	-0.809084	0.683557	0.919734	H	-5.904402	-0.067120	0.276621
H	-2.240336	-0.982635	1.816602	H	-4.848012	1.523915	1.901653
H	1.084196	-0.439662	0.648267	H	-4.276601	0.111287	2.819835
H	-2.917539	-1.985693	-0.983785	H	-3.128706	1.366090	2.312354

Table S15. Atomic coordinates (\AA) of **3a-4** obtained at the B3LYP-D3BJ/6-31G(d) level of theory in the gas phase.

C	1.219203	0.035821	-0.285008	H	1.961457	-3.239105	-0.698870
C	-1.039104	2.359543	-0.449184	H	-0.155451	-2.841156	0.876704
C	-1.399893	1.425578	0.696872	H	-0.289741	-2.238884	-0.781910
C	-1.270646	-0.079921	0.407180	H	-2.451156	1.660233	0.919658
C	0.153975	-0.656419	0.645941	H	-0.835414	1.731455	1.582318
C	-0.896953	3.821173	-0.085150	H	-2.235098	-0.695669	2.260535
C	-2.356180	-0.869121	1.184888	H	-2.197180	-1.941513	1.029772
C	-3.763936	-0.495714	0.786398	H	-4.288241	0.192495	1.448971
C	-4.412021	-0.907365	-0.312830	H	-1.683979	4.142731	0.606464
C	-3.822954	-1.852457	-1.328936	H	0.064461	3.941204	0.427486
C	-5.808909	-0.433025	-0.622016	H	-0.909630	4.436945	-0.986785
C	0.563042	-0.588244	2.130129	H	-5.844422	0.079861	-1.593231
C	0.263543	-2.127278	0.160531	H	-6.507550	-1.278511	-0.691237
C	1.759950	-2.354139	-0.087042	H	-6.182993	0.257098	0.140526
C	2.202087	-1.049587	-0.778629	H	-3.675144	-1.342419	-2.290682
C	3.616448	-0.460213	-0.492170	H	-2.859626	-2.264449	-1.019878
C	4.255351	0.063810	-1.778247	H	-4.506120	-2.690741	-1.520794
C	4.574515	-1.367898	0.268992	H	0.520855	0.429768	2.522677
O	-0.892271	1.970701	-1.596556	H	-0.088804	-1.221107	2.739846
O	1.725722	2.093241	0.944815	H	1.589875	-0.939271	2.276657
O	3.385864	0.707435	0.361688	H	4.183630	-1.614176	1.259527
C	2.083198	1.072385	0.399554	H	4.738429	-2.299007	-0.283415
H	0.701283	0.521653	-1.113160	H	5.539198	-0.868628	0.401192
H	2.099929	-1.183604	-1.859660	H	4.506451	-0.769287	-2.444223
H	-1.482731	-0.207022	-0.661087	H	3.565228	0.730153	-2.306961
H	2.274133	-2.503251	0.866260	H	5.169521	0.621614	-1.553913

Table S16. Key transitions, oscillator strengths, and rotatory strengths in the ECD spectrum of conformer **3a-1** at the CAM-B3LYP/6-311+G(d,p) level of theory in MeOH with IEFPCM solvent model.

Num ^a	Transition ^b	CI-coeff ^b	ΔE (eV) ^d	λ (nm) ^e	f	R _{vel} ^g	R _{len} ^h
1	83->86	0.62435	4.6341	267.55	0.0001	-2.3906	-4.1635
	83->87	0.15896					
	83->89	-0.16429					
2	82->87	0.42848	5.7608	215.22	0.0008	1.0984	1.9196
	82->88	-0.18555					
	82->90	0.3445					
	82->92	0.24503					
3	84->86	0.67388	6.0720	204.19	0.0673	-27.1548	-27.2723
4	84->85	0.41098	6.3404	195.55	0.0103	1.3511	1.2151
	84->87	0.20661					
	84->88	0.28075					
	84->89	-0.33598					
	84->91	0.20517					
5	84->85	0.14882	6.7100	184.78	0.3321	27.5893	28.2197
	84->87	0.22108					
	84->88	0.2324					
	84->89	0.34577					
	84->91	-0.22025					
	84->92	-0.18911					
	84->93	-0.20011					
	84->94	-0.15457					
	84->95	-0.2076					
	84->99	0.14909					
6	83->85	0.48555	6.9038	179.59	0.0555	1.2054	0.9171
	83->87	-0.16483					
	83->88	0.29369					
	83->91	-0.17552					
	83->97	0.15318					
7	84->87	-0.35055	6.9172	179.24	0.0530	-6.8314	-6.578
	84->90	0.35135					
	84->91	-0.21959					
	84->93	0.21917					
	84->95	-0.16829					
	84->96	0.21487					
8	84->85	-0.20651	7.0349	176.24	0.0718	31.8906	31.7853
	84->88	0.33993					
	84->89	0.18117					
	84->90	0.20964					

<i>Num</i> ^a	<i>Transition</i> ^b	<i>CI-coeff</i> ^b	ΔE (eV) ^d	λ (nm) ^e	<i>f</i>	R_{vel} ^g	R_{len} ^h
	84->91	0.32903					
	84->92	-0.15944					
	84->94	0.17847					
	84->96	-0.2068					
9	84->85	-0.30593	7.2033	172.12	0.1101	-13.6914	-14.114
	84->87	0.31693					
	84->90	0.33364					
	84->94	-0.15757					
10	84->87	0.29558	7.4617	166.16	0.0714	-7.0859	-7.6669
	84->89	0.16767					
	84->92	0.16413					
	84->94	0.37958					
	84->100	-0.20416					
	84->101	0.21136					
11	83->87	0.48684	7.5142	165.00	0.0145	5.2705	4.9363
	83->88	0.1855					
	83->89	0.24901					
	83->90	0.14166					
12	81->87	0.36783	7.5378	164.48	0.0852	-64.03	-67.0151
	81->90	0.2406					
	81->92	0.14612					
	82->85	0.21101					
	83->87	-0.14629					
13	84->85	-0.22811	7.5895	163.36	0.0013	13.4785	12.9162
	84->89	-0.19544					
	84->90	-0.18028					
	84->93	-0.21844					
	84->95	-0.22848					
	84->96	0.2515					
	84->98	0.19026					
14	84->85	-0.14593	7.6198	162.71	0.0066	5.8335	6.0802
	84->88	0.15348					
	84->93	-0.15791					
	84->95	0.44171					
	84->96	0.2187					
	84->98	0.14969					
	84->99	-0.14459					
	84->101	-0.18062					
15	81->87	-0.20736	7.6440	162.20	0.0838	8.8213	7.9083
	82->85	0.36796					
	82->86	0.25271					
	82->89	0.16146					

<i>Num</i> ^a	<i>Transition</i> ^b	<i>CI-coeff</i> ^b	ΔE (eV) ^d	λ (nm) ^e	<i>f</i>	R_{vel} ^g	R_{len} ^h
	82->92	0.14185					
	83->90	-0.14546					
16	84->85	-0.146	7.6819	161.40	0.0078	-4.3511	-4.6483
	84->88	0.22254					
	84->90	-0.20953					
	84->92	0.17169					
	84->93	0.27343					
	84->97	0.29038					
	84->98	-0.25942					
	84->99	0.21794					
	84->103	0.15832					
17	82->85	0.15271	7.7402	160.18	0.0216	-12.9433	-13.3126
	83->86	-0.16954					
	83->89	-0.27704					
	83->90	0.33988					
	83->95	-0.28115					
	83->96	0.18742					
18	79->86	-0.22971	7.8202	158.54	0.0140	10.0755	10.2101
	80->86	0.48625					
	80->87	0.15168					
19	84->89	0.14657	7.8707	157.53	0.0205	10.8394	10.7277
	84->91	0.16553					
	84->92	0.2809					
	84->98	0.21336					
	84->99	0.16956					
	84->101	-0.14935					
	84->102	0.16794					
20	82->86	-0.15153	7.9155	156.63	0.0141	-32.6934	-33.7742
	83->85	0.28082					
	83->87	0.24226					
	83->88	-0.26421					
	83->92	0.20392					
	84->101	0.14519					
21	83->85	-0.14378	7.9360	156.23	0.0064	7.9817	7.4315
	84->94	-0.14507					
	84->96	-0.1834					
	84->97	0.17359					
	84->100	0.1899					
	84->101	0.19413					
22	78->86	0.18203	7.9681	155.60	0.0251	1.068	1.1181
	79->86	0.16264					
	83->88	0.26856					

<i>Num</i> ^a	<i>Transition</i> ^b	<i>CI-coeff</i> ^b	ΔE (eV) ^d	λ (nm) ^e	<i>f</i>	R_{vel} ^g	R_{len} ^h
	83->89	-0.16104					
	83->91	0.18857					
	83->92	-0.17411					
23	78->86	0.24664	7.9821	155.33	0.0032	-13.0892	-12.9086
	79->86	0.26496					
	83->85	-0.19322					
	83->89	0.23305					
	83->91	-0.14928					
24	83->91	-0.1686	7.9870	155.23	0.0124	-15.096	-15.2586
	83->92	-0.26936					
	83->93	-0.19503					
	83->95	-0.26662					
	83->96	0.30021					
25	78->87	-0.16537	8.0886	153.28	0.0131	-30.7056	-30.9983
	82->86	0.27416					
	82->87	0.1473					
	84->102	-0.19435					
26	79->86	0.17767	8.0951	153.16	0.0312	-5.932	-5.4421
	82->86	0.29361					
	84->102	0.17022					
27	78->86	0.14546	8.1492	152.14	0.0082	26.3852	27.3169
	80->91	0.15179					
	80->95	0.15294					
28	79->87	-0.14309	8.1587	151.97	0.0071	14.5622	14.3009
	81->85	0.27323					
	84->90	0.17286					
	84->92	0.2308					
	84->93	-0.20383					
	84->102	-0.14934					
29	79->87	0.18703	8.1619	151.91	0.0021	-3.442	-2.9857
	81->85	0.35838					
	81->88	-0.22983					
	81->89	0.17482					
30	78->87	0.23944	8.2188	150.86	0.0015	1.5776	1.6147
	81->85	-0.15602					
	82->86	0.20862					
	82->87	-0.1992					
	82->90	0.14309					
31	84->88	0.1492	8.2349	150.56	0.0041	-1.2884	-1.1274
	84->90	-0.15513					
	84->92	0.29763					
	84->93	0.22179					

<i>Num</i> ^a	<i>Transition</i> ^b	<i>CI-coeff</i> ^c	ΔE (eV) ^d	λ (nm) ^e	<i>f</i>	R_{vel} ^g	R_{len} ^h
	84->97	-0.20934					
	84->99	-0.17477					
	84->102	-0.16372					
	84->103	-0.22328					
	84->104	0.17581					
32	82->87	0.1539	8.2941	149.48	0.0268	0.9495	1.4886
	84->89	0.15709					
	84->91	0.23416					
	84->94	-0.21184					
	84->104	0.17249					
	84->106	-0.18552					
33	78->87	0.1899	8.3021	149.34	0.0219	12.6731	12.4648
	82->85	-0.16441					
	82->87	0.18411					
	84->91	-0.15442					
34	76->87	0.19139	8.3303	148.84	0.0097	-11.0424	-11.5417
	77->87	-0.22446					
	80->87	0.23175					
	82->90	0.15686					
35	84->95	0.17189	8.3456	148.56	0.0047	2.8589	2.9413
	84->96	-0.16495					
	84->97	-0.18781					
	84->98	0.22382					
	84->99	0.32797					
	84->100	-0.174					
	84->103	-0.16509					
	84->106	-0.17442					
36	82->88	0.16619	8.3663	148.19	0.0208	7.4949	7.6645
	83->88	0.15902					
	83->90	-0.18498					
	83->92	0.20842					
	83->99	0.2386					

^aNumber of the excited states; ^bOnly transitions with contribution over 4.0% were listed;

^cConfiguration-interaction coefficient; ^dExcitation energy; ^eWavelength; ^fOscillator strength;

^gRotatory strength in velocity form (10^{-40} cgs); ^hRotatory strength in length form (10^{-40} cgs).

4.4 Computational data of **3b**

Table S17. Conformational analysis of the B3LYP-D3BJ/6-31G(d) optimized conformers of **3b** in the gas phase (T=298.15 K)

Conformer	E (Hartree) ^a	C (Hartree) ^b	G (kcal/mol) ^c	ΔG (kcal/mol) ^d	Population ^e
3b-1	-967.652564	0.3999	-606951.046605	0.0	32.48%
3b-2	-967.650046	0.398224	-606950.518277	0.528327	13.31%
3b-3	-967.650043	0.398236	-606950.509076	0.537529	13.10%
3b-4	-967.650044	0.39824	-606950.507032	0.539573	13.06%
3b-5	-967.651049	0.399474	-606950.363061	0.683543	10.24%
3b-6	-967.65173	0.400249	-606950.304402	0.742203	9.27%
3b-7	-967.651526	0.400124	-606950.254769	0.791835	8.53%

^aElectronic energy obtained at M06-2X-D3/6-311+G(2d,p) level of theory; ^bThermal correction to

Gibbs free energy obtained at B3LYP-D3BJ/6-31G(d) level of theory; ^cGibbs free energy (E + C);

^dThe relative Gibbs free energy; ^eThe Boltzmann distribution of each conformer.

Table S18. Atomic coordinates (Å) of **3b-1** obtained at the B3LYP-D3BJ/6-31G(d) level of theory in the gas phase.

C	1.605357	-0.229326	0.313897	H	3.130442	2.785641	-0.045625
C	-2.970921	1.803632	0.343055	H	0.798802	2.638221	-1.315360
C	-1.880949	1.361711	-0.631994	H	0.715342	2.478921	0.444728
C	-0.849381	0.417514	0.010469	H	-1.402076	2.292826	-0.965166
C	0.573724	0.556627	-0.586157	H	-2.334589	0.915167	-1.523976
C	-4.346934	2.039191	-0.244220	H	-0.627567	-1.712113	0.387065
C	-1.384351	-1.033637	-0.026042	H	-1.517023	-1.342362	-1.066476
C	-2.666222	-1.175017	0.743413	H	-2.585999	-0.936158	1.804126
C	-3.881091	-1.509769	0.282399	H	-4.287933	2.720051	-1.102734
C	-4.195252	-1.858302	-1.150716	H	-4.750958	1.089812	-0.613594
C	-5.068431	-1.562955	1.211612	H	-5.014557	2.453654	0.513548
C	0.615229	0.126238	-2.064015	H	-5.515855	-2.566473	1.227034
C	1.105723	2.013150	-0.470268	H	-4.794691	-1.293250	2.235762
C	2.626908	1.869568	-0.369892	H	-5.859468	-0.875520	0.879624
C	2.788446	0.712260	0.627443	H	-3.328460	-1.796916	-1.811759
C	4.037043	-0.199526	0.521118	H	-4.598208	-2.877939	-1.219346
C	4.403707	-0.781526	1.887963	H	-4.974140	-1.193764	-1.551349
C	5.252493	0.421099	-0.154055	H	0.371005	-0.928382	-2.194240
O	-2.729025	2.007803	1.518582	H	-0.092304	0.725728	-2.647032
O	1.707048	-2.414933	-0.797280	H	1.610283	0.281409	-2.495759
O	3.606843	-1.319212	-0.316077	H	6.078029	-0.296736	-0.179687
C	2.254499	-1.447029	-0.326847	H	5.028402	0.717959	-1.181266
H	1.105188	-0.574742	1.224048	H	5.580948	1.305972	0.401235
H	2.718422	1.111478	1.644416	H	5.159445	-1.564806	1.777580
H	-0.775125	0.725947	1.061707	H	4.802764	0.001725	2.541700
H	3.038090	1.601012	-1.349021	H	3.525290	-1.219053	2.375036

Table S19. Atomic coordinates (\AA) of **3b-2** obtained at the B3LYP-D3BJ/6-31G(d) level of theory in the gas phase.

C	1.420328	-0.409215	0.290169	H	2.937746	2.625487	0.078192
C	-2.145118	2.549616	0.367118	H	0.562263	2.558299	-1.123667
C	-2.072457	1.263608	-0.443781	H	0.547230	2.267577	0.620949
C	-1.049269	0.227637	0.046631	H	-1.945873	1.505624	-1.505701
C	0.373418	0.429066	-0.544310	H	-3.080945	0.828961	-0.363596
C	-2.811051	3.727544	-0.318988	H	-0.782319	-1.928397	-0.004908
C	-1.586285	-1.205964	-0.193708	H	-1.844271	-1.325291	-1.249937
C	-2.761701	-1.516728	0.686701	H	-2.538246	-1.514279	1.755240
C	-4.030687	-1.763862	0.327372	H	-2.154703	4.100722	-1.116085
C	-4.530503	-1.803308	-1.095182	H	-3.751054	3.425945	-0.795858
C	-5.087624	-2.047764	1.366078	H	-2.993762	4.528382	0.400005
C	0.416247	0.091060	-2.046704	H	-4.681748	-2.009807	2.381508
C	0.903628	1.875736	-0.336679	H	-5.911837	-1.323814	1.299925
C	2.426629	1.729463	-0.287619	H	-5.533939	-3.040434	1.213583
C	2.602947	0.520189	0.644237	H	-5.359371	-1.095306	-1.233397
C	3.853665	-0.377644	0.478501	H	-3.759254	-1.566887	-1.831068
C	4.227857	-1.041263	1.805492	H	-4.930433	-2.797753	-1.336298
C	5.063405	0.288277	-0.162379	H	0.173919	-0.953798	-2.240795
O	-1.726846	2.632275	1.507893	H	-0.287254	0.721825	-2.600607
O	1.528374	-2.524091	-0.953908	H	1.412178	0.274520	-2.463743
O	3.423387	-1.445492	-0.424339	H	5.888278	-0.426041	-0.245489
C	2.072259	-1.581003	-0.430656	H	4.829798	0.656784	-1.163931
H	0.933280	-0.814817	1.182628	H	5.397550	1.132141	0.450444
H	2.538975	0.864917	1.681269	H	4.988923	-1.810670	1.645167
H	-0.963379	0.379778	1.130487	H	4.622130	-0.297298	2.506235
H	2.819263	1.513829	-1.287097	H	3.353397	-1.514404	2.265623

Table S20. Atomic coordinates (\AA) of **3b-3** obtained at the B3LYP-D3BJ/6-31G(d) level of theory in the gas phase.

C	1.420217	-0.409323	0.290377	H	2.937753	2.625404	0.079439
C	-2.144822	2.549875	0.367087	H	0.562154	2.558787	-1.122256
C	-2.072614	1.263667	-0.443522	H	0.547300	2.267289	0.622215
C	-1.049398	0.227676	0.046832	H	-1.946391	1.505300	-1.505578
C	0.373370	0.429312	-0.543850	H	-3.081089	0.829091	-0.362779
C	-2.809460	3.728200	-0.319597	H	-0.782468	-1.928390	-0.005542
C	-1.586425	-1.205847	-0.193937	H	-1.844535	-1.324818	-1.250186
C	-2.761759	-1.516910	0.686506	H	-2.538178	-1.514819	1.755024
C	-4.030772	-1.763965	0.327213	H	-2.152375	4.100742	-1.116388
C	-4.530694	-1.803056	-1.095317	H	-3.749435	3.427200	-0.796919
C	-5.087623	-2.048142	1.365948	H	-2.991984	4.529311	0.399149
C	0.416351	0.091870	-2.046368	H	-5.911201	-1.323360	1.300912
C	0.903606	1.875857	-0.335616	H	-5.534885	-3.040233	1.212458
C	2.426618	1.729552	-0.286776	H	-4.681367	-2.011719	2.381287
C	2.603012	0.519851	0.644530	H	-5.360140	-1.095659	-1.233108
C	3.853632	-0.378059	0.478219	H	-3.759677	-1.565600	-1.831132
C	4.228106	-1.042028	1.804955	H	-4.929794	-2.797713	-1.336965
C	5.063282	0.287837	-0.162863	H	0.173601	-0.952819	-2.240856
O	-1.727167	2.632344	1.508105	H	-0.286787	0.723144	-2.600161
O	1.527820	-2.523948	-0.954207	H	1.412434	0.275042	-2.463175
O	3.423016	-1.445651	-0.424762	H	4.829381	0.656787	-1.164187
C	2.071913	-1.581027	-0.430826	H	5.397879	1.131389	0.450149
H	0.933161	-0.814999	1.182794	H	5.887942	-0.426662	-0.246564
H	2.539291	0.864149	1.681718	H	4.622559	-0.298222	2.505773
H	-0.963736	0.379594	1.130743	H	3.353718	-1.515226	2.265174
H	2.819174	1.514433	-1.286391	H	4.989109	-1.811429	1.644286

Table S21. Atomic coordinates (\AA) of **3b-4** obtained at the B3LYP-D3BJ/6-31G(d) level of theory in the gas phase.

C	1.420144	-0.409369	0.290235	H	2.937887	2.625228	0.078856
C	-2.144523	2.550035	0.367152	H	0.562267	2.558600	-1.122799
C	-2.072557	1.263808	-0.443473	H	0.547364	2.267397	0.621737
C	-1.049406	0.227729	0.046809	H	-1.946451	1.505366	-1.505548
C	0.373307	0.429214	-0.544045	H	-3.081083	0.829371	-0.362534
C	-2.808788	3.728543	-0.319583	H	-0.782554	-1.928315	-0.005333
C	-1.586504	-1.205790	-0.193847	H	-1.844578	-1.324824	-1.250093
C	-2.761871	-1.516709	0.686585	H	-2.538366	-1.514382	1.755119
C	-4.030865	-1.763839	0.327273	H	-2.151584	4.100828	-1.116399
C	-4.530695	-1.803236	-1.095286	H	-3.748834	3.427811	-0.796935
C	-5.087758	-2.047910	1.365985	H	-2.991082	4.529726	0.399135
C	0.416165	0.091590	-2.046527	H	-5.534336	-3.040414	1.213152
C	0.903643	1.875779	-0.336032	H	-4.681758	-2.010449	2.381389
C	2.426645	1.729347	-0.287136	H	-5.911799	-1.323726	1.300202
C	2.602896	0.519831	0.644426	H	-5.360549	-1.096315	-1.233096
C	3.853507	-0.378098	0.478394	H	-3.759800	-1.565367	-1.831084
C	4.227718	-1.042063	1.805207	H	-4.929241	-2.798122	-1.336905
C	5.063281	0.287753	-0.162473	H	1.412168	0.274916	-2.463460
O	-1.727009	2.632354	1.508231	H	0.173608	-0.953165	-2.240893
O	1.527875	-2.524021	-0.954288	H	-0.287137	0.722679	-2.600320
O	3.423030	-1.445718	-0.424669	H	4.829548	0.656855	-1.163781
C	2.071932	-1.581088	-0.430892	H	5.397875	1.131201	0.450685
H	0.933089	-0.815103	1.182628	H	5.887889	-0.426811	-0.246147
H	2.539038	0.864329	1.681542	H	3.353237	-1.515254	2.265258
H	-0.963591	0.379681	1.130701	H	4.988741	-1.811476	1.644688
H	2.819177	1.513915	-1.286698	H	4.622044	-0.298266	2.506103

Table S22. Atomic coordinates (\AA) of **3b-5** obtained at the B3LYP-D3BJ/6-31G(d) level of theory in the gas phase.

C	0.991925	-0.196461	0.018049	H	1.968469	-2.982361	-1.664725
C	-4.009728	-0.974180	-0.455712	H	-0.274153	-3.330631	-0.271348
C	-2.734014	-1.451738	0.227497	H	-0.373786	-2.179108	-1.609353
C	-1.540774	-0.515016	0.013669	H	-2.528868	-2.457273	-0.170036
C	-0.186358	-1.197190	0.338562	H	-2.945832	-1.599772	1.294577
C	-5.287836	-1.688733	-0.056840	H	-1.014476	0.929573	1.579451
C	-1.741749	0.837593	0.768876	H	-2.730445	0.832619	1.249092
C	-1.675657	2.019189	-0.161178	H	-2.381733	1.957677	-0.988880
C	-0.873819	3.093525	-0.097312	H	-5.152978	-2.776724	-0.065098
C	0.155553	3.350087	0.973538	H	-5.556727	-1.408259	0.969838
C	-0.966381	4.175351	-1.146179	H	-6.100122	-1.405680	-0.728975
C	-0.149770	-1.732382	1.781418	H	-0.003705	4.311962	-1.659319
C	0.107438	-2.373240	-0.641278	H	-1.726464	3.948686	-1.899999
C	1.627744	-2.372341	-0.822230	H	-1.213625	5.145087	-0.691800
C	1.937674	-0.877933	-0.990845	H	-0.084366	4.272445	1.520842
C	3.338644	-0.369761	-0.584953	H	0.252783	2.540206	1.696751
C	3.674903	0.942156	-1.297618	H	1.145989	3.512500	0.523952
C	4.469209	-1.379138	-0.724247	H	-0.918194	-2.500168	1.916133
O	-4.013347	-0.078429	-1.280111	H	0.816402	-2.195371	2.008545
O	1.606051	0.589521	2.267244	H	-0.305863	-0.945300	2.520435
O	3.207126	-0.062519	0.839748	H	4.277468	-2.273643	-0.126947
C	1.910754	0.160009	1.179403	H	4.579591	-1.676848	-1.772456
H	0.587035	0.745004	-0.364240	H	5.413766	-0.939496	-0.389454
H	1.717922	-0.576912	-2.020675	H	4.575492	1.388193	-0.865246
H	-1.522027	-0.286781	-1.058681	H	3.849485	0.763729	-2.364190
H	2.108898	-2.762925	0.082395	H	2.854868	1.662201	-1.201353

Table S23. Key transitions, oscillator strengths, and rotatory strengths in the ECD spectrum of conformer **3b-1** at the CAM-B3LYP/6-311+G(d,p) level of theory in MeOH with IEFPCM solvent model.

Num ^a	Transition ^b	CI-coeff ^b	ΔE (eV) ^d	λ (nm) ^e	f	R _{vel} ^g	R _{len} ^h
1	83->85	0.60158	4.6142	268.70	0.0000	0.5153	2.1607
	83->86	0.16699					
	83->89	0.16341					
2	82->85	0.17268	5.7444	215.84	0.0008	2.4453	3.2435
	82->87	0.31173					
	82->88	0.32633					
	82->90	0.30858					
	82->92	0.26315					
3	84->85	0.66657	5.9729	207.58	0.0789	32.2528	32.7921
	84->87	-0.16051					
4	84->86	0.46196	6.3128	196.40	0.0074	0.9336	1.0581
	84->88	-0.28394					
	84->89	0.27309					
	84->90	0.16036					
	84->91	-0.18381					
5	84->87	0.41543	6.7005	185.04	0.2622	-37.1462	-38.0493
	84->91	0.38116					
	84->94	0.19645					
6	84->86	-0.16509	6.8526	180.93	0.1219	-3.1981	-3.7867
	84->87	0.36458					
	84->88	0.22498					
	84->89	0.25101					
	84->93	-0.22289					
	84->94	-0.21101					
	84->97	0.17029					
7	83->86	0.45683	6.9473	178.46	0.0973	-10.531	-9.451
	83->87	0.17111					
	83->88	-0.23288					
	83->89	-0.27909					
	83->96	-0.17824					
8	84->86	-0.22402	7.0311	176.34	0.0117	-16.4581	-16.7609
	84->88	-0.19103					
	84->89	-0.18871					
	84->90	0.48395					
	84->93	0.184					
9	84->86	-0.25551	7.2824	170.25	0.0918	-0.0612	0.9901
	84->87	-0.19926					
	84->88	-0.24025					

<i>Num</i> ^a	<i>Transition</i> ^b	<i>CI-coeff</i> ^b	ΔE (eV) ^d	λ (nm) ^e	<i>f</i>	R_{vel} ^g	R_{len} ^h
	84->89	0.29235					
	84->91	0.19027					
	84->92	-0.2475					
	84->95	0.18611					
	84->96	0.18946					
	84->101	-0.15958					
10	84->88	0.26774	7.3513	168.66	0.1375	-15.13	-13.9985
	84->89	0.17089					
	84->90	0.16649					
	84->92	0.20903					
	84->93	0.19019					
	84->94	0.2146					
	84->99	0.32332					
11	81->85	0.16819	7.5191	164.89	0.1095	-62.816	-67.5852
	81->87	0.28373					
	81->88	0.25573					
	81->90	0.21218					
	82->86	0.24607					
	82->89	0.1628					
12	83->85	0.22513	7.5499	164.22	0.0104	-5.8473	-5.9815
	83->87	0.45444					
	83->91	0.20096					
	83->94	-0.20046					
13	84->89	0.21288	7.5582	164.04	0.0054	-5.4761	-5.6019
	84->94	0.32093					
	84->95	-0.30885					
	84->98	0.19502					
	84->101	0.22623					
14	84->86	0.24301	7.6317	162.46	0.0196	28.1935	28.4765
	84->88	0.21943					
	84->92	-0.16008					
	84->94	0.16206					
	84->97	0.33034					
	84->102	-0.19948					
15	81->87	-0.1808	7.6702	161.64	0.0524	-19.0554	-19.3913
	81->88	-0.16813					
	82->86	0.36168					
	82->89	0.21368					
16	84->88	-0.16228	7.6872	161.29	0.0018	4.965	4.5377
	84->90	-0.25435					
	84->93	0.30747					
	84->96	-0.1986					

<i>Num</i> ^a	<i>Transition</i> ^b	<i>CI-coeff</i> ^b	ΔE (eV) ^d	λ (nm) ^e	<i>f</i>	R_{vel} ^g	R_{len} ^h
	84->97	0.24667					
	84->98	-0.21684					
	84->99	0.27099					
17	80->85	-0.25998	7.7685	159.60	0.0406	0.7903	1.0526
	83->88	-0.27818					
	83->91	0.28657					
	83->94	0.17962					
18	84->89	0.21694	7.8255	158.44	0.0018	3.198	3.2801
	84->91	0.23883					
	84->95	-0.21248					
	84->96	0.27603					
	84->97	-0.17743					
	84->98	-0.18192					
	84->100	-0.21913					
19	80->85	0.35005	7.8435	158.07	0.0216	6.6032	6.7566
	83->86	-0.18676					
	83->90	0.26401					
	83->94	0.24432					
20	80->85	0.23301	7.8859	157.22	0.0105	-10.4687	-10.7537
21	80->85	0.22937	7.8978	156.99	0.0273	15.8294	15.7957
	84->92	0.18868					
	84->96	-0.15816					
	84->101	0.15828					
22	78->85	0.22711	7.9531	155.90	0.0030	-3.8295	-4.3328
	83->89	0.22525					
	83->90	0.16756					
	83->91	-0.22631					
	83->94	-0.17347					
23	78->85	0.37508	7.9656	155.65	0.0177	21.9322	22.1875
	83->86	-0.21953					
	83->89	-0.25096					
24	79->85	0.17562	8.0056	154.87	0.0077	-3.701	-3.4509
	83->94	0.2607					
	83->96	0.19314					
	83->99	0.17425					
25	84->88	-0.17968	8.0872	153.31	0.0036	15.2449	15.7164
	84->92	0.2578					
	84->93	-0.24188					
	84->102	-0.23192					
26	81->86	0.2959	8.1259	152.58	0.0067	-21.312	-22.0766
	81->88	0.2005					
	82->85	-0.18369					

<i>Num</i> ^a	<i>Transition</i> ^b	<i>CI-coeff</i> ^b	ΔE (eV) ^d	λ (nm) ^e	<i>f</i>	R_{vel} ^g	R_{len} ^h
27	79->85	-0.16451	8.1415	152.29	0.0007	5.0827	5.7529
	81->86	0.30011					
	81->88	0.20598					
28	82->87	0.16082	8.1695	151.76	0.0020	14.1685	14.968
29	84->87	-0.16488	8.1781	151.61	0.0098	18.8085	19.5295
	84->90	0.16411					
	84->91	0.24495					
	84->96	-0.17732					
	84->102	0.18381					
30	82->87	-0.17122	8.2343	150.57	0.0082	6.1733	6.3661
	82->90	0.16702					
	83->87	0.17034					
	83->88	0.1998					
31	76->85	-0.16647	8.2617	150.07	0.0190	24.8664	25.265
	78->85	-0.19302					
	79->85	0.26667					
	82->85	-0.16056					
32	84->92	0.17177	8.3058	149.27	0.0098	15.0483	15.9032
	84->94	-0.19688					
	84->97	0.16309					
	84->98	0.31282					
	84->103	0.20396					
	84->104	-0.22947					
33	78->87	0.21167	8.3144	149.12	0.0328	0.7371	0.1507
	78->88	0.19534					
34	84->92	0.16317	8.3242	148.94	0.0119	11.281	11.9206
	84->95	-0.20811					
	84->99	-0.16631					
	84->101	-0.22223					
	84->106	0.2455					
35	77->85	0.18307	8.3461	148.55	0.0144	19.7161	20.1525
	77->87	0.30624					
	77->88	0.22919					
	77->90	0.19766					
36	82->86	0.30216	8.3781	147.99	0.0011	1.1873	1.5141
	82->88	0.2117					
	82->89	-0.29732					
	82->92	-0.18609					
	82->95	-0.21038					

^aNumber of the excited states; ^bOnly transitions with contribution over 4.0% were listed; ^cConfiguration-interaction coefficient; ^dExcitation energy; ^eWavelength; ^fOscillator strength; ^gRotatory strength in velocity form (10⁻⁴⁰ cgs); ^hRotatory strength in length form (10⁻⁴⁰ cgs).